2009-07-28

Evidence Based Uncertainty Models and Particles Swarm Optimization for Multiobjective Optimization of Engineering Systems

Kiran Kumar Kishore Annamdas
University of Miami, kiranisonline@yahoo.com

UNIVERSITY OF MIAMI

EVIDENCE BASED UNCERTAINTY MODELS AND PARTICLES SWARM OPTIMIZATION FOR MULTIOBJECTIVE OPTIMIZATION OF ENGINEERING SYSTEMS

By

Kiran Kumar Annamdas

A DISSERTATION

Submitted to the Faculty
of the University of Miami
in partial fulfillment of the requirements for
the degree of Doctor of Philosophy

Coral Gables, Florida

June 2009

UNIVERSITY OF MIAMI

A dissertation submitted in partial fulfillment of
the requirements for the degree of
Doctor of Philosophy

EVIDENCE BASED UNCERTAINTY MODELS AND PARTICLES SWARM OPTIMIZATION FOR MULTIOBJECTIVE OPTIMIZATION OF ENGINEERING SYSTEMS

Kiran Kumar Annamdas

Approved:

_____
Singiresu S. Rao, Ph.D.
Professor and Chairman of Mechanical
& Aerospace Engineering and Chairman
of the Dissertation Commitee

_____
Terri A. Scandura, Ph.D.
Dean of the Graduate School

_____
Jizhou Song, Ph.D.
Assistant Professor of Mechanical &
Aerospace Engineering

_____
Michael R. Swain, Ph.D.
Associate Professor of
Mechanical & Aerospace
Engineering

_____
James Giancaspro, Ph.D.
Assistant Professor of Civil, Architectural, and
Environmental Engineering

ANNAMDAS, KIRAN KUMAR (Ph.D., Mechanical & Aerospace Engineering)

Evidence Based Uncertainty Models And Particle Swarm Optimization For Multiobjective Optimization Of Engineering Systems (June 2009)

Abstract of a dissertation at the University of Miami.

Dissertation supervised by Professor Singiresu S. Rao.
No. of pages in text. (413)

The present work develops several methodologies for solving engineering analysis and design problems involving uncertainties and evidences from multiple sources. The influence of uncertainties on the safety/failure of the system and on the warranty costs (to the manufacturer) are also investigated. Both single and multiple objective optimization problems are considered. A methodology is developed to combine the evidences available from single or multiple sources in the presence (or absence) of credibility information of the sources using modified Dempster Shafer Theory (DST) and Fuzzy Theory in the design of uncertain engineering systems. To optimally design a system, multiple objectives, such as to maximize the belief for the overall safety of the system, minimize the deflection, maximize the natural frequency and minimize the weight of an engineering structure under both deterministic and uncertain parameters, and subjected to multiple constraints are considered. We also study the various combination rules like Dempster's rule, Yager's rule, Inagaki's extreme rule, Zhang's center combination rule and Murphy's average combination rule for combining evidences from multiple sources. These rules are compared and a selection procedure was developed to assist the analyst in selecting the most suitable combination rule to combine various evidences obtained from multiple sources based on the nature of evidence sets. A weighted Dempster Shafer

theory for interval-valued data (WDSTI) and weighted fuzzy theory for intervals (WFTI) were proposed for combining evidence when different credibilities are associated with the various sources of evidence. For solving optimization problems which cannot be solved using traditional gradient-based methods (such as those involving nonconvex functions and discontinuities), a modified Particle Swarm Optimization (PSO) algorithm is developed to include dynamic maximum velocity function and bounce method to solve both deterministic multi-objective problems and uncertain multi-objective problems (vertex method is used in addition to the modified PSO algorithm for uncertain parameters). A modified game theory approach (MGT) is coupled with the modified PSO algorithm to solve multi-objective optimization problems. In case of problems with multiple evidences, belief is calculated for a safe design (satisfying all constraints) using the vertex method and the modified PSO algorithm is used to solve the multi-objective optimization problems. The multiobjective problem related to the design of a composite laminate simply supported beam with center load is also considered to minimize the weight and maximize buckling load using modified game theory. A comparison of different warranty policies for both repairable and non repairable products and an automobile warranty optimization problem is considered to minimize the total warranty cost of the automobile with a constraint on the total failure probability of the system. To illustrate the methodologies presented in this work, several numerical design examples are solved. We finally present the conclusions along with a brief discussion of the future scope of the research.

To my loving parents

Annamdas Janaki and Annamdas Lakshminarayana

ACKNOWLEDGEMENTS

I would like to extend my sincere gratitude and appreciation to my dissertation supervisor and chairman of the committee, Dr. S.S. Rao, for his guidance, support and suggestions throughout this work. Also, my thanks goes to Dr. James Giancaspro of Civil, Architectural and Environmental Engineering, Dr. Michael R. Swain and Dr. Jizhou Song of Mechanical and Aerospace Engineering Department, University of Miami, for accepting the appointment to the dissertation committee, as well as for their helpful suggestions and advice. I must extend sincere gratitude to the Department of Mechanical and Aerospace Engineering, University of Miami for providing me with the financial assistance for my graduate studies as well as for my research-related work. I would like to thank General Motors for their partial financial support during this study.

I would like to thank all my friends and colleagues for their wholehearted help in all moments and the great times we spent together.

I would like to thank my loving wife, Mrs. Swarnalatha Annamdas, for all her love, support and encouragement.

Finally, my deepest sense of gratitude to my parents for their blessing and good will. I am indebted to them for raising me in a healthy and supportive environment with constant encouragement, I would like to thank God with complete faith for making me who I am today.

Kiran Kumar Annamdas

University of Miami

June 2009

TABLE OF CONTENTS

LIST OF FIGURES

LIST OF TABLES

NOMENCLATURE

$\tau_{allowable}$	Allowable shear stress limit
α	Alpha value for a fuzzy number
m_1	Basic probability assignment (bpa) or mass from source 1
m_2	Basic probability assignment (bpa) or mass from source 2
$P_c(\vec{X})$	Beam buckling load
$\delta(\vec{X})$	Beam deflection at the end (Beam is assumed as cantilever beam)
Bel	Belief function
D_{ij}	Bending stiffness
$\sigma(\vec{X})$	Bending stress of the welded beam
$I_n(\cdot)$	Bessel function of the first kind of n^{th} order
c_b	Buyer's cost
m_{12}	Combined basic probability mass of m_1 and m_2
c_s	Compatibility relation

$[S]$	Compliance matrix
$H(G_j)$	Continuous assignment function
C_r	Cost of supplying the repaired product
B_{ij}	Coupling stiffness
$M_d(t)$	Delayed renewal function
$g(r)$	Density function
t	Depth of the cantilever
x_i	Design variable/ multiplicative factor based on the problem
D_i	Diameter
υ_{ij}	Different Poisson's ratios
δ	Discount rate
$F(\bullet)$	Distribution function
erf	Error function
$E[c_s(W)]$	Expected total cost to the manufacturer
E_1, E_2, E_3	Extensional moduli of elasticity along the 1, 2, and 3 directions
A_{ij}	Extensional stiffness
$FP(x_j)$	Failure probability of j^{th} sub-assembly

$r(t)$	Failure rate associated with the failure distribution $F(t)$
Θ	Frame of discernment
ω_n	Fundamental natural frequency of vibration of the truss
$q\{\Theta\}$	Ground probability assignment to Θ
$q\{\phi\}$	Ground probability assignment to ϕ
$q\{A\}$	Ground probability assignment to event A
h	Height of weld
m^U	Inagaki's unified basic probability assignment (bpa) or mass
$P_n(x)$	Incomplete gamma function
iw_{i+1}	Inertia weight for the $(i+1)^{th}$ iteration
σ_6, σ_{12}	inplane shear stress
$\lambda\left(\frac{t}{r}\right)$	Intensity function
τ'_{int}	Interval for primary torsional stress
τ''_{int}	Interval for secondary torsional stress
τ_{int}	Interval for shear stress
$S \times T$	Joint frame

L	Length of the cantilever beam
l	Length of weld
P	Load
σ_1	Longitudinal stress
c_m	Manufacturer's cost
$m\{A\}$	Mass/bpa assigned to event A
$m(\Theta)$	Mass/bpa associated to frame of discernment
$m(\phi)$	Mass/bpa associated to ϕ
MY, MZ	Maximum bending moments in the Y and Z directions
σ_{max}	Maximum bending stress
δ_{max}	Maximum deflection of the beam
τ_{max}	Maximum induced shear stress in the weld
iw_{max}	Maximum inertia weight
i_{max}	Maximum number of iterations
$TFPS_{max}$	Maximum permissible failure probability of the system
$\vec{V}_{max}$	Maximum velocity vector

$r(A,B)$	Measure of intersection of the sets A and B
$iw_{\min}$	Minimum inertia weight
$\vec{V}_{\min}$	Minimum velocity vector
M	Moment of P about center of gravity of the weld group
$\mathbf{X}_{\alpha}$	Monotonically decreasing function of α
κ	Normalization factor
ϕ	Null/empty set
$N_r(W)$	Number of repairs required in [*0, W*)
$N(W)$	Number of replacements in the interval [0,*W*]
$f_i(\vec{X}_i^*)$	Objective function
$M(\bullet)$	Ordinary renewal function
σ_b	Permissible bending stress for the material
Pl	Plausibility function
J	Polar moment of inertia of the weld group
$\vec{X}_k$	Position vector of k^{th} particle
$\gamma(G_j)$	Power of the maximum violated function

2^{Θ}	Power set
τ'	Primary torsional stress
R	Radius of gyration
Rand	Radam number generation function in matlab
τ''	Secondary torsional stress
G_{12}, G_{23}, G_{13}	Shear moduli
G	Shear modulus of the beam
τ	Shear stress
[Q]	Stiffness matrix used in laminate composite analysis
$\{\varepsilon\}$ and $\{\sigma\}$	Strain and stress vectors
$\sigma_{ip}(\vec{X})$	Stress in element i in load condition p
c_s	Supplier's cost
T_s	Thickness of the shell
T_h	Thickness of the spherical head
σ_2	Transverse stress
$X_c(t)$	Total age for the product at time t
$Y_c(t)$	Total usage for the product at time t

R	Usage per unit time or usage rate
$\vec{V}_k$	Velocity vector of k^{th} particle
c_i	Weighting/credibility factor for the source of evidence i
F_{wi}	Worst value of the i^{th} objective function
δ_{xp} , δ_{yp} and δ_{zp}	x, y and z components of displacement at node 1 under load condition p
m^Y	Yager's basic probability assignment (bpa) or mass
E	Young's modulus of the beam

CHAPTER 1

INTRODUCTION

Uncertainty can be considered as the lack of adequate information to make a decision. Uncertainty estimation of engineering systems is sometimes referred to as the simulation of nondeterministic systems. The mathematical model of the system, which includes the influence of the environment on the system, is considered non-deterministic in the sense that: a) the model can produce non-unique system responses because of the existence of uncertainty in the input data of the model, or b) there are multiple alternative mathematical models of the system. The modeling of any mechanical engineering system with stringent performance requirements, in presence of uncertainty, becomes complex and, thus, makes the model impossible to represent the full scope of the uncertainty when the traditional probabilistic approach is used. Thus, it is important to quantify the uncertainties more realistically in developing the mathematical models used for the design and optimization of non-deterministic engineering systems.

The present study uses Dempster-Shafer theory (DST) as the framework for representing uncertainty and investigates the issue of combination of evidence in the scope of this theory. The reasons for selecting DST can be characterized as:

a) Relatively high degree of theoretical development in DST as compared to the other non-traditional theories for characterizing uncertainty.

b) There exists relationship between DST and traditional probability theory and set theory.

c) Applications of DST in engineering are on a rise in the last decade.

d) Versatility of the DST to represent and combine different types of evidence obtained from multiple sources.

In DST, evidence can be associated with multiple possible events, e.g., sets of events. As a result, evidence in DST can be meaningful at a higher level of abstraction without having to resort to assumptions about the events within the evidential set. Where the evidence is sufficient enough to permit the assignment of probabilities to single events, the Dempster-Shafer model collapses to the traditional probabilistic formulation. One of the most important features of Dempster-Shafer theory is that the model is designed to cope with varying levels of precision regarding the information and no further assumptions are needed to represent the information. It also allows for the direct representation of uncertainty of system responses where an imprecise input can be characterized by a set or an interval and the resulting output is a set or an interval.

1.1 RESEARCH OBJECTIVES

The research aims to theoretically combine and analyze the evidences available from single or multiple sources in the presence (or absence) of credibility of the information sources using modify Dempster Shafer Theory (DST) and fuzzy theory in the design of uncertain engineering systems, to optimally design the systems with multiple objectives, such as to maximize the belief for the overall safety of the system, minimize the deflection, maximize natural frequency and minimize the weight of the systems, in the presence of both deterministic and uncertain parameters, and multiple constraints.

The original Particle Swarm Optimization (PSO) algorithm is modified to include dynamic maximum velocity function and bounce method for solving deterministic multi-objective problems and the vertex method is coupled with the modified PSO algorithm for handling the uncertain parameters. A general automobile warranty problem, close to reality, is formulated and the total warranty cost is minimized with a constraint on the total failure probability of the system using a modified particle swarm optimization (PSO) when both continuous and discrete design variables are present. The following aspects are explored in detail in this work:

- Various methods of combining evidences for any uncertain engineering system.
- Comparison and selection procedure to apply a suitable combination rule for combining evidences based on the nature of evidence.
- Develop a DST based approach to combine various evidences available for the uncertain parameters from multiple sources and/or with varying credibilities of the sources and to use the vertex method to calculate the belief and plausibility.
- Develop a fuzzy-based approach to combine evidences available from multiple sources and/or with varying source credibilities and develop a procedure to calculate the margins of safety and failure of the system.
- Develop a general optimization model, called modified particle swarm optimization coupled with modified game theory to solve single/multiple objectives with design variables as continuous, discrete or both.
- Develop a novel procedure to optimally design uncertain engineering systems using modified PSO with modified game theory when uncertainty is present based

on single source of evidence in terms of percentage tolerance about the nominal value.

- Describe a procedure to find the total warranty costs corresponding to different types of warranty policies for repairable and non-repairable products from manufacturer's point of view and compare them to find the best warranty policy i.e., the minimum total warranty cost policy among both repairable and non-repairable warranty policies.
- Formulate an automobile warranty optimization problem, close to reality, to minimize the total warranty cost in which the various sub-assemblies have different warranty policies with different vendors.
- Formulate a composite simply supported beam problem with uncertain parameters, to minimize the weight of the composite and maximize the buckling load with uncertainty present in geometrical, material properties and load.
- Illustrate all the above methodologies with numeric design examples.

1.2 OVERVIEW OF THE THESIS

Following this introduction chapter, Chapter 2 presents a literature review of the Dempster Shafer theory, fuzzy theory, multi-objective optimization, game theory, particle swarm optimization, and warranty policies.

Chapter 3 presents the basic concepts of Dempster Shafer theory, fuzzy theory, α –cut representation, fuzzy arithmetic, particle swarm optimization, game theory, warranty policies, probability and reliability in the context failure distribution, classification of warranty policies, one - and two-dimensional warranty policies.

Chapter 4 studies various combination rules like Dempster's rule, Yager's rule, Inagaki's extreme rule, Zhang's center combination rule and Murphy's average combination rule for combining evidences from multiple sources and several examples are presented for understanding the procedures, and selecting the most appropriate rule based on the nature of evidence sets. These rules are compared and a selection procedure was developed to assist the analyst in selecting the most suitable combination rule to combine various evidences obtained from multiple sources based on the nature of evidence sets. The safety analysis of a welded beam based on maximum induced shear stress is studied using on five different evidence sets.

In chapter 5, the vertex method based on the α-cut concept and interval analysis is considered. A computation procedure to find the belief and plausibility functions is developed. The safety analysis of a welded beam with two and four uncertain parameters, when uncertain parameters are assumed to be available in the form of interval-valued data from multiple sources is also considered. The DST methodology to combine evidence when sources of evidence have different credibilities is also considered in this chapter. The welded beam example is considered with varying credibilities for the sources of evidence when combining evidence.

Chapter 6 explores the fuzzy approach for combining evidences from multiple sources. It describes the procedure to compute bounds on the margin of failure and margin of safety. In this regard, an illustrative example of a welded beam is considered for combining evidences with two and four uncertain parameters by assuming both triangular and trapezoidal membership functions for the maximum allowable shear stress in the weld. A new weighted fuzzy theory for intervals was also proposed in this chapter. The welded

beam example is considered with varying credibilities for the sources of evidence when combining evidence.

Chapter 7 starts with an introduction to the particle swarm optimization followed by a modified particle swarm optimization, approach for constrained optimization with both discrete and continuous design variables. Applications for single objection optimization problems are considered. The procedure to use modified PSO with modified game theory for multi-objective optimization is considered with different engineering applications like design of 2-bar and 25-bar trusses, design of I-beam and gear box.

In chapter 8, a novel method of using modified PSO in conjunction with the vertex method was proposed. It begins with a description of the vertex method and followed by the computational aspects of the vertex method. Engineering applications like design of welded beam and design of 25-bar truss with different number of uncertain parameters are considered. Formulate and design a composite simply-supported beam for minimum weight and maximum buckling load capacity is also considered.

Chapter 9 begins with a description of different warranty policies for repairable and non-repairable products. The warranty policies start with a free replacement warranty (FRW) policy, followed by pro-rated warranty (PRW) policy, combined FRW/PRW policy and two-dimensional FRW warranty policy. This chapter compares the various warranty policies for both repairable and non-repairable products for different failure distributions. The formulation of an automobile warranty optimization problem is considered followed by a sensitivity analysis of the optimal design variables with respect to both total warranty cost and total failure probability of the system.

Chapter 10 is devoted to the conclusion of the current research and the last chapter 11 is devoted to the summarization of future scope of research. Appendix-A describes the various steps involved in the application of the various combination rules and are applied to combine evidences in the context of the robbery and automobile examples considered in chapter 4. Appendix-B describes the procedure to find stress using laminate theory, deflection and buckling load of composite beams. Appendix-C describes main Matlab programs used in the present research work.

CHAPTER 2

LITERATURE REVIEW

2.1 OVERVIEW

It was observed that most of the present literature is concerned with deterministic optimization of engineering structures/systems for specified structural/system parameters including loading conditions/external effects. However, in most practical situations, the structural parameters and loads, for example, are uncertain. For example, the geometry parameters, obtained through construction, manufacturing, or machining processes are usually specified in terms of their nominal values and with tolerances. Many types of loads, such as wind, earthquake and snow loads, are not known in precise terms; only information about past loads is known. Material properties, such as yield strength and Young's modulus, are determined through experiments; they are bound to exhibit variations. Thus all the parameters involved in structural design problems are uncertain. Thus, uncertainty plays a vital role in the investigation of various engineering problems. In section 2.2, a brief literature review of Dempster Shafer frame work has been considered. Literature review of fuzzy set theory in section 2.3, multi-objective optimization in section 2.4, game theory in section 2.5, particle swarm optimization in section 2.6 and warranty policies in section 2.7, respectively, are also considered. We study many new methods proposed in these areas, and are applied successfully to various applications. The chapter concludes with summary at the end.

2.2 DEMPSTER SHAFER THEORY

Many generalized models of uncertainty have been developed to treat different situations; including possibility theory [6, 220] and fuzzy sets, Dempster-Shafer theory of evidence [54, 187], imprecise probabilities [212], convex models [18], random sets [101] and others. These generalized models of uncertainty have a variety of mathematical descriptions [35]. However, they all can typically be described as either random or fuzzy. If the uncertain parameters are treated as random variables, they are described by suitable probability distributions and the response of the structure, such as displacement, strains and stresses, can be computed using probability principles. On the other hand, if the uncertain parameters are treated as fuzzy quantities, they are described using suitable membership functions. For example, the statement, "This beam carries a load of 50 lb with a probability of 0.8" is imprecise because of the randomness in the material properties of the beam, whereas the statement "This beam carries a small load" is imprecise because of the fuzzy meaning of "small load." Examples of imprecisely defined statements are "fiber content in the composite material is very high" and "the probability of pressure acting on the cylinder exceeding a value of 100 psi is greater than 0.9".

Smets [192] showed how the transferable belief model can be used to assess and combine expert opinions. The transferable belief model has the advantage that it can handle weighted opinions and their aggregation without the introduction of any specific methods.

Chang et al. [42] propose a formal methodology for integrating subjective inferential reasoning and geographic information systems (GIS) into a decision support

system for use in these problem domains. The reasoning for inferential spatial models, and the structure and function of a spatial modeling environment based on the Dempster-Shafer theory of evidence are presented.

Vasseur et al. [207] proposed an application of the perceptual organization based on the Dempster-Shafer theory. This method is divided into two parts which prove the segmentation mistakes by restoring the coherence of the segments and detects objects in the scene by forming groups of primitives. Then, the Dempster-Shafer theory, usually used in data fusion is applied, in order to obtain an optimal result between the perceptual organization problem and this tool.

Inagaki [83] explores the application of the Dempster-Shafer theory in system reliability and safety. Inappropriate application of the Dempster- Shafer theory to safety-control policies can degrade plant safety. This is proven in two phases: 1) A new unified combination rule for fusing information on plant states given by independent knowledge sources such as sensors or human operators is developed. 2) Combination rules can not be chosen in an arbitrary manner; i.e., the best choice of combination rules depends on whether the safety-control policy is for fault-warning or safety-preservation.

Kohlas and Monney [112] used evidence theory to represent uncertainty in expert systems, especially in the domain of diagnostics. It can be applied to decision analysis and it gives a new perspective for statistical analysis. Among its further applications are image processing, project planning and scheduling and risk analysis. The computational problems of evidence theory are well described and even though the problem is complex, efficient methods are available.

Chen and Rao [43] introduced a new methodology, based on a modified Dempster-Shafer (DS) theory, for solving multicriteria design optimization problems. The design of a mechanism in the presence of seven design criteria and eighteen design variables is considered to illustrate the computational details of the approach. This work represents the first attempt made in the literature at applying DS theory for numerical engineering optimization.

Shenoy [189] describes how Dempster-Shafer's theory of belief functions will fit in the framework of valuation-based systems (VBS). Since VBS serves as a framework for managing uncertainty in expert systems, this facilitates the use of Dempster's belief functions in expert systems.

Parikh et al. [163] used Dempster-Shafer theory in 'fusion' classifiers. They demonstrated the effectiveness of the approach in a case study involving the detection of static thermostatic valve faults in a diesel engine cooling system.

Bloch [31] describes some key features of Dempster-Shafer evidence theory for data fusion in medical imaging. Examples are provided to show its ability to take into account a large variety of situations, which actually often occur and are not always well managed by classical approaches nor by previous applications of Dempster-Shafer theory in medical imaging.

Data fusion techniques for ventricular suction detection in a heart assist device based on Bayesian, fuzzy logic and Dempster-Shafer theory were evaluated in Boston et al. [34]. Fusion techniques based on fuzzy logic and Dempster-Shafer theory provide a measure of uncertainty in the fused result. This uncertainty measure can be used in the control process, and it can also be used to identify faults in pump operation.

The key feature of the Dempster-Shafer theory as described by Laskey and Cohen [121] is the precision in inputs is required only to a degree justified by available evidence. The output belief function contains an explicit measure of the firmness of output probabilities. They have given an overview of belief function theory and present the basic methodology for application to simulation, and give a simple example of a simulation involving belief functions.

Basti [15] proposed methods that are applicable to the multisensory classification of airborne targets using Dempster-Shafer theory. Several simulations relating to an airborne target classification problem were also presented.

Jiang et al. [94] presented a multisensor multiple-attribute data association method based on Dempster and Shafer evidence theory. This approach was illustrated by simulations involving multi-sensor multiple targets in a dense clutter environment.

The theory of Dempster-Shafer is discussed with emphasis placed on its use in the field of multi-sensor data fusion and data association systems by Tchamova [202]. In this reference, how the structure of multi-sensor integration systems influences the accuracy of objects identification process was discussed and also determined the dependence of the degree of uncertainty on the speed of receiving best evidential intervals as well as the impact of increasing number of sensors on the calculation time.

Luo and Li [131] developed a new multisource information fusion scheme using the plausibility measure. The method avoids using Dempster's rule of combination, so as to overcome the intractability of Dempster-Shafer computations, allowing the theory to be feasible in many more applications. A simple robotic vision system with object recognition data from multi-sensor is presented to highlight benefits of the new method.

Murphy [150] discusses the Dempster-Shafer theory in terms of its utility for sensor fusion for autonomous mobile robots; it exploits two components of DS theory: the weight of conflict metric and the enlargement of the frame of discernment.

Boston [33] describes a signal detection algorithm based on Dempster-Shafer theory: The detector combines evidence provided by multiple waveform features and explicitly considers uncertainty in the detection decision. The detector classifies waveforms as including a signal, not including a signal, or being uncertain, in which case no conclusion regarding presence or absence of a signal is drawn.

As can be noted, this section listed few applications of Dempster Shafer theory in various fields of science and technology. Other applications [9, 36, 37, 183] can be found in literature.

2.3 FUZZY SET THEORY

When the parameters of a system contain information and features that are vague, qualitative and linguistic, a fuzzy approach can be used to predict the response. Various attempts are made to apply fuzzy set theory to solve structural optimization problems since there exists a vast amount of fuzzy information in both the objective and constraint functions for the design optimization of structures. Many papers have discussed the application of fuzzy set theory to structural design and in particular in structural optimization. The theory of fuzzy sets was developed for a domain in which descriptions of activities and observations are not well defined.

The theory was introduced by Zadeh in 1965 [222], and later applied to different practical systems by several researchers. Since then, fuzzy set theory has been widely developed

and various modifications and generalizations have also appeared in literature. Although the theory was recognized as a mathematical concept related to the statistics discipline, its applications were limited to only academic problems for many years. Only in recent years, its utilization was expanded to engineering arena and had attracted more attention in the area of mechanical design. In order to develop a suitable method for processing convex fuzzy input parameters, the concept of $\alpha-$level discretization is followed. In problem solving applications, the $\alpha-$level discretization is advantageous for the numerical processing of fuzzy information. Wood *et al*., [215] adopted this method for solving special problems in structural design. All fuzzy input parameters are discretized using the same sufficiently high number of $\alpha-$levels (α_k , $k=1,2,\cdots,r$) and thus called $\alpha-$level optimization.

Bonarini and Bontempi [32] described the solution of differential equations containing fuzzy parameters. Rao and Sawyer [168] developed the fuzzy finite element approach to analyze imprecisely defined systems. The authors [201] investigate the interrelationships of several concepts of generalized convex fuzzy sets. Dhingra and Rao [59] used non-linear programming technique to model the vague and imprecise information in the problem, thus resulting fuzzy multi-objective problem using this technique. Based on the fuzzy set theory, a general method for fuzzy structural analysis is developed by Moller *et al*., [140] which is formulated in terms of the $\alpha-$level optimization with the application of a modified evolution strategy. The paper describes the coupling between $\alpha-$level optimization and the initial deterministic solution, so that, every known analysis algorithm for the structural analysis may be applied in fuzzy structural analysis in the sense of deterministic solution.

Biondini *et al*., [21] proposed a fuzzy reliability analysis of a concrete structure, where geometrical and mechanical properties of the structure are considered as uncertain. Uncertainties are modeled using a fuzzy criterion in which the model is defined through interval of values, bounded between suitable extremes of minimum and maximum. The reliability problem is formulated at the load level, with respect to several serviceability and ultimate limit states. For the critical interval associated to each limit state, the membership function of the safety factor is deduced by solving a corresponding anti-optimization problem. The strategic planning of this solution process is governed by a genetic algorithm.

Beer [17] has developed a method for uncertain structural design on the basis of nonlinear fuzzy structural analysis. The method is formulated in terms of α-level optimization combined with a modified evolution strategy. The fuzzy structural responses are compared with permissible values and assessed using an analog to the Shannon entropy and de-fuzzification algorithm [41, 56,127].

2.4 MULTIOBJECTIVE OPTIMIZATION

During the past decade the, subject of structural multi-objective optimization has been explored extensively. Some investigators have treated structures subject to static constraints, e.g., maximum stress limit or minimum deflection, while others have considered structures subject to dynamic constraints, e.g. natural frequency. The literature on multi-objective or multi-criteria decision making has grown tremendously in the last decade. Kuhn and Tucker [117] had first mentioned, in mathematical programming, by

calling the multi-objective decision making problem called the "vector maximum" problem.

The weighted approach of objectives is based on the assumption that the objective functions are mutually independent [104]. This method is incapable of generating the entire set of pareto-optimal solutions for non-convex problems. This technique has the drawback of modeling the original problem in an inadequate manner, generating solutions that will require a further sensitivity analysis to become reasonably useful to the designer. The two-level game theory approach presented by Rao *et al.,* [174] overcomes some of the shortcomings of this weighted method but this method is computationally very expensive. No attempt has been made in previous works for modeling vague and imprecise design problem specifications, and uncertain material properties. Rao and Freiheit [166], Dhingra *et al*., [60], Dhingra and Rao [58] studied the game theory approach to multi- objective optimization problems in the fuzzy environment.

Recent advances in area of structures have resulted in the development of techniques for handling optimization problems with large numbers of design variables [7,168,171]. Rao [173] presented a method for solving fuzzy multi-objective optimization problems using ordinary non-linear programming techniques. For simplicity, linear relationships have been assumed to denote membership functions over the transition zones of response quantities. The procedure outlined is expected to work in situations where doubt arises about the exactness of permissible values, correctness of statements and judgments, and so on. Rao *et al.,* [167] proposed two procedures namely the λ-formulation and α-cut approach for solving multi-objective optimization problems where the λ-formulation provides an overall compromise solution while the α-cut approach yields the design

information in a parametric form. Yu *et al.,* [219] have presented three approaches by using different types of generalized fuzzy decision-making: intersection decision, convex decision and product decision in order to reflect various decision ideas and provide a favorable condition in the selection of the structural design scheme. They have emphasized that the intersection decision is the most conservative in generalized fuzzy decision-making in their work.

2.5 GAME THEORY

Game theory is a mathematical tool for the analysis of situations involving conflicting objectives. One way to describe a game is by listing the players (or individuals) participating in the game, and for each player, listing the alternative choices (called actions or strategies) available to that player. Game theory [189, 190] represents multi-objective optimization with multiple decision-makers, each controlling certain design variables [180, 209]. Players make moves (determine strategies) to maximize their payoffs. These moves determine the outcome of the game, based on payoff functions associated with each player [196]. The payoffs to each player are typically determined by some naturally occurring cause and effect situation. Given certain pre-existing conditions, the equilibrium point or final solution to a game is considered the value of the game and is that point at which no player desires to alter his/her position.

One relatively broad classification of games is that of zero-sum and non-zero-sum. A zero-sum game is one in which a payoff to one player directly results in a detriment of equal value to another player. Zero-sum games represent highly competitive situations

and are rare with real world engineering problems. Therefore, this research will consider only non-zero-sum games.

Three common game distinctions are those of matrix, continuous, and differential games. Game Theory has emerged recently as a powerful challenger to the conventional method of examining economics. The first formal fundamental concept of game theory was developed by John Von Neumann and Oskar Morgenstern [213] in 1944. The work stemmed from an effort to model and solve economic problem, in which the objective is typically to maximize utility or profit. The authors used discrete matrix games, now often associated with classical game theory, to prove the existence of optimal strategies in games. In the case of a two player game, it forms a matrix, where the actions of the first player form the rows and the actions of the second player the columns. The entries in the matrix are two numbers representing the utility or payoff to the first and second player respectively. Neumann and Morgenstern [210] introduced the strategic normal game, strategic extensive game, the concept of pure/mixed strategies, coalition games as well as the axiomatization of expected utility theory, which was so useful in the theory of economics under uncertainty. They employed the maximum solution concept derived earlier by Neumann in 1944 [210] to solve simple strategic, zero-sum normal games.

Continuous static games also represent a single move sequence, but the objective functions or payoff functions are represented by continuous functions. With differential games, the pay-off function, dictating a player's best move, changes with time. Lengthy sequences of decisions are knit together. In terms of control theory, state variables represent the status or condition of the game, and players modify control variables, which are functions of the state variables. The strategy used with differential games is

comparable to the scheme of a guidance mechanism [23, 84]. If all but one player is suppressed, in a differential game, the result is a standard optimization problem.

Engineering design problems are best depicted as continuous static games, as described in [209]. In terms of engineering optimization, decision-makers allocate resources (assign values to design variables) to optimize an objective function. The equilibrium point is the optimum.

Game theory can be mainly divided into two broad areas: non-cooperative games and co-operative games.

2.5.1 Non-cooperative Games

A non-cooperative game involves players that do not cooperate with each other. Each player sees only the result of the other players' moves. No information concerning payoff or objective functions is transferred. Each player seeks to maximize his/her own payoff and reacts to the actions of the previous player(s). This is not multi-objective optimization in its truest sense. There are multiple decision-makers. Consequently, certain design variables are associated only with certain objective functions. The results of the game can vary depending on which players attend to which particular objective functions.

2.5.2 Cooperative Games

In cooperative game theory, each player agrees to exchange information concerning payoff or objective functions. Each player moves ultimately to maximize his/her payoff, but they are willing to exchange information and alter their positions in order to benefit other players, as long as there is no personal detriment. Consequently, all players have access to all objective functions. One variable or set of variables is no longer associated with only one objective function. This group rationality, as opposed to individual rationality, results in Pareto optimal solution. An in-depth discussion of Pareto solutions is available in the literature [196,209,167,212]. A point is considered Pareto optimal if no player can move from that point without causing detriment to some other player. This concept results in an infinite set of solutions. A Pareto optimal set is often referred to as a compromise solution set [184].

Graphically, cooperative game theory allows players to move along objective contours rather than just along orthogonal directions, as in case of non-cooperative play.

Kickert distinguishes the subtle differences between team decision theory, group decision theory, and cooperative game theory [105]. Team decision theory, as detailed in [139], involves a single team-objective function, though individuals may have access to different pieces information and may have independent, individual interests. A team struggles to optimize the allocation of tasks or resources among the individuals. Group theory is described in [210] as it applies to social behavior. Group decision theory is concerned with modeling a single consequence of a group of individuals with many independent preferences. Game theory concerns multiple players pursuing personal

gains, with different interests or objective functions. Game theory essentially introduces self-interest to group theory.

Most attention was received by the solutions of cooperative game theory when compared to all other game solutions. This is a result of the fact that cooperative game theory essentially mimics multi-objective optimization with multiple decision-makers. In a two-objective problem, both players seek to optimize both objective functions regardless of association with their own utility functions. Because all decision-makers have access to all objective functions, the result is independent of which decision-makers (variables) are associated with which objective functions. The solution to both multi-objective optimization problems and to cooperative games is a Pareto optimal set. Many algorithms for determining a Pareto optimal set are outlined in the literature [23, 84, 209, 154]. Some of the most popular algorithms are weighted sum (also known as scalarization or utility function), ε-constraint, minimax, lexicographic, global, and ratios.

For determining a single optimal Pareto point, there are essentially two methods. Salukvaze presents a method that minimizes the sum of the differences between the values of each objective function at the optimal Pareto point and at the functions' actual optimum points [184]. If one considers a space of dimension equal to the number of objective functions, the point defined by all of the optima of the individual objectives, is called a "utopia point". Vincent refers to the utopia point as the "single unique point in the cost space where every design criteria takes on its minimum [optimum] value." [208]. Salukvaze uses the Pareto point that is closest (measured with the Euclidean norm) to the utopia point. However, it is suggested that this method may not thoroughly solve the problem of determining a single optimum Pareto point, since the mathematical

definition of "close" can vary [154]. Rao presented a method for selecting a single Pareto optimal point using what he refers to as a "supercriterion". The product of the differences between each objective, evaluated at the Pareto optimal point and at the worst possible position for a specific objective/player, is maximized. In the vein of game theory, players begin with their worst values and negotiate to improve their positions [84, 209].

Concepts and solution methods that apply to game theory have been applied to actual engineering problems [84, 209, 169, 208, 184]. The question that arises is what type of engineering optimization problems or scenarios are most accurately modeled by a given game. Though team members/engineers work towards a common goal, there will rarely exist the type of defensive play that is inherent in min-max problems. Though the min-max (security) game is common in game theory literature, its application to engineering problems is minimal.

Though direct, competitive opposition is rare, engineers with separate and partially conflicting objectives do not typically cooperate completely; communication is not constant. Often, an engineer is the decision-maker and his/her objective function is unique. There may be no explicit by defined objective function. Therefore, it becomes difficult to completely share the objective function information. Consequently, each engineer or designer is actually reacting to the position of another engineer(s). In such a situation the Nash equilibrium point, determined through non-cooperative game theory, indicates the best in terms of what the set of players (engineers) can do (the optimum design). Rarely, except with small, and simple systems, are all engineers familiar with all of the objective functions and with what is required to alter each of the design variables.

To improve on the Nash equilibrium point with cooperative game theory, all players/engineers are required to communicate all information concerning strategy and objective functions. If explicit objective functions or even "black box" functions, such as finite element analysis software, are available, then the Nash equilibrium point can be improved upon with a Pareto optimal set. An optimal Pareto point can then be selected using Rao's method, as discussed earlier. Usually several Pareto-optima exist for a vector optimization problem and additional information is needed to find a specific Pareto-optimal point. This clearly makes it possible to bring in additional considerations not included in the optimization model (besides the original objectives), thus, making the multi-objective approach a flexible technique for most design problems. Several numerical methods have been suggested for solving a vector optimization problem. In general, each method generates a different Pareto-optimal solution.

2.6 PARTICLE SWARM OPTIMIZATION

Over the last decade, the particle swarm optimization (PSO) has gained rapid importance as an optimization tool to facilitate the design of many engineering systems. The original version of PSO algorithm was introduced by Kennedy and Eberhart in 1995 [103] for the solution of single objective optimization problems. The PSO algorithm is found to be suitable for non convex and continuous function optimization with continuous design variables. Many practical engineering applications involve both continuous and discrete design variables. In most of the cases, the discrete design variables are transformed into continuous ones by several approaches [70, 5, 40, 119].

There are methods that treat discrete design variables as constraints and use a penalty function approach to augment the objective function to include discrete variable conditions [109, 108]. Thus the problem is reduced to an unconstrained optimization problem which can be solved using a continuous variable based solution method. Unlike these methods, this work uses an approach termed the closest discrete approach [206] (CDA) to handle discrete design variables. In the real world, a large number of engineering systems involve a number of competing quantitative measures that define the quality of a design solution. For instance, in the design of an automobile, a firm may wish to minimize its production cost, maximize its fuel efficiency, maximize its crash resistance and/or maximize its reliability. These objectives cannot be met by a single solution; so, by adjusting the various design parameters, the firm may like to find all available possible combinations of these objectives, given a set of constraints (for instance legal requirements and dimensional limits of the product). A true Pareto front, defined as the optimal trade-off possibilities between objectives, is represented by a curve (for two objectives) or surface (more than two objectives). A feasible solution lying on this true Pareto front cannot improve any objective without worsening at least one of the others while satisfying all the given constraints of the model; no solutions exist beyond the true Pareto front. The goal of any multiobjective algorithm is to find this Pareto front that indicates the non-dominated solutions. These types of problems are effectively solved by various multiobjective evolutionary search algorithms as these algorithms maintain a population of solutions which are capable of exploring several parts of the Pareto front simultaneously for any complex problem. Similar characteristics are also associated with the PSO and several results are reported in the literature comparing PSO

with evolutionary algorithm techniques in the case of single objective problems. It is obvious that the next stage is the application of PSO to multiobjective problems. Some researchers have published studies on multiobjective PSO starting from 2002 [206, 88, 178]. The PSO algorithm can be viewed as a distributed behavioral algorithm which can perform a multi-dimensional search to find the solution of various optimization problems [88, 80, 165, 206].

2.7 WARRANTY POLICIES

The literature on warranty models and policies is very broad since it involves many interdisciplinary areas of application. Warranty models and policies have been analyzed by many economists, engineers, statisticians, management consultants, mathematical modelers, marketing professionals and people from many other disciplines. Each discipline has investigated different aspects of the warranty. For example, the marketing literature has considered warranties as a marketing tool and analyzed their effects on product sales and the impact of warranties on customers' perceptions of risk and the economics literature on product warranties focuses on social welfare and regulatory issues [139]. The approach used for warranty modeling in this research pertains to development of analytical models and strategies that minimize the expected cost of warranty servicing (to the manufacturer) and we shall confine the attention only to those aspects.

For many years, we have seen warranty policies in existence for both products and services. Often, product warranties are perceived as signals of product quality by customers and the strategies made by the manufacturer to service the product greatly

influences this perception [139]. As an important component of post-sale support service, warranty offered by a manufacturer or a dealer establishes liability among the two parties (manufacturer and buyer) in the event when product fails. It is a contractual obligation in connection with the sale of a product [146]. Warranty cost is important to manufacturers for several reasons. First, the warranty cost is included into the price of the product and thus necessary for determining pricing policy. Second, the knowledge of warranty cost helps sellers compare different policies and select the best policy in some sense. Finally, it increases seller's ability to manage future cash flows. From customers' point of view, the knowledge of warranty cost may help customers to decide between products with different warranties, and whether to buy an extended warranty when such an option exists. However, in most cases, customers cannot get access to this information. The warranty cost estimation is a very challenging task since product failures occur randomly, and operating conditions and customers' usage greatly vary. The literature in this area can be grouped as one and two-dimensional warranty cost modeling.

2.7.1 One-dimensional warranty policies

One-dimensional policies are characterized by a single variable such as age or usage of the product since purchase. While 1-D policies have been researched over many years, the majority of research in 1-D models have been focused on estimation of the expected cost per product during the warranty period and the expected total cost during the product life cycle from both customers' and sellers' perspective. The major drawback in 1-D warranty modeling is that analytical models often involve cumbersome expressions in terms of convolutions of integrals, transforms, and limited to very few

probability distribution functions. Products which usually characterize the terms warranty in terms of one variable are high mix and high volume manufactured goods.

Blischke and Scheuer [30] analyzed Free Replacement Warranty (FRW) and Pro-Rated Warranty (PRW) policies from the view point of both customer and manufacturer. Customers have the choice of buying the product with or without a warranty. The author [30] calculated the cost (profit) to the customer (seller) at which the customer (seller) would be indifferent between buying (selling) the product with or without a warranty.

Balachandran *et. al.* [11] developed a Markov model. They assumed that the product consists of three independent components whose failure times are governed by exponential distribution. The seller repairs a component on the first two failures and replaces the component on its third failure during the warranty period. According to this policy, they estimated the expected warranty cost.

Anderson [4] developed a non-specific profit maximization model framework for optimally specifying the product price and warranty period. Glickman and Berger [72] considerably extend the work [4] by considering a displaced log-linear demand function of product price and warranty period, to maximize manufacturer's profit function embedded with demand function to yield optimal product price and warranty period.

Thomas [201] developed a combination warranty policy for non-repairable products. The warranty period was divided into two intervals. Products failing in the interval $[0, W_1]$ are replaced with a new one, and failures in the interval $[W_1, W_2]$ result in prorated rebates. He derived a unit warranty cost formulation for different failure distributions. He also developed a procedure to minimize the expected warranty cost to find the optimum warranty period.

Blischke and Scheuer [29] applied renewal theoretic arguments to obtain the expected number of replacements during the product life cycle. They studied several failure time distributions, including exponential, uniform, gamma, and Weibull, and due to the inherent difficulties in analytical modeling, they developed a simulation program to evaluate the effect of different failure time distributions.

Nguyen and Murthy [156] developed a general model for repairable products sold with FRW. It was assumed that the failure time distribution is arbitrary, and the repair cost depends on the number of repairs carried out. They estimated the expected total warranty cost and its confidence interval for a fixed lot size, and the expected number of units returned for repair and expected warranty cost incurred in any time interval during the product life cycle when sales occur continuously.

Mamer [133,134] examined the expected warranty cost for a product sold with a free replacement warranty (FRW) policy and a pro-rated warranty (PRW) policy. In the first paper, he derived an expression for the expected total warranty cost assuming that the product would be replaced by an identical one until the end of the life cycle. He also found the average costs for three cases: no warranty, PRW and FRW. In the second paper, he assumed that some customers might switch to another seller because of their bad experience with the first purchase, *i. e.,* there is a certain probability that the customer will not replace the product from the same manufacturer if it fails after the warranty period. He assumed that damage occurs according to Poisson process, and calculated the expected discounted profit to the manufacturer and the expected discounted cost to customers for FRW and PRW policies. He also introduced a random

damage process into the model so that a product will fail either because it wears out or because it has been damaged accidentally.

Ritchken and Tapiero [179] investigated the optimal age replacement policies for non-repairable products sold with PRW from the customers' point of view. In the age replacement policy, a product is replaced upon its failure or at a fixed time interval whichever comes first. This type of policy is often used when the product has an increasing failure rate with age. They minimize the expected average cost to calculate the optimal replacement period after the expiration of warranty.

Balcer and Sahin [12] found the mean and variance of the total replacement cost for a PRW and FRW during the product life cycle. They also investigated the case where the failure distribution depends continuously on time.

Nguyen and Murthy [156] considered a special case where the product is replaced with a new one if it fails in the interval [0, W-t] and with a repaired one if it fails in the interval [W-t, W]. Further, they assumed that a failed unit is repaired and added to the collection of repaired products only if it was not subjected to repair earlier and its age at failure is less than or equal to α. They minimize the expected warranty cost to find the optimal replacement interval.

Frees [68] considered approximation techniques to estimate renewal density function for obtaining expected warranty costs. Frees and Nam [69] investigated a combination warranty in which manufacturer replaced all product failures in (0,W) free of cost to the customer, and all failures in the region (W;$W + T$) the customer buys new product paying pro-rated cost. They derived the expected costs for warranty servicing using straight line approximation technique during the product lifetime.

Sahin and Polatoglu [182] study two types of replacement policies following the expiration of warranty for products with Increasing Failure Rate (IFR) distribution. A type-1 policy involves minimal repair for a fixed duration of time followed by a replacement, and in a type-2 policy, there is replacement of the product by the user after the first failure following the minimal repair period. They considered renewing and non-renewing options of the above policy and obtain the long run mean cost to the customer. Sahin [183] investigates the impact of quality conformance on manufacturers and users replacement costs for products under free-replacement and pro-rata warranty. He concluded that consumer's cost is severely influenced by the both quality improvement and the manufacturer's quality inspection.

Chukova and Hayakawa [45] modeled warranty claims and evaluated warranty costs allowing non-zero repair time. They use alternating renewal process in finite horizon and derive warranty costs for finite life cycle of the product and attribute a cost for the duration of repair time.

Thomas [201] predicted total warranty reserves for a product sold under a nonrenewal PRW. He calculated total warranty costs for several failure distributions. He also considered discounting value of the money since warranty claims are realized in the future.

In the warranty cost estimation models, it is often assumed that the product is used continuously. This is true for some industrial products, but most consumer products are used intermittently during their lifetimes. In general, the product failure rate is less when product is idle. Additionally, the product failure depends not only on its age but also on its usage frequency. Murthy [148] proposed two different models to model the failure

times for both repairable and non-repairable products. In the first model, the product failure depended on its age and usage without considering whether it is in use or not in use at the time of failure. In the second model, he assumed a constant failure rate when the product is idle. He used a Markov process to model the failure distribution function.

In the next sub-section we shall study the literature concerning two-dimensional policies.

2.7.2 Two-dimensional warranty policies

The 2-D policies have not received much attention from researchers as 1-D policies, but recent research in this area has began due to its applicability across various products and industries. Murthy et. al. [150] studied two-dimensional, FRW policies for non-repairable products. They proposed three alternative two-dimensional warranty policies that sellers should consider beside fixed *x*-year-*y*-usage warranty coverage. For each two-dimensional warranty policy, they have calculated the expected unit warranty cost and the life cycle cost of the product.

One-dimensional point process approach assumes a relationship between the two-variables in the model, namely age and usage. Moskowitz and Chun [142] assume a linear relationship between age and usage of the product and model FRW warranties using conditional Poisson process. They developed a Poisson regression model for obtaining the expected warranty costs. Chun and Kwei [47] studied two-attribute policy using an approach similar to that of Moskowitz and Chun [141] and developed decision models to obtain the expected total warranty cost and determine the effective warranty period. Moskowitz and Chun [142] developed two types of two-dimensional warranty models based on a Poisson regression model and expected utility theory. First, they

determined the optimal warranty price per product that is sold with a fixed two-dimensional warranty. Later, they generated different two-dimensional warranty plans for a given warranty price so that all customers will have the same expected repair or replacement cost.

Jack and Murthy [90] proposed a new repair-replacement strategy for products sold with non-renewing free replacement warranty policy by splitting the rectangular warranty period into three parts, namely regions 1, 2, and 3. The repair strategy consisted of minimal repair in regions-1 and 3 and replacement in intermediate region-2. They developed a control limit sub-optimal strategy with minimal expected cost for servicing. Iskandar and Murthy [85] consider a repairable item under FRW policy and derived expected cost of servicing the warranty, and they compare two strategies in a rectangular region. Iskandar et al. [87] study a 2-D combination warranty policy which combines the features of FRW and PRW polcies in 2-D. They discuss renewing and non-renewing options and perform cost analysis of expected servicing costs among combinations of policies developed. Baik et al. [10] extend the concept of minimal repair form of 1-D policy to a 2-D policy. They compare the strategy of minimal repair to the strategy of replacement upon failure. Iskandar et al. [86] develop a new strategy to replace the failed product for the first time in a specified region of the rectangular warranty and minimally repair for all other failures during the warranty period.

Eliashberg et. al. [65] developed a two dimensional model for a FRW in order to find the optimal warranty reserve. They assumed that the usage is a monotonically increasing function of time. A “stochastic logistic function” was used for this purpose. They also assumed that the seller repairs the product and the type of repair is imperfect. They

defined a loss function associated with having established a warranty reserve and calculated the warranty reserve that minimizes the loss function.

2.8 SUMMARY

In this chapter, we have reviewed representative research papers and articles in the areas of Dempster Shafer theory, fuzzy set theory, multi-objective game theory, particle swarm optimization, and warranty policies to show the wide range of applications and development of various new methods and their applications to a variety of problems. In the next chapter, we present the basic concepts of these topics in the context of the proposed research work.

CHAPTER 3
REVIEW OF BASIC CONCEPTS

3.1 OVERVIEW

In general, uncertainty can be broadly classified in to three types. The first one is aleatory uncertainty (also referred to as stochastic or inherent or irreducible or objective or type A uncertainty or variability) - It results from the fact that a system can behave in random ways. For example, the failure of an engine can be modeled as an aleatory uncertainty because the failure can occur at a random time. One cannot predict exactly when the engine will fail even if a large quantity of failure data is gathered (available). The second one is epistemic uncertainty (also known as subjective or reducible or type B uncertainty or ignorance) - It is the uncertainty of the outcome of some random event due to lack of knowledge or information in any phase or activity of the modeling process. By gaining information about the system or environmental factors, one can reduce the epistemic uncertainty. For example, a lack of experimental data to characterize new materials and processes leads to epistemic uncertainty. The third one is numerical uncertainty (also known as error) – It is present, for example, when there is numerical error due to round-off errors, truncation errors, errors associated with the solution of ordinary and partial differential equations.

Conventionally, probability theory has been used to characterize both aleatory and epistemic uncertainties. However, the recent developments in the characterization of uncertainty reveal that traditional probability theory provides an inadequate model to capture epistemic uncertainty. It is recognized that probability theory is best suited to deal with aleatory uncertainty. A traditional probabilistic analysis follows *Principle of Insufficient Reason* and axiom of additivity. For example, the failure of a gear can occur as a result of bending fatigue, pitting, micropitting, scuffing and wear. An expert assigns a probability of failure of gear due to bending fatigue as 0.4. The expert knows nothing about other failure modes of the gear. Principle of insufficient reason follows that all simple events with unknown probability distribution in a given sample space are equally likely. The axiom of additivity follows that all probabilities satisfying specific properties must add to 1. Thus, according to probabilistic analysis, one could assign a probability of failure of gear 0.15 to each of the four remaining modes of failure. This implies that probabilities of failure of these four modes are assigned a precise probability even in the face of the complete ignorance on these modes on the part of the expert.

It is known in the probability theory that the knowledge of the probability of likelihood of the event occurrence can be translated in to the knowledge of the probability of likelihood of that event not occurring. For example, if an expert believes that a failure of the system due to the failure of a particular component is 0.4, then this does not mean that expert believes that the failure of the system will not occur due to that component with likelihood of 0.6. Thus these assumptions of axiom of additivity and the principle of insufficient reason can model the random events associated with aleatoric uncertainty but not sufficient belief or knowledge is applied. Analysis of these situations, where there is

little information to evaluate a probability or when the given information is nonspecific, ambiguous or conflicting, is required in many engineering applications (for example, in the case of risk assessment). It is evident in these situations where precise probability cannot characterize the uncertainty and thus makes us to consider an interval or set as the measure of probability. To summarize the important implications in the characterization of the measure of probability as an interval are a) the principle of insufficient reason is not applicable, b) the axiom of additivity is not applicable, and c) the precise probability from an experiment or an expert is not mandatory. Thus, probability theory cannot be applied to every situation involving more than one kind of uncertainty. Apart from probability theory, several other theories like fuzzy theory, evidence theory and so on are introduced to handle these uncertainties. The main difference among these theories is in the assignment of belief and commonality is in the determination of degree of belief to uncertain events which are likely to occur.

We present four different types of evidences from multiple sources that impact the choice of how the evidence is to be combined:

The first one is *consonant evidence*- it represents the situation where each evidential set is supported by the next larger evidential set and implies an agreement on the smallest evidential set; however, there is conflict between the additional evidence that the larger set represents in relation to the smaller set. For example, let the failure data from four different service stations (S1, S2, S3 and S4) of an automobile be as demonstrated in Fig 3.1 with

S1: mainly due to failures of gearbox

S2: mainly due to failure of gearbox and brakes

S3: mainly due to failure of front shock absorber and gearbox

S4: mainly due to failure of gearbox, brakes, front shock absorber and engine.

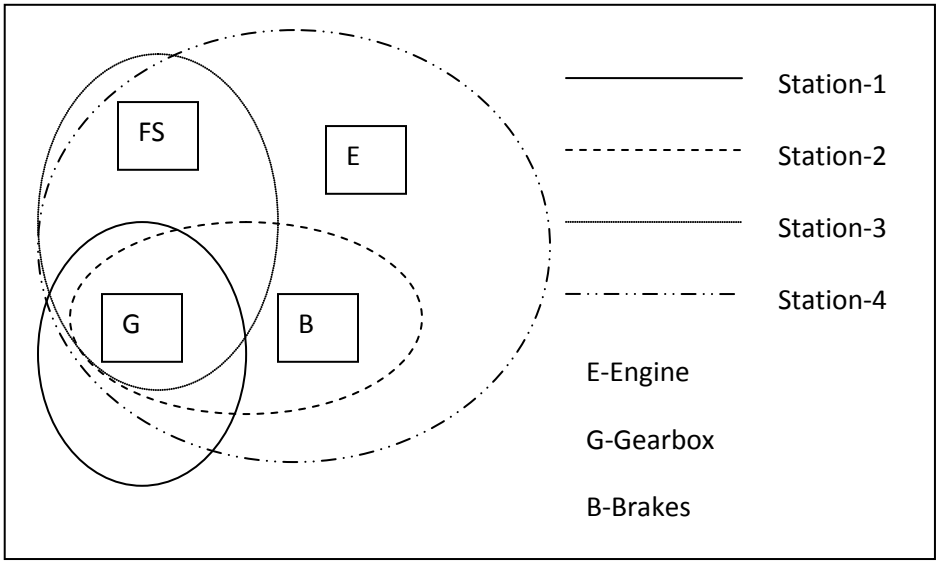

Figure 3.1 Consonant evidence obtained from multiple sources [185]

The second one is *consistent evidence*- it implies an agreement on atleast one evidential set or element. For example, let the failure of automobiles from different service stations be as shown in Fig 3.2 with

S1: mainly due to failure front shock absorber

S2: Gearbox and front shock absorber

S3: Brakes and front shock absorber

S4: Front shock absorber and engine.

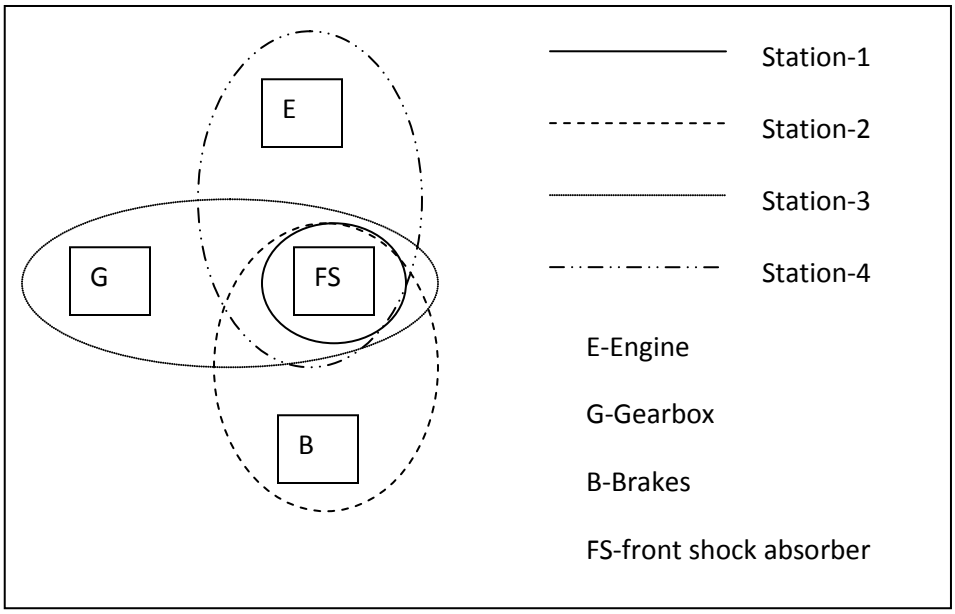

Figure 3.2 Consistent evidence obtained from multiple sources

The third one is a*rbitrary evidence*- in this case, there is some agreement between some sources but there is no consensus among sources on any one element. For example, let the failure of automobiles from different service stations be as shown in Fig 3.3 with

S1: mainly due to failure of front shock absorber

S2: Gearbox and brakes

S3: Front shock absorber and gearbox

S4: Brakes and engine.

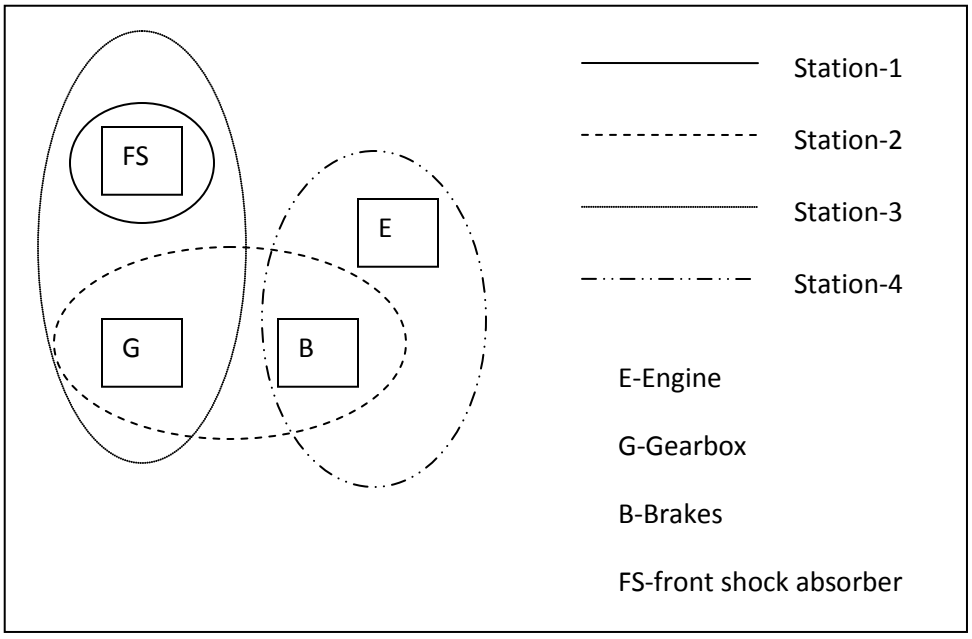

Figure 3.3 Arbitrary evidence obtained from multiple sources

The fourth one is *disjoint evidence*- in this case, all of the sources supply conflicting evidence. For example, let the failure of automobiles from different service stations be as shown in Fig 3.4 with

S1: mainly due to failure of front suspension

S2: Bakes

S3: Gearbox

S4: Engine

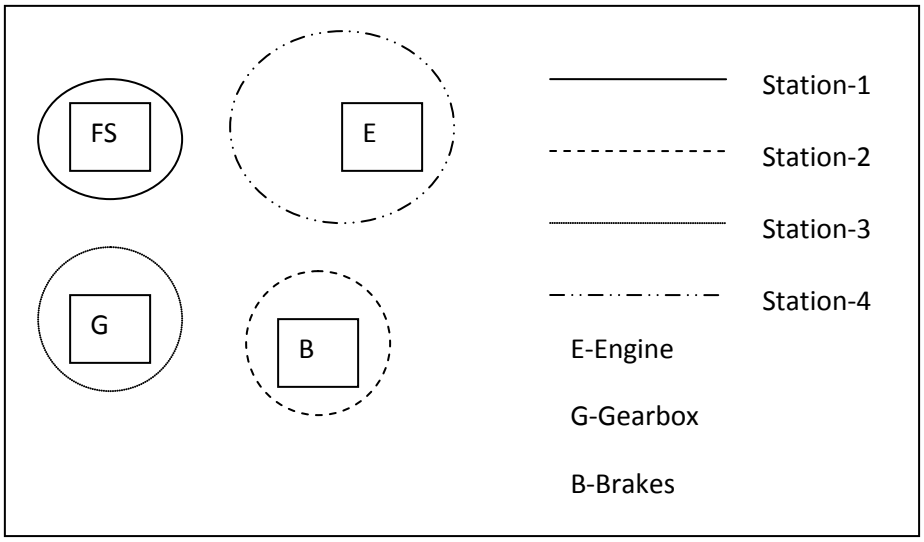

Figure 3.4 Disjoint evidence obtained from multiple sources

3.2 DEMPSTER SHAFER THEORY (DST)

DST, also called evidence theory, is a branch of mathematics that concerns with the combination of empirical evidence in an individual's mind in order to construct a coherent picture of reality. Evidence theory is a generalization of classical probability and possibility theories from the perspective of bodies of evidence and their measures, even though the methodologies for manipulation of evidence are totally different [222,210,212,218]. It can handle both epistemic uncertainty and aleatory uncertainty in its framework. When the evidence is sufficient enough to permit the assignment of probabilities to single events, the DST model collapses to the traditional probabilistic formulation. One of the most important features of DST is that the model is designed to cope with varying levels of precision regarding the information and no further assumptions are needed to represent the information. DST theory [55] is found by adding the third category "don't know", to the familiar dichotomy "it's true" or "it's false". More precisely, let the non negative probabilities (a, b, c) represent the triad "known to be

true", "known to be false", and "don't know" then as per DST, it implies that a + b + c = 1 that is 'a' – your evidence "for truth" , 'b' – evidence "against" and c = 1 - a - b for residual ambiguity.

Frame of discernment: The theory assumes that there is a fixed set of mutually exclusive and exhaustive elements called the Environment or Frame or Frame of Discernment (FOD) or sample space(Θ) which is given as

$$\Theta = \{\theta_1, \theta_2, \theta_3, \theta_4, ...\theta_n\} \tag{3.1}$$

We assume that all possible elements of the universe are present in this set and therefore the set is exhaustive. For simplicity, we assume that Θ is a finite set in equation (3.1). Each subset of Θ can be interpreted as a possible solution to a question. There can be only one correct solution subset to a question. The term "discern" means that it is possible to distinguish the one correct answer from all the other possible answers to a question. The power set of the environment/FOD has elements as answers to all the possible questions of the frame of discernment. This means that there is a one to one correspondence between the elements of the power set (Θ) and the subsets of Θ .

Three important functions are defined in DST: the *basic probability assignment* (*or mass*) *function,* the *Belief* function (*Bel*), and the *Plausibility* function (*Pl*).

3.2.1 Basic probability assignment

The basic probability assignment (bpa) is a primitive of evidence theory. Another term for bpa is mass (m). It is customary in DST to think about the degree of belief in evidence as analogous to the mass of a physical object i.e., mass of evidence supports a

belief. Generally, the term "basic probability assignment" does *not* refer to probability in the classical sense. The bpa, represented by *m*, defines a mapping of the power set to the interval between 0 and 1, where the bpa of the null set is 0 and the summation of the bpa's of all the subsets of the power set is 1. The value of the bpa for a given set *A*, represented as *m*(*A*), expresses the proportion of all relevant and available evidence that supports the claim that a particular element of Θ (the universal set) belongs to the set *A* but to no particular subset of *A* . The value of *m*(*A*) pertains only to the set *A* i.e., portion of total belief assigned exactly to proposition A and makes no additional claims about any subsets of *A*. Any further evidence on the subsets of A would be represented by another bpa, *i.e.* $B \subset A$, *m*(*B*) would the bpa for the subset *B*. Formally, this description of bpa, *m,* can be represented with the following three axioms/equations:

$$\mathrm{m}(A) \geq 0 \text{ for any } A \in 2^{\Theta} \tag{3.2}$$

$$\mathrm{m}(\phi) = 0 \tag{3.3}$$

$$\sum_{A \in 2^{\Theta}} m(A) = 1 \tag{3.4}$$

A belief structure is defined as the collection of all values of *m(A)* for $A \subset \Theta$, denoted as $\{m(A) : A \subset \Theta\}$.

Properties of bpa:

1. Additivity does not necessarily hold $m(\{x_1\}) + m(\{x_2\}) \neq m(\{x_1, x_2\})$ (3.5)
2. Monotonicity does not necessarily hold

   $m(\{x_1\}) \geq m(\{x_1, x_2\})$ even though $\{x_1\}$ is a subset of $\{x_1, x_2\}$ (3.6)

3. It is not required that $m(\Theta) = 1$, but $m(\Theta) \leq 1$ (3.7)

For example, when there is a robbery in a house and there are three suspects, the frame of discernment consists of three elementary propositions, $\Theta = \{A, B, C\}$, where $\{A\}$ means that A is the thief. If there is a witness (E_1, evidence), and she gave her testimony for only A, let's say $m(\{A\})$ is 0.7. However, we cannot assign the remaining 0.3 to $m(\{B\}), m(\{C\})$ or $m(\{B, C\})$, because the evidence given by the witness is just for suspect A, and she did not testify against suspects B and C. Therefore, 0.3 is assigned to the degree of uncertainty $m(\{\Theta\})$.

From the basic probability assignment, the upper and lower bounds of an interval can be defined. This interval contains the precise probability of a set of interest (in the classical sense) and is bounded by two nonadditive continuous measures called Belief and Plausibility.

3.2.2 Belief function (*Bel*)

The belief for a set A is defined as the sum of all the basic probability assignments of the proper subsets B of the set of interest A (B $\subseteq$ A). Belief [75] can be seen to be a lower bound on the interval which contains the precise probability of a set of interest (in the classical sense) [3]

$$Bel(A) = \sum_{B|B \subseteq A} m(B) \tag{3.8}$$

3.2.3 Plausibility function (*Pl*)

The plausibility for a set A is defined as the sum of all the basic probability assignments of the sets B that intersect the set of interest A ($B \cap A \neq \phi$). Thus, for all sets A that are elements of the power set 2^n where n is the number of elements in the frame of discernment, the plausibility is given by

$$Pl(A) = \sum_{B|B\cap A\neq\phi} m(B) \tag{3.9}$$

Thus plausibility can be seen as the upper bound of the interval which contains the precise probability of a set of interest (in the classical sense) [3]. Although the Bel(A) and Pl(A) have been defined in terms of the bpa, they can also be derived from each other as

$$Pl(A) = 1 - Bel(\overline{A}) \tag{3.10}$$

where $\overline{A}$ is the complement of A.

We also define $\text{Doubt(A)} = Bel(\overline{A})$

Due to a lack of information, it is more reasonable to present bounds for the result of uncertainty quantification, as opposed to a single value of probability. This precise probability of an event (in the classical sense) lies within the lower and upper bounds given by Belief and Plausibility, respectively.

$$Bel(A) \leq P(A) \leq Pl(A) \tag{3.11}$$

The total degree of belief in a proposition "A" is expressed within a bound [*Bel(A), Pl(A)*], which lies in the unit interval [0,1], as shown in Figure 3.5.

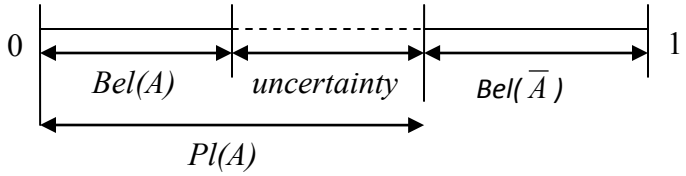

Figure 3.5 Belief (*Bel*) and Plausibility (*Pl*)

Note that the belief interval [*Bel(A), Pl(A)*] reflects the uncertainty and ignorance associated with *A,* and the following two parameters play an important role:

- The actual values of *Bel(A)* and *Pl(A)* (to measure the uncertainty about A)
- Size/length of the interval (to measure the ignorance)

For example, the Belief interval [05, 0.8] for a proposition, for example, " the person in the house is dead" implies that the statement is true with a confidence of 0.5, false with a confidence of 0.2 and the difference 0.3 is indeterminate – meaning that the person could either be dead or alive. Thus DST allows one to specify a degree of ignorance in the specific situation instead of being forced to supply prior probabilities that add to unity. The inferences can be drawn from the belief interval as shown in Table 3.1.

Table 3.1 Inferences from the belief interval

Case	Condition	Example
Ignorance	*Bel(A)<< Pl(A)*	[0,1]
Maximum information	*Bel(A) = Pl(A)*	[0.7,0.7]
Certainty	*Bel(A) & Pl(A)* ≈ 1	[0.99,1]
Uncertainty	*Bel(A) & Pl(A)* ≈ 0.5	[0.49,0.5]

Focal elements: Those propositions in the FOD (Θ) that possess nonzero masses are called focal elements of FOD:

$$F(\Theta) = \{A \subseteq \Theta : m(A) > 0\} \tag{3.12}$$

Core: The union of all focal elements corresponding to a bpa assigned to the FOD (Θ) is referred to as its core.

Body of Evidence (BoE): The triple $\{\Theta, F, m\}$ is referred to as the body of evidence (BoE)

For the automobile example considered in section 3.1, let the two evidences for the failure of the automobile be given as

$m_1 : m_1(G) = 0.6 \quad m_1(B) = 0.1 \quad m_1(\Theta) = 0.3$

$m_2 : m_2(G) = 0.2 \quad m_2(B) = 0.4 \quad m_2(\Theta) = 0.4$

so, we have $\Theta = \{\phi, \{G\}, \{B\}, \{G, B\}\}$

and $F = \{\{G\},\{B\}\}$

First body of evidence $(BoE)_1 = \{\Theta, F, m_1\}$ and second body of evidence $(BoE)_2 = \{\Theta, F, m_2\}$

3.3 FUZZY SET THEORY

Zadeh introduced the fuzzy set theory in 1965 [220]. Fuzzy set theory is a generalization of classical set theory as a mathematical way to represent the impreciseness and vagueness present in the everyday life. It was successfully applied in a variety of applications including those from artificial intelligence, consumer electronics, optimization, decision theory, and control system design. In real life engineering problems, several uncertain conditions exist during the analysis of the problem. Some of the uncertain information is vague, incomplete, imprecise, linguistic, or qualitative, which makes it impossible to use conventional or probabilistic methods to handle it. Thus, fuzzy sets are introduced to model the incomplete, linguistic or vague information encountered in real world engineering problems. In classical set theory, an element may or may not belong to a certain set. In fuzzy set theory, an element can belong to a certain set partially. Some researchers [22] suggested the use of fuzzy sets in order to handle the uncertainties present in the analysis of engineering problems

3.3.1 Concept of fuzzy sets

In conventional set theory, crisp (deterministic) sets are defined such that $F = \{x / x = 3\}$, then for a given number, it can only reside in one set, that is, the level of

presumption or level of membership α of "x is 3" is one, while α of "x is not 3" is zero. Therefore, a given crisp number is either in this set, or not. For a fuzzy set, things are different. A fuzzy set B in U (the universe set) can be treated as the coupling between the level of presumption α and the interval of confidence $[A_\alpha^-, A_\alpha^+]$ at level α , where α is within the range of zero to one, A_α^- and A_α^+ are, respectively, the lower and upper bounds of A at the α level. A fuzzy set can be represented as:

$$B = \{(x, \mu_B(x)) \mid x \in U\}, \text{where } \propto = \mu_B: U \to [0,1] \tag{3.13}$$

It denotes the collection of all points $x \epsilon U$ with the associated membership function $\mu_B(x)$.

A fuzzy set B is convex if and only if every ordinary subset defined by [51]

$$B_\propto = \{x \mid \mu_F(x) \geq \propto\}, \propto \in [0,1] \tag{3.14}$$

is convex. Another definition is $\forall\, x^{(1)}, x^{(2)} \in R, \forall\, \lambda \in [0,1]$

$$\mu_B[\lambda x^{(1)} + (1-\lambda)x^{(2)}] \geq \mu_B(x^{(1)} \wedge x^{(2)}) \tag{3.15}$$

where $X \wedge Y$ means minimum of X and Y.

A fuzzy set is any set that allows its members to have different grades of membership function in the interval [0, 1]. The crisp value of a fuzzy number is the value corresponding to a membership function value of one. A fuzzy number can also be represented by a set of discrete pairs containing a value x and its associated membership value α as $B = \{x, \mu_B(x)\}$. As an example, the fuzzy number, "x is not 3", may be described by the membership function shown in equation (3.16). In discrete form, B can

be represented as: B = {0.0/0.0, 0.5/2.5, 0.9/2.9, 1.0/3.0, 0.8/3.4, 0.25/4.5, 0.0/5.0}. A membership value of one indicates a full membership while a value of zero indicates non-membership.

$$\propto = \mu_F(x) = \begin{cases} 0, & for \quad x < 2 \\ x - 2, & for \quad 2 \leq x \leq 3 \\ \frac{5-x}{2}, & for \quad 3 \leq x \leq 5 \\ 0, & for \quad x > 5 \end{cases} \tag{3.16}$$

For the fuzzy number described in equation (3.16), the element x = 3.4 has a membership value of 0.8 in the fuzzy set "about 3". The membership function can have a linear or a nonlinear form.

3.3.2 Fuzzy set relations

The following terminologies are important in describing fuzzy relations:

- The ∝-level (∝-cut) of a fuzzy set B in U is defined as $B_\propto = \{x \in U : \mu_B(x) \geq \propto\}$
- Two fuzzy sets A and B are said to be equal, A=B, if $\mu_A(x) = \mu_B(x)$, for all $x \in U$
- A fuzzy set A is said to be contained in $B, A \subseteq B,$ if $\mu_A(x) \leq \mu_B(x),$ for all $x \in U$

Now a number of definitions and operations on fuzzy sets are given:

- Fuzzy complement: $\mu_{\bar{A}}(x) = 1 - \mu_A(x)$
- Fuzzy union: $\mu_{A \cup B}(x) = \mu_A(x) \vee \mu_B(x)$
- Fuzzy intersection: $\mu_{A \cap B}(x) = \mu_A(x) \wedge \mu_B(x)$
- For fuzzy sets A and its complement set $\overline{A}$, $A \cup \bar{A} \neq A \cap \bar{A} \neq \varphi$

3.3.3 α-Cut representation

In general, when a fuzzy set is discretized, the number of elements in the set could become quite large. Thus, in numerical computations, it is convenient to express fuzzy numbers as sets of lower and upper bounds of a finite number of α-cut subsets as shown in Fig 3.6. Corresponding to a level of α (α-cut), the value of x is extracted in the form of an ordered pair with a closed interval $[x_l, x_u]$. The α-cut can be taken anywhere ranging from α = 0 (total uncertainty) to α = 1(total certainty). An interval number is represented as an ordered pair $[x_l, x_u]$ where $x_l \leq x_u$. In case $x_l = x_u$, the interval is called a fuzzy-point interval, e.g. [a, a]. Thus membership functions are constructed in terms of intervals of confidence at several levels of α-cuts. The level of α, $\alpha \in [0,1]$, gives an interval of confidence $\mathbf{X}_\alpha$, defined as

$$\mathbf{X}_\alpha = \{x \in \mathbf{R}, \mu_{\mathbf{X}}(x) \geq \alpha\}. \tag{3.17}$$

where $\mathbf{X}_\alpha$ is a monotonically decreasing function of α, that is

$$(\alpha_1 < \alpha_2) \Rightarrow (\mathbf{X}\alpha_2 \subset \mathbf{X}\alpha_1) \tag{3.18}$$

or

$$(\alpha_1 < \alpha_2) \Rightarrow [a_1^{\alpha 2}, a_2^{\alpha 2}] \subset [a_1^{\alpha 1}, a_2^{\alpha 1}] \text{ for every } \alpha_1, \alpha_2 \in [0,1] \tag{3.19}$$

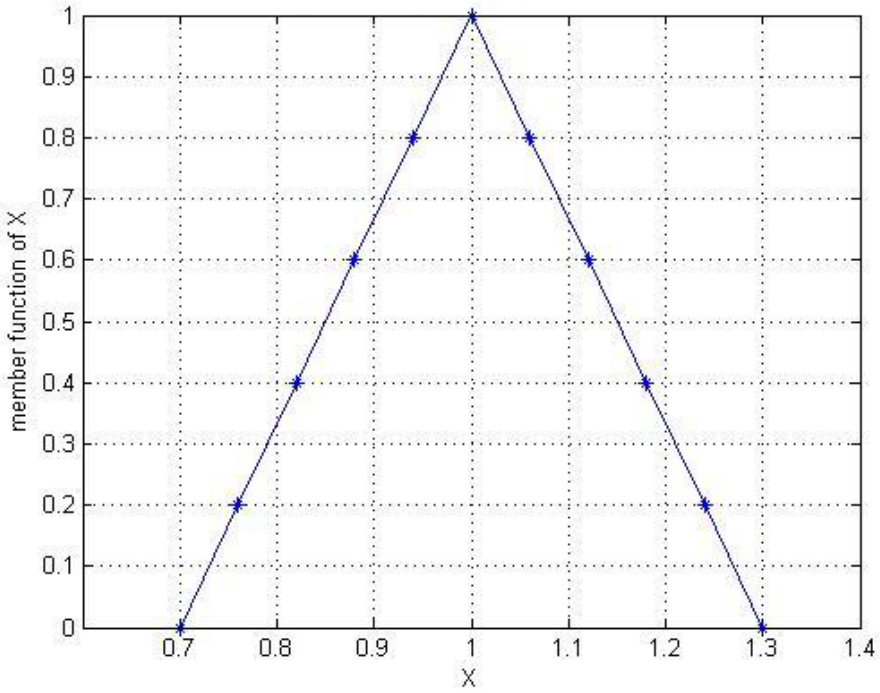

Figure 3.6 Typical fuzzy number, X

The fuzzy numbers thus defined are known as intervals. Once the intervals or ranges of a fuzzy quantity corresponding to specific α – cuts are known, the system response at any specific α – cut, can be found using interval analysis. Thus in the application of a fuzzy approach to uncertain engineering problems, interval analysis can be used.

3.3.4 Fuzzy arithmetic [100]

With fuzzy quantities expressed in interval form, fuzzy arithmetic operations can be carried out using interval operations at each of the n α –levels independently. The addition of two fuzzy numbers A and B with

$$A = \{(a^L, a^R)_i\} \text{ and } B = \{(b^L, b^R)_i\} \tag{3.20}$$

can then be expressed as

$$A(+)B = \{(a^L + b^L, a^R + b^R)_i\};\ \text{i= 1, 2, 3, ……n} \tag{3.21}$$

The addition operation of fuzzy numbers is both commutative and associative. The subtraction of fuzzy numbers A and B can be expressed as

$$A(-)B = \{(a^L - b^R, a^R - b^L)_i\};\ \text{i= 1, 2, 3, ……n} \tag{3.22}$$

The subtraction operation of fuzzy numbers is neither commutative nor associative. The multiplication of fuzzy numbers A and B can be expressed as

$$A(\times)B = \left\{\min[a^L.b^L, a^L.b^R, a^R.b^L, a^R.b^R]_i, \max[a^L.b^L, a^L.b^R, a^R.b^L, a^R.b^R]_i\right\};$$

$$\text{i= 1, 2, 3, …… n} \tag{3.23}$$

The multiplication operation of fuzzy numbers is both commutative and associative but is not distributive in **R**. The inverse of a fuzzy number A can be expressed as

$$A^{-1} = \left\{\left(\frac{1}{a^R}, \frac{1}{a^L}\right)_i\right\};\ \text{i= 1, 2, 3 …n} \tag{3.24}$$

The division of fuzzy numbers A and B can be expressed as

$$A(\div)B = A(\times)B^{-1};\ \text{i= 1, 2, 3 …n} \tag{3.25}$$

The square root can be defined only for positive fuzzy numbers. Let $A^{1/2}$ be the square root of a fuzzy number A. It can be defined as the fuzzy number C such that $C^2 = A$. Then, by using Eq. (3.23), the square root of a fuzzy number is written as

$$C = A^{1/2} = [c^L, c^R]_i;\ \text{i= 1, 2, 3 …n} \tag{3.26}$$

where $c_i^R = [a^R]_i^{1/2}$ (3.27)

$$c_i^L = \begin{Bmatrix} [a^L]_i^{1/2} & if \;\; a^L \geq 0 \\ \left(\frac{a^L}{c^R}\right)_i & if \;\; a < 0 \end{Bmatrix} \tag{3.28}$$

3.4 PARTICLE SWARM OPTIMIZATION (PSO)

The PSO algorithm is based on the swarm intelligence techniques [13,67]. The concept of swarm intelligence was inspired by the social behavior of groups of animals such as a flock of birds, ants, or a school of fish. It is also a population based algorithm in which individuals are called particles and the population is called swarm. The PSO is similar to evolutionary algorithms (EA) in the sense that both approaches are population-based and each individual has a fitness function. Based on the bounds or limits on the design variables, randomly generated values are taken as initial population in the algorithm. Another major difference between PSO and EA is that in PSO each individual depends from its history whereas no such mechanism exists in EA [64]. A PSO is an inherently continuous algorithm. In order to apply for discrete optimization problems, it should be modified suitably. Kennedy and Eberhart [103] proposed the first PSO algorithm where the k^{th} particle travels in the search space with velocity $\vec{V}_k$ at position $\vec{X}_k$. If the search space is *n*-dimensional, the k^{th} individual of the population can be represented by an *n*-dimensional vector $\vec{X}_k = [x_{k1}, x_{k2}, ..., x_{kn}]^T$ and its velocity vector $\vec{V}_k = [v_{k1}, v_{k2}, ..., v_{kn}]^T$. Let $pbest_{ik}$ and $gbest_i$ denote the best previous position of the k^{th} particle at i^{th} iteration and the best particle in the population at the end of i^{th} iteration,

respectively. The adaptable velocity and position of the particle k is updated using the following equation at $i + 1$ iteration as:

$$\vec{V}_k^{i+1} = \vec{V}_k^{i} + c_1\, rand()\ (pbest_{ik} - \vec{X}_k^{i}) + c_2\, Rand()\ (gbest_i - \vec{X}_k^{i}) \tag{3.29}$$

$$\vec{X}_k^{i+1} = \vec{X}_k^{i} + \vec{V}_k^{i+1}, \quad k = 1, 2, \ldots, K \tag{3.30}$$

where $rand()$ and $Rand\ ()$ are two different random numbers in the range [0,1], and c_1 and c_2 are positive constants, referred to as cognitive and social learning rates. Cognitive rate represents the particle's own experience as to where the best solution is present in the design space where as social learning rate represents the entire swarm as to where the best solution is present in the design space. Eberhart and Shi [63] introduced a parameter, called inertia weight, *iw*, to control the velocity over time in the PSO algorithm and termed the procedure the modified PSO. In the modified PSO, Eq. (3.29) for the updating velocity is changed to

$$\vec{V}_k^{i+1} = i\, w_{i+1} \vec{V}_k^{i} + c_1\, rand()\ (pbest_{ik} - \vec{X}_k^{i}) + c_2\, Rand()\ (gbest_i - \vec{X}_k^{i}) \tag{3.31}$$

where iw_{i+1} is the inertia weight for the $(i+1)^{th}$ iteration, assumed to be linearly decreasing, as (Eberhart and Shi 2000 [42], Naka *et al.* 2001 [109]):

$$iw_{i+1} = iw_{\max} - \frac{iw_{\max} - iw_{\min}}{i_{\max}}\ (i+1) \tag{3.32}$$

where $i_{\max}$ represents the maximum number of iterations with $iw_{\min}$ and $iw_{\max}$ denoting the initial and final inertia weights, respectively. After meeting the convergence criteria set by the user, the algorithms gives the global best value as the optimum solution of the algorithm.

The relation between the inertia weight and cognitive and social learning rates should satisfy the following relation in order to have guaranteed convergence, as given by Van den Bergh [204]:

$$\frac{c_1 + c_2}{2} - 1 < iw$$

3.5 GAME THEORY

In many real-world problems, several objectives must be satisfied simultaneously in order to obtain an optimal solution. The multiple objectives are typically conflicting and non-commensurable, and must be satisfied simultaneously. For example, we might want to minimize the total weight of a truss while minimizing its maximum defection and maximizing its allowable stress or, in the design of an automobile, an engineer may wish to maximize crash resistance for safety and minimize the weight for fuel economy. These are some examples of multi-objective problems with conflicting objectives, *i. e*., a step towards improving one of the objectives, worsens the other objective, is a step away from improving the other, increasing the first objective. The common approach in these types of problems is to choose one objective and incorporate the other objectives as constraints. This approach has the disadvantage of limiting the choices available to the designer, making the optimization process a rather difficult task. Another common approach is the combination of all the objectives into a single objective function. This technique has the disadvantage of modeling the original optimization problem in an inadequate manner, generating solutions that will require a further sensitivity analysis to become reasonably useful to the designer. A more appropriate approach to deal with multiple objectives is to

use techniques that were originally designed for that purpose as used in the field of Operations Research. Many approaches have been refined and commonly applied in economics and control theory. Several techniques have been suggested for the solution of a multiobjective structural optimization problem. The game theory approach has been found to be superior to many other techniques since it finds not only the best compromise (Pareto-optimal) solution but also the relative contributions of the various objective functions to the best compromise solution.

In the game theory, two concepts, namely the non-cooperative and cooperative game theories, are available. For a basic understanding of these theories, the number of design variables (n) is assumed to be same as the number of objective functions (k). The values of n and k need not be same in the general approach presented later. In game theory, each objective function is associated with a player. Thus the i^{th} player aims to minimize his/her own objective function f_i. It is further assumed, for simplicity, that the i^{th} player will have control over only one design variable x_i (and not on any other design variable). Although the i^{th} player would like to minimize his/her own objective function $f_i(x_1, x_2, ..., x_i, ..., x_n)$, other players can also influence the value of f_i by controlling the design variables $x_1, x_2, \ldots, x_{i-1}, x_{i+1}, \ldots, x_n$. Similarly, the i^{th} player can influence the values of the objectives of other players, $f_1, f_2, \ldots, f_{i-1}, f_{i+1}, \ldots, f_n$ by controlling his/her own design variable x_i.

The game theory approach can be seen graphically by considering a multiobjective optimization problem involving two objective functions in two design variables. Let $f_1(x_1, x_2)$ and $f_2(x_1, x_2)$ represent the two objectives and x_1 and x_2 the two design variables. As indicated earlier, one player is associated with each objective. Thus the first

player wants to select a design variable x_1, which will minimize his/her objective f_1 and similarly the second player seeks a variable x_2, which will minimize his/her own objective f_2. Assuming f_1 and f_2 to be continuous, let the contours of constant values of f_1 and f_2 be as shown on Fig. 3.7. The dotted and dashed lines passing through O_1 and O_2, respectively, represent the loci of rational (minimizing) choices for the first and second player for a fixed value of x_2 and x_1, respectively. The intersection of these two lines, if exists, is a candidate for the two objective minimization problem assuming that the players do not cooperate with each other (non-cooperative game). In Fig. 3.7, the point $N(x_1^*, x_2^*)$ represents such a point. This point, called the Nash equilibrium solution, represents a stable equilibrium condition in the sense that no player can deviate unilaterally from this point for further improvement of his/her own criterion. The Nash equilibrium point has the characteristic that

$$f_1(x_1^*, x_2^*) \le f_1(x_1, x_2^*) \tag{3.33}$$

and

$$f_2(x_1^*, x_2^*) \le f_2(x_1^*, x_2) \tag{3.34}$$

where x_1 may be to the left or right of x_1^* in Eq. (3.33) and x_2 may lie above or below x_2^* on Eq. (3.34). This idea can be extended to define the Nash equilibrium solution of a multiobjective optimization problem in *k* design variables and *k* objective functions as follows:

$$\begin{aligned} &f_1(x_1^*, x_2^*, \dots, x_k^*) \le f_1(x_1, x_2^*, \dots, x_k^*) \\ &f_2(x_1^*, x_2^*, \dots, x_k^*) \le f_2(x_1^*, x_2, \dots, x_k^*) \\ &\qquad\qquad \vdots \\ &f_k(x_1^*, x_2^*, \dots, x_k^*) \le f_k(x_1^*, x_2^*, \dots, x_k) \end{aligned} \tag{3.35}$$

The Nash equilibrium solution denotes the solution of a non-cooperative game. In the above discussion, only one Nash equilibrium point has been assumed, i.e. the dotted and dashed lines in Fig. 3.7 intersect only at one point. An interesting situation occurs when the two lines intersect at more than one point. In such a case, since the values of f_1 and f_2 are different at the multiple Nash equilibrium points, any player can have the advantage of declaring his/her move first (by choosing a proper value of his/her design variable) there by forcing the other players to play at the equilibrium point of his/her own choice.

In a cooperative game, the two players agree to cooperate with each other and hence any point in the shaded region S of Fig. 3.7 will provide both of them with a better solution than their respective Nash equilibrium solutions. Since the region S does not provide a unique solution, the concept of Pareto-optimal (non-inferior) solutions can be introduced to eliminate many solutions from the region S. A feasible solution $\vec{X}$ of a multiobjective problem is called Pareto optimal if there exists no other feasible solution $\vec{Y}$ such that $f_i(\vec{Y}) \leq f_i(\vec{X})$ for $i = 1, 2, \ldots, k$ with $f_j(\vec{Y}) < f_i(\vec{X})$ for at least one j (Rao 1996) [169]. In other words, a feasible vector $\vec{X}$ is called Pareto optimal if there is no other feasible solution $\vec{Y}$ that would reduce some objective function without causing a simultaneous increase in at least one other objective function. Using the definition of a Pareto optimal solution, all the points lying on the continuous line $O_1ACQDBO_2$, which represent the loci of tangent points between the contours of f_1 and f_2, can be seen to be Pareto optimal points. Thus every point on this line has the property that it is not dominated by any other point in its neighborhood, i.e.

$$f_1(Q) \leq f_1(P) \tag{3.36}$$

and

$$f_2(Q) \leq f_2(P) \tag{3.37}$$

where Q is a point lying on the line O_1O_2 and P is a neighborhood point. Thus all points of S that do not lie on the fine O_1O_2 need not be considered in finding a cooperative game solution. The set of all points lying on the line AB denotes the Pareto-optimal set, denoted as S_p. The first task in the cooperative game theory is to find the Pareto optimal set S_p. After determining the Pareto-optimal set, the second task is to find a particular element (design vector) from the set S_p which represents a compromise solution that is acceptable to all the players. For this, the players establish specific rules of negotiation which can be used to formulate a supercriterion or bargaining model. The supercriterion can then be used to convert the multiobjective optimization problem into an equivalent single objective optimization problem whose solution yields a mutually agreeable compromise solution (an element of the Pareto optimal set S_p).

A procedure for finding not only the Pareto optimal set S_p but also the compromise solution (an element of S_p) based on a supercriterion, is presented in chapter 7, in the form of a modified game theory. The procedure is termed modified game theory because it not only simplifies the computational procedure but also considers the solution of the general multiobjective optimization problem involving *n* design variables and *k* objective functions ($n = k$ has been assumed in the game theory approach presented above).

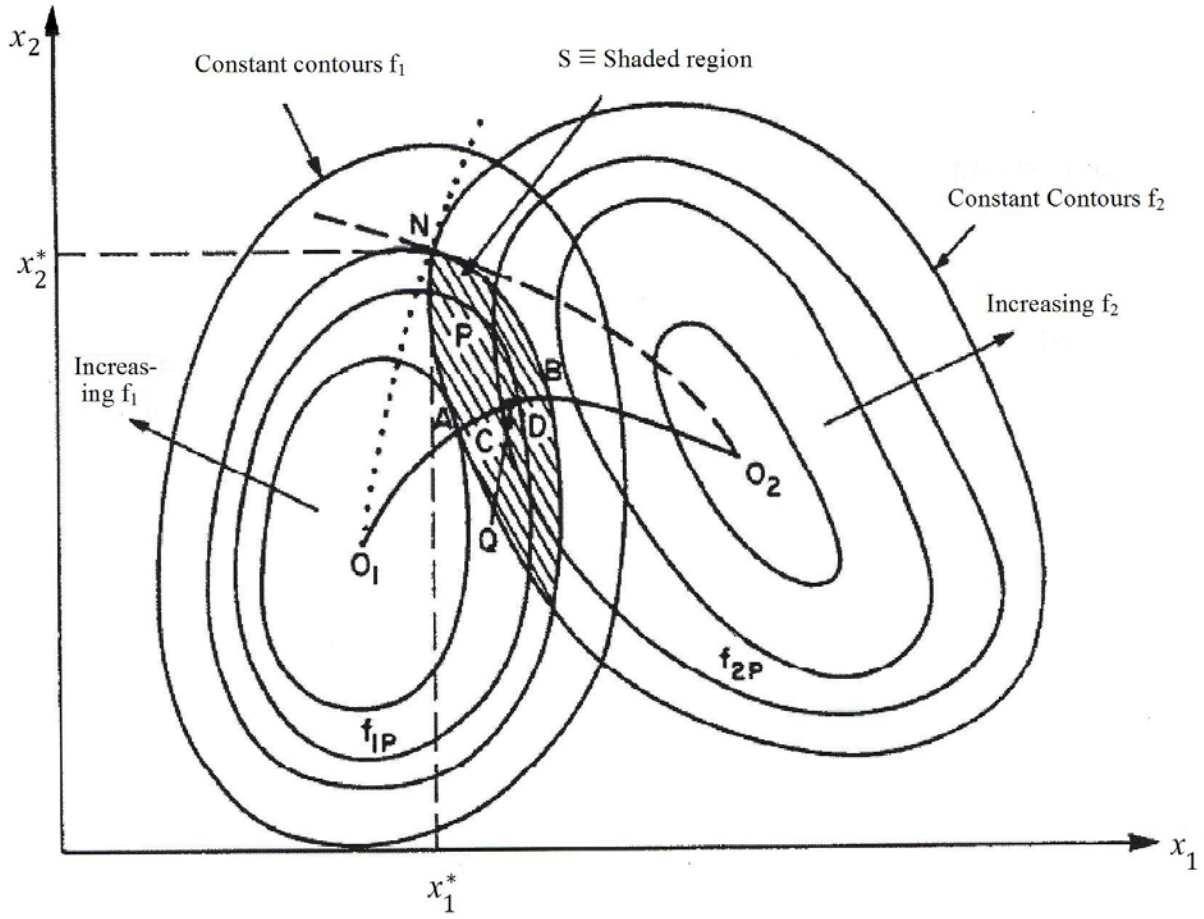

Figure 3.7 Cooperative and non-cooperative game solutions [170]

3.6 WARRANTY POLICIES

In today's competitive market, product warranties have become an important consideration for both the manufacturer (or seller) and the customer (or consumer). A warranty is an assurance given by the manufacturer to the buyer at the time of sale that the product will perform its intended functions satisfactorily for a specified length of warranty. The purpose of a warranty is to establish liability to the manufacturer when the product fails during the warranty period (when the product is properly used by the

customer). The common interpretation of warranty implies quality, reliability, product desirability, limitations of liability, and superior workmanship.

Warranties are important to both manufacturers and customers. Manufacturers often use warranties as a marketing tool to increase the sales of the product. These warranties act as a means of protection to the manufacturers against exceptional claims by requiring certain responsibilities on the part of customers, for example warranties do not cover any product failures due to misuse of the product. Customers usually interpret a longer warranty period as a sign of quality and reliability. This is especially true for new products introduced in the market for which customers have little or no information about quality and reliability. For the customers, warranty provides a means of redress for product failures.

There are four stages involved in the product purchase decision by a rational customer. They are a) perception of a need for the product, b) search for information, c) evaluation of alternatives, and d) product choice. It is seen that warranty plays an important role in the last three stages. Customers often compare the warranties apart from price, style and other characteristics of products before purchase. According to the Magnuson-Moss Warranty Federal Trade Commission Improvement Act, manufacturers of consumer products must provide any warranty information available to customers so that they can compare different product warranties. Manufacturers incur additional costs by offering warranty. However when warranty is used as a marketing tool to increase the sales, then it will increase the revenue. If the revenue generated by the warranty program exceeds the warranty cost, it is more sensible to sell the product with a warranty. Thus the

cost of the warranty program (i.e., warranty cost analysis) is, to be considered while designing an effective warranty program.

A review of some basic concepts of probability and reliability is given in section 3.6.1 followed by a description of different warranty policies in section 3.6.2. An automobile warranty problem is formulated in section 9.3 and the results of the optimization problem along with a sensitivity analysis are given in section 9.4.

3.6.1 Basic concepts of probability and reliability [173]

Let *T* be any continuous random variable in the interval (0,∞). The uncertainty in the values of failure time, *T,* can be described through a continuous distribution function $F(t;\theta)$ which denotes the probability $P(T \leq t)$ [27]:

$$F(t;\theta) = P(T \leq t) \text{ for } 0 \leq t \leq \infty \tag{3.38}$$

where θ represents distribution function parameter set and *t* represents time. If there exists a function, $f(t;\theta)$, such that

$$f(t,\theta) = \frac{dF(t;\theta)}{dt} \tag{3.39}$$

over the interval $0 < t < \infty$, $f(t;\theta)$ is called the density function associated with the distribution function $F(t;\theta)$. Integrating equation (3.39), we obtain,

$$F(t) = \int_0^t f(t)dt \tag{3.40}$$

The hazard function or failure rate function $r(t;\theta)$ associated with $F(t;\theta)$ is defined as

$$r(t;\theta) = \frac{f(t;\theta)}{1-\mathrm{F(t\,;\,\theta)}} \tag{3.41}$$

The hazard function $r(t;\theta)$ can be interpreted as the probability that the product will fail in $(t, t+\delta t)$ provided that it has not failed at or prior to *t*. The reliability of the product, $R(t)$, is given by

$$R(t) = P(T > t) = 1 - P(T \leq t) = 1 - F(t) \tag{3.42}$$

The hazard function, $r(t)$, in terms of reliability can be defined as

$$r(t) = -\frac{1}{R(t)}\frac{dR(t)}{dt} \tag{3.43}$$

Integrating equation (3.43), we obtain

$$R(t) = \exp\left[-\int_0^t r(t)dt\right] \tag{3.44}$$

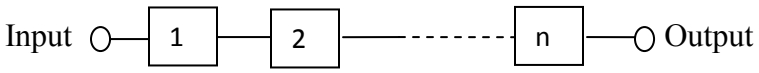

Figure 3.8 Block diagram of a series system

A system is called a series system when it fails whenever any one of its components fails. The components need not be physically connected in series for the system to be called a series system. A typical block diagram of a series system is shown in Figure 3.8. For example, the two tires of a bicycle are considered to be in series to find its reliability because the failure of any one tire makes the bicycle inoperative.

If $F_i(t)$ denotes the probability distribution function of failure time of the i^{th} component, then the failure time distribution of the series system, $F_s(t)$, can be obtained as

$$F_s(t) = P(t_s \leq t) = 1 - \prod_{i=1}^{n} P(t_i > t) = 1 - \prod_{i=1}^{n}(1 - F_i(t)) \tag{3.45}$$

and the reliability of the series system, $R_s(t)$, can be found as

$$R_s(t) = \prod_{i=1}^{n}(1 - F_i(t)) \tag{3.46}$$

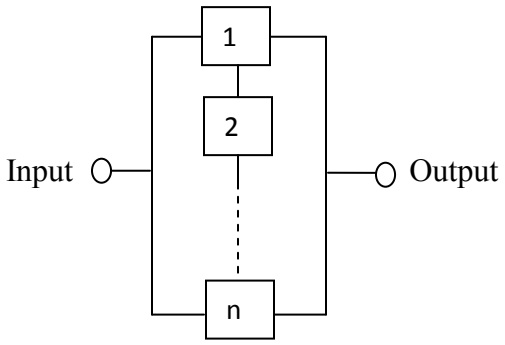

Figure 3.9 Block diagram of a parallel system

A system is called parallel system when it fails only when all of its components fail. The components need not be physically connected in parallel for the system to be called a parallel system. A typical block diagram of a parallel system is shown in Figure 3.9. The failure time distribution of a parallel system, $F_p(t)$, can be obtained as

$$F_p(t) = P\left(t_p \leq t\right) = \prod_{i=1}^{n} F_i(t) \tag{3.47}$$

and its reliability, $R_p(t)$, can be obtained as

$$R_p(t) = 1 - \prod_{i=1}^{n} F_i(t) \tag{3.48}$$

There are many different warranty policies available in practice. Depending upon the type of product, customer and manufacturer, warranty policies can be very simple or very sophisticated. Effective warranty management requires a proper evaluation of the alternative warranty policies. This work considers only consumer warranties, which can further be classified into several categories as indicated below.

(i) Based on the type of remedial action

1) Lump-sum rebate (money- back guarantee)

2) Free replacement

3) Replacement at a reduced cost

4) Some combination of all the above

(ii) Based on the number of criteria used to determine the length of warranty eligibility

1) One dimensional

2) Two dimensional

3) Multi dimensional (more than two)

(iii) Based on whether the warranty is renewal or non-renewal

1) Renewing: Under this warranty all replaced or repaired products are covered whose warranty is identical to that of the original purchased product.

2) Non-renewing: Under this warranty, the coverage extends only over the time remaining in the original warranty period.

3.6.2 Taxonomy for classification of warranties

If a warranty does not require product development after the sale of a product, then the warranty is classified to be of group A, consisting of policies applicable for the sale of a single product, and group B, consisting of policies applicable for the sale of a group of products (called a lot or batch sales). If a product development is involved, then the warranty is classified to be of group C. This division and the remainder of the taxonomy are shown in Figure 3.10. This classification can be further extended based on the dimensionality of the warranty policy.

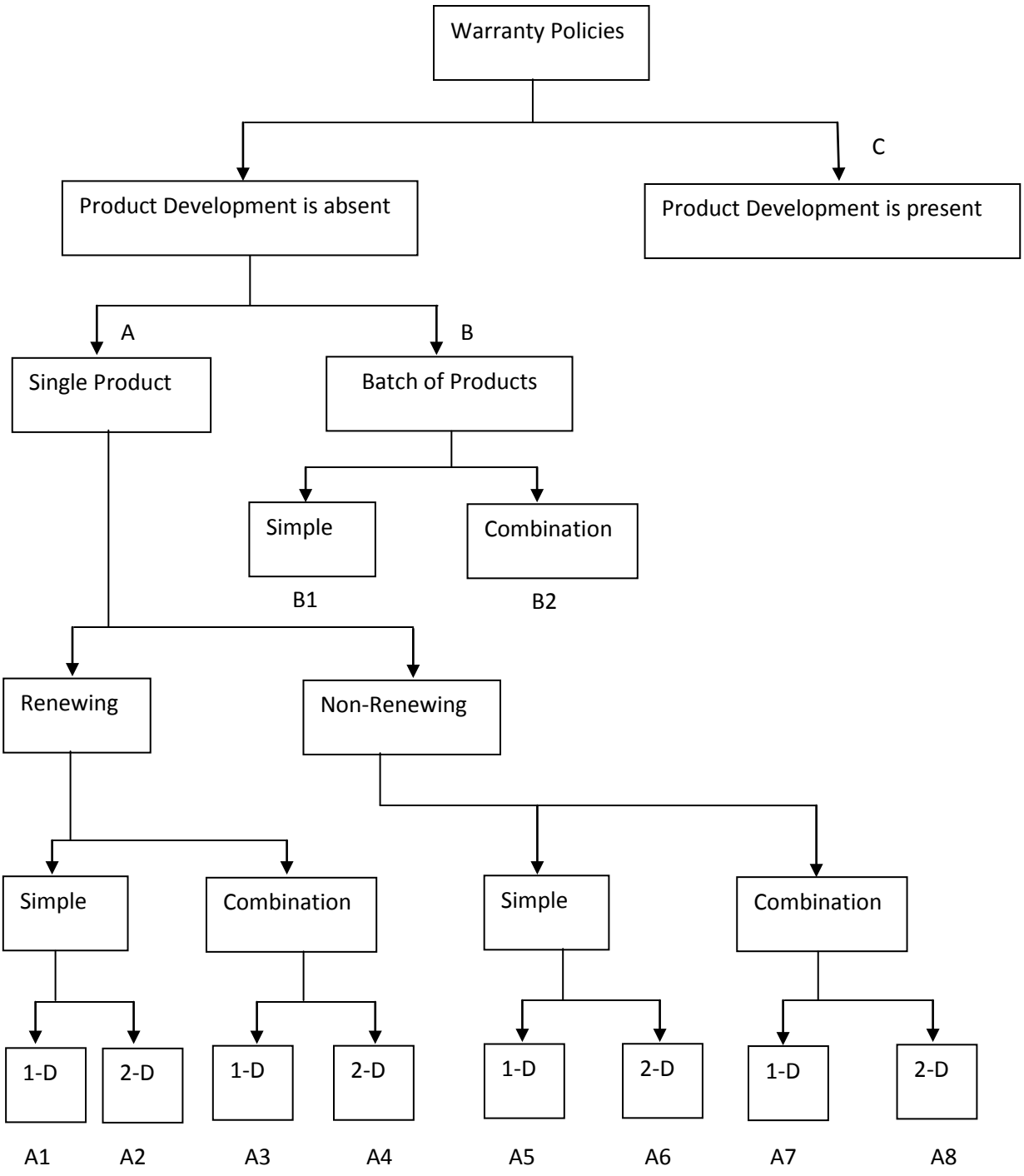

Figure 3.10 Classification of warranty policies [1, 2, 3]

This work considers policies which fall under the category A5, A6 and A7 shown in Figure 3.10. All the warranty policies discussed in this work are non-renewing type. It is assumed that the repair time for all repairable products is equal to zero.

3.6.3 One-dimensional warranty policies

In the one-dimensional warranty policies [30,133], two simple policies, namely Free Replacement Warranty (FRW) and Pro-Rated Warranty (PRW), as well as a combination policy, namely FRW/PRW, are possible.

3.6.3.1 Policy-1: Free Replacement Warranty (FRW) Policy

The manufacturer agrees to repair or provide replacement for failed items free of charge up to a time W from the time of initial purchase. This is a non-renewing and one-dimensional warranty policy applicable for both non-repairable and repairable products.

3.6.3.2 Policy 2: Pro-Rated Warranty (PRW) Policy

The manufacturer agrees to refund a fraction of the purchase price when the product fails before time W from the time of the initial purchase. The buyer or customer receives a cash rebate and is not constrained to buy a replacement product. The cash rebate to the customer may be of different types:

Policy 2a: When the refund is a linear function given by

$$q_1 = \begin{cases} \left(1 - \frac{t}{W}\right) c_b, & 0 \le t < W \\ 0, & \text{otherwise} \end{cases} \tag{3.49}$$

where c_b is the purchase price of the product.

Policy 2b: When the refund is a proportional linear function given by

$$q_2 = \begin{cases} \propto \left(1 - \frac{t}{W}\right) c_b, & 0 \le t < W \\ 0, & \text{otherwise} \end{cases} \tag{3.50}$$

where $0 < \propto < 1$.

Policy 2c: The refund is a quadratic function given by

$$q_3 = \begin{cases} \left(1 - \frac{t}{W}\right)^2 c_b, & 0 \le t < W \\ 0, & \text{otherwise} \end{cases} \tag{3.51}$$

3.6.3.3 Policy-3: Combined Free Replacement Warranty/Pro-Rated Warranty (FRW/PRW) policy

Under this policy, the manufacturer agrees to provide a free replacement of the original product up to time W_1 from the time of initial purchase and any failure in the interval from W_1 *to* W $(> W_1)$ results in a pro-rated refund. The warranty does not renew. From the manufacturer's view point, the rebate function as per the policy is represented as

$$q(t) = \begin{cases} c_s, & 0 \le t < W_1 \\ c_b(W - t)(W - W_1), & W_1 \le t < W \\ 0, & otherwise \end{cases} \tag{3.52}$$

where c_b is the purchase or buyer's price of the product.

3.6.4 Two-dimensional warranty policy [One-dimensional approach]

In the two-dimensional warranty policies [135, 142], a simple non renewing policy, namely the Free Replacement Warranty (FRW), is considered. The procedure to find the corresponding expected warranty cost from the manufacturer's view point can be computed as indicated below.

Policy-4: Free Replacement Policy (FRP)

Under this policy the manufacturer agrees to repair or provide a replacement for the failed product free of charge up to a time *W* or up to a usage *U*, whichever occurs first, from the time of initial purchase. The warranty region is a rectangle [*0, W*) × [*0, U*) as shown in Figure 3.11. *U* and *W* are the parameters of the policy. This policy does not renew. Let $X_c(t)$ and $Y_c(t)$ represent the age and usage for the product at time t, respectively. Let *Y(t)* represent the total usage over the interval [0,*t*), with the first sale at $t = 0$. If no product failure has occurred in [0, *t*), then

$$X_c(t) = t \quad \text{and} \quad Y_c(t) = Y(t) \tag{3.53}$$

This is also true if all the failed items are repaired with their repair times equal to zero. In contrast, if the product is not repairable and if there have been one or more failures in [0, *t*) then $X_c(t) < t$ and $Y_c(t) < Y(t)$ (3.54)

In the one-dimensional approach, we model $Y_c(t)$ as a function of $X_c(t)$. This function characterizes the product usage as a function of the age of the product. This relationship is assumed to be linear with a non negative coefficient *R* as:

$$Y_c(t) = R.X_c(t) \tag{3.55}$$

where *R* represents the usage per unit time or usage rate, and may vary from user to user. We can model it as a random variable with density function *g(r)* so that

$$G(r) = P(R \leq r) \tag{3.56}$$

Three different forms of *G(r)* reflecting different usage rates across the population of buyers are given below:

i) *R* uniformly distributed over [*a, b*], with $0 \leq a \leq b$:

$$g(r) = \begin{cases} \frac{1}{[b-a]}, & for\ a \leq r \leq b \\ 0, & otherwise \end{cases} \tag{3.57}$$

ii) $R = a + A[b\text{-}a]$, with $0 \leq a \leq b$, and A is a random variable with a Beta density function:

$$f_A(x) = \frac{dF_A(x)}{dx} = \frac{x^{p-1}(1-x)^{q-1}}{B(p,q)}, \qquad 0 \leq x \leq 1 \tag{3.58}$$

where $B(p, q)$ is the Beta function. We assume that all the values of R are in the interval $[a, b]$.

iii) R distributed according to the Gamma distribution :

$$g(r) = \frac{r^{p-1}\exp(-r)}{\Gamma(p)}, \qquad 0 \leq r < b,\ p > 0 \tag{3.59}$$

We assume the first form for R i.e., uniformly distributed as defined by equation (3.57) in this policy.

When the usage rate $R = r$ warranty stops at time X_r or W, if

(i) $X_r = \frac{U}{r}$ when $r \geq \gamma_1$ (3.60)

(ii) W when $r < \gamma_1$ where $\gamma_1 = U/W$ (3.61)

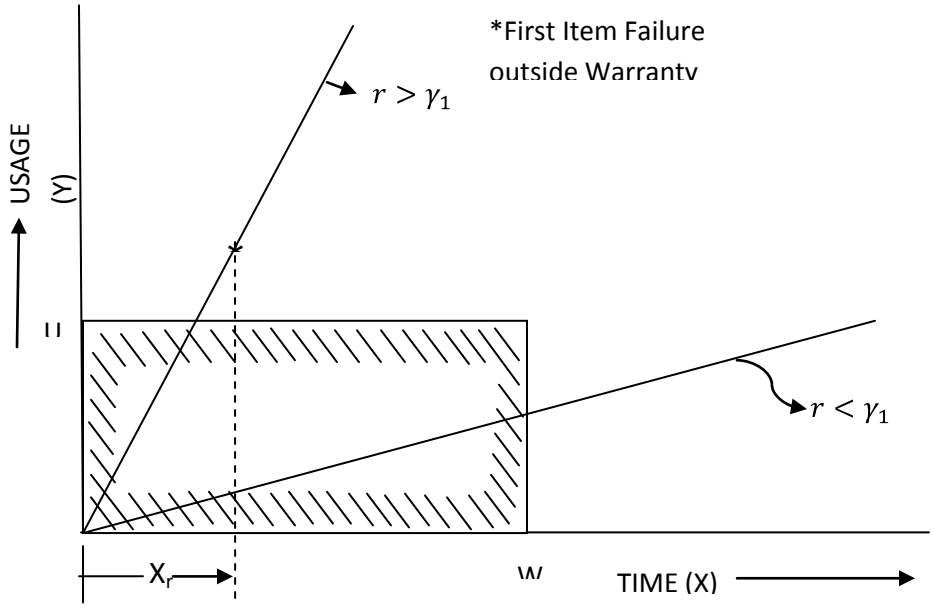

Figure 3.11 Warranty region for policy 4

3.7 SUMMARY

In this chapter, a complete description and basic differences present in different types of evidences are considered through an example. It also describes the important functions of Dempster Shafer theory in detail. This chapter describes the basic concepts of fuzzy theory. It also describes the basic principle of particle swarm optimization algorithm. Game theory was studied for multi-objective optimization problems in detail. Classification of several warranty policies with the one-dimensional and two-dimensional warranty policies studied in detail. In the next chapter, a selection procedure is described to select the most suitable combination rule to combine various evidences obtained from multiple sources.

CHAPTER 4

COMPARISON OF VARIOUS EVIDENCE-COMBINATION RULES

4.1 OVERVIEW

For the uncertainty quantification (UQ), both deterministic and non-deterministic analysis is used in many engineering applications. Various UQ methods are applied to propagate and quantify the uncertainty present in a system based on the nature of uncertainty. As stated in chapter 3, in general, uncertainty can be broadly classified in to two types. The first one is aleatory uncertainty (also referred to as stochastic or inherent or irreducible uncertainty) - It results from the fact that a system can behave in random ways. The second one is epistemic uncertainty (also known as subjective or reducible uncertainty) - It is the uncertainty of the outcome of some random event due to lack of knowledge or information in any phase or activity of the modeling process. By gaining more information about the system and its environmental factors, one can reduce the epistemic uncertainty [50].

Conventionally, probability theory has been used to characterize both aleatory and epistemic uncertainties. However, the recent developments in the characterization of uncertainty reveal that traditional probability theory provides an inadequate model to capture epistemic uncertainty. It is recognized that probability theory is best suited to deal with aleatory uncertainty. The present study uses Dempster-Shafer theory (DST) as the framework for representing uncertainty and investigates the issue of combination of evidence. The application of various combination rules like Dempster's rule, Yager's

rule, Inagaki's extreme rule, Zhang's center combination rule and Murphy's average combination rule for representing uncertainty and combining evidences from multiple sources is investigated. In section 3.2, a review of the DST, along with some important functions, is given. Following that, in section 4.2, we state and explain in detail all the five different types of combination rules in the context of both robbery and automobile examples. The detailed procedures to apply all the evidence combinations rules are described in Appendix-A for these two examples. After understanding the basic characteristics of all the combination rules for combining evidence from multiple sources, we outline a procedure for selecting an appropriate rule in section 4.3. In section 4.4, an engineering application, the welded beam design problem, is solved for combining evidence from various evidence sets based on the proposed selection procedure to find the most suitable combination rule to be applied. In section 4.5, results are presented along with a comparative analysis of the combination rules when applied to each of the evidence sets. A summary of the chapter is given in the last section 4.6.

4.2 COMBINATION RULES BASED ON DST

The versatility of DST is the motivation for selecting DST to represent and combine different types of evidence obtained from multiple sources [74,185,181,190]. The various combination rules to combine evidence obtained from multiple sources are discussed in this section.

4.2.1 Dempster's rule of combination

Dempster's rule of combination was introduced to enable the computation of the orthogonal sum of given evidences from multiple sources. Dempster's rule uses bpa's to combine multiple evidences. Although the bpa's are assumed to be from independent bodies of evidence, they are defined on the same frame of discernment. One of the important areas of research in DST is the effect of independence of the bodies of evidence when combining evidence [96, 97, 98]. The Dempster's rule involves a conjunctive operation (AND) for combining evidence. Two bpa's m_1 and m_2 can be combined to yield a new bpa m_{12} denoted as $m_{12} = m_1 \oplus m_2$ .Specifically, the combined bpa (m_{12}) is calculated from the two bpa's m_1 and m_2 as [1]:

$$m_{12}(A) = \frac{\sum_{B \cap C = A} m_1(B) m_2(C)}{1 - k_I} \quad where \quad A \neq \phi \tag{4.1}$$

$$m_{12}(\phi) = 0 \tag{4.2}$$

$$\text{where } k_I = \sum_{B \cap C = \phi} m_1(B) m_2(C) \tag{4.3}$$

Equation (4.1) can be generalized to obtain $m_{12\ldots n} = m_1 \oplus m_2 \ldots \oplus m_n$, for combining the bpa structures m_1, m_2, m_3 .... m_n from 'n' different sources of evidences as

$$m_{12\ldots n}(A) = \frac{\sum_{A_1 \cap A_2 \ldots \cap A_n = A} m_1(A_1).m_2(A_2) \ldots m_n(A_n)}{1 - k_{II}} \quad where \quad A \neq \phi \tag{4.4}$$

$$m_{12\ldots n}(\phi) = 0 \tag{4.5}$$

$$\text{where } k_{II} = \sum_{A_1 \cap A_2 \ldots A_n = \phi} m_1(A_1) m_2(A_2) \ldots m_n(A_n). \tag{4.6}$$

The denominators in equations (4.1) and (4.4), $1-k_I$ and $1-k_{II}$, are called the normalization factors while k_I and k_{II} are called conflicts. Thus the normalization process not only ignores conflict but also attributes the bpa associated with conflict to the null set [57, 66, 71, 81, 128]. In addition, the normalization will yield counterintuitive results when significant conflict is present in certain contexts. Thus, the DST rule is not suitable for situations where there is considerable inconsistency in the available evidence. However, it is applicable, when there is some degree of consistency or sufficient agreement among the opinions of different sources. Thus the normalization of the DST rule yields counter intuitive results if the DST combination rule is applied to Zadeh's example [190]. In the Zadeh's example, there is one failed sensor among three sensors; *A*, *B* and *C*. The frame of discernment consists of three elementary propositions, $\Theta = \{A, B, C\}$, where $\{A\}$ means that *A* is the failed sensor. Let E_1 be the evidence which states that $m(\{A\})$ is 0.99 and $m(\{C\})$ is 0.01. Let E_2 be the evidence which states that $m(\{B\})$ is 0.99 and $m(\{C\})$ is 0.01. If, DST rule is used to combine the evidences E_1 and E_2, it yields, with certainty, that *C* is the failed sensor which is counter intuitive in the presence of the given evidences E_1 and E_2. The results given by different combination rules, when applied to Zadeh's example, are shown in Table 4.1.

Table 4.1 Results given by different combination rules when applied to Zadeh's example

	A	B	C
E1	0.99	0	0.01
E2	0	0.99	0.01
Dempster's rule	0	0	1
Yager's rule	0	0	0.0001
Inagaki's rule	0	0	1
Zhang's rule	0	0	1
Murphy's rule	0.499	0.499	0.0002

Robbery example: There was a robbery in a house and there are three suspects, *A*, *B* and *C*, the frame of discernment consists of three elementary propositions, $\Theta = \{A, B, C\}$, where, for example, $\{A\}$ means that *A* is the thief. Let the witnesses or evidences (E_1 and E_2) be as shown in Table 4.2.

Table 4.2 Evidence for the robbery problem

	A	B	C	Θ
E1	0.5	0.1	0.1	0.3
E2	0.6	0.1	0.1	0.2

Dempster's rule is applied. The resulting belief intervals for the three suspects are tabulated in Table 4.3.

4.2.2 Yager's rule of combination

Subsequent to DST, Yager proposed an alternative rule of combination in which all contradiction is attributed to total ignorance. He introduced the concept of a quasi-associative operator because in many cases the evidence combination requires a non-associative operator. Yager's combination rule differs from Dempster's rule in the way of handling the conflict. Yager used the term "ground probability mass assignment", designated q [214]. The main differences between the basic probability assignment and the ground probability assignment lie in the normalization factor and the mass assigned to the frame of discernment (Θ), which implies total ignorance. According to Yager's rule, the combined ground probability mass assignment is defined as follows

$$q(A) = \sum_{B \cap C = A} m_1(B) m_2(C) \tag{4.7}$$

where $q(A)$ denotes the ground probability assignment associated with *A*. Equation (4.7) is same as Equation (4.1) with no denominator. Because Yager's combination rule is not associative, for combining bpa structures $m_1, m_2, m_3 \ldots m_n$ from '*n*' different sources of evidence, Yager's defines the combined bpa structure for any focal element *A* as

$$q(A) = \sum_{A_1 \cap A_2 \cap \ldots A_n = A} m_1(A_1).m_2(A_2) \ldots m_n(A_n) \tag{4.8}$$

In this formulation, normalization is avoided by allowing the ground probability mass assignment of the null set to be greater than zero, i.e., $q(\phi) \geq 0$. It is calculated exactly as k_1 in equation (4.3) of the Dempster's rule. The ground probabilities are converted to the basic probability assignment of the universal set $m^Y(\Theta)$ as:

$$m^Y(\Theta) = q(\Theta) + q(\phi) \tag{4.9}$$

where $q(\phi)$ and $q(\Theta)$ are the ground probability assignment of the null set and universal set, respectively.

When the conflict is equal to zero, (k=0 or $q(\phi) = 0$), Yager's rule yields the same result as Dempster's rule, and implies that

$$m^Y(\phi) = 0. \tag{4.10}$$

$$m^Y(A) = q(A) \tag{4.11}$$

The bpas associated with Yager's rule (m^Y) and Dempster's rule (m) are not the same. The following relations are valid between the ground probability assignments and the bpas of Dempster's rule:

$$m(\phi) = 0 \tag{4.12}$$

$$m(\Theta) = \frac{q(\Theta)}{1 - q(\phi)} \tag{4.13}$$

$$m(A) = \frac{q(A)}{1 - q(\phi)} \text{ where } A \neq \phi, \Theta \tag{4.14}$$

In Yager's rule, there is no normalization or scaling to the resulting combined evidence and the mass associated with conflict, $m(\phi)$, will appear as ignorance in the belief interval. The distinctive feature of Yager's combination rule is shown in equation (4.9). When there is any contradiction among the evidences from different sources, the Yager's combination rule treats that contradiction as coming from ignorance. If there is any additional knowledge, then this contradiction might be resolved. The Yager's combination rule is more conservative than the Dempster's combination rule. In the case of Zadeh's example, Yager's rule combines the evidences E_1 and E_2 to indicate, with very small evidence, that *C* is the failed sensor which is closer to the intuitively expected result

based on the given evidences $E_1$and E_2; this is better than the one indicated by the Dempster-shafer theory. For the robbery example, with evidences given in Table 4.2, the belief intervals for the three suspects given by Yager's rule are tabulated in Table 4.3. It can be seen that Dempster's and Yager's rules give the same combined result3ing bpa structures when $q\{\phi\} = 0$.

4.2.3 Inagaki's rule of combination

Inagaki [83] proposed a combination rule using the ground probability assignment function (q), introduced by Yager, to define a continuous parameterized class of rules to combine evidences which include both Dempster's and Yager's rules. According to Inagaki, any combination rule can be expressed as

$$m(C) = q(C) + f(C)q(\phi) \quad \text{where } C \neq \phi \tag{4.15}$$

$$\sum_{C\subset\Theta, C\neq\phi} f(C) = 1 \tag{4.16}$$

$$f(C) \geq 0 \tag{4.17}$$

In Eq. (4.15), the function f can be called a scaling function for $q(\phi)$ with the conflict (k) defined by

$$k = \frac{f(C)}{q(C)} \text{ for any } C \neq \phi, \Theta \tag{4.18}$$

Inagaki's class of combination rules is constrained to satisfy the property:

$$\frac{m(C)}{m(D)} = \frac{q(C)}{q(D)} \tag{4.19}$$

for any nonempty sets C and D which are distinct from Θ or ϕ. If a weighting factor is applied to the evidence, based on some additional knowledge about the credibilities of the

sources, then it would change the ratio in Eq. (4.19) and thus the equality is not satisfied. As a result of constraint of Eq. (4.19) and its implication, Inagaki's rule applies only to situations where information regarding the credibilities or reliabilities of the sources is not available. From Eq. (4.15), the constraint of Eq. (4.16) and the definition of *k* (Eq. (4.18)), Inagaki's unified combination rule (denoted m^U) is derived as follows:

$$m^U(C) = [1 + kq(\phi)]q(C), \quad \text{where} \quad C \neq \Theta, \phi \tag{4.20}$$

$$m^U(\Theta) = [1 + kq(\phi)]q(\Theta) + [1 + kq(\phi) - k]q(\phi) \tag{4.21}$$

$$\text{where } 0 \leq k \leq \frac{1}{1 - q(\phi) - q(\Theta)} \tag{4.22}$$

From Inagaki's rule, Dempster's rule can be obtained by setting $k = [1 - q(\phi)]^{-1}$ and Yager's rule can be realized when *k* = 0 in equations (4.20) to (4.22). Since *k* is continuous-valued, the unified rule of combination results in an infinite number of rules of combination, as shown in Figure 4.1.

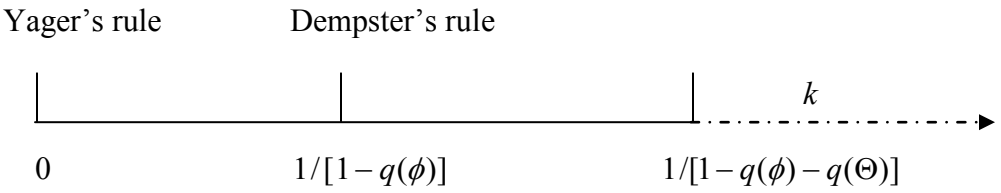

Figure 4.1 Inagaki's rule of combination with different values of the parameter *k*

Inagaki's extreme rule, also called "the extra rule", can be obtained by setting the value of *k* equal to the upper bound indicated in equation (4.22) so that

$$m^U(C) = \frac{1 - q(\Theta)}{1 - q(\phi) - q(\Theta)} . q(C), \quad \text{where} \quad C \neq \Theta \tag{4.23}$$

$$m^U(\Theta) = q(\Theta) \tag{4.24}$$

It is clear from Figure 4.1 that Inagaki's extreme rule is nothing but the extrapolation of Yager's and Dempster's rules of combination with k set equal to its upper bound. As Inagaki's extra combination rule is not associative when combining bpa structures m_1, m_2, m_3, ..., m_n from 'n' different sources of evidences, Yager's ground probability function for the combined bpa structure for any focal element C, can be used, with equations (4.8) and (4.23), to obtain Inagaki's combined bpa.

The difference between DST's rule and Inagaki's extreme rule is that only conflict, $m(\phi)$, is used in the normalization/scaling of the combined evidence in DST's rule while both conflict and the degree of ignorance (mass associated with the universal set, $m(\Theta)$) are used in the scaling of the combined evidence in Inagaki's extreme rule. For the Zadeh's example considered in section 4.2.1, the Inagaki's extreme rule is used to combine the evidences E_1 and E_2 to indicate with certainty, that C is the failed sensor which is same as the one indicated by Dempster's rule. This result is counter intuitive with the given evidences E_1 and E_2. The results are tabulated in Table 4.1. For the robbery example, with evidences shown in Table 4.2, Inagaki's extreme rule yields the belief intervals for the three suspects as shown Table 4.3.

4.2.4 Zhang's combination rule

Zhang [221] introduced a combination rule as an alternative to the Dempster's rule in which a two frame interpretation of DST is offered. Let S and T denote two frames of discernment- these could be the opinions of two experts. Let C, a subset of the Cartesian product $S \times T$, be a compatibility set between the two frames. In this case, we are concerned with the truth in T but the probability P is available for the truth in S. The

information about S provides some information on T due to the presence of the compatibility relation. This information on T is described in the form of a belief function for any subset A of T, which can be written as

$$Bel(A) = P\{s \mid s \in S \text{ such that for all } t \text{ if } (s,t) \in C, \text{then } t \in A\} \tag{4.25}$$

This two frame interpretation of DST is used to propagate evidence through logical links. We get evidence in one frame of discernment from its logical link to another frame. If the information available for the elements of S and T is denoted by s and t respectively, through the compatibility relation (C), then DST can represent the relationship, C, between s and t by a subset of the joint frame $S \times T$. For the two frame model, a subset C_s of T is defined for each $s \in S$ through the compatibility relation $C_s = \{t \mid (s,t) \in C\}$. Thus, the bpa over T can be defined by

$$m(A) = \sum \{P(C_s) \mid s \in S \text{ such that } C_s = A\} \tag{4.26}$$

The belief function of A, as calculated using equation (4.26), is exactly the same as given by equation (4.25) :

$$Bel(A) = \sum \{P(s) \mid C_s \subset A\} \tag{4.27}$$

The plausibility function is given by

$$Pl(A) = \sum \{P(s) \mid C_s \cap A \neq 0\} \tag{4.28}$$

where bpa of $P(s)$ is assigned to C_s.

We use a moderate approach to include only a portion of *P(s)* in equation (4.27) which leads to the center probability P_c given by

$$P_c(A) = \sum_s \frac{|A \cap C_s|}{|C_s|} P(s) \tag{4.29}$$

where $|.|$ represents cardinality.

Zhang's rule of combination introduces a measure of the intersection of the two sets A and B assuming them to be finite. The measure of intersection is the ratio of the cardinality of the intersection of the two sets divided by the product of the cardinality of the individual sets. Thus the measure of intersection of the sets A and B, denoted *r*(A,B), is given by

$$r(A,B) = \frac{|A \cap B|}{|A||B|} = \frac{|C|}{|A||B|} \tag{4.30}$$

where $A \cap B = C$. The use of equation (4.30) in the combination rule reduces to the moderate approach indicated by equation (4.29). Zhang's combination rule scales the products of the bpa's of the intersecting sets ($A \cap B = C$) with *r*(A,B), given by equation (4.30). This process is repeated for all intersecting pairs that give C. The scaled products of all bpa's whose intersection equals C are added and then multiplied by a factor $\tilde{k}$ where $\tilde{k}$ denotes a renormalization factor which is independent of C, m_1, and m_2. This renormalization factor makes the summation of the bpa's equal to 1:

$$m(C) = \tilde{k} \sum_{A \cap B = C} [\frac{|C|}{|A||B|} m_1(A) m_2(B)] \tag{4.31}$$

It can be seen that this rule corresponds to the Dempster's rule when |C| = |A||B|. Dempster's rule fails to consider the intersection of focal elements. There are many other ways to define the measure of intersection instead of equation (4.30) and thus many combination rules can be devised from the Zhang's combination by defining a particular measure of intersection in equation (4.31). This rule is commutative but not associative, idempotent, or continuous. As Zhang's combination rule is not associative when

combining bpas $m_1, m_2, m_3, ..., m_n$ from 'n' different sources of evidence, equation (4.31) can be modified as

$$m(C) = \tilde{k} \sum_{A_1 \cap A_2 \ldots \cap A_n = C} [\frac{|C|}{|A_1||A_2|\ldots|A_n|} m_1(A_1) m_2(A_2) \ldots m_n(A_n)] \quad (4.32)$$

where $C = |A_1 \cap A_2 \ldots \cap A_n|$.

For the Zadeh's example considered in section 4.2.1, Zhang's rule combines the evidences $E_1$and E_2 to state, with certainty, that *C* is the failed sensor which is same as the one given by the Dempster's rule a counter intuitive result with the given evidences $E_1$and E_2 and the results are shown in Table 4.1. For the robbery example with evidences shown in Table 4.2, the application of Zhang's rule gives the belief intervals for the three suspects as indicated in Table 4.3.

4.2.5 Murphy's average combination rule

Murphy's average rule [145] of combination uses the average of all bpas to define a new combined bpa. This average method has many attractive properties like convergence towards certainty of any particular event. To improve the performance of convergence, Murphy introduced the average belief in the combination rule. Thus, the initial averaging of bpas is followed by combining the evidence using DST 'n-1' times where 'n' is the number of evidences [216]. This approach solves the problem of combining conflicting evidences efficiently. The average of all bpas is recommended in situations where one source of evidence contradicts with several other sources of evidence that are consistent, to preserve the opinion from the majority of sources. When one of the sources is unreliable, but it is not clear which source it is, to reduce the effect

of that particular source on combination to some extent, Murphy's average combination rule is used. Thus, the averaging process identifies the combination problems, shows the distribution of belief and preserves a record of unassigned belief (ignorance). For the Zadeh's example considered in section 4.2.1, the Murphy's rule combines the evidences $E_1$and E_2 to state equal evidences of 0.499 for *A* and *B* with very small evidence for *C* , which means that the failed sensor can be *A* or *B* and the results are shown in Table 4.1. For the robbery example with evidences as shown in Table 4.2, the application of Murphy's average combination rule gives the belief intervals for the three suspects as indicated in Table 4.3.

Table 4.3 Robbery example: Results given by various combination rules

Rule used to combine evidences E1 and E2	Belief Interval for A	Belief Interval for B	Belief Interval for C	$m(\Theta)$
Dempster's rule	[0.7631,0.8421]	[.0789,0.1578]	[.0789,0.1578]	0.0789
Yager's rule	[0.5800,0.8800]	[0.0600,0.3600]	[0.0600,0.3600]	0.3000
Inagaki's rule	[0.7788,0.8388]	[0.0805,0.1405]	[0.0805,0.1405]	0.0600
Zhang's rule	[0.8428,0.8857]	[0.0571,0.1000]	[0.0571,0.1000]	0.0428
Murphy's rule	[0.7598,0.8421]	[0.0789,0.1611]	[0.0789,0.1611]	0.0822

4.2.6 Discussions and Additional Examples [202]

The following observations can be made from the results given by the various combination rules applied to the robbery example.

1. As evidences, in terms of the mass assigned to thief *A,* differ by 0.1, it makes consonant type of evidence available for combination.
2. It is clear that all combination rules converge to prove that *A* is the thief but the degree of the belief assigned to *A* by different combination rules is different.
3. The belief assigned to thief *A* has been predicted to lie between 0.7 to 0.8 based on the evidences E_1 and E_2.
4. The ignorance is less and belief assigned to thief *A* is high in case of Zhang's rule which indicates that convergence is much quicker with this rule.
5. The Yager's rule yields pessimistic conclusion for the belief (low value) assigned to *A* and hence the associated ignorance is very high (0.3).
6. The belief for *A* has slightly larger values in the values predicted by the Murphy's rule, Dempster's rule and Inagaki's rule in this order, but the conclusion about the thief is same for all these three rules. There is slight change in the scaling done on the combined evidence for the results obtained by using Dempster and Inagaki combination rules.
7. There is slow decrease in the degree of ignorance associated with thief A in the same order of rules as in point 6. This shows that the degree of ignorance and the belief are inversely proportional to each other.
8. If there is any additional evidence available or any information available on the reliabilities of the sources of evidence then we can physically justify which one of these three (Dempster's, Inagaki's, and Murphy's) rules can be applied.

Automobile example:

Consider an automobile with two states- safe to drive and unsafe to drive. The frame of discernment, consisting of the two states can be denoted as $\Theta = \{I, II\}$, where $\{I\}$ means that the automobile is safe to drive and $\{II\}$ means that it is unsafe to drive. Let the evidences (E_1 and E_2) be as shown in Table 4.4.

Table 4.4 Evidence for the automobile problem

	A	B	Θ
E1	0.5	0.3	0.2
E2	0.6	0.1	0.3

When the safety analysis of the automobile is conducted using the various rules of combination (using the procedures described in the case of the robbery example), the results shown in Table 4.5 can be obtained.

Table 4.5 Results given by different combination rules for the safety analysis of an automobile

Rule used to combine evidences E1 and E2	Belief Interval for I	Belief Interval for II	$m(\Theta)$
Dempster's rule	[0.7402,0.8181]	[0.1818,0.2597]	0.0779
Yager's rule	[0.57,0.86]	[0.14,0.43]	0.29
Inagaki's rule	[0.7546,0.8146]	[0.1853,0.2453]	0.06
Zhang's rule	[0.7909,0.8454]	[0.1545,0.2090]	0.0545
Murphy's rule	[0.7403,0.8205]	[0.1794,0.2596]	0.0801

The following observations can be made from the results of the automobile safety problem regarding the characteristics of the various combination rules:

1. All the combination rules predict that the automobile is safe to drive but the degree of the belief assigned to *I* is different for different rules.
2. The belief assigned to the condition, automobile is safe (I) can be intuitively predicted to be around 0.75 based on the given evidences (as by summing the evidences given E_1 and E_2).
3. Zhang's rule gives a maximum belief (more than 0.75) for the safe condition of the automobile (I). Hence, this rule is not applicable for this example.
4. In the safety analysis of the automobile, the rule that predicts the lowest belief for the safe condition of the automobile (I) is considered to be the best rule of evidence combination (a conservative result). From this point of view, the Yager's rule can be considered as the best combination rule for this example.
5. In the failure analysis of the automobile, the rule that predicts the highest belief for the unsafe condition of the automobile (II) is considered to be the best rule of evidence combination. Inagaki's extreme rule can be considered as the best combination rule for this example.

Fault sensor example:

There are three sensors out of which there is one faulty sensor. The frame of discernment consists of three states, $\Theta = \{A, B, C\}$, where $\{A\}$ means that sensor A is identified to be faulty. The evidences E_1 and E_2 are as follows.

$$E_1: \begin{array}{l} m\{A\} = 0,\ m\{B\} = 0, m\{C\} = 0, m\{A, B\} = 0.1, m\{B, C\} = 0.2, m\{C, A\} = .3, \\ m\{\Theta\} = 0.4 \end{array}$$

$$E_2: \begin{array}{l} m\{A\}=0,\ m\{B\}=0, m\{C\}=0, m\{A,B\}=0.1, m\{B,C\}=0.2, m\{C,A\}=.3, \\ m\{\Theta\}=0.4 \end{array}$$

When the fault sensor evidence is combined using all the five rules of combination (using the procedure indicated for the robbery example), the results are as shown in Table 4.6. Here we observe that all combination rules, except Zhang's rule, give the same combined evidence.

Table 4.6 Results of various combination rules for a fault sensor example

Combination rule E1 & E2	Belief Interval for A	Belief Interval for B	Belief Interval for C
DST	[0.06,0.64]	[0.04,0.49]	[0.12,0.81]
Yager's	[0.06,0.64]	[0.04,0.49]	[0.12,0.81]
Inagaki's	[0.06,0.64]	[0.04,0.49]	[0.12,0.81]
Zhang's	[0.0443,0.6650]	[0.2955,0.4975]	[0.0886,0.8325]
Murphy's	[0.06,0.64]	[0.04,0.49]	[0.12,0.81]

Target identification example:

There are three targets A, B, and C out of which there is one required target. The frame of discernment consists of three states, $\Theta = \{A, B, C\}$, where $\{A\}$ means that target A is the required target. The evidences E_1 and E_2 are as follows.

$$E_1: \begin{array}{l} m\{A\}=a_1, m\{B\}=b_1, m\{C\}=c_1, m\{A,B\}=d_1, m\{B,C\}=e_1, m\{C,A\}=f_1, \\ m\{\Theta\}=1-a_1-b_1-c_1-d_1-e_1-f_1 \end{array}$$

$$E_2: \begin{array}{l} m\{A\}=a_2, m\{B\}=b_2, m\{C\}=c_2, m\{A,B\}=d_2, m\{B,C\}=e_2, m\{C,A\}=f_2, \\ m\{\Theta\}=1-a_2-b_2-c_2-d_2-e_2-f_2 \end{array}$$

such that $a_i + b_i + c_i + d_i + e_i + f_i \le 1$

$a_i, b_i, c_i, d_i, e_i, f_i \ge 0$ and $a_i, b_i, c_i, d_i, e_i, f_i \le 1$ where $i = 1, 2$

The evidences E_1 and E_2 are generalized to combine two sources of evidence by using all rules of combination. Thus, we can formulate ten optimization problems so that we can make comparisons among the five different combination rules. These optimization problems are formulated as follows:

Maximize (i) $\left|bel\{A\}_{dst} - bel\{A\}_{Yager}\right|$, (ii) $\left|bel\{A\}_{dst} - bel\{A\}_{Inagaki}\right|$,

(iii) $\left|bel\{A\}_{dst} - bel\{A\}_{Zhang}\right|$, (iv) $\left|bel\{A\}_{dst} - bel\{A\}_{Murphy}\right|$

(v) $\left|bel\{A\}_{Yager} - bel\{A\}_{Ingaki}\right|$, (vi) $\left|bel\{A\}_{Yager} - bel\{A\}_{Zhang}\right|$

(vii) $\left|bel\{A\}_{Yager} - bel\{A\}_{Murphy}\right|$, (viii) $\left|bel\{A\}_{Ingaki} - bel\{A\}_{Zhang}\right|$

(ix) $\left|bel\{A\}_{Ingaki} - bel\{A\}_{Murphy}\right|$, (x) $\left|bel\{A\}_{Zhang} - bel\{A\}_{Murphy}\right|$

to find the values of $a_i, b_i, c_i, d_i, e_i,$ and f_i where i = 1, 2. The evidence and optimization results are tabulated for the ten optimization problems (which are solved by using MATLAB optimization toolbox) in Table 4.7. The examples discussed so far indicate that the five rules of combination have some distinct features and some similarities which are summarized in section 4.

Table 4.7(a) Results of Optimization problems for target identification example

Optimization prob. no.	Evidence	Optimization result
(i)	$\mathrm{E}_1 : m\{A\} = 0.025602, m\{B\} = 0, m\{C\} = 0.974397,$ $m\{A,B\} = 0, m\{B,C\} = 0, m\{C,A\} = 0, m\{\Theta\} = 0$ $\mathrm{E}_2 : m\{A\} = 0.659464, m\{B\} = 0.340535, m\{C\} = 0,$ $m\{A,B\} = 0, m\{B,C\} = 0, m\{C,A\} = 0, m\{\Theta\} = 0$	$bel\{A\}_{dst} = 1$ $bel\{A\}_{Yager}$ =0.026287
(ii)	$\mathrm{E}_1 : m\{A\} = 0, m\{B\} = 0.459944, m\{C\} = 0.0380693,$ $m\{A,B\} = 0, m\{B,C\} = 0.001957, m\{C,A\} = 0, m\{\Theta\} = 0$ $\mathrm{E}_2 : m\{A\} = 0.719157, m\{B\} = 0, m\{C\} = 0,$ $m\{A,B\} = 0, m\{B,C\} = 0, m\{C,A\} = 0, m\{\Theta\} = 0$	$bel\{A\}_{dst}$ =0.5614 $bel\{A\}_{Ingaki}$ =0.6181
(iii)	$\mathrm{E}_1 : m\{A\} = 0.000022, m\{B\} = 0.368645, m\{C\} = 0,$ $m\{A,B\} = 0, m\{B,C\} = 0.631332, m\{C,A\} = 0, m\{\Theta\} = 0$ $\mathrm{E}_2 : m\{A\} = 0.999927, m\{B\} = 0, m\{C\} = 0,$ $m\{A,B\} = 0, m\{B,C\} = 0, m\{C,A\} = 0.000072, m\{\Theta\} = 0$	$bel\{A\}_{dst}$ =0.3337 $bel\{A\}_{Zhang}$ =0.6670
(iv)	$\mathrm{E}_1 : m\{A\} = 0, m\{B\} = 0.569640, m\{C\} = 0.162148,$ $m\{A,B\} = 0, m\{B,C\} = 0.268210, m\{C,A\} = 0, m\{\Theta\} = 0$ $\mathrm{E}_2 : m\{A\} = 0.999999, m\{B\} = 0, m\{C\} = 0,$ $m\{A,B\} = 0, m\{B,C\} = 0, m\{C,A\} = 0.000001, m\{\Theta\} = 0$	$bel\{A\}_{dst} = 0$ $bel\{A\}_{Murphy}$ =0.5508
(v)	$\mathrm{E}_1 : m\{A\} = 0.009722, m\{B\} = 0.012754,$ $m\{C\} = 0.762340, m\{A,B\} = 0, m\{B,C\} = 0.215182,$ $m\{C,A\} = 0, m\{\Theta\} = 0$ $\mathrm{E}_2 : m\{A\} = 1.00000, m\{B\} = 0, m\{C\} = 0,$ $m\{A,B\} = 0, m\{B,C\} = 0, m\{C,A\} = 0., m\{\Theta\} = 0$	$bel\{A\}_{Yager}$ =1 $bel\{A\}_{Ingaki}$ =0.0097

Table 4.7(b) Results of Optimization problems for target identification example

Optimization prob. no.	Evidence	Optimization result
(vi)	$\mathrm{E}_1 : m\{A\}=0, m\{B\}=0.965897, m\{C\}=0,$ $m\{A,B\}=0.034102, m\{B,C\}=0, m\{C,A\}=0, m\{\Theta\}=0$ $\mathrm{E}_2 : m\{A\}=0.002895, m\{B\}=0, m\{C\}=0.689361,$ $m\{A,B\}=0, m\{B,C\}=0, m\{C,A\}=0.307743, m\{\Theta\}=0$	$bel\{A\}_{Yager}$ =0.01059 $bel\{A\}_{Zhang}$ =1
(vii)	$\mathrm{E}_1 : m\{A\}=0, m\{B\}=0.5000, m\{C\}=0.5000,$ $m\{A,B\}=0, m\{B,C\}=0, m\{C,A\}=0, m\{\Theta\}=0$ $\mathrm{E}_2 : m\{A\}=1.0000, m\{B\}=0, m\{C\}=0,$ $m\{A,B\}=0, m\{B,C\}=0, m\{C,A\}=0, m\{\Theta\}=0$	$bel\{A\}_{Yager}$ =0 $bel\{A\}_{Murphy}$ =0.6666
(viii)	$\mathrm{E}_1 : m\{A\}=0.999147, m\{B\}=0, m\{C\}=0,$ $m\{A,B\}=0.000852, m\{B,C\}=0, m\{C,A\}=0, m\{\Theta\}=0$ $\mathrm{E}_2 : m\{A\}=0.000315, m\{B\}=0, m\{C\}=0.259569,$ $m\{A,B\}=0, m\{B,C\}=0.740115, m\{C,A\}=0, m\{\Theta\}=0$	$bel\{A\}_{Ingaki}$ =0.3332 $bel\{A\}_{Zhang}$ =0.6664
(ix)	$\mathrm{E}_1 : m\{A\}=0, m\{B\}=0.756344, m\{C\}=0,$ $m\{A,B\}=0.243655, m\{B,C\}=0, m\{C,A\}=0, m\{\Theta\}=0$ $\mathrm{E}_2 : m\{A\}=0.775325, m\{B\}=0, m\{C\}=0.224674,$ $m\{A,B\}=0, m\{B,C\}=0, m\{C,A\}=0, m\{\Theta\}=0$	$bel\{A\}_{Ingaki}$ =1 $bel\{A\}_{Murphy}$ =0.4823
(x)	$\mathrm{E}_1 : m\{A\}=0, m\{B\}=0.994440, m\{C\}=0,$ $m\{A,B\}=0.005559, m\{B,C\}=0, m\{C,A\}=0, m\{\Theta\}=0$ $\mathrm{E}_2 : m\{A\}=0.002833, m\{B\}=0, m\{C\}=0.997166,$ $m\{A,B\}=0, m\{B,C\}=0, m\{C,A\}=0., m\{\Theta\}=0$	$bel\{A\}_{Zhang}$ =1 $bel\{A\}_{Murphy}$ =0.000019

The following observations can be made from the results of the optimization problems in Tables 4.7(a) and 4.7(b) for the target identification problem: given

1. The results obtained using DST rule in comparison with other combination rules indicate that the difference in the belief for the target A between DST and Yager's rules is 0.9738 (maximum) while it is 0.0567 (minimum) between DST and Inagaki's rules.
2. The results obtained using Yager's rule in comparison with other combination rules indicate that the difference in the belief for the target A between Yager's and Inagaki's rules is 0.9903 (maximum) while it is 0.6666 (minimum) between Yager's and Murphy's rules.
3. The results obtained using Inagaki's rule in comparison with other combination rules indicate that the difference in the belief for the target A between Inagaki's and Yager's rules is 0.9903 (maximum) while it is 0.3332 (minimum) for between Inagaki's and Zhang's rules.
4. The results obtained using Zhang's rule in comparison with other combination rules indicate that the difference in the belief for the target A between Zhang's and Murphy's rules is 0.9999 (maximum) while it is 0.3333 (minimum) between Zhang's and DST rules.
5. The results obtained using Murphy's rule in comparison with other combination rules indicate that the difference in the belief for the target A between Murphy's and Zhang's rules is 0.9999 (maximum) while it is 0.5177 (minimum) between Murphy's and Inagaki's rules.

4.3 PROPOSED SELECTION PROCEDURE

The following guidelines are proposed to provide an insight in to the use of different combination rules depending on the nature of evidence available from different sources. The situations or conditions under which each of the combination rules is applicable are given below:

Dempster's rule:

-When the sum of the masses of all focal elements in the body of evidence is very large compared to the mass associated with the frame of discernment.

-When the evidences from different sources are not conflicting.

-When there is no measure of intersection among the different evidences.

-When similarities exit among the bodies of evidence from different sources, i.e., when evidences are consistent with each other.

Yager's rule:

-When the mass associated with the frame of discernment is comparable to the sum of the masses of all focal elements in the body of evidence.

-When the evidences from different sources have some conflict.

-When there is no measure of intersection among the different evidences.

-When only partial evidences are available from different bodies of evidence obtained from different sources.

- When the analysis is conducted from the point of view of the safety of the system.

Inagaki's rule:

-When the mass associated with the frame of discernment is high or comparable to all other evidences.

-When the evidences from different sources have some conflict.

-When there is no measure of intersection among the various evidences.

-When evidence is available for every interval of the required output parameter, such as the factor of safety, of the system.

- When the analysis is conducted from the point of view of the failure of the system.

Zhang's rule:

- When the measure of intersection among the various evidences is available.

-When the mass associated with the frame of discernment is low or comparable to all other evidences.

-When the evidences from different sources do not have much conflict.

- When similarities exit among the bodies of evidence obtained from different sources.

Murphy's average combination rule:

- When the evidences from different sources are conflicting in nature.

-When one body of evidence highly conflicts with other bodies of evidence.

--When there is no measure of intersection among the various evidences.

-When evidence is available for every interval of the required output parameter, such as the factor of safety, of the system.

4.4 ENGINEERING APPLICATION – A WELDED BEAM PROBLEM

The application of the various models for combining evidence is illustrated by considering the failure analysis of a welded beam [169] in the presence of different bodies of evidence in the various evidence sets. Consider a beam of length L and cross-sectional dimensions *t* and *b* that is welded to a fixed support as shown in Figure 4.2. The weld length is *l* on both the top and bottom surfaces and the beam is required to support a load *P*. The weld is in the form of a triangle with a depth of h. The maximum shear stress developed in the weld, τ , is given by

$$\tau = \sqrt{(\tau')^2 + 2\tau'\tau''\cos\theta + (\tau'')^2} \tag{4.33}$$

where

$$\tau' = \frac{P}{\sqrt{2}.h.l} \tag{4.34}$$

$$\tau'' = \left[P\left(L + \frac{l}{2}\right)\right] \frac{\sqrt{\left[\frac{l^2}{4} + \left(\frac{h+t}{2}\right)^2\right]}}{2\left(\frac{hl}{\sqrt{2}}\left[\frac{l^2}{12} + \left(\frac{h+t}{2}\right)^2\right]\right)} \tag{4.35}$$

$$\cos\theta = \frac{l}{2\sqrt{\left[\frac{l^2}{4} + \left(\frac{h+t}{2}\right)^2\right]}} \tag{4.36}$$

where θ is the angle between τ' and τ''.

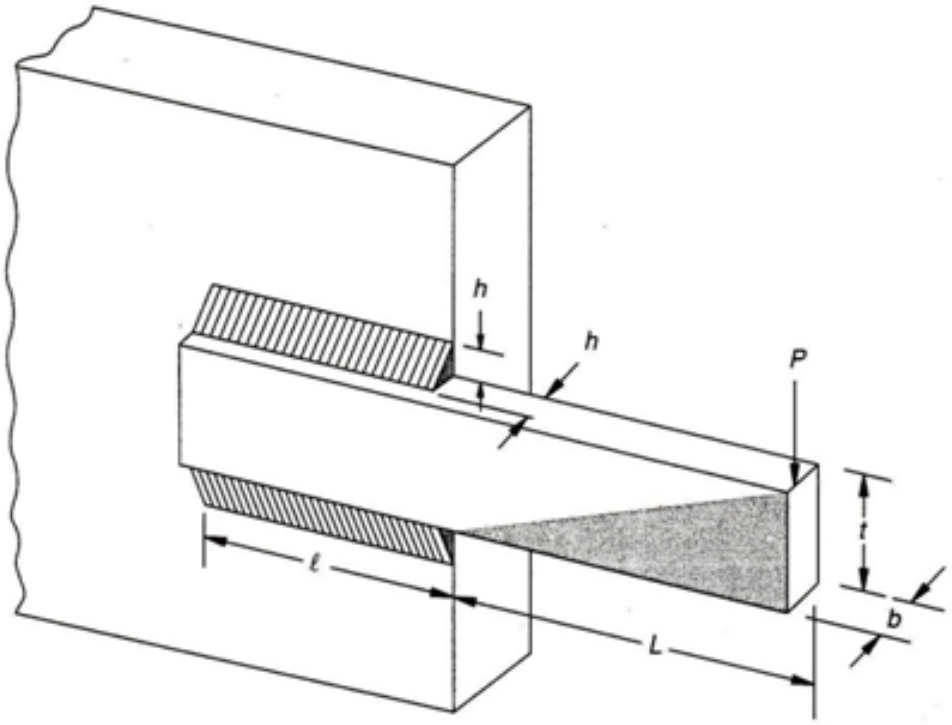

Figure 4.2 Welded beam

The intervals of the factor of safety (FS) are classified into three categories based on the maximum induced shear stress as follows.

Category I: $FS = \{I\} = [1.3,1.5]$

Category II: $FS = \{II\} = [1.5,1.7]$

Category II: $FS = \{III\} = [1.7,2.0]$

The allowable or permissible shear stress corresponding to a factor of safety of 1 is assumed to be $13600\, lb/in^2$. The beam is considered safest if the factor of safety falls in the range of 1.7 to 2.0. Let x_1 and x_2 denote the uncertain multiplication factors that define the ranges for the length of the weld (l) and the height of the weld (h), respectively. These multiplication factors are considered to be low, medium and high based on the following ranges:

$x_i = L = [0.85, 0.92],\ i = 1,2.$

$x_i = M = [0.92, 1.0],\ i = 1,2.$

$x_i = H = [1.0, 1.1],\ i = 1,2.$

The available evidence is assumed to be of five different types or forms as indicated in Table 4.8 to illustrate the applicability of each of the five different models for combining the evidences. Let s_1, s_2, s_3 and s_4 represent four different sources of evidence that provide information in each of the five cases. The mathematical formulation of the problem is used in formulating the five different evidence sets to some extent and the rest can be attributed to ignorance about the credibility of the source. The number of sources in each evidence set is assumed to be four. The number of available sources for combining evidence using rules such as Inagaki and Zhang rules is limited to two in the available literature. In this work, four sources are assumed which increases the complexity involved to combining the evidences. The results of calculation and the subsequent comparison of the various parameters associated with the evidence sets given in Table 4.8 are shown in Tables 4.9 and 4.10. In Table 4.9, k_1, k_2 and k_3 represent k_I in Eq. (4.3) when combining the bodies of evidence from sources S_1 and S_2, S_2 and S_3, and S_3 and S_4, respectively. If the values of k_I are less than 0.4, then the extent of conflict is assumed to be low, and the current analysis is done on the evidence sets to find the nature of evidences such as conflicting, similar, etc.

Table 4.8 Five sets of evidence

Evidence Set No.	Evidence
1	$s_1 : x_1 = L,\ x_2 = L, m\{I\} = 0.8, m\{II) = 0.1$ $s_2 : x_1 = L,\ x_2 = H, m\{I\} = 0.5, m\{II) = 0.2, m\{III\} = 0.1$ $s_3 : x_1 = L\ or\ M,\ x_2 = H, m\{I\} = 0.6, m\{II) = 0.2, m\{III\} = 0.1$ $s_4 : x_1 = L,\ x_2 = L\ or\ M, m\{I\} = 0.55, m\{II) = 0.1, m\{III\} = 0.15$
2	$s_1 : x_1 = L,\ x_2 = L, m\{I\} = 0.4, m\{II) = 0.4$ $s_2 : x_1 = L,\ x_2 = H, m\{I) = 0.5, m\{III\} = 0.3$ $s_3 : x_1 = L\ or\ M,\ x_2 = H, m\{I\} = 0.6, m\{II) = 0.25$ $s_4 : x_1 = L,\ x_2 = L\ or\ M, m\{I\} = 0.7, m\{II) = 0.2$
3	$s_1 : x_1 = L,\ x_2 = L, m\{I\} = 0.7$ $s_2 : x_1 = L,\ x_2 = H, m\{II) = 0.4, m\{III\} = 0.2$ $s_3 : x_1 = L\ or\ M,\ x_2 = H, m\{I\} = 0.6, m\{II) = 0.2$ $s_4 : x_1 = L,\ x_2 = L\ or\ M, m\{I\} = 0.6, m\{II) = 0.1, m\{III\} = 0.1$
4	$s_1 : x_1 = L,\ x_2 = L, m\{I \cup II\} = 0.8, m\{II \cup III) = 0.1$ $s_2 : x_1 = L,\ x_2 = H, m\{II\} = 0.5, m\{I \cup III) = 0.2, m\{III\} = 0.1$ $s_3 : x_1 = L\ or\ M,\ x_2 = H, m\{I\} = 0.6, m\{II \cup III) = 0.2$ $s_4 : x_1 = L,\ x_2 = L\ or\ M, m\{I\} = 0.6, m\{II) = 0.1, m\{II \cup III\} = 0.2$
5	$s_1 : x_1 = L,\ x_2 = L, m\{I\} = 0.8, m\{II) = 0.1$ $s_2 : x_1 = L,\ x_2 = H, m\{I\} = 0.1, m\{II) = 0.5, m\{III\} = 0.3$ $s_3 : x_1 = L\ or\ M,\ x_2 = H, m\{I\} = 0.6, m\{II) = 0.2, m\{III\} = 0.1$ $s_4 : x_1 = L,\ x_2 = L\ or\ M, m\{I\} = 0.7, m\{III\} = 0.2$

In addition $m\{\Theta_1\}$, $m\{\Theta_2\}$ and $m\{\Theta_3\}$ represent the masses associated to the frame of discernment when combining the bodies of evidence from sources S_1 and S_2, S_2 and S_3,

and s_3 and s_4, respectively. If these values are less than 0.04 then we call that they have low mass attributed to frame of discernment.

Table 4.9 Various parameters calculated for all evidence sets

Combination rule	Evidence set-1	Evidence set-2	Evidence set-3	Evidence set-4	Evidence set-5
Dempster's					
k_1	0.30	0.44	0.42	0.08	0.68
k_2	0.37	0.38	0.40	0.36	0.62
k_3	0.355	0.295	0.26	0.30	0.37
Yager's					
$m\{\Theta_1\}$	0.02	0.04	0.12	0.02	0.01
$m\{\Theta_2\}$	0.02	0.03	0.08	0.04	0.01
$m\{\Theta_3\}$	0.02	0.015	0.04	0.02	0.01
Inagaki's					
Conflict	Low	High	High	Low	High
Frame of discernment	Low	Low	High	Low	Low
Zhang's Intersection measure	No	No	No	Yes	No
Murphy's $\max(k_1, k_2, k_3)$	0.37	0.44	0.42	0.36	0.68

Table 4.10 Selection criteria for all evidence sets

Evidence Set No	Inferences from the evidence	Selected combination rule
1	k1 , k2 and k3 are low (k1 & k2) and (k2 & k3) are comparable to each other $m\{\Theta\}$ is low compared to k1 , k2 and k3 Intersections are not available	Dempster's
2	$m\{\Theta\}$ are comparable to k1 , k2 and k3 Max(k1,k2, k3) is high Evidence for all events is not available. i.e., less data. Intersections are not available	Yager's
3	$m\{\Theta\}$ is high $m\{\Theta\}$ are comparable to k1 , k2 and k3 Intersections are not available Evidence for all events are available	Inagaki's
4	Intersections are available Evidences are given for shared events k1 , k2 and k3 are low	Zhang's
5	k1 , k2 and k3 are high highly conflicting evidence are available from different sources Intersections are not available $m\{\Theta\}$ is very low	Murphy's

Case-1: Evidence type 1

The four sources of evidence given by evidence set 1 (Table 4.8) indicate the situation where Dempster's rule is the most suitable rule to combine evidence based on the inferences described in Table 4.10. As the Dempster's combination rule is associative, the order of combination of the sources does not matter on the solution. The evidence from sources s_1 and s_2 are combined using Dempster's rule using a procedure similar to the one described in the case of robbery example (in section 3.1), to obtain $m\{I\} = 0.87142,\ m\{II\} = 0.08571,\ m\{III\} = 0.01428,$ and $m\{\Theta\} = 0.02867.$ Similarly, the evidence from sources s_3 and s_4 are combined using Dempster's rule to obtain $m\{I\} = 0.782946,\ m\{II\} = 0.108527,\ m\{III\} = 0.077519,$ and $m\{\Theta\} = 0.031008.$ By combining the combined evidences obtained from sources s_1 & s_2 and s_3 & s_4 using DST, we obtain $m\{I\} = 0.97376,$ and $m\{II\} = 0.02004,\ m\{III\} = 0.00501,$ $m\{\Theta\} = 0.00117.$ The belief values are calculated as *Bel{I}* = $m\{I\}$ = 0.97376, *Bel{II}* = $m\{II\}$ = 0.02004 and *Bel*$\{III\}$ = $m\{III\}$=0.00501. The plausibility values are calculated by using equation (3.10) as *Pl*{I} = 1 - *Bel{II}* - *Bel{III}* = 0.97494, *Pl{II}* = 0.02122 and *Pl{III}* = 0.00619. The belief and plausibility intervals for the factor of safety are tabulated in Table 4.11.

Case-2: Evidence type 2

The four sources of evidence given by evidence set 2 (Table 4.8) indicate the situation where Yager's rule is the most suitable rule to combine evidence based on the inferences described in Table 4.10. As Yager's rule is not associative in nature, we have to combine evidence from all sources at the same time using equation (4.8). A matlab program was

written using procedure similar to the one described for combining two sources of evidence in the case of the robbery example (in section 4.2.1), but for combining four evidences (from four different sources) to form four dimensional product bpa matrix (similar to Table A.1). Using Yager's rule, we obtain $q\{I\} = 0.2514$, $q\{II\} = 0.0138$, $q\{III\} = 0.0009$, and $m^Y\{\Theta\} = 0.6611$. The belief values are calculated as *Bel{I}* = *q{I}* = 0.2514, *Bel{II}* = *q{II}* = 0.0138 and *Bel{III}* = *q{III}* = 0.0009. The plausibility values are calculated by using equation (3.10) as *Pl{I}* = 1 - *Bel{II}* - *Bel{III}* = 0.9853, *Pl{II}* = 0.7477 and *Pl{III}* = 0.7348. The belief and plausibility intervals for the factor of safety are tabulated in Table 4.11.

Case 3: Evidence type 3

The four sources of evidence given by evidence set 3 (Table 4.8) indicate the situation where Inagaki's extra rule is the most suitable rule to combine evidence based on the inferences described in Table 4.10. As Inagaki's extra rule is not associative in nature, we have to combine evidence from all sources at the same time using equation (4.8) in equation (4.23). A matlab program was written using a procedure similar to the one described for combining two sources of evidence in the case of the robbery example (in section 3.3), but for combining four evidences (from four different sources) to form four dimensional product bpa matrix (similar to Table A.1). Using Inagaki's extra rule, we obtain $m^U\{\Theta\} = 0.0048$, $p = 3.5391$, $m^U\{I\} = 0.8890$ $m^U\{II\} = 0.0849$, and $m^U\{IIII\} = 0.0212$. The belief values are calculated as *Bel{I}* = $m^U\{I\}$=0.8890, *Bel{II}* =0.0849 and *Bel{III}* =0.0212. The plausibility values are calculated by using

equation (3.10) as *Pl{I}* = 0.8938, *Pl{II}* = 0.0897 and *Pl{III}* = 0.0260. The belief and plausibility intervals for the factor of safety are tabulated in Table 4.11.

Case 4: Evidence type 4

The four sources of evidence given by evidence set 4 (Table 4.8) indicate the situation where Zhang's rule is the most suitable rule to combine evidence based on the inferences described in Table 4.10. As Zhang's rule is not associative in nature, we have to combine evidence from all sources at the same time using equation (4.32). A matlab program was written using a procedure similar to the one described for combining two sources of evidence in the case of the robbery example (in Appendix-A), but for combining four evidences (from four different sources) to form four dimensional product bpa matrix (similar to Tables A.1, A.2 and A.3). Using Zhang's rule, we obtain $m\{I\} = 0.7306$, $m\{II\} = 0.2514$, $m\{III\} = 0.0087$, $m\{I \cup II\} = 0.0028$, $m\{II \cup III\} = 0.0057$, $m\{I \cup III\} = 0.00035$, and $m\{\Theta\} = 0.000356$. The belief and plausibility values are calculated as *Bel{I}* = 0.7306, *Bel{II}* = 0.2514 and *Bel{III}* = 0.0087. The plausibility values are calculated by using equation (3.10) as *Pl{I}* = 1 - *Bel{II}* - *Bel{III}* - *Bel{* $II \cup III$ *}* = 0.7342, *Pl{II}* = 0.2603 and *Pl{III}* = 0.0151. The belief and plausibility intervals for the factor of safety are tabulated in Table 4.11.

Case 5: Evidence type 5

The four sources of evidence given by evidence set 5 (Table 4.8) indicate the situation where Murphy's rule is the most suitable rule to combine evidence based on the inferences described in Table 4.10. The evidences from source s_1, s_2, s_3 and s_n are

combined using Murphy's rule to obtain the average bpas as $m\{I\} = 0.55$, $m\{II) = 0.2, m\{III\} = 0.15$, and $m\{\Theta\} = 0.1$. Now, apply Dempster's rule to the overall combined bpa (using a procedure similar to the one described for the robbery example (in Appendix-A). As four evidences from four different sources are added, we use Dempster's rule 3 times to obtain $m\{I\} = 0.93744$, $m\{II) = 0.04204$, $m\{III\} = 0.0200$, and $m\{\Theta\} = 0.000525$. The belief and plausibility intervals for the factor of safety are tabulated in Table 4.11.

4.5 RESULTS

The belief and plausibility intervals for the factor of safety for all five evidence sets are tabulated in Table 4.11. If all the combination rules are applied to all the evidence sets (Table 4.8) without following the selection procedure described in section 4.3 (to apply just one particular most suitable combination rule) then we obtain five different solutions (belief interval for the factor of safety) for each evidence set. All the results are tabulated in Table 4.12.

Table 4.11 Belief Interval for factor of safety (FS)

Evidence Set No.	FS	Belief Interval	
Evidence set 1	FS = {I}	0.97377	0.97494
	FS = {II}	0.02004	0.02122
	FS = {III}	0.00501	0.00619
Evidence set 2	FS = {I}	0.2514	0.9853
	FS = {II}	0.0138	0.7477
	FS = {III}	0.0009	0.7348
Evidence set 3	FS = {I}	0.8890	0.8938
	FS = {II}	0.0849	0.0897
	FS = {III}	0.0212	0.0260
Evidence set 4	FS = {I}	0.7306	0.7342
	FS = {II}	0.2514	0.2603
	FS = {III}	0.0087	0.0151
Evidence set 5	FS = {I}	0.93744	0.93796
	FS = {II}	0.04204	0.04256
	FS = {III}	0.02000	0.02053

Table 4.12 Comparison of various combination rules applied on all evidence sets

Rule	Evidence set-1		Evidence set-2		Evidence set-3		Evidence set-4		Evidence set-5	
Dempster's										
m(I)	0.97377	0.97494	0.87090	0.87527	0.91819	0.91885	0.62374	0.63636	0.91819	0.91885
m(II)	0.02004	0.02122	0.11816	0.12254	0.07003	0.07068	0.32828	0.35354	0.07003	0.07068
m(III)	0.00501	0.00619	0.00656	0.01094	0.01113	0.01178	0.02146	0.03788	0.01113	0.01178
Yager's										
m(I)	0.3304	0.9915	0.2514	0.9853	0.2512	0.9700	0.1976	0.8848	0.1007	0.9942
m(II)	0.0068	0.6679	0.0138	0.7477	0.0240	0.7428	0.1040	0.7952	0.0035	0.8970
m(III)	0.0017	0.6628	0.00090	0.73480	0.0060	0.7248	0.0068	0.6952	0.0023	0.8958
Inagaki's										
m(I)	0.9745	0.9749	0.9442	0.9448	0.8890	0.8938	0.6243	0.6360	0.9454	0.9455
m(II)	0.0201	0.0205	0.0518	0.0524	0.0849	0.0897	0.3286	0.3530	0.0329	0.0330
m(III)	0.0050	0.0054	0.0034	0.0040	0.0212	0.0260	0.0215	0.0370	0.0216	0.0217
Zhang's										
m(I)	0.9917	0.9918	0.9826	0.9828	0.9442	0.9477	0.7306	0.7342	0.9829	0.9829
m(II)	0.0074	0.0075	0.0169	0.0171	0.0461	0.0496	0.2514	0.2603	0.0105	0.0106
m(III)	0.0008	0.0009	0.0003	0.0004	0.0062	0.0097	0.0087	0.0151	0.0066	0.0066
Murphy's										
m(I)	0.96906	0.97052	0.92030	0.92279	0.86068	0.87652	0.58050	0.62222	0.93744	0.93796
m(II)	0.02180	0.02326	0.06831	0.07081	0.09775	0.11360	0.34304	0.39543	0.04204	0.04256
m(III)	0.00768	0.00913	0.00890	0.01139	0.02573	0.04157	0.02123	0.03889	0.02000	0.02053

Analysis of the results of the welded beam problem given by the various combination rules:

1. In the evidence set-1, there is high evidence available from all sources for *m{I}* and hence belief for *{I}* should be high. This is exactly the one followed using Dempster's rule as the best rule to be applied for this evidence set.
2. In the evidence set-2, there is less evidence or data available from all sources and hence ignorance/uncertainty is high. This indicates that plausibility should be high apart from a large belief interval. This is exactly the one followed using Yager's rule as the most suitable rule to be applied for this evidence set.
3. In the evidence set-3, even though the 2nd source has no evidence for {I} but all the other sources state that a high evidence is available for {I}. There is one bpa from the 1st source and all three bpas are from 4th source. This nature of evidence set is most suitable for use of Inagaki's rule to get the belief intervals.
4. In the evidence set-4, there is evidence for more than one event combined and hence the cardinality for the events is found to be more than one. Hence, the best rule for this evidence set is Zhang's rule.
5. In the evidence set-5, the 2nd source of evidence is totally conflicting with the other sources for the evidence given to *{I}*. The other sources, namely the 1st, 3rd and 4th sources, haven high evidence for *{I}* and there is no reliability information for the sources. The best rule for this nature of evidence, where evidence from each source is to be preserved in finding the final combined evidence is none other than the Murphy's average combination rule.

4.6 COMBINING DIFFERENT FORMS OF EVIDENCE

We consider five aspects of a car namely control and stability (brakes), comfort (suspension), power train design (drive), body style and Interior (cab design) and features & accessories (features) and assume different forms of evidence as tabulated in Tables 4.13 to 4.22.

Table 4.13 Different various forms of evidence, reliability and cost for the brakes

Brakes	I	II	III	IV	V
JD rating	2.5	3	4	4.5	3.5
Customer review	Poor	Average	Poor	Better	Good
Probability of survival from the manufacture	0.96	0.97	0.98	0.98	0.97
reliability	0.90	0.92	0.98	0.99	0.96
cost	200	220	265	280	250

Evidence in the form of bpa for the brakes is assumed as tabulated in Table 4.14.

Table 4.14 Evidence in the form of bpa for the brakes

Life	Evidence for brakes I	Evidence for brakes II	Evidence for brakes III	Evidence for brakes IV	Evidence for brakes V
< 3 years	0.2	0.1	0.1	-	0.2
3-5 years	0.4	0.2	0.1	-	0.1
> 5 years	0.2	0.4	0.7	0.7	0.5

Table 4.15 Different various forms of evidence, reliability and cost for the suspension

Suspension	I	II	III	IV	V
JD rating	3.5	4	4	4.5	2.5
Customer review	Poor	Better	Average	Better	Average
Failure probability from manufacture	0.95	0.97	0.96	0.98	0.92
reliability	0.94	0.95	0.92	0.96	0.90
cost	440	460	415	500	400

Evidence in the form of bpa for the suspension is assumed as tabulated in Table 4.16.

Table 4.16 Evidence in the form of bpa for the suspension

Life	Evidence for suspension I	Evidence for suspension II	Evidence for suspension III	Evidence for suspension IV	Evidence for suspension V
< 3 years	0.2	0.2	0.1	0.1	0.2
3-5 years	0.1	0.1	0.2	-	0.1
> 5 years	0.5	0.5	0.6	0.8	0.4

Table 4.17 Different various forms of evidence, reliability and cost for the drive

Drive	I	II	III	IV	V
JD rating	3	4	4.5	3	4
Customer review	Good	Average	Poor	Good	Better
Failure probability from manufacture	0.95	0.97	0.98	0.96	0.98
reliability	0.93	0.90	0.88	0.95	0.98
cost	290	260	250	330	380

Evidence in the form of bpa for the drive is assumed as tabulated in Table 4.18.

Table 4.18 Evidence in the form of bpa for the drive

Life	Evidence for drive I	Evidence for drive II	Evidence for drive III	Evidence for drive IV	Evidence for drive V
< 3 years	-	-	0.4	0.2	-
3-5 years	0.1	0.2	0.1	-	0.1
> 5 years	0.6	0.5	0.2	0.5	0.8

Table 4.19 Different various forms of evidence, reliability and cost for the cab design

Cab design	I	II	III	IV	V
JD rating	3.5	3	2.5	4.5	4
Customer review	Average	Poor	Poor	Better	Good
Failure probability from manufacture	0.92	0.90	0.85	0.98	0.95
reliability	0.90	0.85	0.88	0.95	0.92
cost	325	300	310	400	450

Evidence in the form of bpa for the cab design is assumed as tabulated in Table 4.20.

Table 4.20 Evidence in the form of bpa for the cab design

Life	Evidence for cab design I	Evidence for cab design II	Evidence for cab design III	Evidence for cab design IV	Evidence for cab design V
< 3 years	-	0.1	0.2	-	0.1
3-5 years	0.1	0.2	-	0.1	-
> 5 years	0.6	0.5	0.5	0.7	0.7

Table 4.21 Different various forms of evidence, reliability and cost for the features

Features	I	II	III	IV	V
JD rating	3	2.5	4	4.5	3
Customer review	Average	Poor	Better	Better	Average
Failure probability from manufacture	0.9	0.85	0.95	0.90	0.88
reliability	0.93	0.9	0.96	0.97	0.94
cost	240	220	280	300	250

Evidence in the form of bpa for the features is assumed as tabulated in Table 4.22.

Table 4.22 Evidence in the form of bpa for the features

Life	Evidence for the features I	Evidence for the features II	Evidence for the features III	Evidence for the features IV	Evidence for the features V
< 3 years	-	0.2	0.1	0.1	0.2
3-5 years	0.3	-	0.1	0.3	0.2
> 5 years	0.5	0.6	0.7	0.4	0.5

As we know the JD power ratings are given on the scale of 5. The unit of cost is dollars. We assume reasonable credibilities for each source. Let us assume credibility = 0.9 for JD power rating. (experts). For example, the bpa for the brakes (type-I), the JD power rating is equal to 0.9×0.5 (= 0.45). Let us assume credibility = 0.5 for custom review (not experts) and corresponding bpas are indicated in Table 4.23.

Table 4.23 Equivalent evidence for customer review for various sub-systems of car

Rating	Interval range	bpa
Poor	0-0.3	0.15
Average	0.4-0.5	0.25
Good	0.6-0.7	0.325
Better	0.8-1.0	0.45

For example, the bpa for the brakes (Type-I) from customer reviews is equal to 0.5*[0, 0.3]. Thus, the average value for bpa = 0.15. Let us assume credibility = 1 for probability of survival from the manufacture for life greater than 5 years and also assume credibility = 1 for the source where evidence are given in the form of bpas. The procedure to compute the combined evidence for life greater than 5 years for the brakes (Type-I), suspension (Type-I), drive (Type-I), cab design (Type-I) and features (Type-I) are summarized as follows.

$E_1 : m\{III\} = 0.45, m\{\Theta\} = 0.55$
$E_2 : m\{III\} = 0.15, m\{\Theta\} = 0.85$
$E_3 : m\{III\} = 0.96, m\{\Theta\} = 0.04$
$\mathrm{E}_4 : m\{I\} = 0.2, m\{II) = 0.4, m\{III\} = 0.2$ and $m\{\Theta\} = 0.2$

$E_1 : m\{III\} = 0.63, m\{\Theta\} = 0.37$
$E_2 : m\{III\} = 0.15, m\{\Theta\} = 0.85$
$E_3 : m\{III\} = 0.95, m\{\Theta\} = 0.05$
$\mathrm{E}_4 : m\{I\} = 0.2, m\{II) = 0.1, m\{III\} = 0.5$ and $m\{\Theta\} = 0.2$

$E_1 : m\{III\} = 0.54, m\{\Theta\} = 0.46$
$E_2 : m\{III\} = 0.325, m\{\Theta\} = 0.675$
$E_3 : m\{III\} = 0.95, m\{\Theta\} = 0.05$
$\mathrm{E}_4 : m\{II) = 0.1, m\{III\} = 0.6$ and $m\{\Theta\} = 0.3$

$E_1 : m\{III\} = 0.63, m\{\Theta\} = 0.37$
$E_2 : m\{III\} = 0.25, m\{\Theta\} = 0.75$
$E_3 : m\{III\} = 0.92, m\{\Theta\} = 0.08$
$\mathrm{E}_4 : m\{II) = 0.1, m\{III\} = 0.6$ and $m\{\Theta\} = 0.3$

$E_1 : m\{III\} = 0.54, m\{\Theta\} = 0.46$
$E_2 : m\{III\} = 0.25, m\{\Theta\} = 0.75$
$E_3 : m\{III\} = 0.9, m\{\Theta\} = 0.1$
$\mathrm{E}_4 : m\{II) = 0.3, m\{III\} = 0.5$ and $m\{\Theta\} = 0.2$

Similarly, we have obtained the evidences for other types namely Type-II, Type-III, Type-IV, and Type-V for each sub-system of the car.. These evidences from four different sources for each type and for each sub-system are used in the matlab program to combine the evidence. We can observe the conflict between the JP rating and the customer reviews for the brakes Type-III, suspension Type-V and drive Type-III when compared to the other types in their respective sub-system category. We can observe partial evidences from different bodies of evidence obtained from different sources. We can also observe that the bpas associated with the frame of discernment is comparable to the sum of the masses of all focal elements in the body of evidence. When the analysis is conducted from the point of view of the safety of the system, by using the selection procedure described in section 4.3, Yager's combination rule is best suited to combine these four different types of evidence for each type of the sub-system of the car. We can also observe the bpas associated with the frame of discernment is high or comparable to

all other evidences. When the analysis is conducted from the point of view of the failure of the system, by using the selection procedure described in section 4.3, Inagaki's combination rule is best suited combination rule to combine these four different types of evidence for each type of the sub-system of the car. The belief interval obtained from the matlab program (used in section 4.4) is used in the discrete modified PSO matlab program. Now, for combining evidence from each sub-system level to the overall system level, we use DST rule successively four times to combine these resulting combined bpas to get belief for the life greater than 5 years. All these sub-systems form a series system. We assumed reliabilities for each type of the sub-system and their associated cost as tabulated in Tables 4.13, 4.15, 4.17, 4.19 and 4.21. The cost is assumed to vary increasingly non-linear with respect to its reliability with theoretically reaching cost to infinite when reliability is equal to 1. The belief is maximized to solve a discrete optimization problem to find one particular type of each sub-system of the car to have maximum performance ratings with design space of $5^5 = 3125$ discrete points with reliability range from 0.545 to 0.867 and the total cost vary from \$1370 to \$1860. An optimization problem thus formulated to maximize the belief for the car to have life greater than 5 years with constraints on total cost and total reliability of the car as follows.

Maximize belief subject to $TC \leq 1500$ and $TR \leq 0.75$.

This problem is solved by using two different analysis types namely case 1 using Yager's rule and case 2 using Inagaki's rule to combine evidence at sub-system level for each type. We used modified PSO algorithm to solve this optimization problem along with Dempster's and yager's rule of combined evidence program in the developed matlab

program to solve this problem. These optimization problems are solved to combine evidences at the sub-system level and the system level. For the PSO parameters, namely, population size = 12, $i_{\max}$= 800, $c_1 = c_2$ = 2, iw_{max}= 0.9, iw_{min}= 0.4, $\vec{V}_{f\max} = 1 \text{and} \vec{V}_{i\max} = 4$ for all i, stopping convergence criterion (in terms of change in the objective function value) = 10^{-8} for over 350 continuous iterations. The optimum solutions are obtained using the above described matlab program and tabulated in Table 4.24. We have observed that the total reliability of the car has decreased when we use Inagaki's rule at the sub-system level as expected. The selection of particular types for sub-systems like brakes, drive and cab design are changed compared to the optimum solution obtained when we use Yager's rule for combination of evidence at sub-system level. The optimum solutions obtained for both cases have an active constraint for the cost.

Table 4.24 Optimal solutions for combination of evidence for the car

Optimal solution	Case 1	Case 2
Brakes	Type-IV	Type-III
Suspension	Type-III	Type-III
Drive	Type-II	Type-III
Cab design	Type-I	Type-V
Features	Type-II	Type-II
Total cost	$ 1500	$ 1500
Total Reliability	0.6639	0.6569

4.7 SUMMARY

This chapter studied various combination rules to combine evidence from multiple sources to understand the procedure of combining evidence in depth and how the conflict among the evidence can be treated. The proposed selection procedure described in section 4.3 guides the user or analyst to select the most suitable combination rule to combine various evidences obtained from multiple sources based on the nature of the evidence sets. At the same time, it will not restrict from the application of other rules for combining evidences. Evidence sets (Table 4.8) are constructed in such a way that the applied combination rule gives the most satisfactory/logical results compared to the other combination rules (in each of the five cases described in section 4.4). For these cases, described in the section 4.4, if the combination rules, which are not suggested as the most suitable one, are used for combining evidence then they can give misleading results and may not convergence to the actual reality when more and more evidence/information becomes available. In the next chapter, the DST methodology to combine evidence when sources of evidence have different credibilities is considered.

CHAPTER 5

DEMPSTER-SHAFER THEORY FOR THE SAFETY ANALYSIS OF UNCERTAIN ENGINEERING SYSTEMS

5.1 OVERVIEW

A methodology for the safety analysis of uncertain engineering systems in the presence of multiple sources of evidence based on Dempster-Shafer Theory (DST) is presented. DST can be used when it is not possible to obtain a precise estimation of system response due to the presence of multiple uncertain input parameters. The information for each of the uncertain parameters is assumed to be available in the form of interval-valued data from multiple sources implying the existence of large epistemic uncertainty in the parameters [74,114]. The vertex method, described in section 5.2, is used to reduce the widening of the function value set due to multi-occurrences of variables when interval analysis is used in finding the response function of the system [9, 44]. It is followed by a computation procedure to find belief and plausibility functions using vertex method in section 5.3. The safety analysis of a welded beam with two and four uncertain parameters, when uncertain parameters are assumed to be available in the form of interval-valued data from multiple sources, is considered in section 5.4. A new method, called Weighted Dempster Shafer Theory for Interval-valued data (WDSTI), is proposed in section 5.5, for combining evidence when different credibilities are associated with different sources of evidence. The application of the methodology is illustrated by considering the safety analysis of a welded beam in the presence of two and

four multiple uncertain parameters and in presence three sources of evidence. The chapter concludes with a discussion and a summary in the penultimate and end sections.

5.2 VERTEX METHOD [61]

When $y = f(x_1, x_2, x_3, ..., x_n)$ is continuous in the n-dimensional rectangular region with no extreme points in the region (including the boundaries), then the interval value of the function can be obtained as

$$Y = f(X_1, X_2, ..., X_n) \quad = \left[\min_j (f(c_j)), \max_j (f(c_j)) \right], \; j = 1,2,...., N \tag{5.1}$$

where c_j denotes the ordinate of the j-th vertex. If m extreme points $E_k (k = 1, 2, \ldots\ldots, m)$, exist among the vertices, then Eq. (5.1) is to be modified as

$$Y = \left[\min_{j,k} (f(c_j), f(E_k)), \max_{j,k} (f(c_j), f(E_k)) \right] \tag{5.2}$$

The vertex method is based on the α-cut concept and interval analysis. The α-cut is a discretization technique on membership value domains of uncertain variables instead of on the domains of the variables themselves. The vertex method reduces the widening of the function value set due to multi-occurrences of a variables when interval analysis is implemented on the expression of the function.

5.3 COMPUTATION OF BELIEF AND PLAUSIBILITY FUNCTIONS

The following procedure can be used to determine the belief and plausibility functions.

1. Use DST or Zhang's rule corresponding to Dempster's rule (i.e., when $|C| = |A||B|$) to combine the evidences that are available in the form of interval valued data.

2. Find bpa's as simple products of the evidences.
3. Let the sum of all the bpa's be n. Using the normalization factor 1/n, each of the bpa's is multiplied by 1/n.
4. The number of uncertain parameters used to find the combined evidence determines the dimensionality of the product table of bpas.
5. Apply DST to combine the bpa values obtained in step 4.
6. Calculate the belief and plausibility functions using the vertex method [40]. A matlab program has been developed for this purpose in this work.

5.3.1 Computational aspects of the vertex method:

The following step-by-step procedure is used to implement the vertex method for determining the belief and plausibility functions:

1. Initialize the interval ranges of the uncertain parameters as $X_1, X_2 \ldots\ldots X_n$, and the corresponding bpa's as $Y_1, Y_2 \ldots\ldots Y_n$ respectively where 'n' is the number of uncertain parameters.

2. Construct the bpa product table using $Y_1, Y_2 \ldots\ldots Y_n$ and store the result in a matrix A where 'n' represent the dimensionality of A

3. Each element of A, corresponding to the interval ranges of $X_1, X_2 \ldots\ldots X_n$, represents a n-sided hyper cube where each vertex denotes a different combination of the values of the uncertain parameters.

4. The belief is calculated as the sum of the bpa's (or elements of A) corresponding to n-sided hyper cube where the response function evaluated at each vertex is less than the limit value of the response (or output) function.

5. The plausibility is calculated as the sum of all those bpa's from the matrix A that not only correspond to the belief but also any n-sided hyper cube for which any of its vertices has a function value less than the limit value of the output/response function.

6. The number of function evaluations can be optimized (minimized) in the computation of plausibility in identifying the function values at the vertices of the n-sided hyper cube that has values less than the limit value of the response function.

5.4 SAFETY ANALYSIS OF A WELDED BEAM

The failure/safety analysis of the welded beam described in section 4.4 of chapter 4 is considered. The beam is considered unsafe if the maximum shear stress in the weld is greater than $9066.67\, lb/in^2$ ($=\tau_{\max}$ / Factor of Safety $= 13{,}600/1.5$). The nominal (input) data is P = 6000 lb, L = 14 in., $E = 30x10^6$ psi, $\sigma_{\max} = 30{,}000$ psi, $\delta_{\max} = 0.25$ in, $\tau_{\max} = 13{,}600$ psi, $h = 0.2455$ in. , $l = 6.196$ in. , $b = 0.2455$ in. and t = 8.273 in..

The safety analysis of the welded beam is investigated for two cases. In the first case, the beam is assumed to have two uncertain parameters while four uncertain parameters are assumed in the second case. The nondeterministic character of the system is due to the presence of uncertainty in the parameters embodied in the mathematical model of the welded beam.

Figure 5.1 shows a three-dimensional representation of the shear stress induced in the weld, τ, over the range of possible values of x_1 and x_2 with several level curves, or response contours of τ. The rectangle defined by $0.7 \le x_1 \le 1.3$ and $0.8 \le x_2 \le 1.3$ is referred to as the input product space. Figure 5.2 shows the limit shear stress contour in the x_1- x_2 plane for $\tau = 9066.67\, lb/in^2$ in the weld.

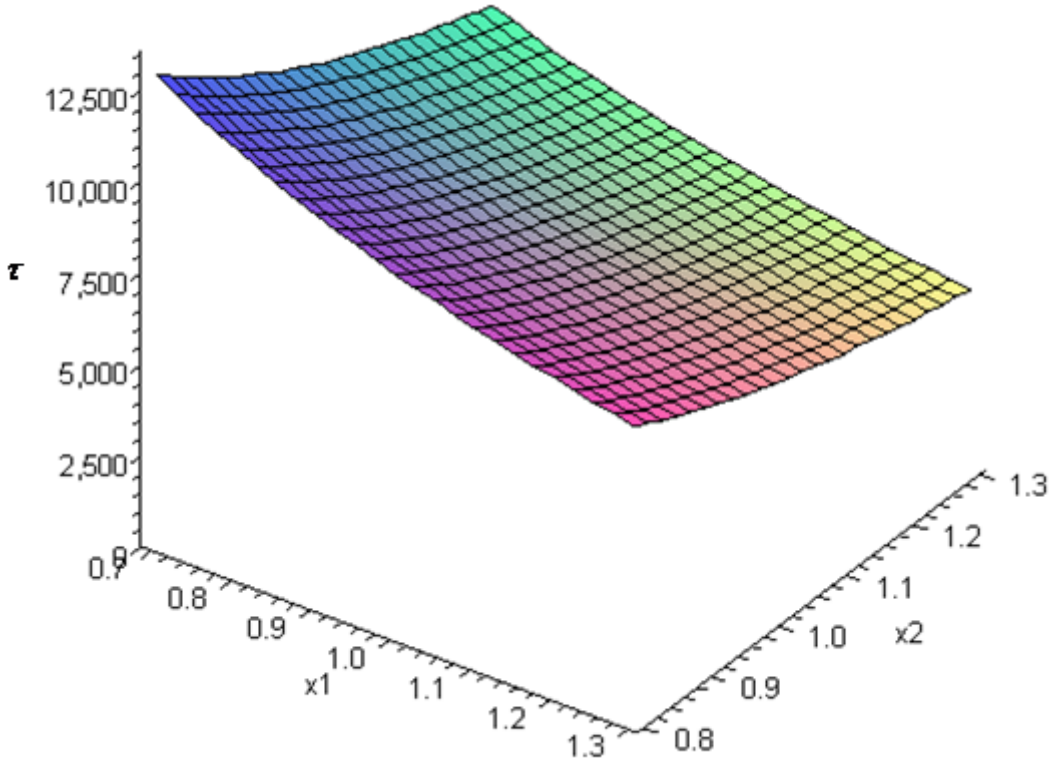

Figure 5.1 Representation of shear stress (τ) in the weld in the range $0.7 \leq x_1 \leq 1.3$ and $0.8 \leq x_2 \leq 1.3$

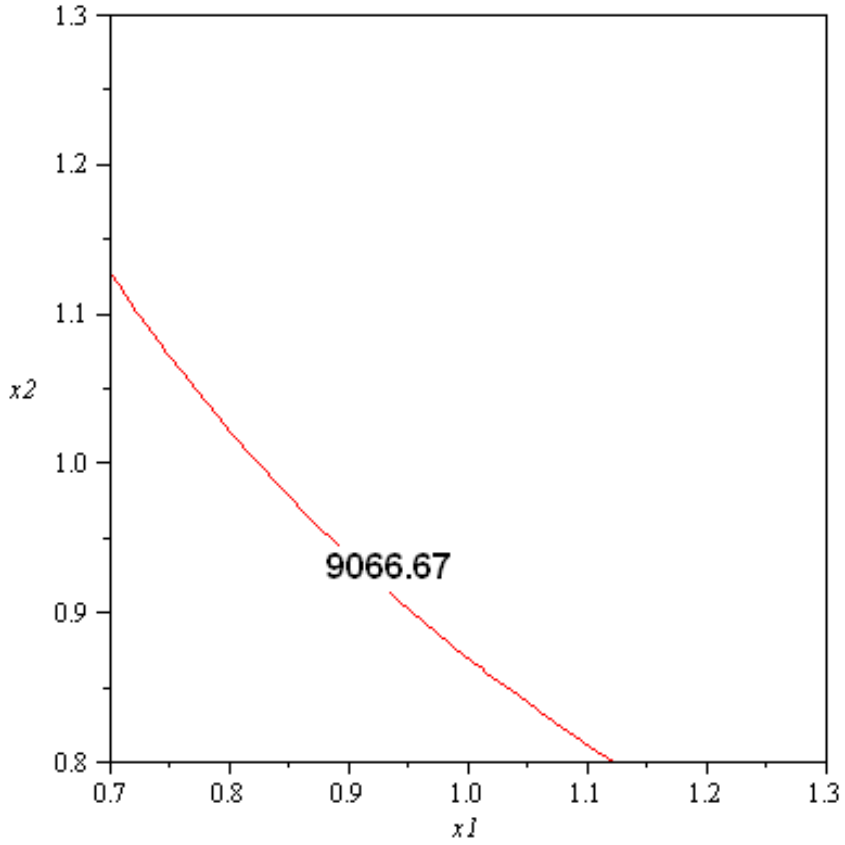

Figure 5.2 Contour of the shear stress in the weld (τ) in the range $0.7 \leq x_1 \leq 1.3$ and $0.8 \leq x_2 \leq 1.3$

5.4.1 Analysis with two uncertain parameters

The length of the weld (l) and the height of the weld (h) are treated as the uncertain parameters. The beam is considered unsafe if this maximum shear stress is greater than $9066.67\, lb/in^2$. Let x_1 and x_2 be the multiplication factors that denote the uncertainties of the parameters l and h, respectively. It is assumed that two sources of evidence (experts) provide the possible ranges (intervals) of x_1 and x_2 along with the corresponding bpa's as indicated in Table 5.1.

Table 5.1 Evidences for the uncertain parameters

x_1	Expert1 (Evidence1) (S1)	Interval	[0.7,0.8]	[0.8,1.1]	[1.0,1.2]	[1.2,1.3]
		Bpa	0.1	0.4	0.4	0.1
	Expert2 (Evidence2) (S2)	Interval	[0.7,0.9]	[0.8,1.0]	[1.0,1.2]	[1.1,1.3]
		Bpa	0.1	0.4	0.3	0.2
x_2	Expert1 (Evidence1) (S1)	Interval	[0.8,0.9]	[0.9,1.1]	[1.0,1.2]	[1.2,1.3]
		Bpa	0.1	0.4	0.4	0.1
	Expert2 (Evidence2) (S2)	Interval	[0.7,0.9]	[0.9,1.0]	[1.0,1.2]	[1.1,1.3]
		Bpa	0.2	0.4	0.2	0.2

The belief and plausibility are computed as follows:

Step 1: Find the intersections of intervals for the uncertain variable x_1 from the two sources of evidence (experts) as shown in Table 5.2:

Table 5.2 Combined interval ranges of x_1

		Expert 2			
	Interval	[0.7,0.9]	[0.8,1.0]	[1.0,1.2]	[1.1,1.3]
Expert 1	[0.7,0.8]	[0.7,0.8]			
	[0.8,1.1]	[0.8,0.9]	[0.8,1.0]	[1.0,1.1]	
	[1.0,1.2]			[1.0,1.2]	[1.1,1.2]
	[1.2,1.3]				[1.2,1.3]

Step 2: Find the bpa for the interval ranges calculated in Step1 as indicated in Table 5.3:

Table 5.3 Combined bpa values of x_1

		Expert 2				
		Interval	[0.7,0.9]	[0.8,1.0]	[1.0,1.2]	[1.2,1.3]
Expert 1	Interval	Bpa (m)	0.1	0.4	0.3	0.2
	[0.7,0.8]	0.1	0.01			
	[0.8,1.1]	0.4	0.04	0.16	0.12	
	[1.0,1.2]	0.4			0.12	0.08
	[1.1,1.3]	0.1				0.02

Step 3: Find the normalization factor for x_1 as shown in Table 5.4 and scale the bpa's to obtain $\sum m = 1$. Use a similar procedure for x_2 and combine the evidences for both x_1 and x_2 as shown in Table 5.5.

Table 5.4 Normalization factor of x_1

x_1	
Interval	M
[0.7,0.8]	0.01
[0.8,0.9]	0.04
[0.8,1.0]	0.16
[1.0,1.1]	0.12
[1.0,1.2]	0.12
[1.1,1.2]	0.08
[1.2,1.3]	0.02
$\sum m$	0.55

Table 5.5 Combined normalized evidence (bpas) from experts 1 and 2 of x_1 and x_2

x_1		x_2	
Interval	m	Interval	m
[0.7,0.8]	0.01818	[0.8,0.9]	0.04545
[0.8,0.9]	0.07272	[0.9,1.0]	0.3636
[0.8,1.0]	0.29091	[1.0,1.1]	0.1818
[1.0,1.1]	0.21818	[1.0,1.2]	0.1818
[1.0,1.2]	0.21818	[1.1,1.2]	0.1818
[1.1,1.2]	0.14545	[1.2,1.3]	0.04545
[1.2,1.3]	0.03636		

Step 4: Since there are two uncertain parameters in the problem, the dimensionality of the bpa product table is 2. Apply DST for the evidences obtained for x_1 and x_2 to find the bpa product table of order 7 x 6 as shown in Table 5.6.

Table 5.6 Bpa product table of x_1 and x_2

x_1		x_2					
		[0.8,0.9]	[0.9,1.0]	[1.0,1.1]	[1.0,1.2]	[1.1,1.2]	[1.2,1.3]
Interval	m	0.04545	0.3636	0.1818	0.1818	0.1818	0.04545
[0.7,0.8]	0.01818	0.00083	0.00661	0.00331	0.00331	0.00331	0.00083
[0.8,0.9]	0.07272	0.00331	0.02644	0.01322	0.01322	0.01322	0.00331
[0.8,1.0]	0.29091	0.01322	0.10577	0.05289	0.05289	0.05289	0.01322
[1.0,1.1]	0.21818	0.00992	0.07933	0.03967	0.03967	0.03967	0.00992
[1.0,1.2]	0.21818	0.00992	0.07933	0.03967	0.03967	0.03967	0.00992
[1.1,1.2]	0.14545	0.00661	0.05289	0.02644	0.02644	0.02644	0.00661
[1.2,1.3]	0.03636	0.00165	0.01322	0.00661	0.00661	0.00661	0.00165

Step 6: Use the vertex method to handle the two uncertain parameters represented by interval numbers to obtain an assessment of the likelihood of the maximum induced shear stress not exceeding the specified limit state value of $9066.67\,lb/in^2$ (using the matlab program developed in this work).

Table 5.7 Bpa product table of x_1 and x_2 represent matrix A

x_1		x_2					
		[0.8,0.9]	[0.9,1.0]	[1.0,1.1]	[1.0,1.2]	[1.1,1.2]	[1.2,1.3]
Interval	m	0.04545	0.3636	0.1818	0.1818	0.1818	0.04545
[0.7,0.8]	0.01818	A(1,1)	A(1,2)	**A(1,3)**	**A(1,4)**	**A(1,5)**	*A(1,6)*
[0.8,0.9]	0.07272	A(2,1)	**A(2,2)**	**A(2,3)**	**A(2,4)**	*A(2,5)*	*A(2,6)*
[0.8,1.0]	0.29091	**A(3,1)**	**A(3,2)**	**A(3,3)**	**A(3,4)**	*A(3,5)*	*A(3,6)*
[1.0,1.1]	0.21818	**A(4,1)**	*A(4,2)*	*A(4,3)*	*A(4,4)*	*A(4,5)*	*A(4,6)*
[1.0,1.2]	0.21818	**A(5,1)**	*A(5,2)*	*A(5,3)*	*A(5,4)*	*A(5,5)*	*A(5,6)*
[1.1,1.2]	0.14545	**A(6,1)**	*A(6,2)*	*A(6,3)*	*A(6,4)*	*A(6,5)*	*A(6,6)*
[1.2,1.3]	0.03636	*A(7,1)*	*A(7,2)*	*A(7,3)*	*A(7,4)*	*A(7,5)*	*A(7,6)*

Belief is calculated as the sum of all bpas of matrix A whose corresponding hyper cube satisfies all the design constraints and maximum induced shear stress less than 9066.67 lb/in^2 using the procedure described in section 5.3. These bpas are indicated by italic letters in Table 5.7. Similarly, plausibility is calculated as the sum of all the bpas of the matrix for which atleast one vertex of the corresponding hyper cube satisfies the condition that the maximum induced shear stress is less than 9066.67 lb/in^2. These bpas are represented by both bold and italic letters in Table 5.7. This procedure is implemented in matlab program to obtain belief and plausibility values for the safety of the welded beam.

If the program is not optimized for the number of function evaluations, the required number of function evaluations using the vertex method would be $(2^2)(7)(6) = 168$ to

find the belief and plausibility for realizing the maximum induced shear stress to be less than the limit value $9066.67\,lb/in^2$. In the optimized program, when computing plausibility, we do not evaluate function values (maximum induced shear stress) at all other vertices of the hypercube once the program finds atleast one vertex that corresponds to a function value less than $9066.67\,lb/in^2$ and atleast one vertex with a function value (τ) greater than $9066.67\,lb/in^2$. When the current procedure/program is optimized, the number of function evaluations required is 166. Thus, a reduction of 1.19% function evaluations is achieved by the program. This reduction increases with an increase in the number of uncertain input parameters and/or an increase in the number of interval data for the uncertain input parameters. The numerical results indicate a belief of 0.67515 and a plausibility of 0.98927 (for the maximum shear stress less than $9066.67\,lb/in^2$). Thus the degree of plausibility, 0.98927, is the maximum limit state violation for the design while there is atleast 0.67515 belief for a safe design. The belief and plausibility are nothing but lower and upper bounds on the unknown probability. The DST, thus, indicates that the probability of a safe design with $\tau < 9066.67\,lb/in^2$ will be as low as 0.67515 and as high as 0.98927 with the given body of evidence.

Table 5.8 Evidences for the uncertain parameters x_1 and x_2

	x1		x2	
	Expert1 (Evidence1) (S1)	Expert2 (Evidence2) (S2)	Expert1 (Evidence1) (S1)	Expert2 (Evidence2) (S2)
Interval	Bpa	Bpa	Bpa	Bpa
[0.85,0.86]	0.02	0.03	0.03	0.04
[0.86,0.87]	0.04	0.03	0.05	0.05
[0.87,0.88]	0.04	0.04	0.04	0.05
[0.88,0.89]	0.05	0.05	0.05	0.04
[0.89,0.90]	0.06	0.05	0.04	0.04
[0.90,0.91]	0.06	0.07	0.08	0.07
[0.91,0.92]	0.08	0.08	0.08	0.08
[0.92,0.93]	0.09	0.1	0.1	0.1
[0.93,0.94]	0.11	0.1	0.09	0.08
[0.94,0.95]	0.09	0.09	0.1	0.11
[0.95,0.96]	0.06	0.05	0.08	0.08
[0.96,0.97]	0.05	0.05	0.05	0.05
[0.97,0.98]	0.06	0.06	0.06	0.06
[0.98,0.99]	0.04	0.04	0.04	0.04
[0.99,1.00]	0.05	0.05	0.05	0.05
[1.00,1.01]	0.04	0.04	0.03	0.02
[1.01,1.02]	0.04	0.05	0.02	0.03
[1.02,1.03]	0.02	0.02	0.01	0.01

The procedure described above is also applied to another set of evidence as shown in Table 5.8. For this data, the belief and plausibility values for the maximum induced shear stress less than $9066.67\,lb/in^2$ are computed as 0.61767 and 0.766872, respectively. If the program is not optimized for the number of function evaluations, the required number of function evaluations using the vertex method would be $(2^2)(18)(18) = 1296$ to find the belief and plausibility. When the current procedure/program is optimized, the number of function evaluations required is 1290. Thus, a reduction of 0.46% in function evaluations is achieved by the program.

The use of the vertex method is justified to overcome the complexity involved in the mathematical formation of the welded beam. The equations to find the interval (range) of the maximum induced shear stress can be rewritten in the form:

$$\tau_{\text{int}} = \sqrt{(\tau'_{\text{int}})^2 + 2\tau'_{\text{int}}\,\tau''_{\text{int}}\cos\theta + (\tau''_{\text{int}})^2} \tag{5.3}$$

where

$$\tau'_{\text{int}} = \frac{P}{\sqrt{2}.[h_{.a}, h_b].[l_a, l_b]} \tag{5.4}$$

$$\tau''_{\text{int}} = \frac{MR}{J} = \left[P\left(L + \frac{[l_a, l_b]}{2}\right)\right] \frac{\sqrt{\left[\frac{[l_a, l_b]^2}{4} + \left(\frac{[h_{.a}, h_b] + t}{2}\right)^2\right]}}{2\left(\frac{[h_{.a}, h_b].[l_a, l_b]}{\sqrt{2}}.\left[\frac{[l_a, l_b]^2}{12} + \left(\frac{[h_{.a}, h_b] + t}{2}\right)^2\right]\right)} \tag{5.5}$$

$$\cos\theta_{\text{int}} = \frac{[l_a, l_b]}{2\sqrt{\left[\frac{[l_a, l_b]^2}{4} + \left(\frac{[h_{.a}, h_b] + t}{2}\right)^2\right]}} \tag{5.6}$$

where $[l_a, l_b]$ and $[h_{.a}, h_b]$ are the intervals (range) of the uncertain parameters, namely, the length of the weld and height of the weld. The subscript int is used in Eqs. (5.3) – (5.6) to represent the interval for the corresponding parameters in Eqs. (4.33) - (4.36). The computation of the interval of the induced shear stress becomes tedious with large values of the uncertain parameters (when combinatorial approach is used).

5.4.2 Analysis with four uncertain parameters

The failure/safety analysis of the welded beam is considered using four uncertain parameters to find the maximum induced shear stress developed in the weld. As in the previous case, the welded beam is considered unsafe if the maximum shear stress exceeds

$9066.67\,lb/in^2$. x_1, x_2, x_3 and x_4 are assumed to be the multiplication factors for the four uncertain parameters, namely the depth of the beam (*t*), length of the beam (*L*), weld length (*l*) and height of the weld (*h*), respectively. Evidences from two sources (experts 1 and 2) are assumed to be available in the form of intervals of the uncertain parameters as shown in Table 5.9. The credibility of each of the two sources of evidence is assumed to be equal to 1.

The maximum induced shear stress in the weld is calculated using Eqs. (4.33) and (5.3). In this case, the Matlab program considers four uncertain parameters, denoted in the form of interval numbers, to assess the likelihood that the maximum induced shear stress does not exceed the limit state value of $9066.67\,lb/in^2$. If the Matlab program is not optimized for the number of function evaluations then the required number of function evaluations using the vertex method, to find the belief and plausibility will be $(2^4)(18)(18)(18)(18) = 1679616$. The present optimized program required 1543072 function evaluations. Thus, a reduction of 8.12% in function evaluations has been achieved by the optimized program. The numerical results indicate that the belief is 0.521151 and the plausibility is 0.730883 for a safe design. This shows that the degree of plausibility of 0.730883 is the maximum limit state violation for the design while there is atleast 0.521151 belief for the safe design. The belief and plausibility denote the lower and upper bounds on an unspecified probability. Thus, the probability of safety, $\tau < 9066.67\,lb/in^2$, can be as low as 0.521151 and as high as 0.730883 in the presence of given (assumed) body of evidence. This is evident from the present results that the belief intervals (difference between belief and plausibility) for the maximum shear stress less than $9066.67\,lb/in^2$ increases with an increase in the number of uncertain parameters.

Table 5.9 Evidences (experts) for the uncertain parameters x_1, x_2, x_3 and x_4

	x1		x2		x3		x4	
	Expert1 (Evidence1) (S1)	Expert2 (Evidence2) (S2)	Expert1 (Evidence1) (S1)	Expert2 (Evidence2) (S2)	Expert1 (Evidence1) (S1)	Expert2 (Evidence2) (S2)	Expert1 (Evidence1) (S1)	Expert2 (Evidence2) (S2)
Interval	Bpa	Bpa	Bpa	Bpa	Bpa	Bpa	Bpa	Bpa
[0.85,0.86]	0.01	0.01	0.03	0.03	0.02	0.03	0.03	0.04
[0.86,0.87]	0.02	0.02	0.04	0.03	0.04	0.03	0.05	0.05
[0.87,0.88]	0.03	0.02	0.04	0.03	0.04	0.04	0.04	0.05
[0.88,0.89]	0.04	0.04	0.04	0.04	0.05	0.05	0.05	0.04
[0.89,0.90]	0.05	0.04	0.05	0.04	0.06	0.05	0.04	0.04
[0.90,0.91]	0.06	0.04	0.08	0.07	0.06	0.07	0.08	0.07
[0.91,0.92]	0.06	0.05	0.08	0.07	0.08	0.08	0.08	0.08
[0.92,0.93]	0.08	0.07	0.1	0.09	0.09	0.1	0.1	0.1
[0.93,0.94]	0.09	0.09	0.09	0.08	0.11	0.1	0.09	0.08
[0.94,0.95]	0.1	0.1	0.11	0.11	0.09	0.09	0.1	0.11
[0.95,0.96]	0.08	0.08	0.1	0.11	0.06	0.05	0.08	0.08
[0.96,0.97]	0.08	0.09	0.05	0.05	0.05	0.05	0.05	0.05
[0.97,0.98]	0.06	0.07	0.05	0.05	0.06	0.06	0.06	0.06
[0.98,0.99]	0.06	0.07	0.04	0.05	0.04	0.04	0.04	0.04
[0.99,1.00]	0.05	0.05	0.04	0.04	0.05	0.05	0.05	0.05
[1.00,1.01]	0.05	0.06	0.03	0.04	0.04	0.04	0.03	0.02
[1.01,1.02]	0.05	0.06	0.02	0.04	0.04	0.05	0.02	0.03
[1.02,1.03]	0.03	0.04	0.01	0.03	0.02	0.02	0.01	0.01

5.5 DST METHODOLOGY WHEN SOURCES OF EVIDENCE HAVE DIFFERENT CREDIBILITIES

When the credibilities of the various expert opinions are different, a modified DST, proposed in this section, can be used for combining evidences. Let c_i be the weighting/credibility factor for the source of evidence i where $0 \le c_i \le 1$. The combined bpa with all the available evidence is determined as:

$$\begin{aligned} m_{12..n} &= m_1(S1) * m_2(S2).....m_n(Sn) + (1 - c_1) * (1 - m_1(S1)) * m_2(S2)....m_n(Sn) \\ &+ (1 - c_2) * m_1(S1) * (1 - m_2(S2)) * m_3(S3).....m_n(Sn) + ... \\ &+ (1 - c_n) * m_1(S1) * m_2(S2) * m_3(S3).....m_{n-1}(Sn-1) * (1 - m_n(Sn)) \end{aligned} \quad (5.7)$$

where $m_1(S1), m_2(S2) \ldots .. m_n(Sn)$ are the bpa's for a particular interval range from sources 1,2,..n (S1, S2, ..., Sn), respectively, and $m_{12...n}$ is the combined bpa obtained from the DST rule for the same interval range. For example, if the number of sources is two (n = 2), Eq. (5.7) gives

$$m_{12} = m_1(S1) * m_2(S2) + (1 - c_2) * (1 - m_2(S2)) * m_1(S1) + (1 - c_1) * (1 - m_1(S1)) * m_2(S2) \quad (5.8)$$

where $m_1(S1)$ and $m_2(S2)$ are the bpa's for a particular interval range from sources 1 and 2, respectively, and m_{12} is the bpa obtained from the DST rule for the same interval range.

Note that the degree of uncertainty, $m(\Theta)$, itself is not multiplied by the weighting factor and Eq. (5.8) reduces to Eq. (4.1) when all the credibility factors are equal to 1. Also, when $c_1 = 0$ or $c_2 = 0$, Eq. (5.7) reduces to the formula corresponding to the case with only n-1 sources of evidence. Once the modified bpa is determined, the DST can be used

to combine evidences. The procedure, termed the Weighted Dempster Shafer Theory for Interval-valued data (WDSTI), is outlined below.

5.5.1 Solution procedure with Weighted Dempster Shafer Theory for Interval-valued data (WDSTI)

The procedure to determine the belief and plausibility functions using WDSTI is indicated in the following steps:

1. Use DST or Zhang's rule corresponding to Dempster's rule (i.e., when $|C| = |A||B|$) to combine the evidences from interval valued input data.
2. Find the bpa's using Eq. (5.8) for the product of evidences.
3. Let the sum of all the bpa's be n. Using the normalization factor 1/n, multiply each of the bpa's by 1/n.
4. The number of uncertain parameters used to find the combined evidence determines the dimensionality of the product table of bpa.
5. Calculate the belief and plausibility functions using the vertex method as described earlier.

5.5.2 Safety analysis of a welded beam

The safety analysis of the welded beam described in section 4.4 is considered again. The maximum shear stress induced in the welded beam can be calculated using Eqs. (4.33) – (4.36). The problem is solved with two and four uncertain parameters. For the two-uncertain parameter case, the length of weld (l) and the height of the weld (h) are considered to be uncertain. For the four-uncertain parameter case, the length of weld (l),

height of the weld (h), depth of the cantilever (t) and length of the cantilever (L) are considered to be uncertain. In each case, the problem is solved using data from two and three sources of evidence. The beam is considered unsafe if the maximum induced shear stress in the weld is greater than $9066.67\, lb/in^2$. If the credibilities of the sources of evidence 1 and 2 are 1 and c $(0 \le c \le 1)$, respectively, the belief and plausibility can be determined as follows:

(i) The intervals are combined in the usual manner (as in the case of equal credibilities for all sources of evidence) except that the bpa's are calculated using Eq. (5.7).

(ii) The DST or Zhang's rule corresponding to Dempster's rule (i.e., when $|C| = |A||B|$) is used to combine the evidences as per the WDSTI method to compute the combined bpa values and the resulting values are normalized as indicated earlier.

(iii) The belief and plausibility functions are computed using the vertex method.

5.5.3 Numerical results

The methodology of WDSTI is illustrated for the safety analysis of a welded beam by considering the following six cases.

Case 1: Two uncertain parameters with evidence from two different sources

Let x_1 and x_2 denote the multiplication factors for the uncertain parameters l and h, respectively. The two sources of evidence are assumed to provide possible ranges or intervals of x_1 and x_2 along with the corresponding bpa's as given in Table 5.8. The values of belief and plausibility computed for different values of the credibility (c) of source 2, with $(0 \le c \le 1)$, are shown in Fig. 5.3.

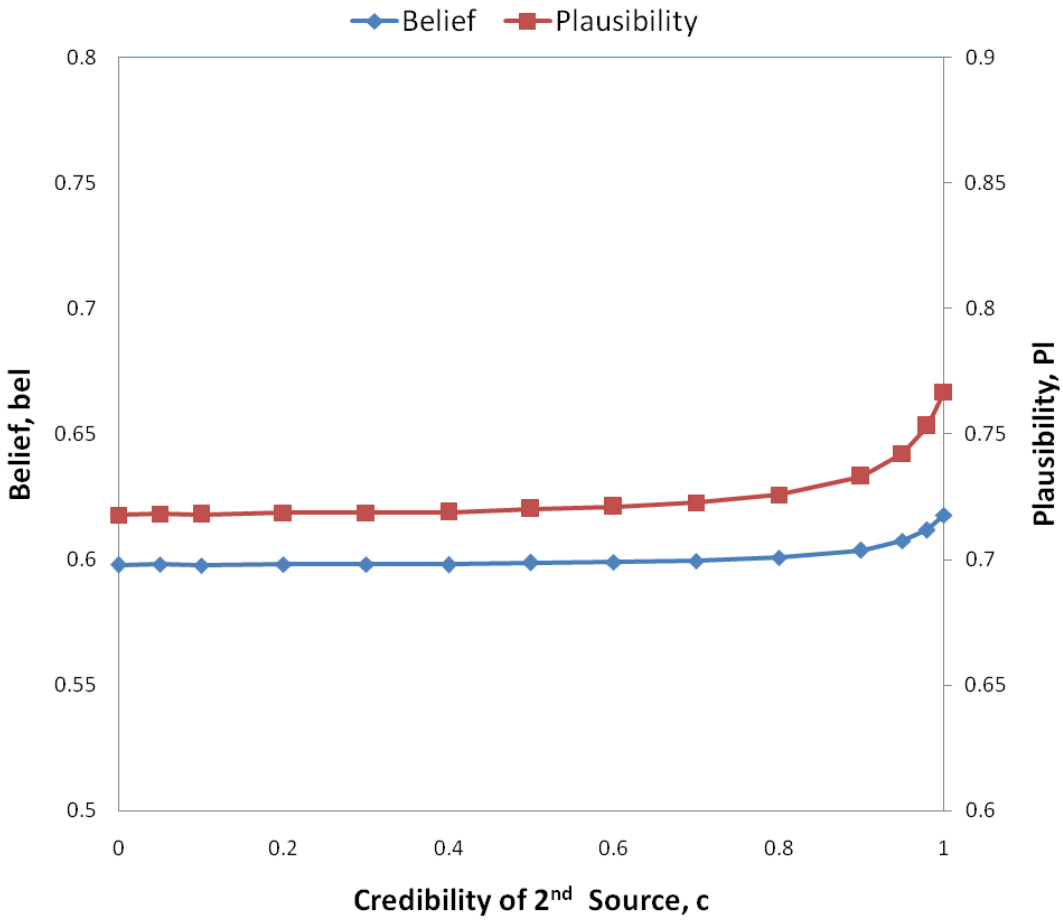

Figure 5.3 Variations of belief and plausibility with credibility (c) of source 2

Case 2: Two uncertain parameters with evidence from three different sources

The uncertain parameters are assumed to be the length of the weld (*l*) and height of the weld (*h*) with their uncertainties described by the multiplication factors x_1 and x_2, respectively. Three sources of evidence are assumed to give possible ranges of the intervals of x_1 and x_2 along with the corresponding bpa's as indicated in Table 5.8 (sources 1 and 2) and Table 5.10 (source 3) along with Table 5.8. The credibilities of

sources 1, 2 and 3 are assumed to be 1, 1 and c $(0 \le c \le 1)$, respectively. The resulting belief and plausibility values are shown in Fig. 5.4.

Table 5.10 Evidence for the uncertainty factors x_1 and x_2 from sources 3

	x_1	x_2
	Expert3 (Evidence3) (S3)	Expert3 (Evidence3) (S3)
Interval	Bpa	Bpa
[0.85,0.86]	0.025	0.035
[0.86,0.87]	0.035	0.05
[0.87,0.88]	0.04	0.045
[0.88,0.89]	0.05	0.045
[0.89,0.90]	0.055	0.04
[0.90,0.91]	0.065	0.075
[0.91,0.92]	0.08	0.08
[0.92,0.93]	0.095	0.1
[0.93,0.94]	0.105	0.085
[0.94,0.95]	0.09	0.105
[0.95,0.96]	0.055	0.08
[0.96,0.97]	0.05	0.05
[0.97,0.98]	0.06	0.06
[0.98,0.99]	0.04	0.04
[0.99,1.00]	0.05	0.05
[1.00,1.01]	0.04	0.025
[1.01,1.02]	0.045	0.025
[1.02,1.03]	0.02	0.01

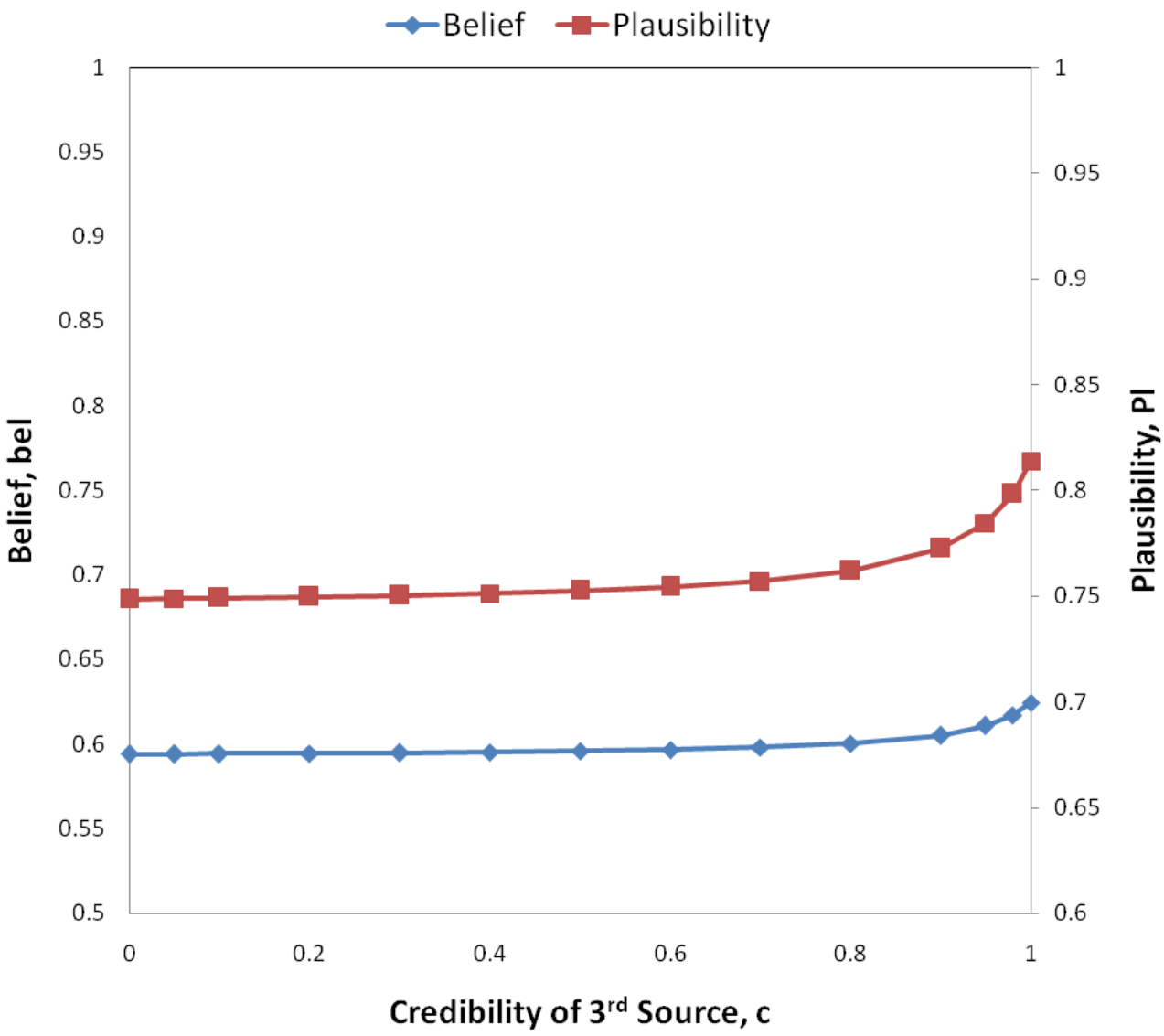

Figure 5.4 Variations of belief and plausibility with varying values of credibility (c) of source 3

Case 3: Four uncertain parameters with evidence from two different sources

The depth of the cantilever (*t*), length of the cantilever (*L)*, length of the weld (*l*) and height of the weld (*h*) are considered as the uncertain parameters with x_1, x_2, x_3 *and* x_4 indicating their corresponding multiplication factors. The evidences, in the form of interval ranges of the factors x_1, x_2, x_3 *and* x_4, from two different sources are assumed to

be as indicated in Table 5.9. The values of belief and plausibility computed for different values of the credibility (c) of source 2, with $(0 \le c \le 1)$, are shown in Fig. 5.5.

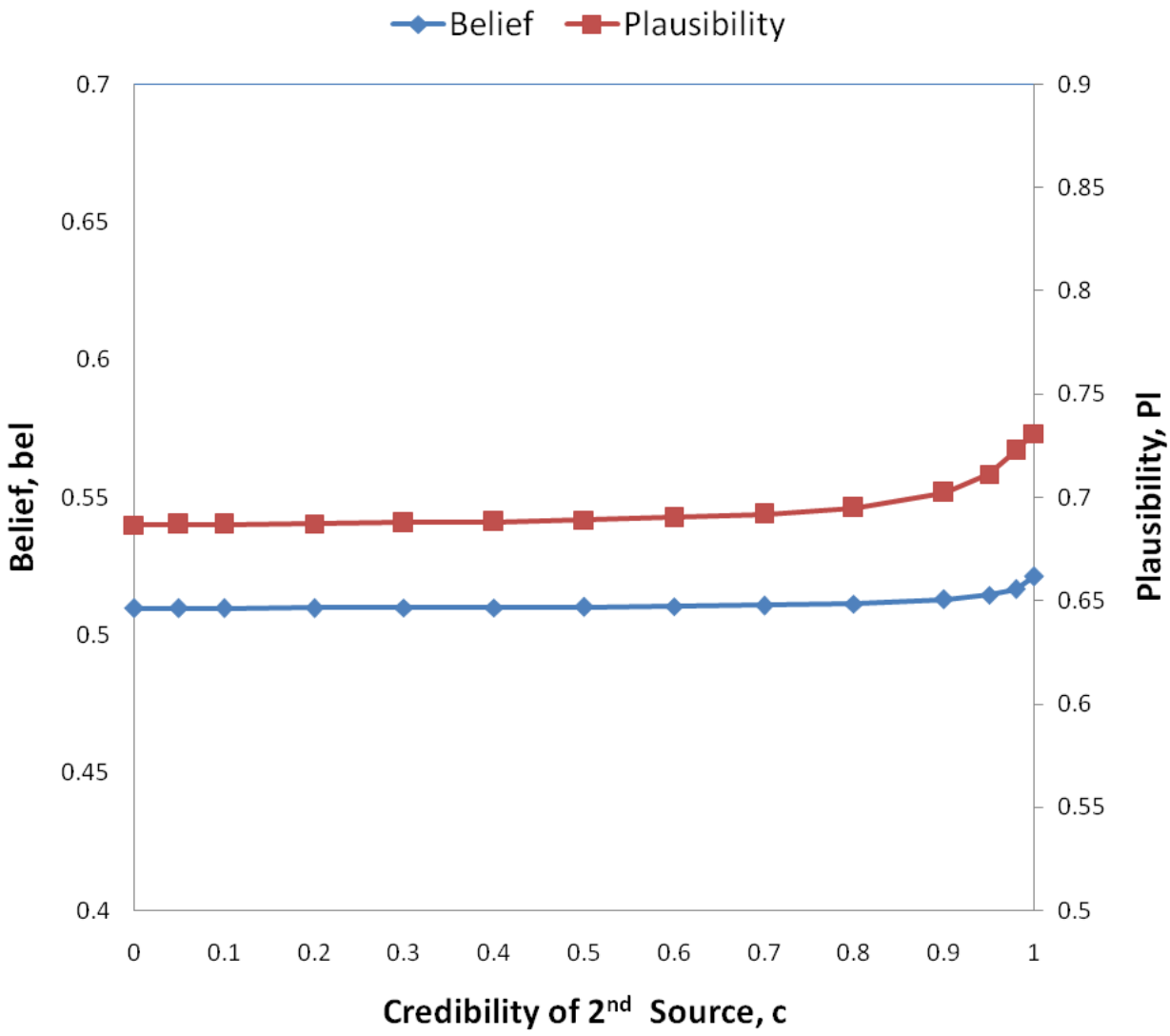

Figure 5.5 Variations of belief and plausibility with credibility (c) of source 2

Case 4: Four uncertain parameters with evidence from three different sources

In this case, evidences for the four uncertain parameters and the associated multiplication factors x_1, x_2, x_3 *and* x_4 considered in Case 3 are assumed to be available from three

sources as indicated in Table 5.9 (sources 1 and 2) and Table 5.11 (source 3). The values of belief and plausibility obtained with different values of the credibility (c) of source 3, with $(0 \le c \le 1)$, are shown plotted in Fig. 5.6.

Table 5.11 Evidence for the uncertain factors of , x_1, x_2, x_3 , and x_4 from sources 3

	x1	x2	x3	x4
	Expert3 (Evidence3) (S3)	Expert3 (Evidence3) (S3)	Expert3 (Evidence3) (S3)	Expert3 (Evidence3) (S3)
Interval	Bpa	Bpa	Bpa	Bpa
[0.85,0.86]	0.01	0.08	0.025	0.035
[0.86,0.87]	0.01	0.08	0.035	0.05
[0.87,0.88]	0.01	0.08	0.04	0.045
[0.88,0.89]	0.02	0.09	0.05	0.045
[0.89,0.90]	0.02	0.09	0.055	0.04
[0.90,0.91]	0.02	0.09	0.065	0.075
[0.91,0.92]	0.02	0.1	0.08	0.08
[0.92,0.93]	0.03	0.09	0.095	0.1
[0.93,0.94]	0.03	0.07	0.105	0.085
[0.94,0.95]	0.04	0.05	0.09	0.105
[0.95,0.96]	0.09	0.05	0.055	0.08
[0.96,0.97]	0.09	0.03	0.05	0.05
[0.97,0.98]	0.09	0.03	0.06	0.06
[0.98,0.99]	0.09	0.02	0.04	0.04
[0.99,1.00]	0.1	0.02	0.05	0.05
[1.00,1.01]	0.1	0.01	0.04	0.025
[1.01,1.02]	0.11	0.01	0.045	0.025
[1.02,1.03]	0.12	0.01	0.02	0.01

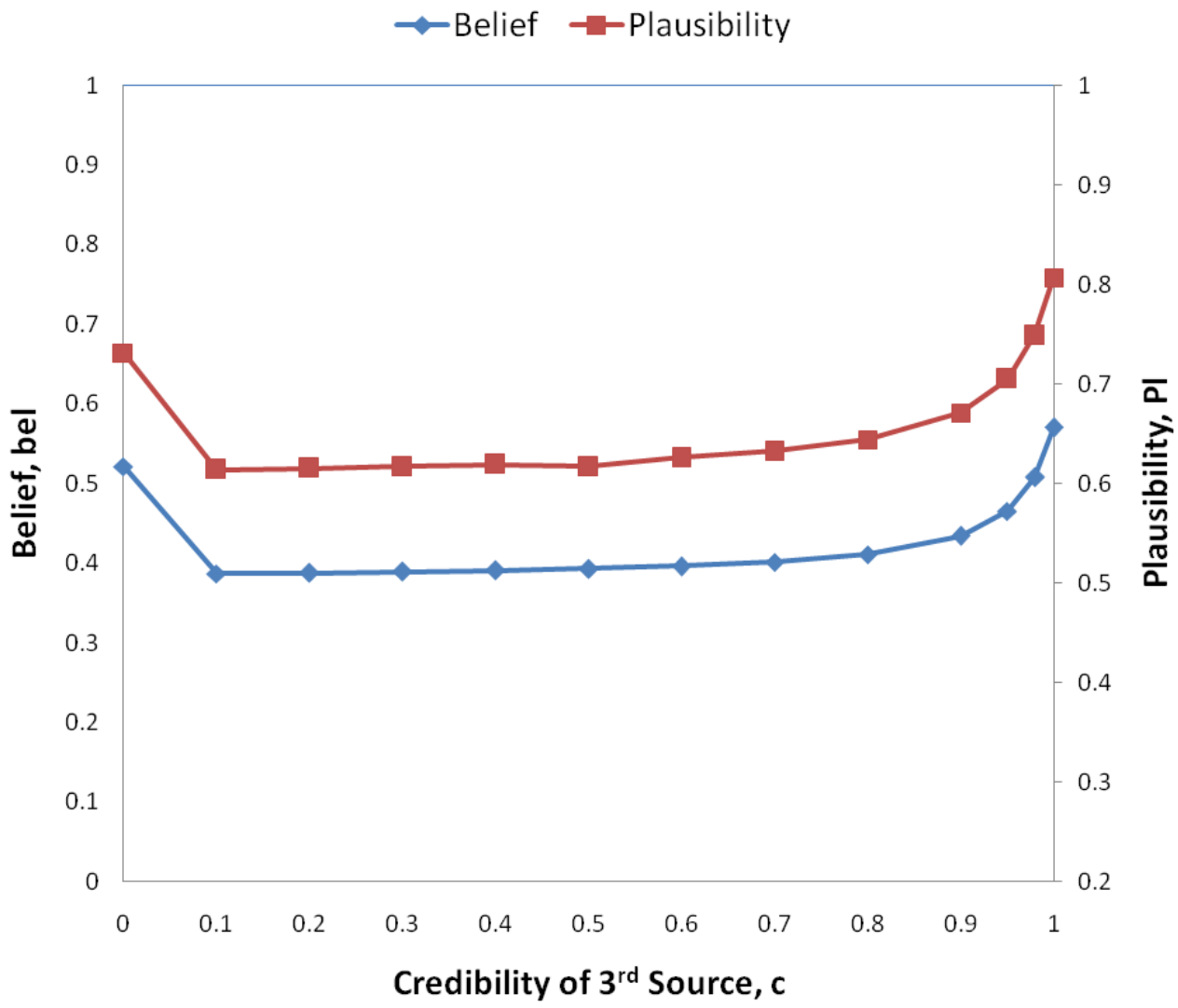

Figure 5.6 Variations of belief and plausibility with the credibility (c) of source 3

Case 5: Two uncertain parameters with evidence from three different sources (Same as case 2) with varying credibilities for two sources

The uncertain parameters are assumed to be the length of the weld (*l*) and height of the weld (*h*) with their uncertainties described by the multiplication factors x_1 and x_2, respectively, as in case2. The credibilities of sources 1, 2 and 3 are assumed to be c1, c2 and c3, respectively, with c1 assumed to be equal to 1 and the other two credibilities (c2

and c3) assumed to have values indicated in Table 5.12. The resulting belief and plausibility values are shown in Figs. 5.7 and 5.8, respectively

Table 5.12 Credibilities c2 and c3 for the sources 2 and 3

c2	c3
0.1	0.1 0.3 0.5 0.7 0.9 1.0
0.3	0.1 0.3 0.5 0.7 0.9 1.0
0.5	0.1 0.3 0.5 0.7 0.9 1.0
0.7	0.1 0.3 0.5 0.7 0.9 1.0
0.9	0.1 0.3 0.5 0.7 0.9 1.0

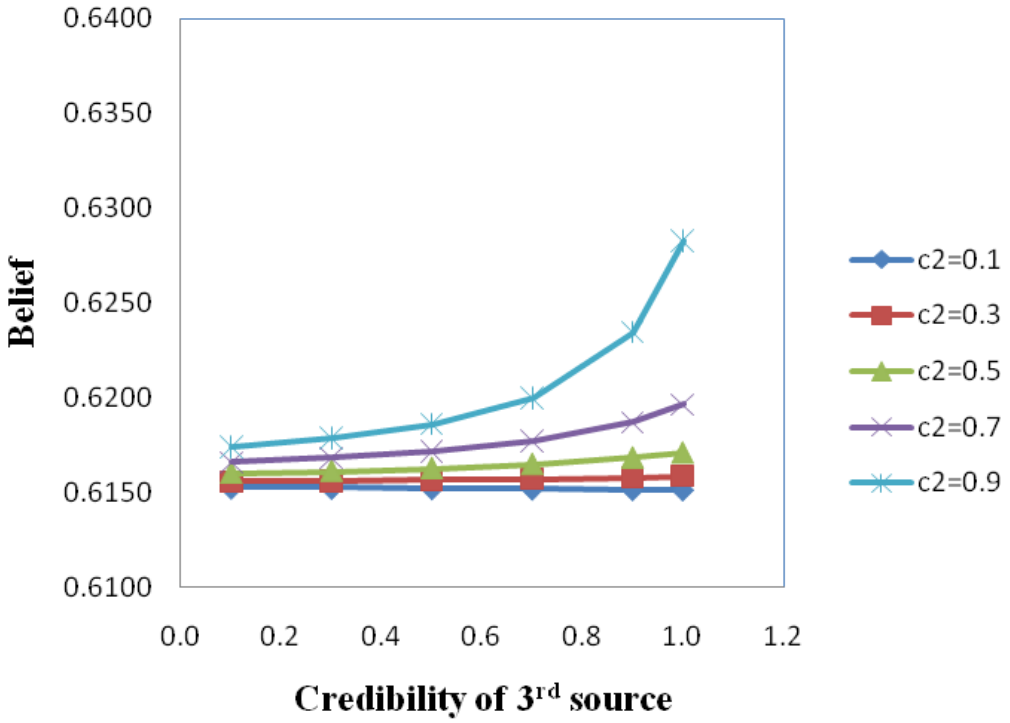

Figure 5.7 Variations of belief with varying values of credibilities of sources 2 and 3

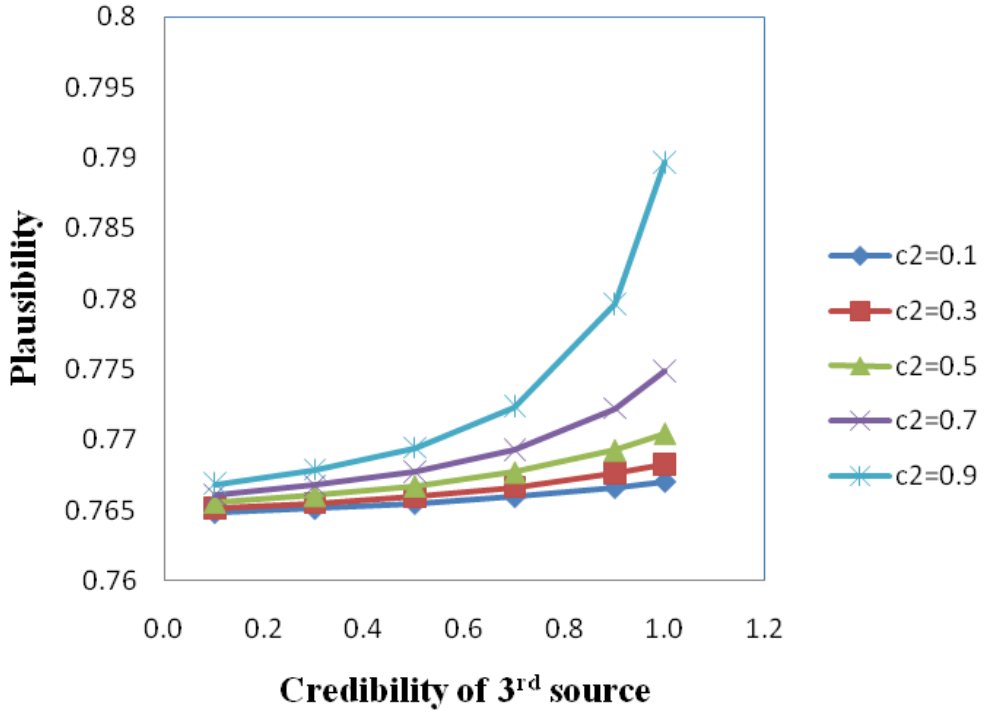

Figure 5.8 Variations of plausibility with varying values of credibilities of sources 2 and 3

Case 6: Four uncertain parameters with evidence from three different sources (Same as case 4) with varying credibilities for two sources

The depth of the cantilever (*t*), length of the cantilever (*L)*, length of the weld (*l*) and height of the weld (*h*) are considered as the uncertain parameters with x_1, x_2, x_3 *and* x_4 indicating their corresponding multiplication factors. The evidences for these multiplication factors x_1, x_2, x_3 *and* x_4 from three different sources are assumed to be same as in case 4. The credibilities of sources 1, 2 and 3 are assumed to be c1, c2 and c3, respectively, with c1 assumed to be equal to 1 and the other two credibilities (c2 and c3) assumed to have values indicated in Table 5.12. The resulting belief and plausibility values are shown in Figs. 5.9 and 5.10, respectively

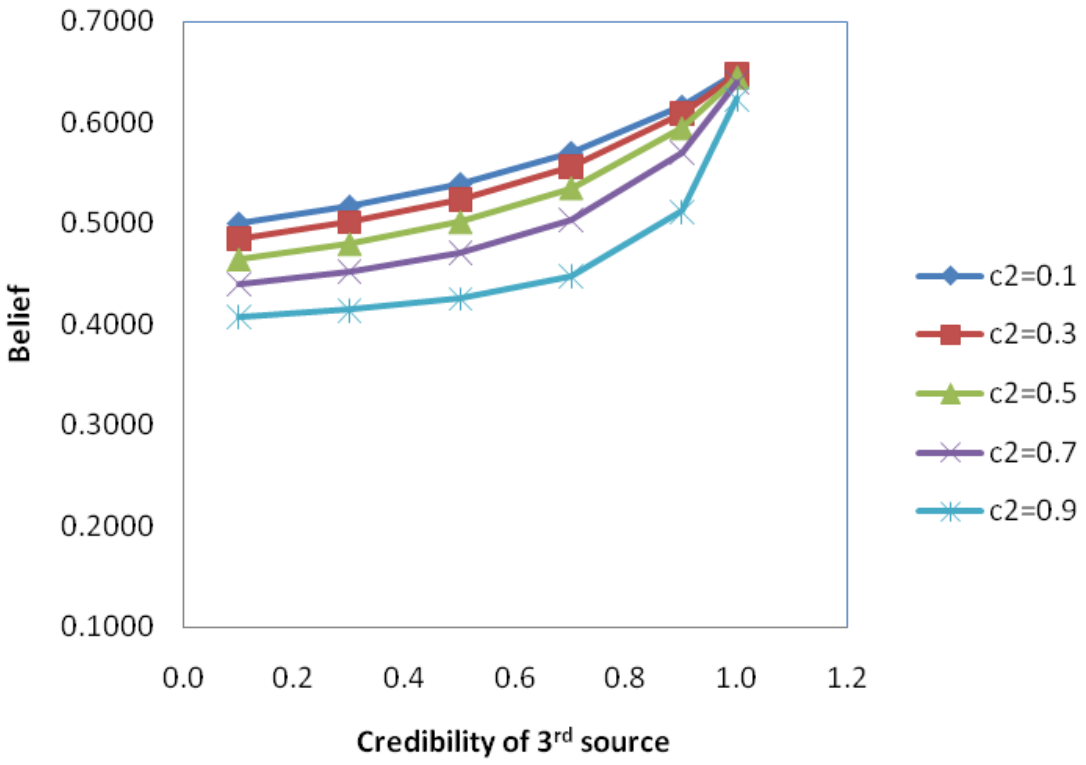

Figure 5.9 Variations of belief with varying values of credibilities of sources 2 and 3

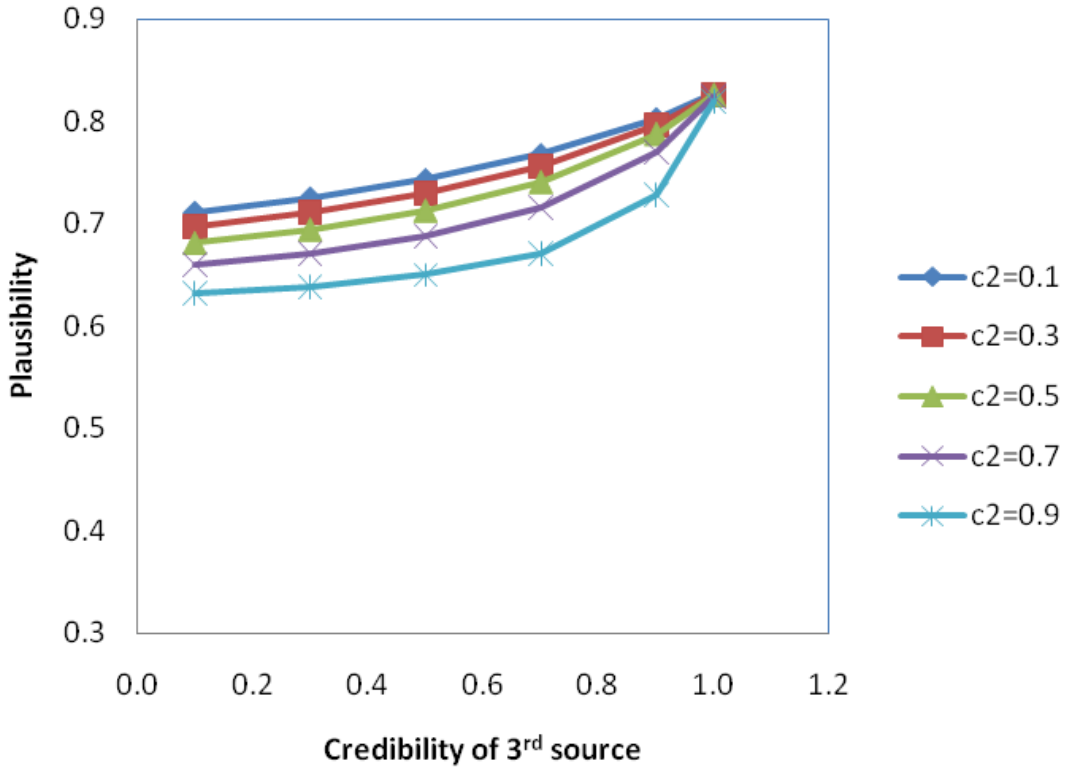

Figure 5.10 Variations of plausibility with varying values of credibilities of sources 2 and 3

5.6 DISCUSSION

A methodology is presented for the safety analysis of uncertain systems in the presence of multiple sources of evidence based on DST. The information on the uncertain parameters is assumed to be available in the form of interval- valued data from multiple sources. The vertex method is used in computing the interval- valued response of the system using known mathematical expressions.

The methodology is extended for combining evidence from multiple sources when different values of credibility are associated with different sources. Figures 5.3 – 5.6 indicate that irrespective of the number of sources, the belief and plausibility values converge to those corresponding to the ones obtained by considering evidences from (n-

1) sources when the credibility of one of the sources (n^{th} source) is reduced to zero. The belief and/or plausibility will increase with an increase in the number of sources of evidence and decrease with an increase in the number of uncertain parameters in the model. It can also be observed that the variations of the belief and plausibility values with varying values of the credibility of the source are similar, i.e., when the belief curve rises, the corresponding plausibility curve also rises. A sudden variation can be seen in the curves (Fig 5.6) when the credibility of one of the sources varies between 0 to 0.1 as it involves combining n-1 intervals for $c = 0$ and n intervals for $c > 0$ (such as $c > 0.1$) and due to less credibility value of the 3^{rd} source ($c = 0.1$) (as it increases the uncertainty in the model thereby causing a decrease in both belief and plausibility values ; the belief and plausibility values tend to improve with an increase in the credibility of the 3^{rd} source.) The effect of credibility can be seen to become more significant when its value is closer to 1 (i.e., large changes in the slopes of the curves can be seen near $c = 1$). The curves shown in Figs 5.7 to 5.11 indicate that both belief and plausibility increase with an increase in the credibility of the 3^{rd} sources while the credibilities of the other sources are kept constant. This increase is observed to be very high when the credibility is close to 1. The belief and plausibility values increase with the number of sources of evidence and thus the results obtained through the application of DST are justified as there is consistency of the evidences among different sources.

The results indicate that evidence theory can deal with situations in which epistemic uncertainties are represented by interval-valued parameters. This capability is important in many engineering applications because the precision of the available data can only permit representation as interval- valued information (as in the case of tolerance values).

In addition, evidence theory does not require the assumption of probability distributions of input parameters if none is available. It can be seen that evidence theory is able to propagate the interval-valued input data to system response in the form of bounds known as interval-valued probabilities consistent with the available evidence on the input data; in other words, evidence theory gives the highest and the lowest possible probabilities consistent with the available evidence on the input data. It is to be noted that the method of combining evidences is dependent on the available data in the specific situation and a unified method, suitable for combining evidences in all possible situations, dealing with epistemic uncertainty, cannot be given in the form of a simple mathematical expression.

5.7 SUMMARY

When evidences on several uncertain parameters are available from a number of sources (experts) in an engineering problem, and if the response of the system involves mathematical expressions, DST or Zhang's combination rule can be used. In the case of the welded beam problem, evidences of two and four uncertain parameters are combined to find the maximum shear stress induced in the weld. A modified DST method is also presented to combine evidences from multiple sources, when the multiple sources of evidence have different credibilities. The variations in the belief and plausibility have been observed to depend on the number of interval ranges for the interval-valued data for combining the evidence. In the next chapter, a methodology is proposed to combine evidence when sources of evidence have different credibilities by using fuzzy theory in conjunction with the vertex method.

CHAPTER 6

AN EVIDENCE-BASED FUZZY APPROACH FOR THE SAFETY ANALYSIS OF UNCERTAIN SYSTEMS

6.1 OVERVIEW

The application of Dempster Shafer theory for combining multiple sources of evidence to handle the uncertainties present in engineering systems is well established. In this chapter, a fuzzy approach is presented for the safety analysis of uncertain engineering systems in the presence of multiple sources of evidence (in section 6.2). The α-cut approach described in section 3.3 of chapter 3 is used to represent the fuzzy membership functions of the uncertain parameters. The large epistemic uncertainty information for each of the uncertain parameters is assumed to be available in the form of interval-valued data from multiple sources. The fuzzy membership function of the response of the system (such as the margin of safety) is computed by applying fuzzy arithmetic to the mathematical formulation of the system. A new procedure is introduced to calculate the bounds on the response of the system such as the margin of failure and margin of safety in section 6.3. After the presentation of an illustrative example in section 6.4, a new methodology, termed the Weighted Fuzzy Theory for Intervals (WFTI), is proposed in section 6.5, for combining evidence when different credibilities are associated with the various sources of evidence. The application of the proposed method is illustrated by considering the design of a welded beam involving multiple uncertain parameters in section 6.5. A summary of this chapter is included on section 6.6.

6.2 FUZZY APPROACH FOR COMBINING EVIDENCES

When evidences from multiple sources are available regarding the uncertainty of a system, Dempster-Shafer theory has traditionally been used to combine the evidences. This theory was studied and described in detail by Dempster [54] and Shafer [186]. Dempster-Shafer theory is considered as a generalization of probability theory where probabilities are assigned to sets instead of mutually exclusive events. In Dempster-Shafer theory, evidence can be associated with multiple or sets of events. By combining evidence from multiple sources, Dempster-Shafer theory provides the lower and upper bounds, in the form of belief and plausibility, for the probability of occurrence of an event. In this work, an uncertain parameter is modeled as a fuzzy variable and the available evidences on the ranges of the uncertain parameter, in the form of basic probability assignments (bpa's), are represented in the form of membership functions of the fuzzy variable [38,113,143]. The membership functions constructed from the available evidences from multiple sources are added as multiple fuzzy data to find the combined membership of the uncertain or fuzzy parameter. The resulting combined membership function of the fuzzy parameter is then used to estimate the lower and upper bounds of any response quantity of the system, (such as the margin of safety or margin of failure) in the context of the safety analysis of an engineering system.

6.3 COMPUTATION OF BOUNDS ON THE MARGIN OF FAILURE/SAFETY

The following procedure is used to calculate the bounds on the margin of failure of the system based on the membership function of the margin of failure curve shown in Fig. 6.1. We define margin of failure as

Margin of failure = Maximum induced stress - Maximum permissible stress

Let A represent the area under the membership function curve until the margin of failure equals to zero, B indicate the area under the membership function value curve for the margin of failure greater than zero. The lower and upper bounds on the margin of failure (greater than zero) can be expressed as

$$\text{Lower bound} = 0$$
$$\text{Upper bound} = \frac{B}{A+B} \tag{6.1}$$

where A>>B.

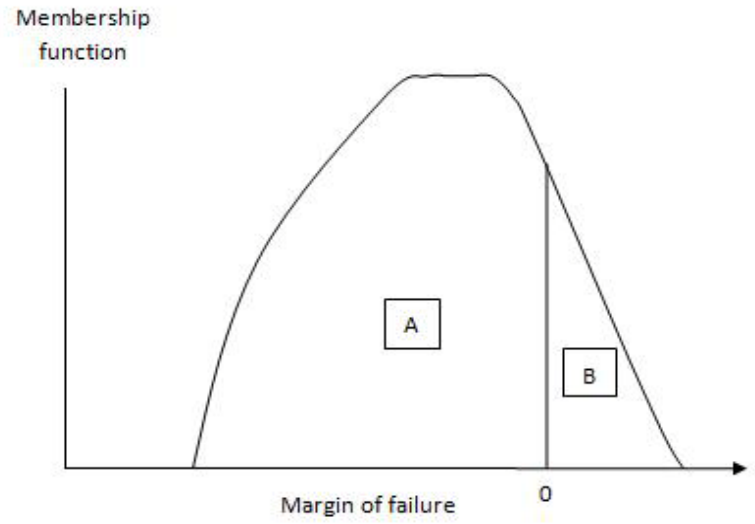

Figure 6.1 General membership function of the margin of failure

Similarly, the bounds on the margin of safety of the system can be computed using the membership function of the margin of safety curve shown in Fig. 6.2. We define margin of safety as

Margin of safety = Maximum permissible stress - Maximum induced stress

Let A represent the area under the membership function curve until the margin of safety equals to zero, B indicate the area under the membership function value curve for the margin of safety greater than zero. The lower and upper bounds on the margin of safety can be expressed as

$$\begin{aligned} \text{Lower bound} &= \frac{B}{A+B} \\ \text{Upper bound} &= 1 \end{aligned} \tag{6.2}$$

where A<<B.

Figure 6.2 General membership function of the margin of safety

6.4 ILLUSTRATIVE EXAMPLE: A WELDED BEAM PROBLEM

To illustrate the methodology of combining evidences using a fuzzy approach, the safety/failure analysis of the welded beam introduced in section 4.4 of chapter 4 is considered. The beam is considered unsafe if the maximum shear stress in the weld is greater than the permissible stress of $\tau_{\max}$ for the data [122]: P = 6000 lb, L = 14 in., $E = 30x10^6$ psi, $\tau_{\max} = 13{,}600$ psi, h = 0.3437 in., l = 8.149 in. and t = 8.273 in. b = 0.2455 in. The bounds on the margin of safety and margin of failure of the welded beam are computed for two types of data. In the first type, the uncertain parameters are assumed to be fuzzy with triangular membership functions. In the second type, the ranges of the uncertain parameters are assumed to be available in the form of evidences from multiple sources.

6.4.1 With assumed triangular membership functions for uncertain parameters

Two cases are considered: one with two uncertain parameters and the other with four uncertain parameters. A matlab program is developed to implement the fuzzy arithmetic required to handle both the two and the four uncertain parameters and obtain an assessment of the likelihood of the maximum induced shear stress exceeding the specified permissible value.

Case 1: **Two uncertain parameters**

The length of the weld (l) and the height of the weld (h) are treated as the uncertain parameters. Let x_1 and x_2 denote the multiplication factors that define the uncertainties of these parameters about their respective nominal values. The membership functions of x_1 and x_2 are assumed to be triangular as shown in Figs. 6.3(a) and (b).

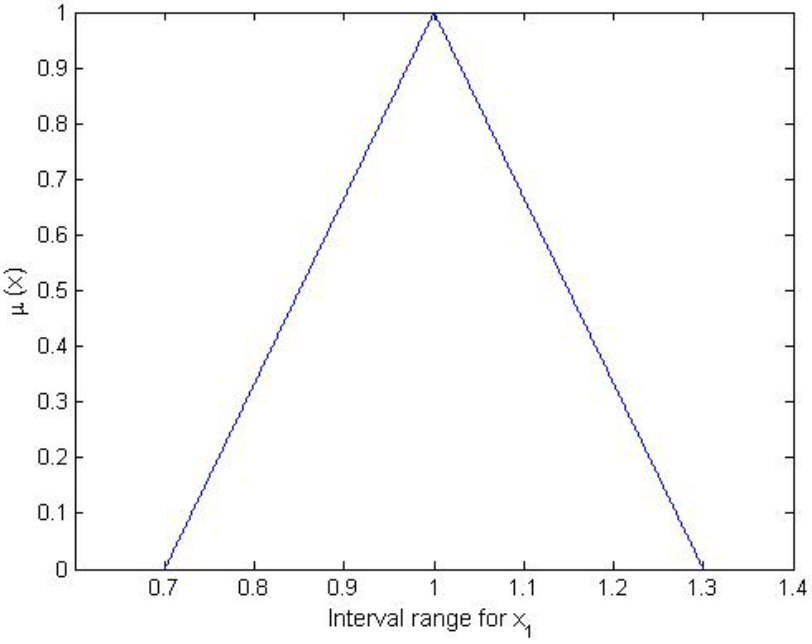

(a)

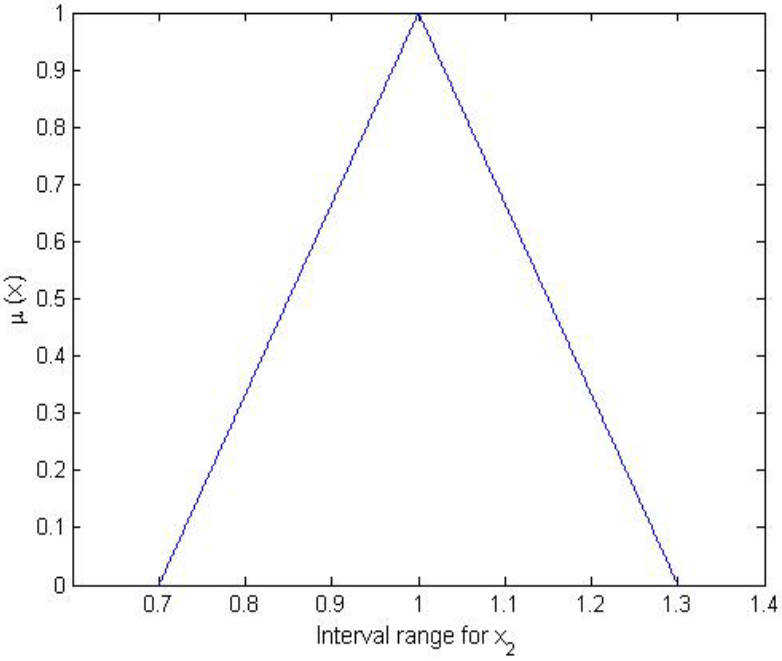

(b)

Figure 6.3 Fuzzy membership functions of x_1 and x_2

The permissible stress, $\tau_{allowable}$, is assumed to be a fuzzy quantity with a triangular membership function in the range of ± 15% of $\tau_{\max}$ ($0.85\,\tau_{\max}$ psi to $1.15\,\tau_{\max}$ psi) with $\tau_{\max} = 13{,}600$ psi as shown by the solid line in Fig. 6.4. The dotted curve in Fig. 6.4 shows the fuzzy description of the maximum shear stress induced in the beam. The margin of safety is calculated as the fuzzy difference between $\tau_{allowable}$ and $\tau_{\max}$ as shown in Fig. 6.5. Similarly, the margin of failure is calculated as the fuzzy difference between $\tau_{\max}$ and $\tau_{allowable}$ as shown in Fig. 6.6.

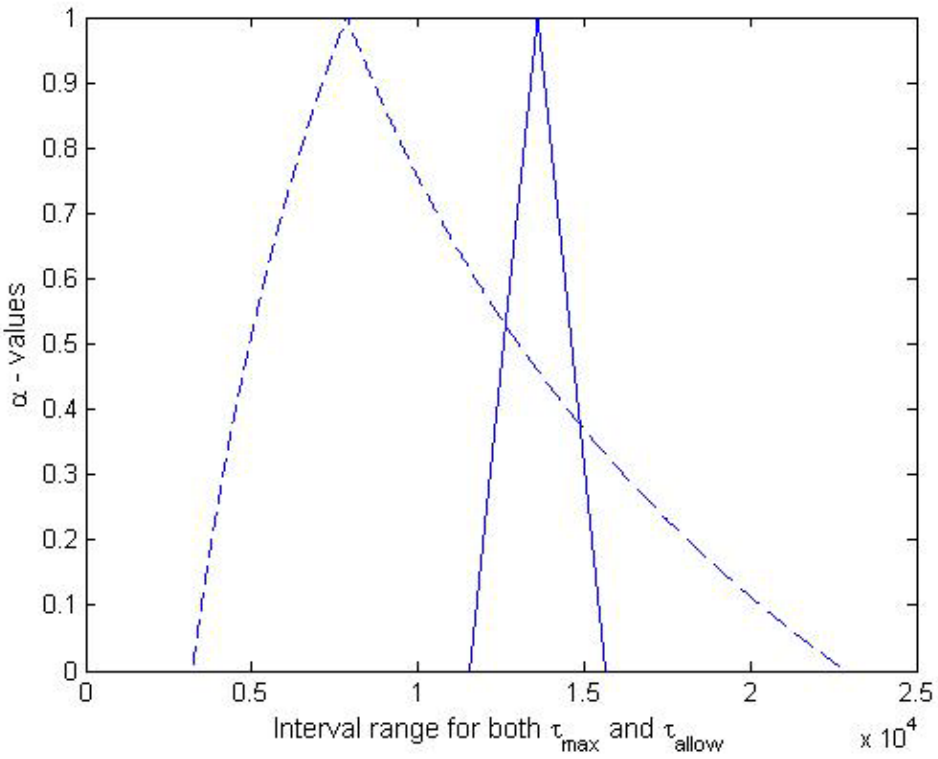

Figure 6.4 Fuzzy membership functions of $\tau_{\max}$ and $\tau_{allowable}$

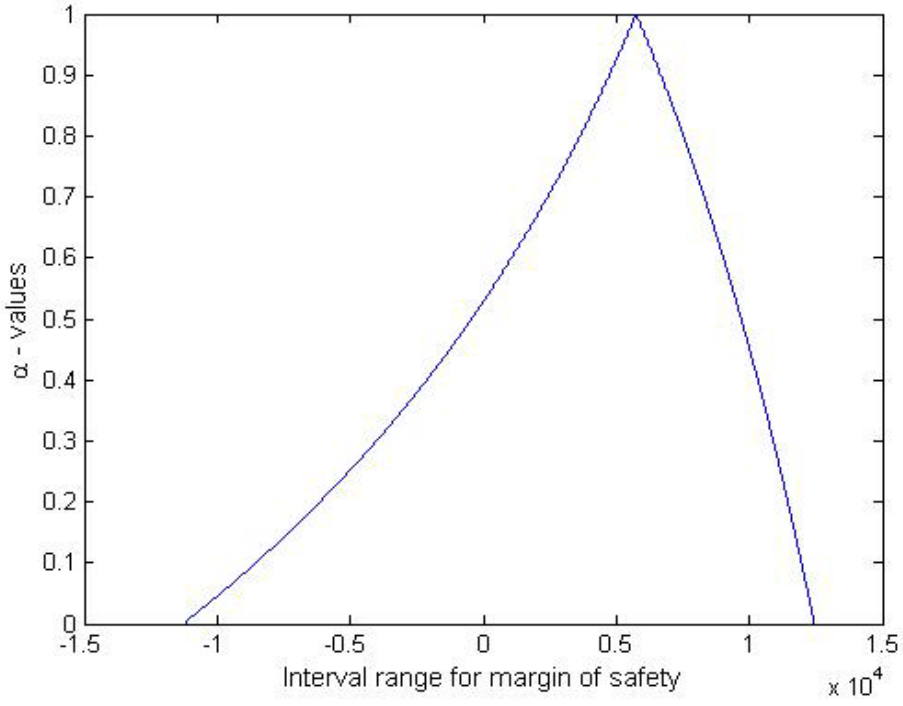

Figure 6.5 Fuzzy membership function of the margin of safety

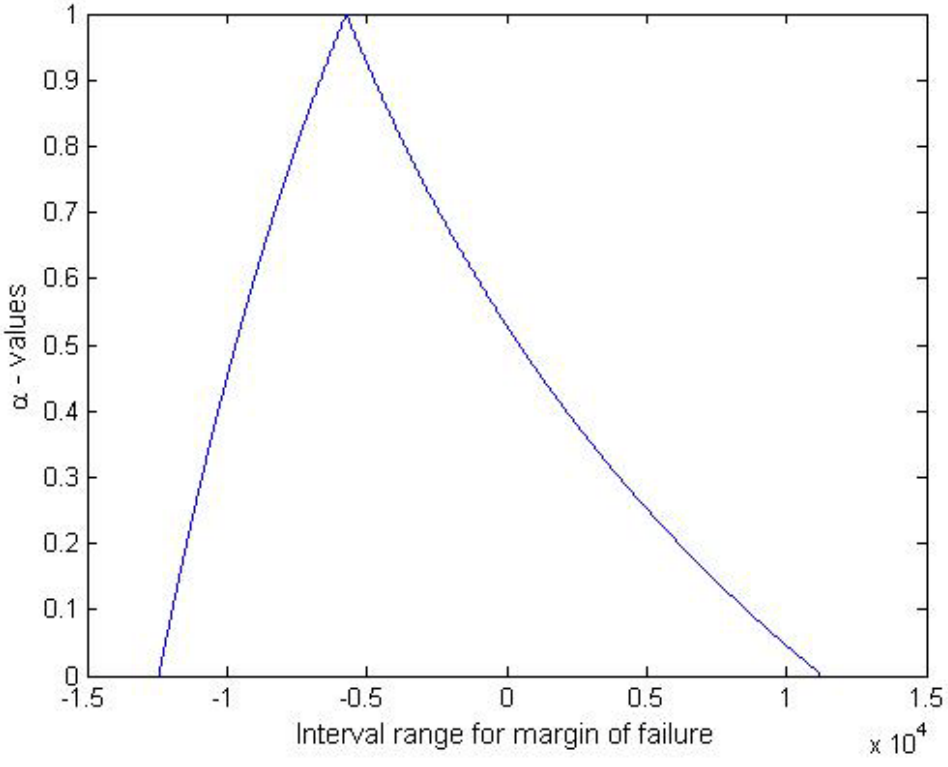

Figure 6.6 Fuzzy membership function of the margin of failure

Equations 6.1 and 6.2 are used to find the lower and upper bounds on the margin of failure as well as the margin of safety based on the curves shown in Figs. 6.5 and 6.6, respectively, and the results are shown in Table 6.1.

Table 6.1 Lower and upper bounds on the margins of failure and safety

Response quantity	Case-1		Case-2	
	Lower bound	Upper bound	Lower bound	Upper bound
Margin of failure	0	0.24873	0	0.52194
Margin of safety	0.75127	1	0.47806	1

Case 2: Four uncertain parameters

In this case, the depth of the cantilever (t), length of the cantilever (L), length of the weld (l) and height of the weld (h) are considered as the four uncertain parameters with x_1, x_2, x_3 and x_4 indicating their corresponding multiplication factors (representing variations about their respective nominal values). The membership functions for x_1 and x_2 are assumed to be same as in Case-1 (Fig. 6.3). The membership functions of the possible ranges or intervals of x_3 and x_4 are assumed to be triangular as shown in Fig. 6.7.

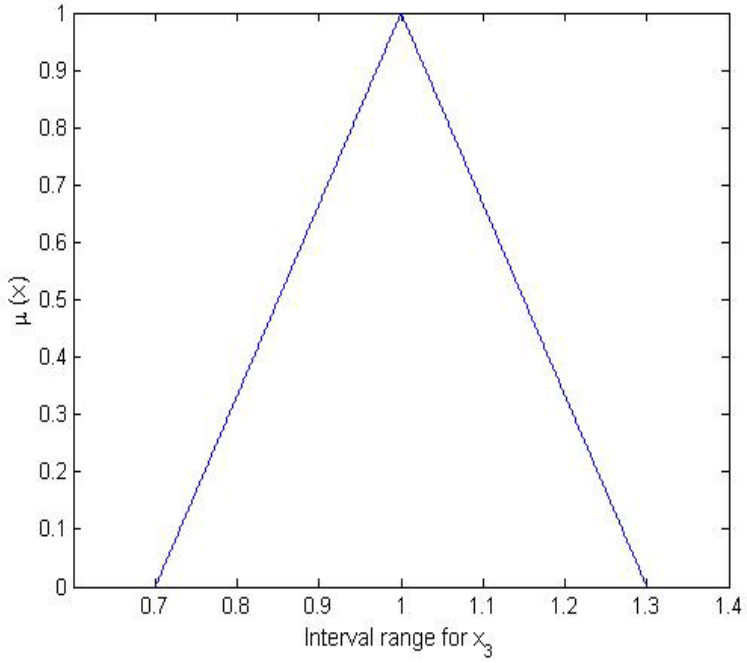

(a)

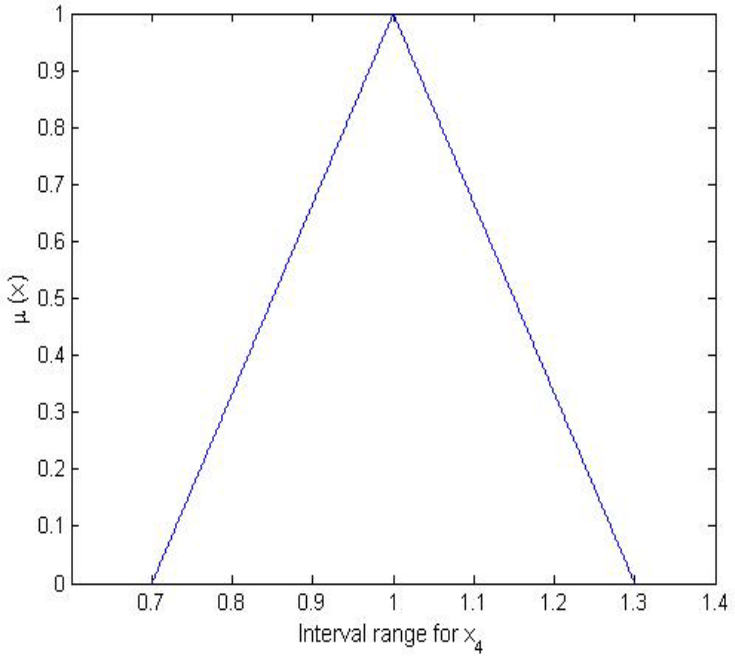

(b)

Figure 6.7 Fuzzy membership functions of x_3 and x_4

The procedure indicated earlier is used to find the likelihood of the maximum induced shear stress exceeding the specified permissible/allowable value, $\tau_{allowable}$, which is considered to be a fuzzy quantity with a triangular membership function with a range of ± 15% of $\tau_{\max}$ (0.85 $\tau_{\max}$ psi to 1.15 $\tau_{\max}$ psi) with $\tau_{\max} = 13{,}600$ psi as shown by the solid line in Fig. 6.8. The dotted curve in Fig. 6.8 shows the fuzzy description of the maximum shear stress induced in the beam.

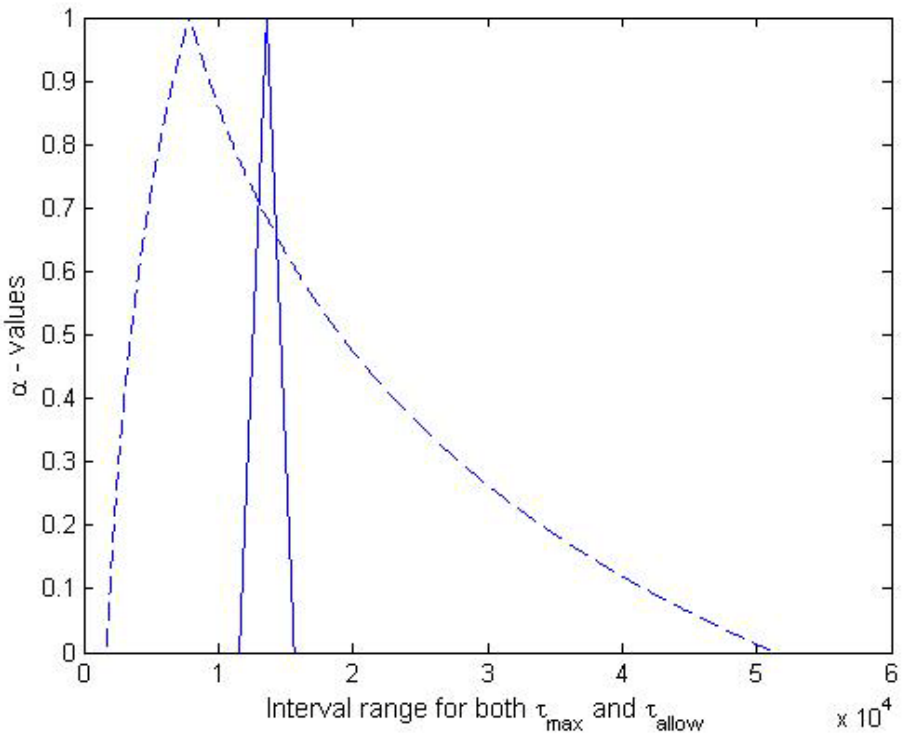

Figure 6.8 Fuzzy membership functions of $\tau_{\max}$ and $\tau_{allowable}$

The margin of safety, calculated as the fuzzy difference between $\tau_{allowable}$ and $\tau_{\max}$, i.e., $\tau_{allowable} - \tau_{\max}$ and is shown in Fig. 6.9. Similarly, the margin of failure, calculated as the fuzzy difference between $\tau_{\max}$ and $\tau_{allowable}$, i.e., $\tau_{\max} - \tau_{allowable}$, is shown in Fig. 6.10.

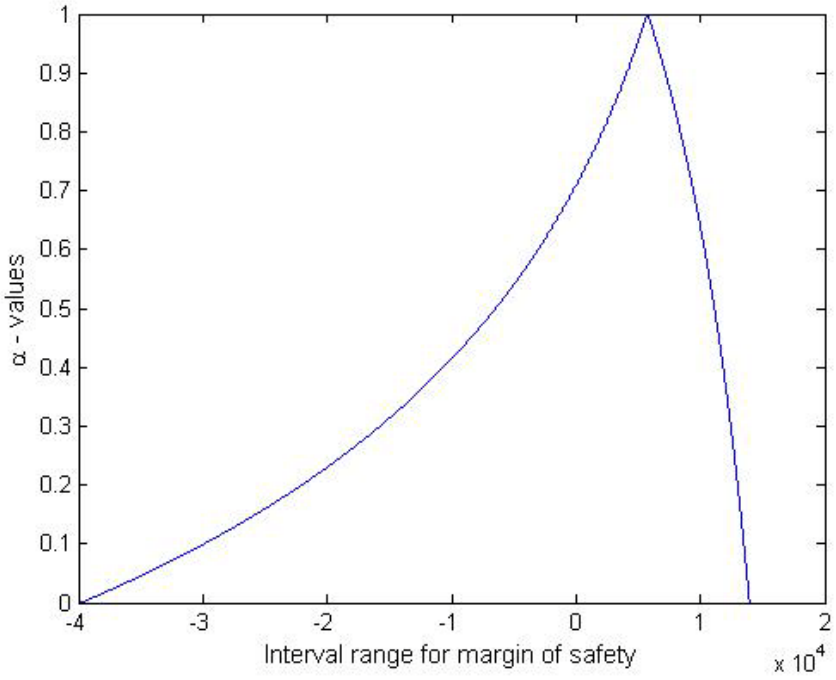

Figure 6.9 Fuzzy membership function of the margin of safety

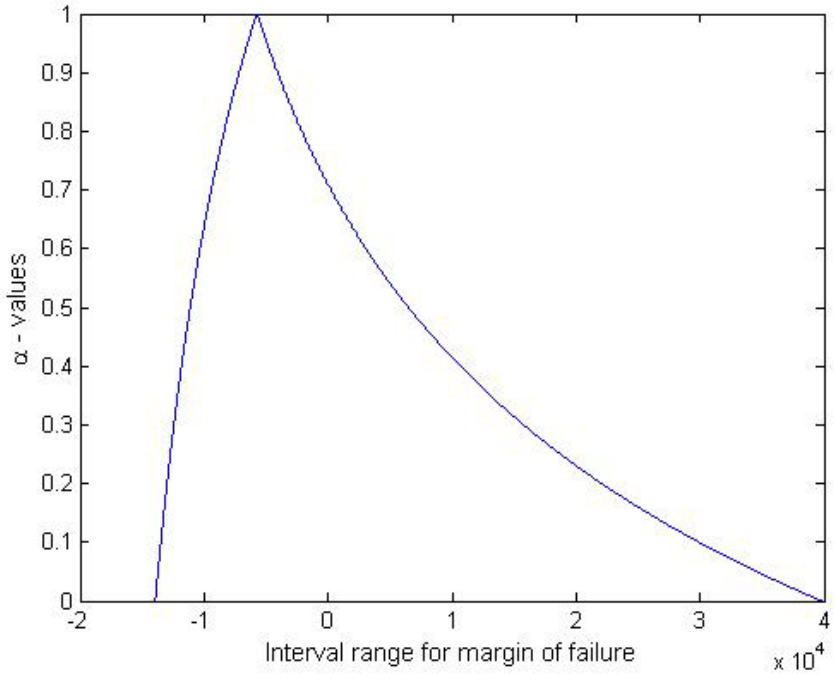

Figure 6.10 Fuzzy membership function of the margin of failure

Using the procedure indicated in Case 1, the lower and upper bounds on the margins of safety and failure are computed from the membership function curves shown in Figs. 6.9 and 6.10, respectively, to obtain the results indicated in Table 6.1.

6.4.2 With membership functions of uncertain parameters constructed using evidences from multiple sources

The methodology is illustrated for the safety/failure analysis of a welded beam by considering two cases. In each case, two types of membership functions - triangular and trapezoidal – are assumed. The range of triangular membership function for $\tau_{allowable}$ is assumed as ± 15% of $\tau_{\max}$ ($0.85\,\tau_{\max}$ to $1.15\,\tau_{\max}$) with center at $\tau_{\max}$ and the range of trapezoidal membership function is assumed to be ± 15% of $\tau_{\max}$ ($0.85\,\tau_{\max}$ to $1.15\,\tau_{\max}$) at $\alpha = 0$ and ± 3 % of $\tau_{\max}$ ($0.97\,\tau_{\max}$ to $1.03\,\tau_{\max}$) at $\alpha = 1$. Matlab programs are developed to incorporate the evidences for the various interval ranges of the uncertain parameters for the following cases.

Case 1: **Two uncertain parameters with evidence from three different sources**

The length of the weld (*l*) and the height of the weld (*h*) are the uncertain parameters with x_1 and x_2 denoting the multiplication factors that indicate their respective uncertainties. It is assumed that three sources of evidence provide possible ranges or intervals of x_1 and x_2 along with the corresponding bpa's (as in the case of Dempster Shafer theory) as given in Table 6.2. The bpa's are normalized so that the maximum value corresponds to a membership value of one for modeling the uncertain factors as fuzzy quantities and

the resulting fuzzy descriptions of factors x_1 and x_2 from the evidences available from sources 1, 2 and 3 are shown in Figs. 6.11(a)-(c) and 6.12(a)-(c), respectively. The two evidences (fuzzy descriptions) available for each of the factors x_1 and x_2 are added to obtain the combined fuzzy representations of x_1 and x_2 shown in Figs. 6.11(d) and 6.12(d), respectively. These combined fuzzy representations are approximated as shown in Figs. 6.13(a) and (b) (smoothed by neglecting the valleys in the curves of Figs. 6.11(d) and 6.12(d) to avoid multiple disjointed ranges of the variables corresponding to any specific value of α-cut in an α-cut representation of the fuzzy quantities).

The fuzzy maximum induced shear stress in the weld, $\tau_{\max}$, computed using the fuzzy parameters x_1 and x_2 is shown in Fig. 6.14(a). A triangular membership function is assumed for the allowable shear stress as shown in Fig. 6.14(b). The maximum induced shear stress and the allowable shear stress are shown in the same graph in Fig. 6.14(c). The fuzzy margin of safety and margin of failure are computed to obtain Figs. 6.14(d) and (e), respectively. Similarly, when a trapezoidal form of membership function is assumed for the allowable shear stress (τ_{allow}) as shown in Fig. 6.15(a), the fuzzy margins of safety and failure can be obtained as shown in Figs. 6.15(c) and (d), respectively.

Table 6.2 Evidences for the uncertain factors x_1 and x_2 from sources S_1, S_2 and S_3

x_1	Source1 (S_1)	Interval	[0.7,0.8]	[0.8,1.1]	[1.0,1.2]	[1.2,1.3]
		Bpa	0.1	0.4	0.4	0.1
	Source2 (S_2)	Interval	[0.7,0.9]	[0.8,1.0]	[1.0,1.2]	[1.1,1.3]
		Bpa	0.1	0.4	0.3	0.2
	Source3 (S_3)	Interval	[0.9,1.1]	[1.0,1.2]	[1.2,1.3]	
		Bpa	0.3	0.4	0.3	
x_2	Source1 (S_1)	Interval	[0.8,0.9]	[0.9,1.1]	[1.0,1.2]	[1.2,1.3]
		Bpa	0.1	0.4	0.4	0.1
	Source2 (S_2)	Interval	[0.7,0.9]	[0.9,1.0]	[1.0,1.2]	[1.1,1.3]
		Bpa	0.2	0.4	0.2	0.2
	Source3 (S_3)	Interval	[0.9,1.1]	[1.0,1.2]	[1.2,1.3]	
		Bpa	0.4	0.4	0.2	

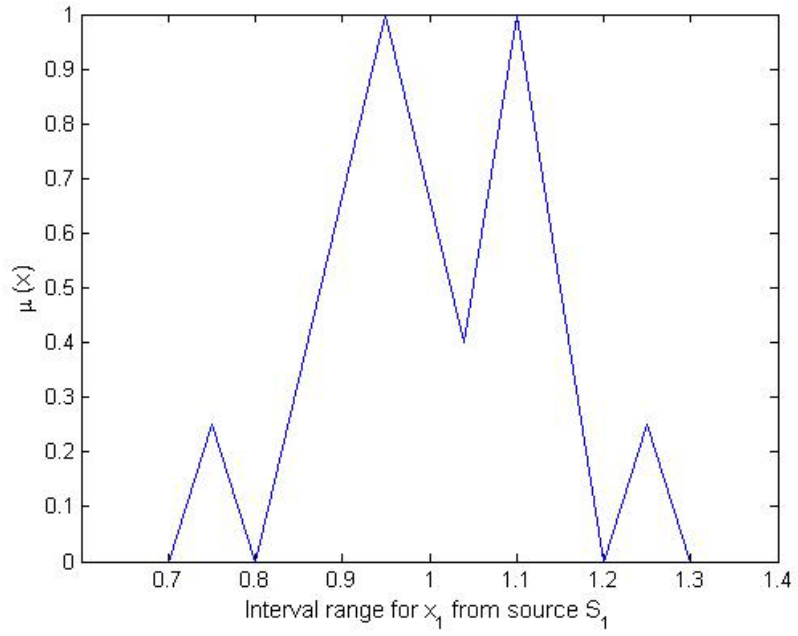
μ (x)
Interval range for x1 from source S1

(a)

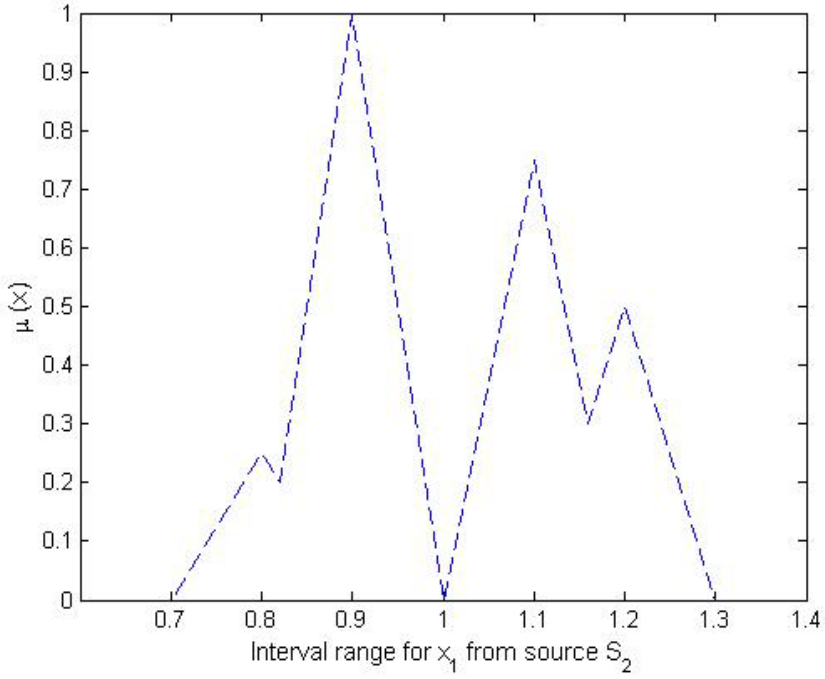
μ (x)
Interval range for x1 from source S2

(b)

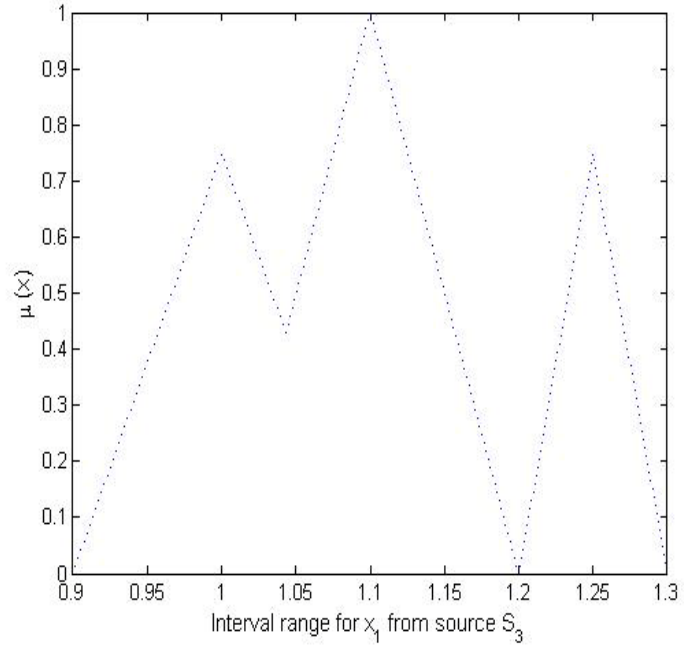

(c)

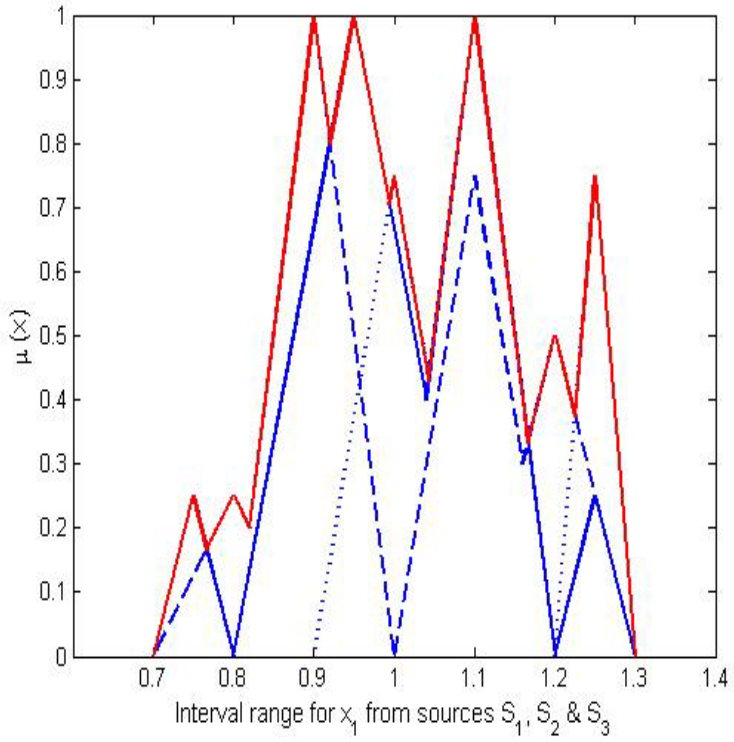

(d)

Figure 6.11 Combined fuzzy membership function of x_1 from sources S_1, S_2 and S_3

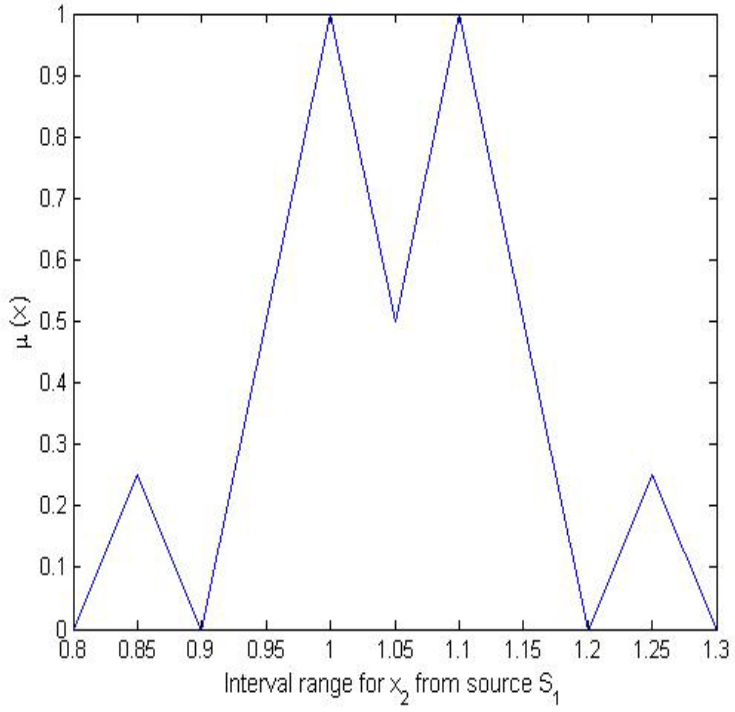
μ (x)
Interval range for x2 from source S1

(a)

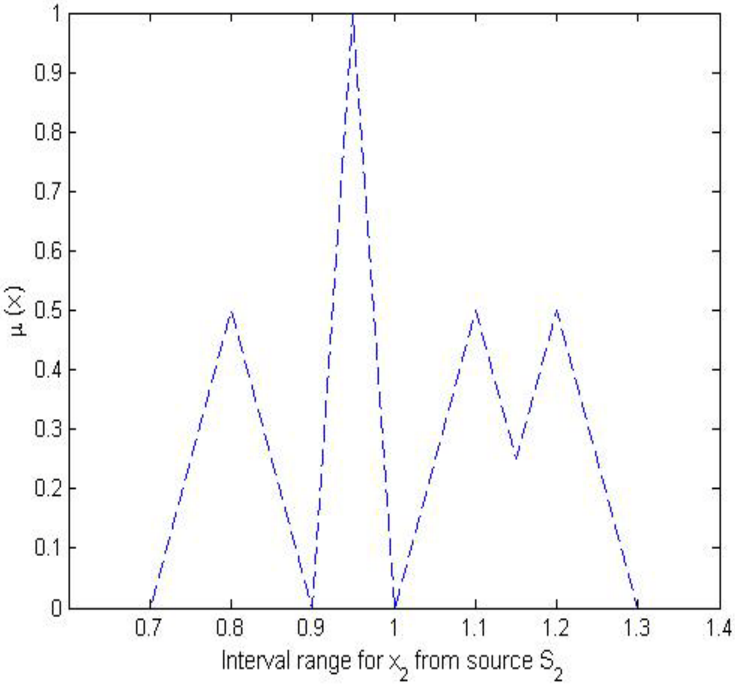
μ (x)
Interval range for x2 from source S2

(b)

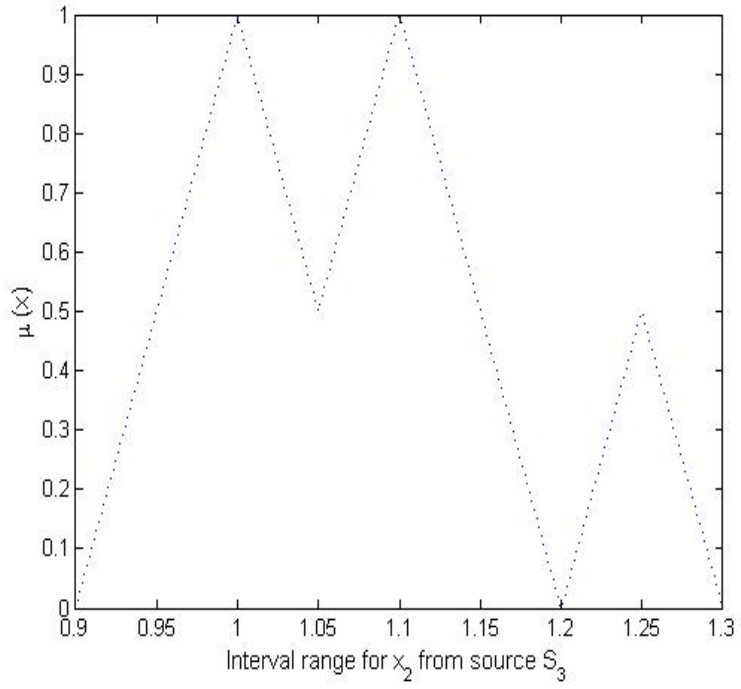

(c)

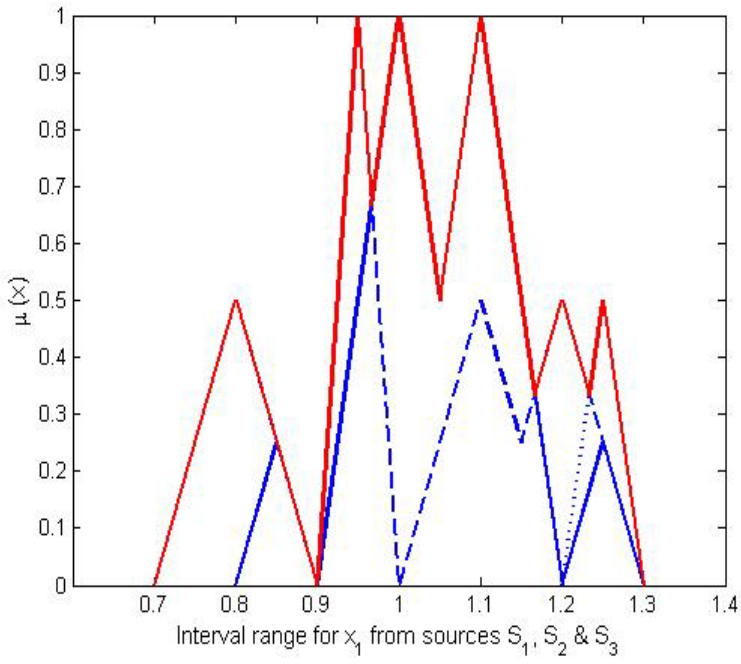

(d)

Figure 6.12 Combined fuzzy membership function of x_2 from sources S_1, S_2 and S_3

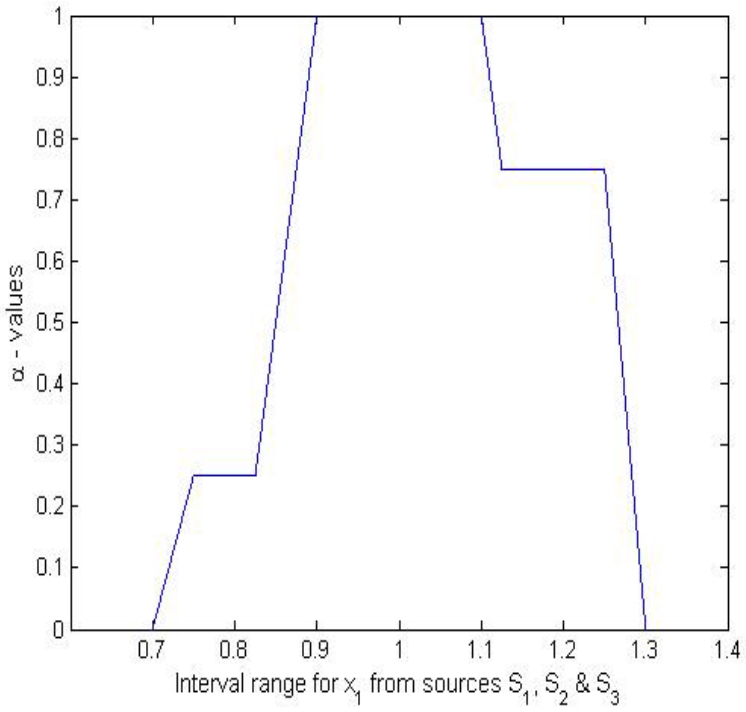

(a)

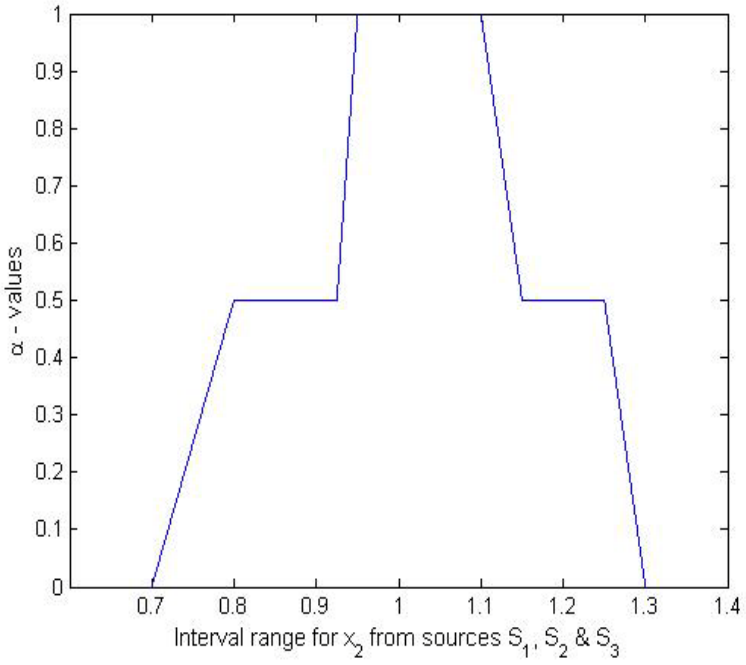

(b)

Figure 6.13 α - cuts for combined x_1 and x_2 from sources S_1, S_2 and S_3

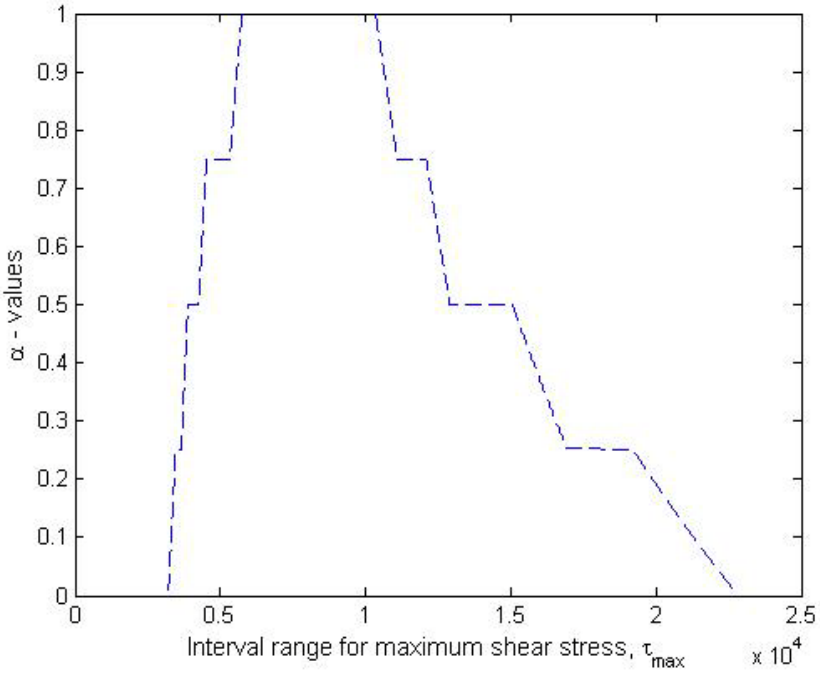
α - values
Interval range for maximum shear stress, τ_{max}
x 10^4

(a)

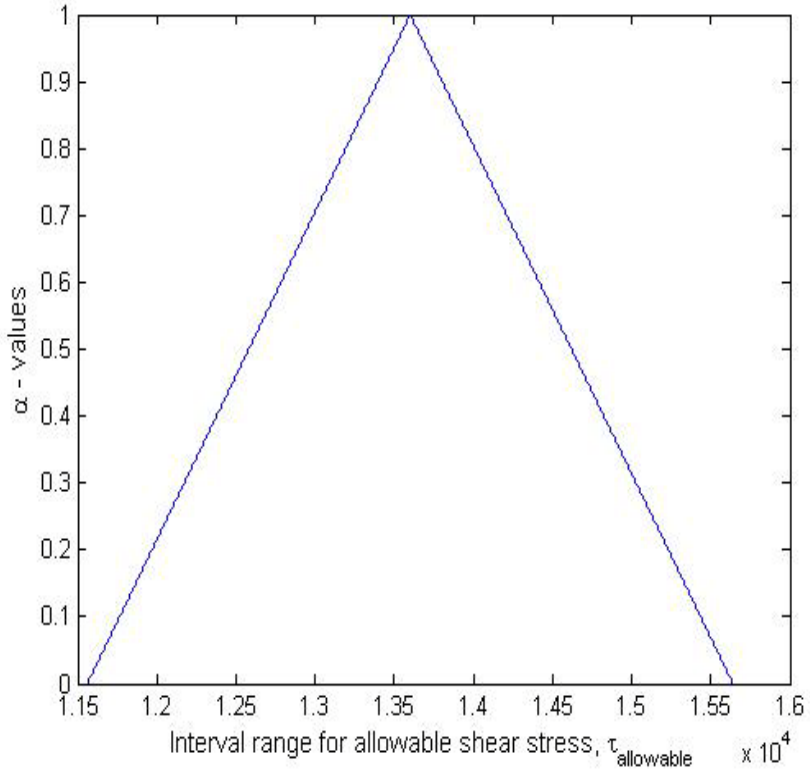
α - values
Interval range for allowable shear stress, $\tau_{allowable}$
x 10^4

(b)

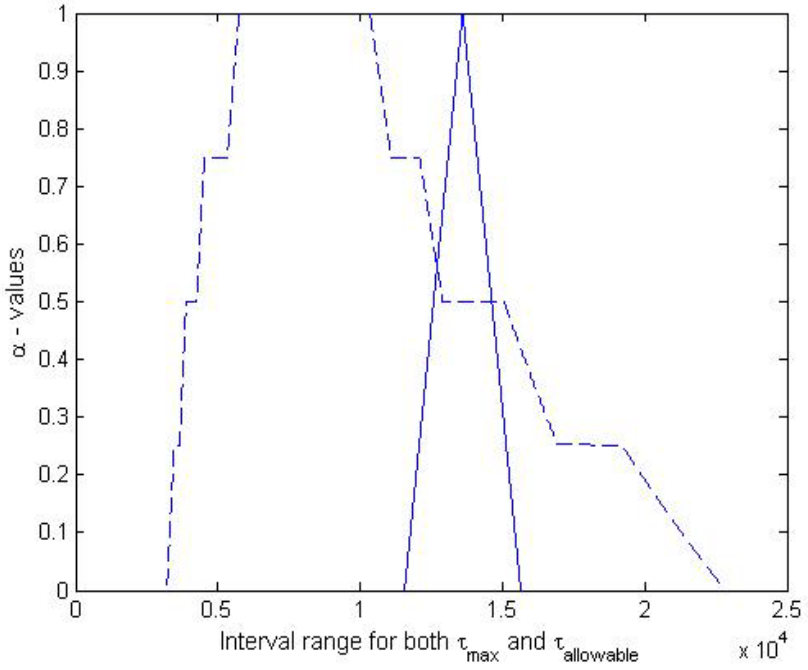
α - values
Interval range for both τ_{max} and $\tau_{allowable}$
x 10^4

(c)

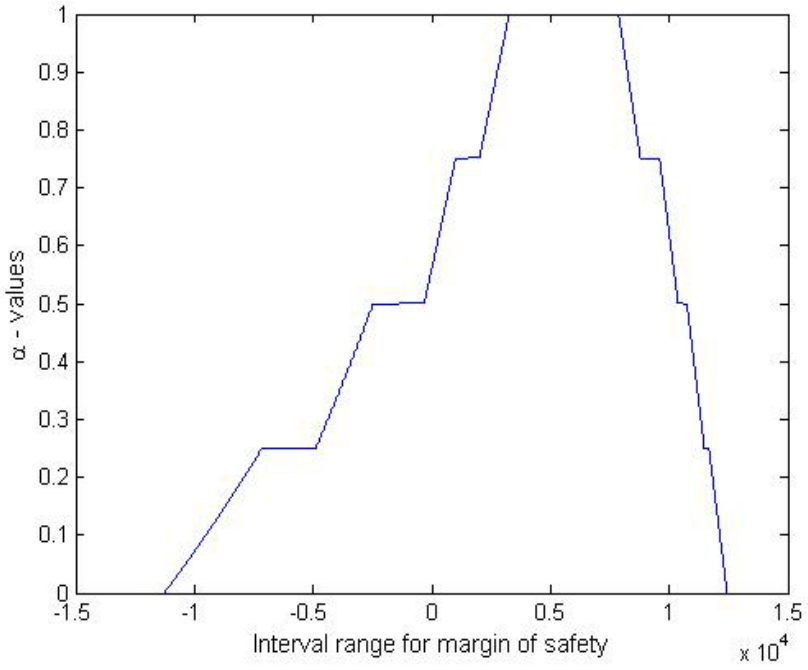
α - values
Interval range for margin of safety
x 10^4

(d)

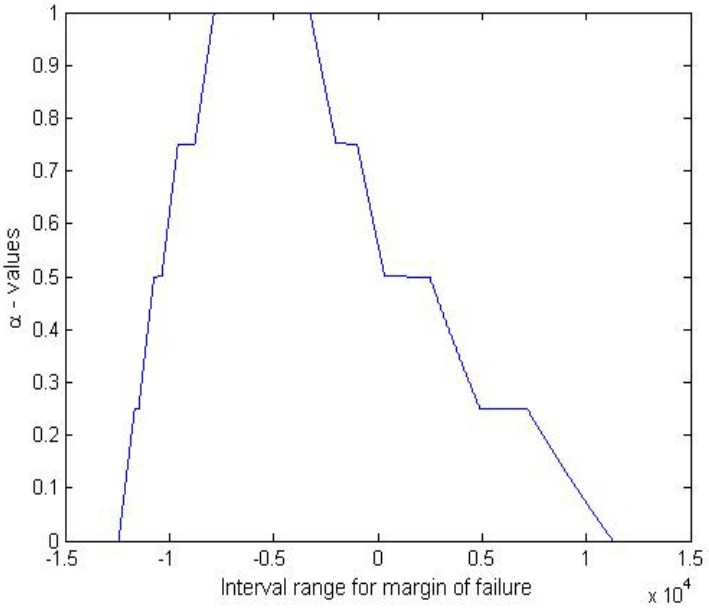

(e)

Figure 6.14 α - cut representation of $\tau_{\max}$, $\tau_{allowable}$ and margins of safety and failure

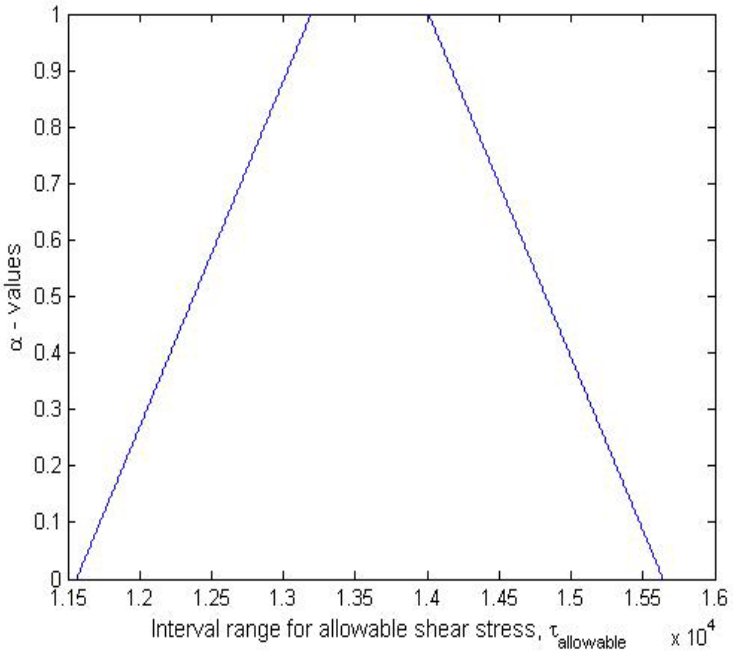

(a)

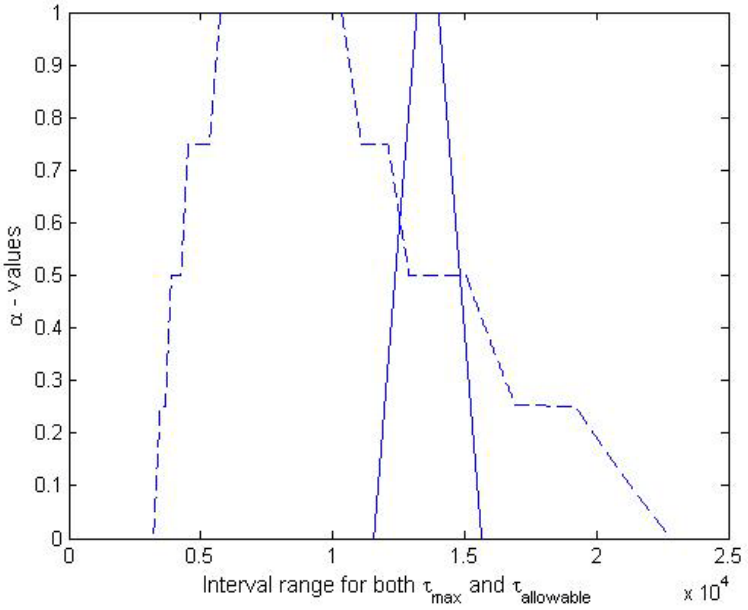
α - values
Interval range for both τ_{max} and $\tau_{allowable}$
x 10^4

(b)

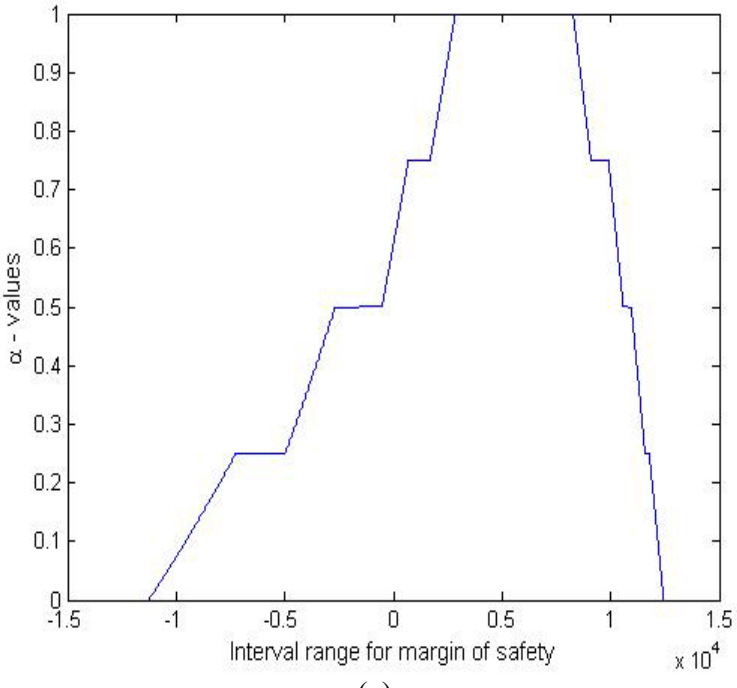
α - values
Interval range for margin of safety
x 10^4

(c)

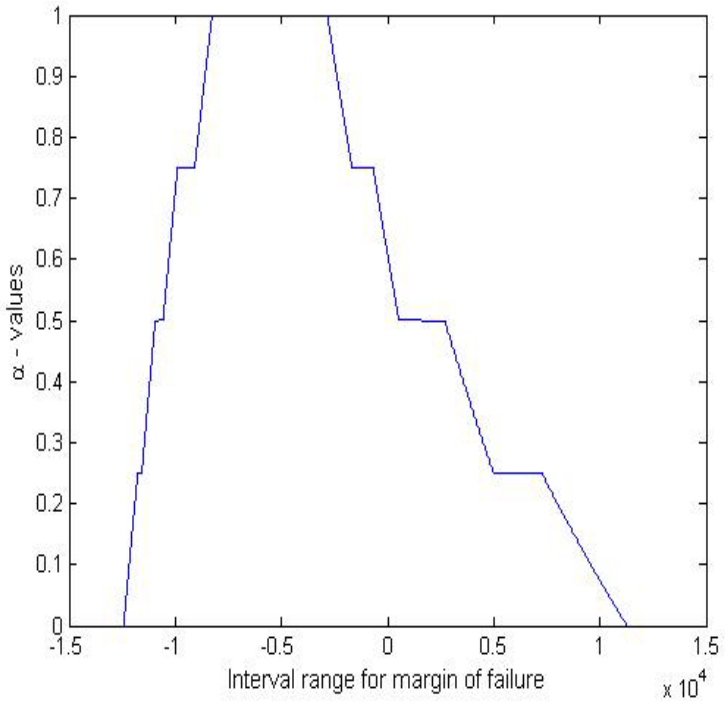

(d)

Figure 6.15 α - cut representation of $\tau_{\max}$, $\tau_{allowable}$ and margins of safety and failure

Case 4: **Four uncertain parameters with evidence from three different sources**

In this case, the four uncertain input parameters are assumed to be the length of the weld (l), height of the weld (h), depth of the cantilever (t) and length of the cantilever (L) with x_1, x_2, x_3 and x_4 indicating their corresponding multiplication factors (representing variations about their respective nominal values). The evidences for x_1 and x_2 are assumed to be same as those considered in Case 1. The evidences for x_3 and x_4 are assumed to be as indicated in Table 6.3.

Table 6.3 Evidences for the uncertain factors x_3 and x_4 from sources S_1, S_2 and S_3

x_3	Source1 (S_1)	Interval	[0.8,0.9]	[0.9,1.1]	[1.0,1.2]	
		Bpa	0.2	0.4	0.4	
	Source2 (S_2)	Interval	[0.7,0.9]	[0.9,1.0]	[1.0,1.2]	[1.1,1.2]
		Bpa	0.1	0.5	0.2	0.2
	Source3 (S_3)	Interval	[0.8,1.0]	[1.0,1.2]	[1.1,1.3]	
		Bpa	0.3	0.5	0.2	
x_4	Source1 (S_1)	Interval	[0.7,0.8]	[0.8,1.1]	[1.0,1.2]	[1.2,1.3]
		Bpa	0.2	0.3	0.3	0.2
	Source2 (S_2)	Interval	[0.7,0.9]	[0.8,1.0]	[1.0,1.2]	[1.1,1.3]
		Bpa	0.1	0.5	0.2	0.2
	Source3 (S_3)	Interval	[0.9,1.1]	[1.0,1.2]	[1.2,1.3]	
		Bpa	0.1	0.5	0.4	

The combined membership functions of x_1 and x_2, obtained from the individual membership functions shown in Figs. 6.11(a)-(c) and 6.12(a)-(c), are shown in Figs. 611(d) and 6.12(d), respectively. The membership functions of x_3 and x_4 from sources S_1, S_2 and S_3 are shown in Figs. 6.16(a) – (c) and 6.17(a) – (c), respectively. Their combined membership functions are obtained as indicated in Figs. 6.16(d) and 6.17(d). The α-cuts of the combined smoothed out, fuzzy representations of x_3 and x_4 are shown in Fig. 6.18. The fuzzy representation of the maximum induced shear stress, $\tau_{\max}$, is shown in Fig. 6.19(a). If the allowable shear stress, $\tau_{allowable}$, is assumed to be fuzzy with a

triangular membership function as shown in Fig. 6.19(b), the fuzzy representations of the margins of safety and failure can be determined as shown in Figs. 6.19(d) and (e), respectively. Similarly, if the fuzzy representation of the allowable shear stress, $\tau_{allowable}$, is assumed to be trapezoidal as indicated in Fig. 6.20(a), the fuzzy representations of the margins of safety and failure can be obtained as shown in Figs. 6.20(c) and (d), respectively.

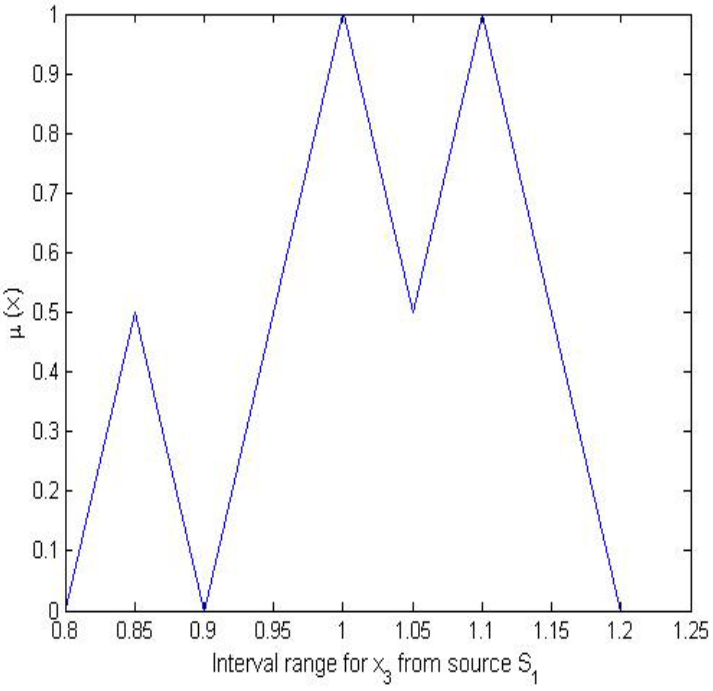

(a)

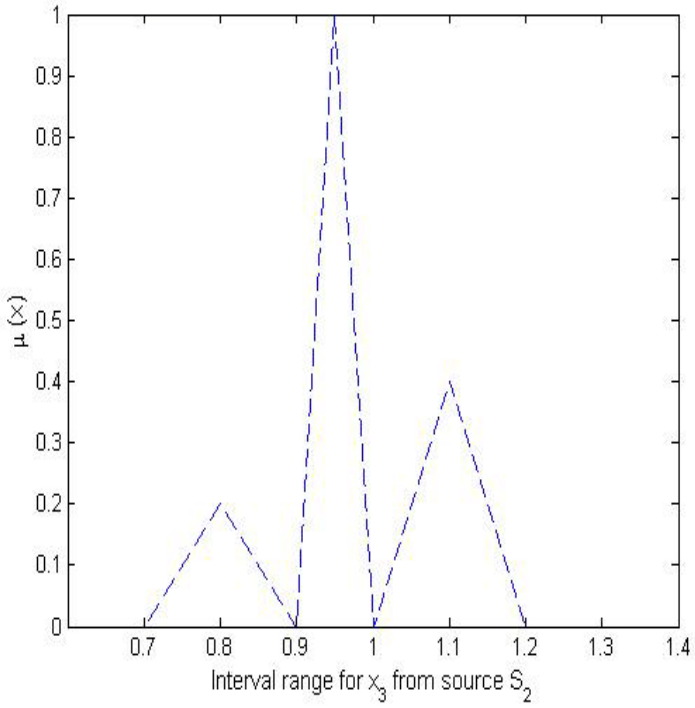
μ (x)
Interval range for x_3 from source S_2

(b)

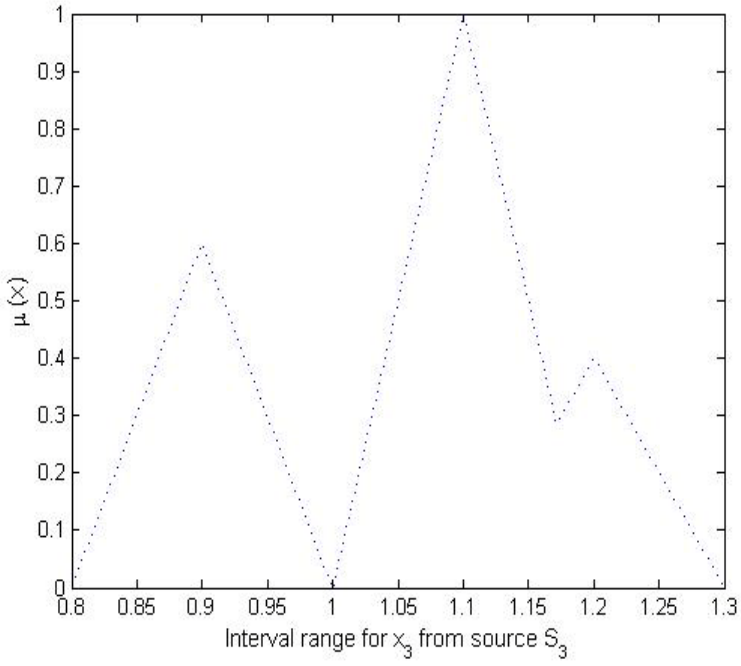
μ (x)
Interval range for x_3 from source S_3

(c)

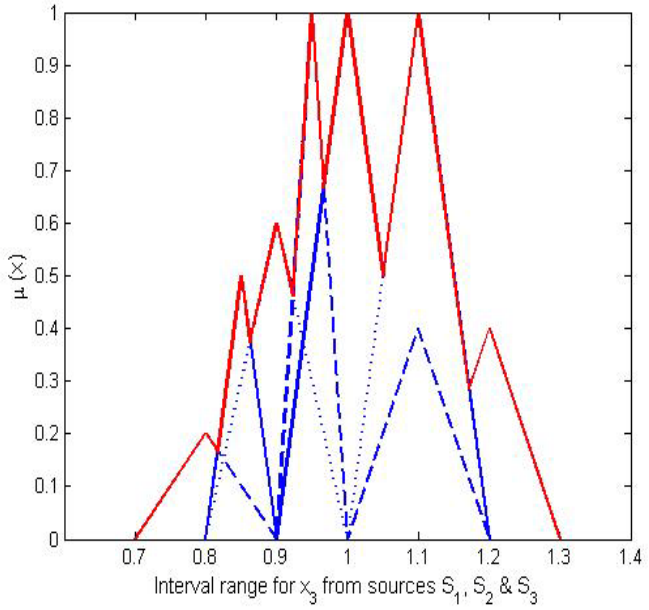

(d)

Figure 6.16 Combined fuzzy membership function of x_3 from sources S_1, S_2 and S_3

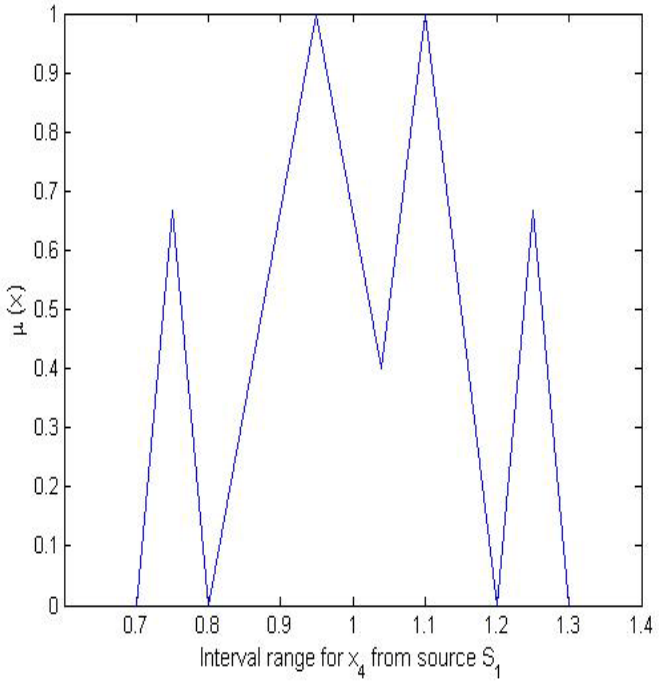

(a)

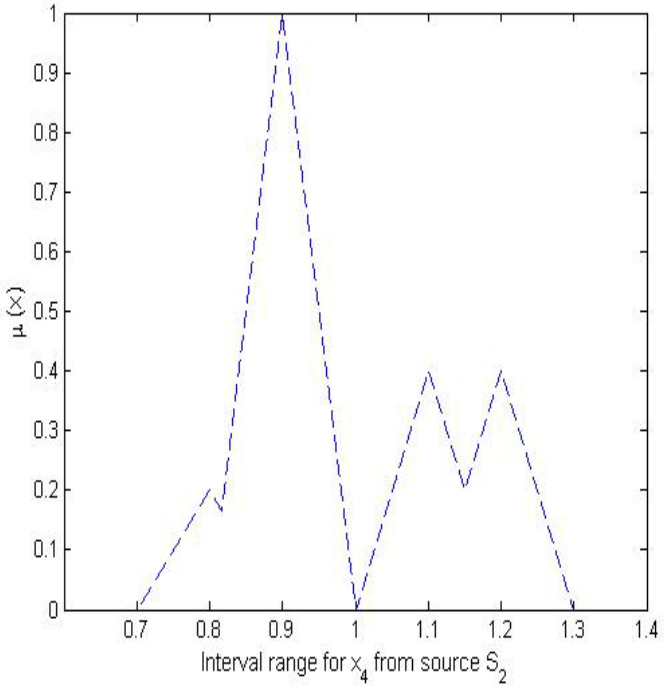
μ (×)
Interval range for x4 from source S2

(b)

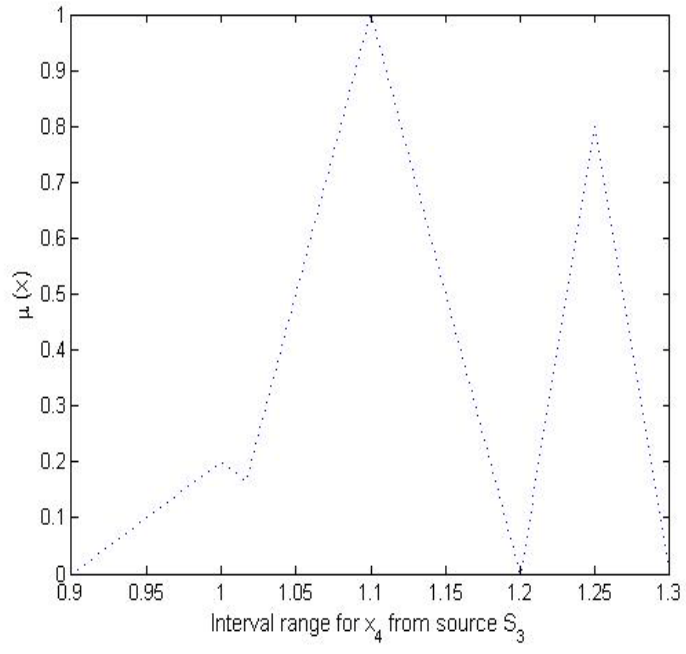
μ (×)
Interval range for x4 from source S3

(c)

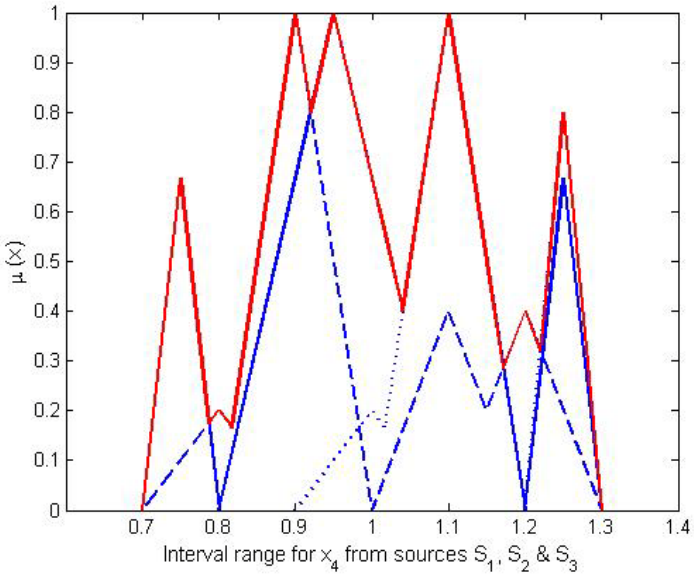

(d)

Figure 6.17 Combined fuzzy membership function of x_4 from sources S_1, S_2 and S_3

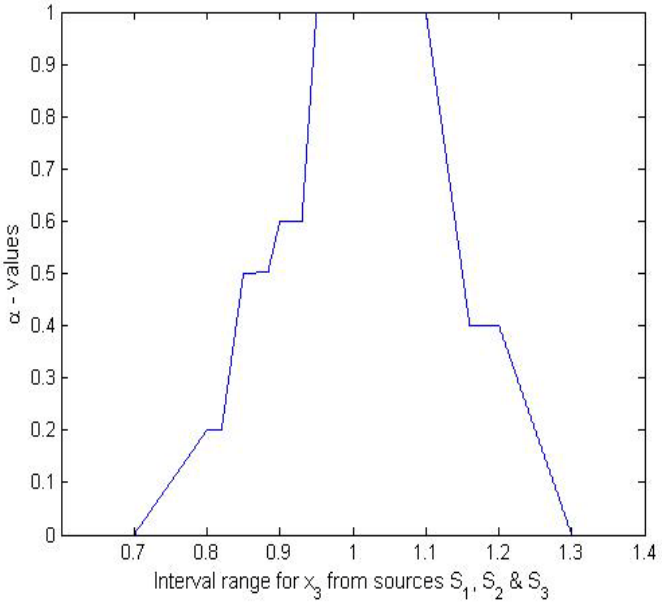

(a)

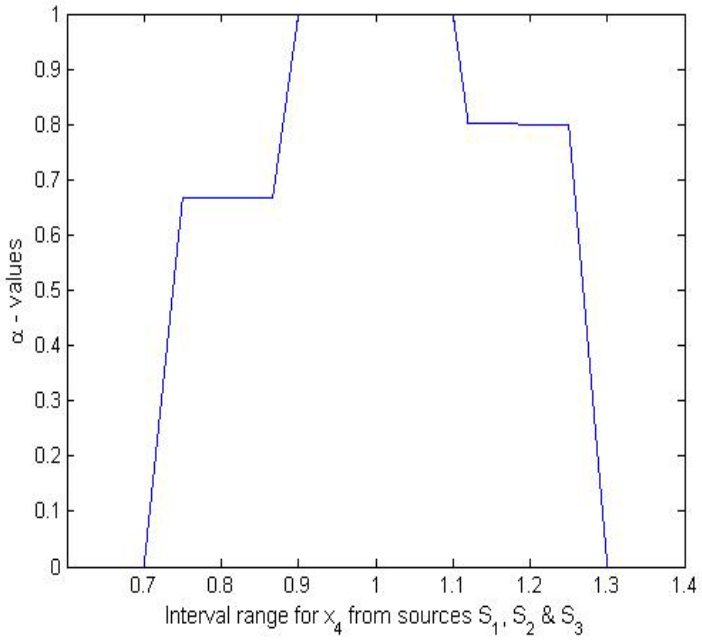

(b)

Figure 6.18 α - cuts for combined x_1, x_2, x_3 and x_4 from sources S_1, S_2 and S_3

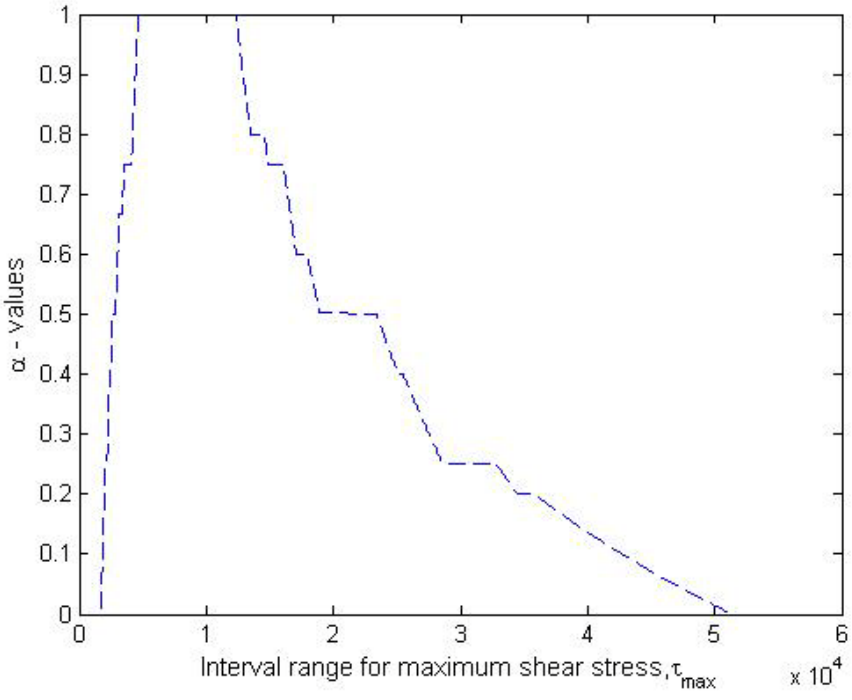

(a)

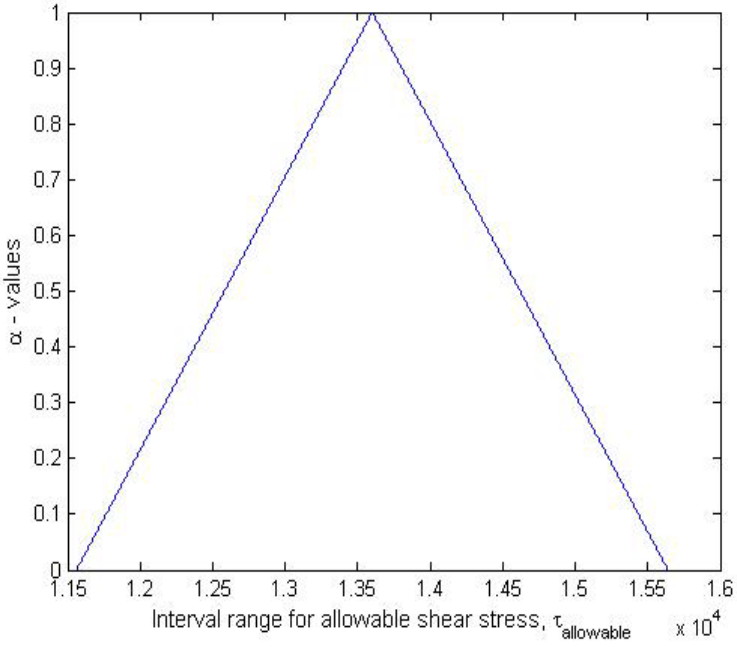
α - values
Interval range for allowable shear stress, $\tau_{allowable}$
x 10^4

(b)

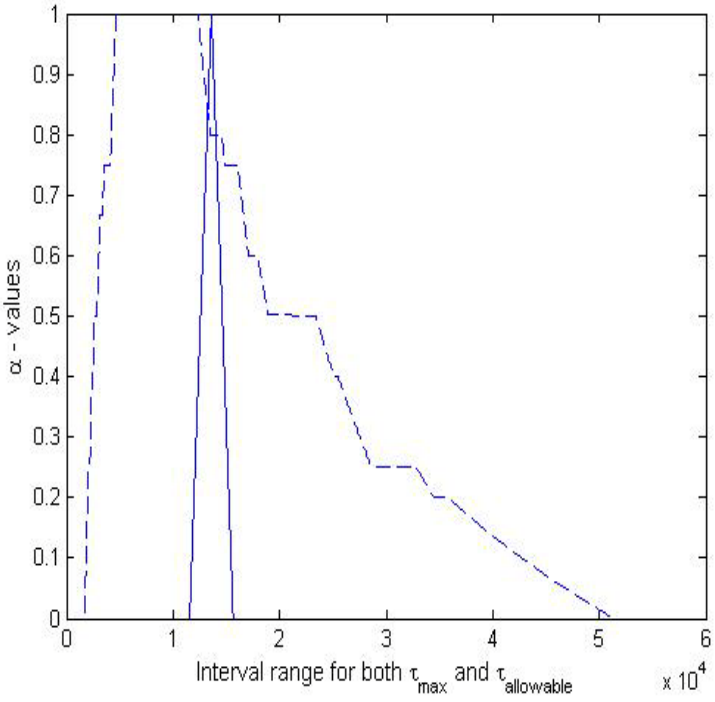
α - values
Interval range for both τ_{max} and $\tau_{allowable}$
x 10^4

(c)

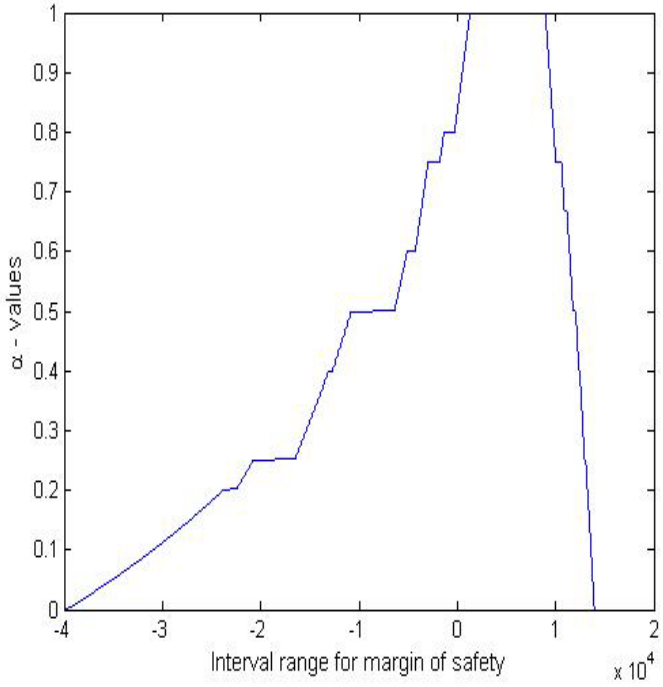

(d)

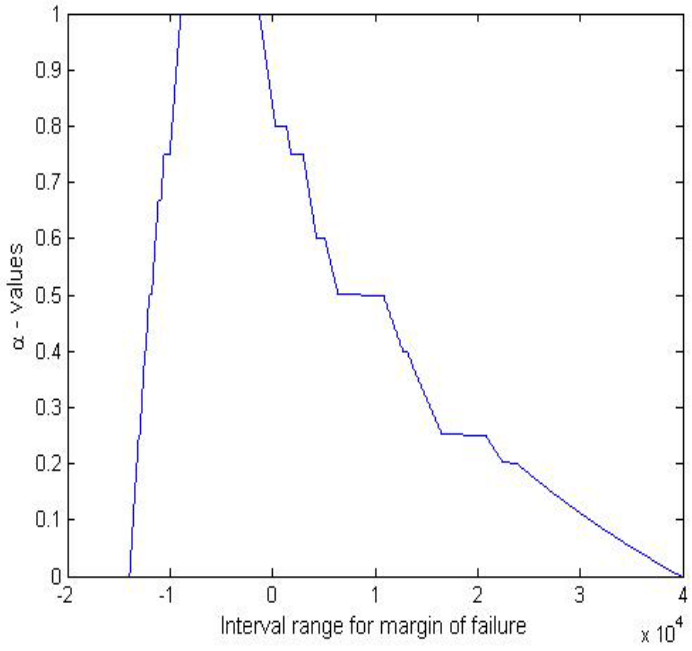

(e)

Figure 6.19 α - cut representation of $\tau_{\max}$, $\tau_{allowable}$ and margins of safety and failure

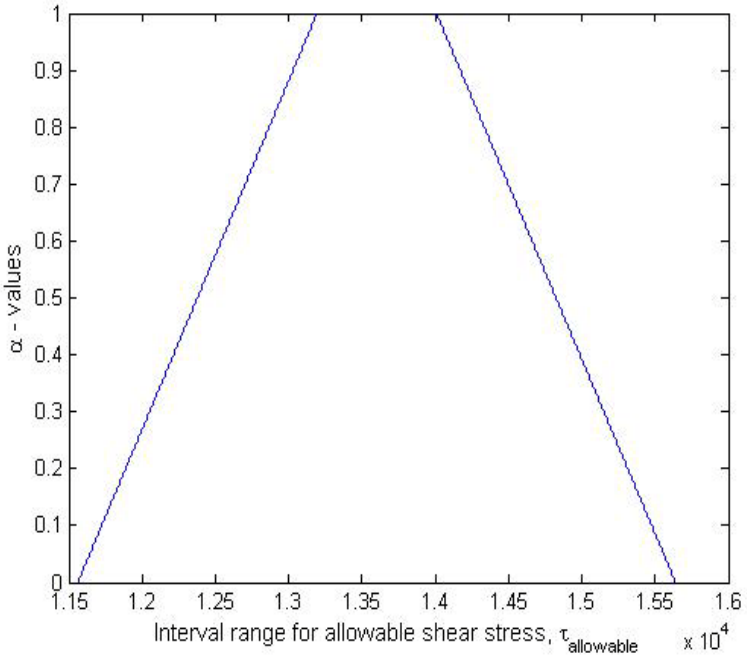
α - values
Interval range for allowable shear stress, $\tau_{allowable}$
x 10^4

(a)

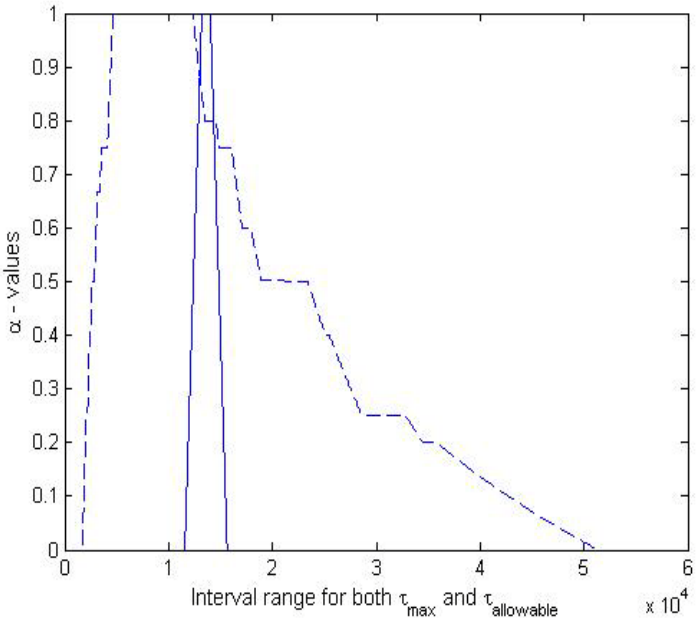
α - values
Interval range for both τ_{max} and $\tau_{allowable}$
x 10^4

(b)

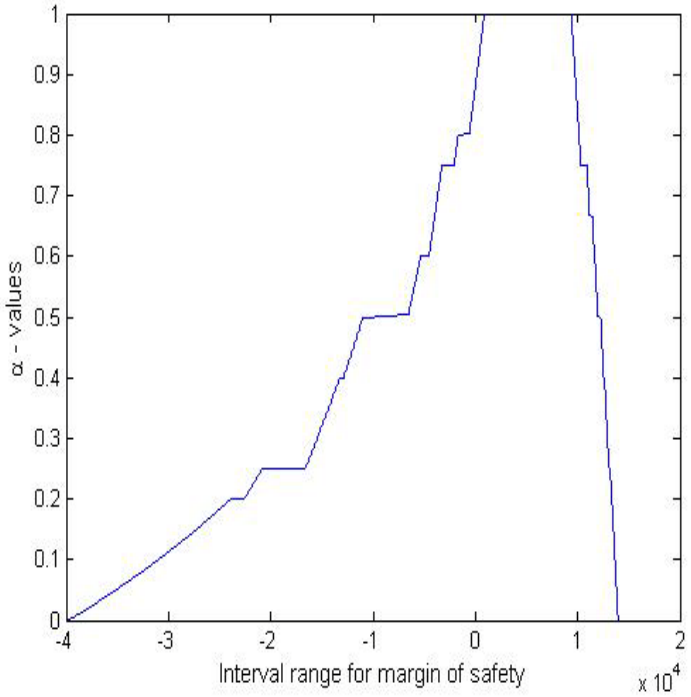

(c)

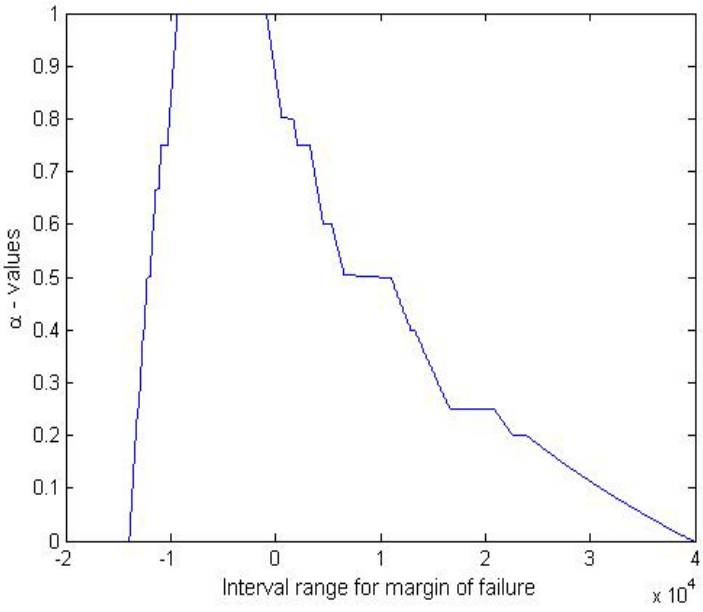

(d)

Figure 6.20 α - cut representation of $\tau_{\max}$, $\tau_{allowable}$ and margins of safety and failure

6.4.3 Bounds on margins of safety and failure

Using the procedure outlined in section 6.2, the lower and upper bounds on the margins of safety and failure are computed. The results are shown in Tables 6.4 and 6.5 for Cases 1 and 2, respectively. The Dempster Shafer theory (DST) is also used to combine the evidences in each case. In DST, the criteria are $\tau_{allowable} \leq \tau_{\max}$ and $\tau_{allowable} > \tau_{\max}$ are used for the margin of safety and margin of failure, respectively, to obtain the results shown in the last rows of Tables 6.4 and 6.5.

Table 6.4 Lower and upper bounds on the margin of safety (Cases 1 and 2)

Allowable shear stress, $\tau_{allowable}$ fuzzy function	Two uncertain parameters (Margin of safety)		Four uncertain parameters (Margin of safety)	
	Lower bound	Upper bound	Lower bound	Upper bound
Triangular	0.74966	1	0.49257	1
Trapezoidal	0.75215	1	0.49496	1
DST	1	1	0.98698	1

Table 6.5 Lower and upper bounds on the margin of failure (Cases 1 and 2)

Allowable shear stress, $\tau_{allowable}$ fuzzy function	Two uncertain parameters (Margin of failure)		Four uncertain parameters (Margin of failure)	
	Lower bound	Upper bound	Lower bound	Upper bound
Triangular	0	0.25034	0	0.50743
Trapezoidal	0	0.24785	0	0.50504
DST	0	0	0	0.013017

6.5 WEIGHTED FUZZY THEORY FOR INTERVAL-VALUED DATA FROM MULTIPLE SOURCES WITH DIFFERENT CREDIBILITIES

In practice, the credibilities of the different sources of evidence for the uncertain parameters may be different. To consider the credibilities associated with the sources of evidence, a procedure, termed the weighted fuzzy theory for intervals (WFTI), is proposed in this work for determining the lower and upper bounds on the margins of safety and failure. The general procedure is described by the following steps:

1. Normalize the evidences from each source before considering the credibilities of that source.
2. Multiply the normalized evidences by the credibilities of the corresponding sources. Each of the credibilities is assumed to lie in the range 0 to 1.

3. Obtain the combined outer envelope of the fuzzy membership function of each uncertain parameter by superposing all the membership functions (normalized evidences) of the uncertain parameter given by the various sources.
4. Compute the alpha-cuts of the combined outer envelopes (or the combined fuzzy membership functions).
5. Calculate the response or output of the system using the algebra of interval numbers or parameters.
6. Determine the lower and upper bounds on the response or output parameter using the procedure described in Section 6.2.

The procedure is illustrated by considering the following two cases. The range of trapezoidal membership function for $\tau_{allowable}$ is assumed to be ± 15% of $\tau_{\max}$ ($0.85\,\tau_{\max}$ to $1.15\,\tau_{\max}$) at α = 0 and ± 3% of $\tau_{\max}$ ($0.97\,\tau_{\max}$ to $1.03\,\tau_{\max}$) at α = 1. A Matlab program is developed to incorporate the WFTI procedure to include the credibility information of the various sources in the calculation of lower and upper bounds on the margins of safety and failure.

Case 1: Two uncertain parameters with evidence from three different sources

The length of the weld (*l*) and the height of the weld (*h*) are considered to be the uncertain parameters with x_1 and x_2 denoting the multiplication factors for these parameters. Three sources of evidence are assumed to provide possible ranges or intervals of x_1 and x_2 along with the corresponding bpa's as given in Table 6.2. The credibility of source S_3 is assumed to be less than one and is varied from 0 to 1 in increments of 0.1. Figure 6.23 shows the variation of the lower bound on the margin of

safety with varying values of the credibility of source S_3. Figure 6.24 shows the variations of the upper bound on the margin of failure with varying values of the credibility of source S_3. It can be observed that the lower bound on the margin of safety and the upper bound on the margin of failure vary in complementary way to each other as the credibility of source S_3 varies from 0 to 1 and nature of the variation depends on the evidence given to the intervals of the source S_3. Consider the case when credibility of 3rd source is equal to 0.7. The step 2 of the WFTI procedure described in section 6.5 can be illustrated as shown in Figures 6.21 and 6.22. It can be seen that Figures 6.11(c) and 6.12(c) are transformed to 6.21(a) and 6.22(a) and thus the resulting combined fuzzy membership functions as shown in Figures 6.21(b) and 6.22(b) are obtained as different from corresponding Figures 6.11(d) and 6.12(d). The upper bound for the margin of failure is found to be 0.2524, same as the value obtained from the curve in Figure 6.24.

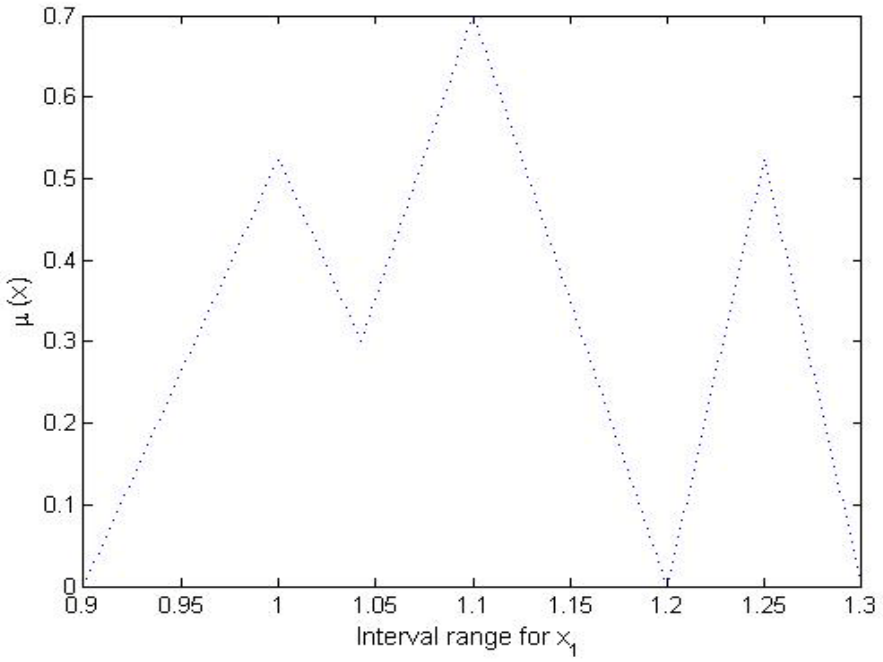

(a)

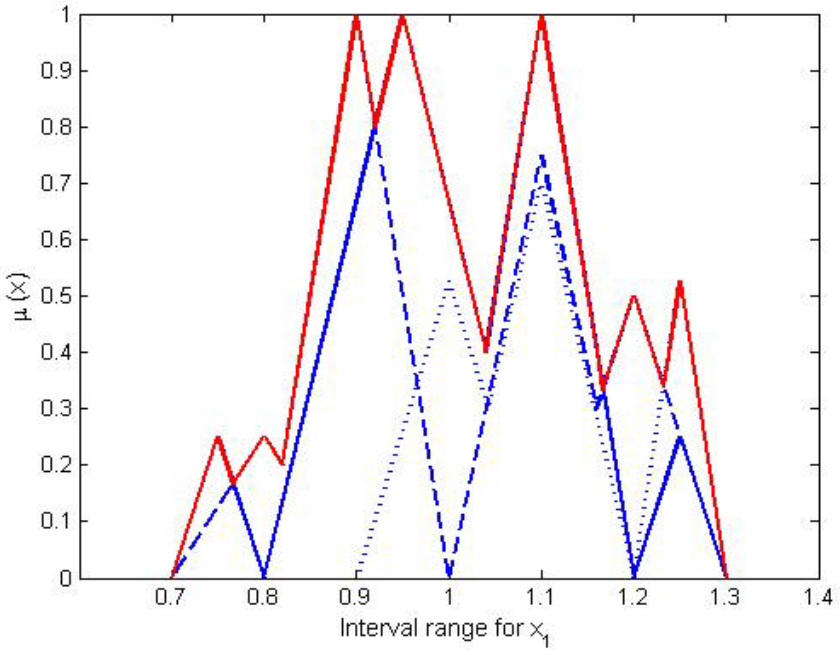

(b)

Figure 6.21 Combined fuzzy membership function of x_1 from sources S_1, S_2 and S_3

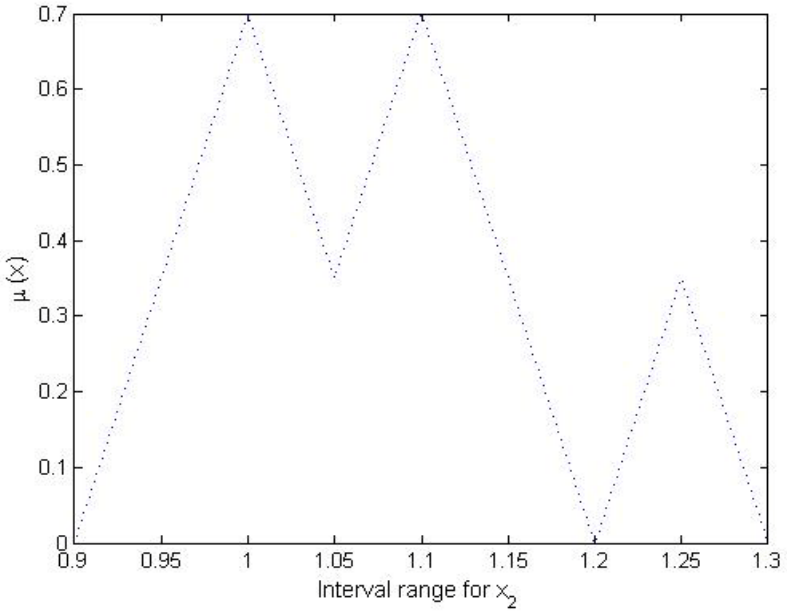

(a)

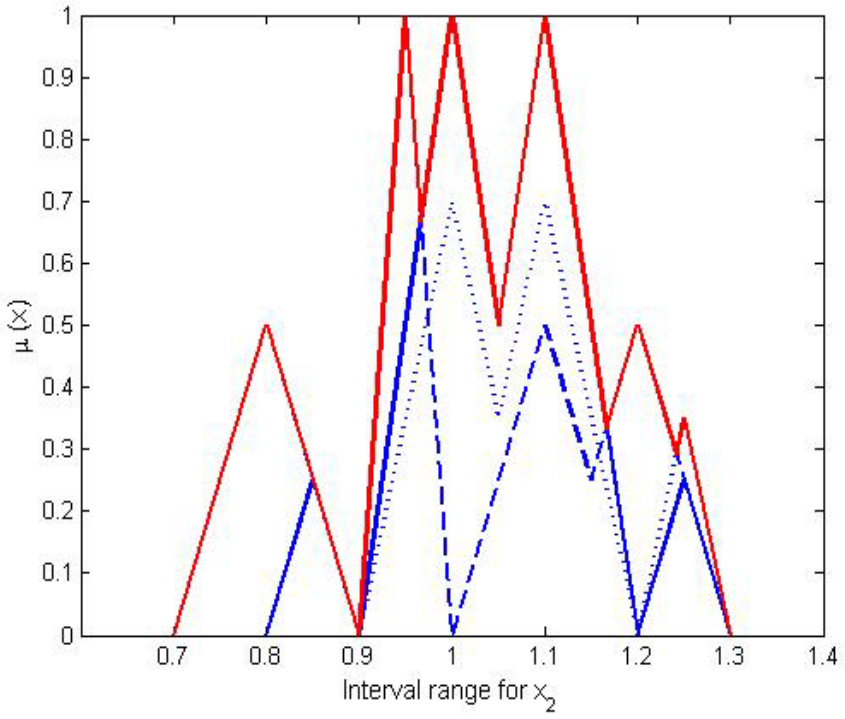

(b)

Figure 6.22 Combined fuzzy membership function of x_2 from sources S_1, S_2 and S_3

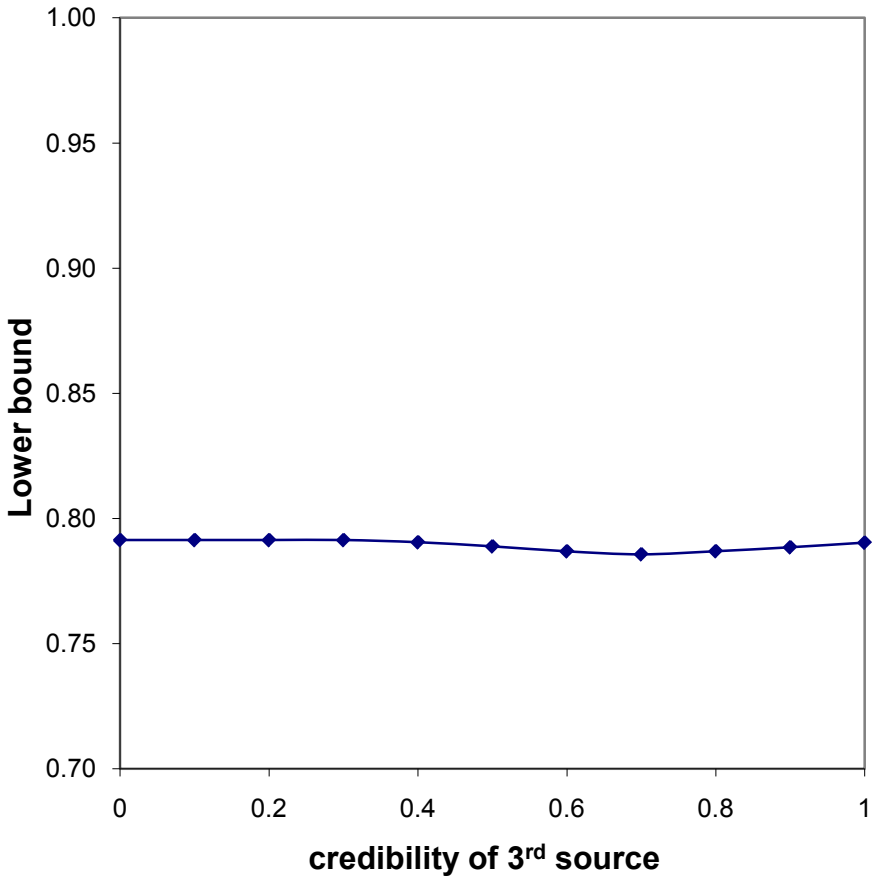

Figure 6.23 Variation of lower bound on margin of safety with the credibility of source S_3

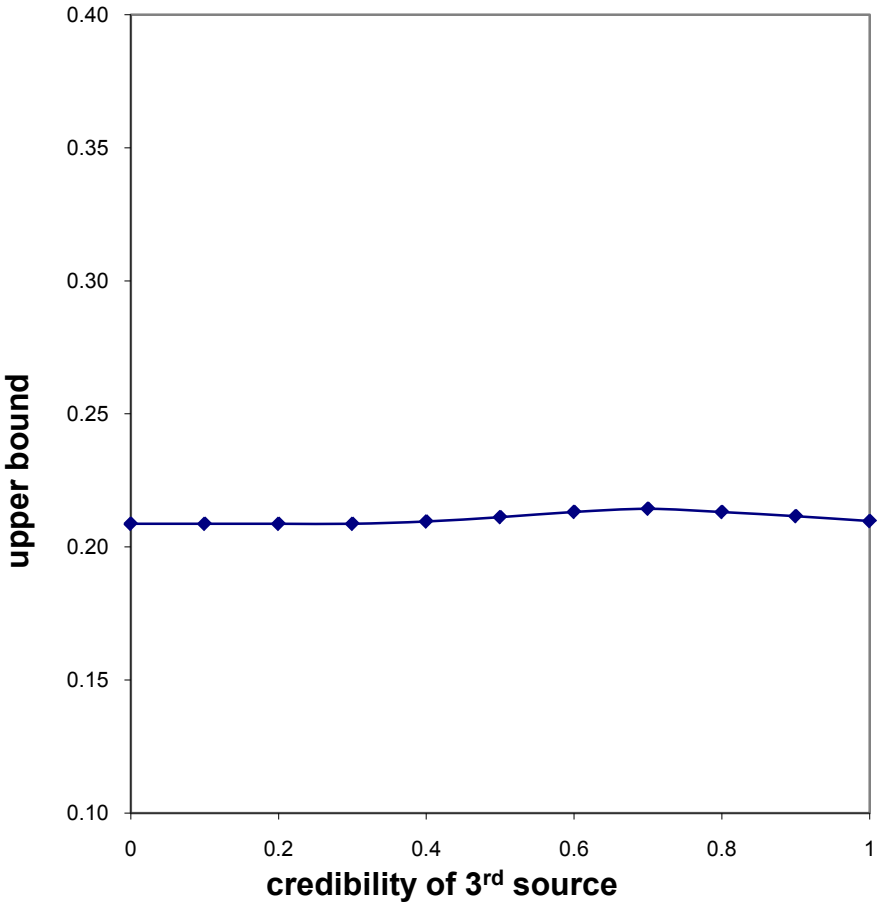

Figure 6.24 Variation of upper bound on margin of failure with the credibility of source S_3

Case 2: Four uncertain parameters with evidence from three different sources

In this case, the length of the weld (l), height of the weld (h), depth of the cantilever (t) and length of the cantilever (L) are assumed to be the uncertain parameters with x_1, x_2, x_3 and x_4 indicating their corresponding multiplication factors. The evidences for x_1 and x_2 are assumed to be same as those considered in Case 1. The evidences for x_3 and x_4 are assumed to be same as those shown in Table 6.3. Figure 6.25 shows the

variation of the lower bound on the margin of safety with varying values of the credibility of source S_3 while Fig. 6.26 shows the variation of the upper bound on the margin of failure with varying values of the credibility of source S_3

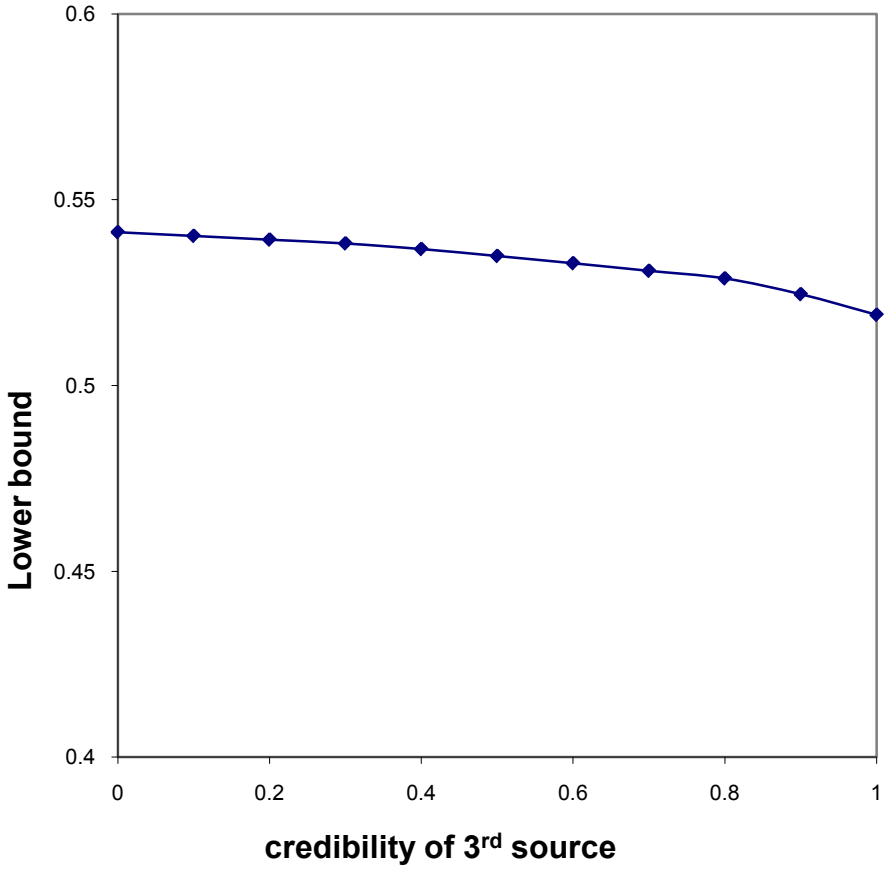

Figure 6.25 Variation of lower bound on margin of safety with the credibility of source S_3

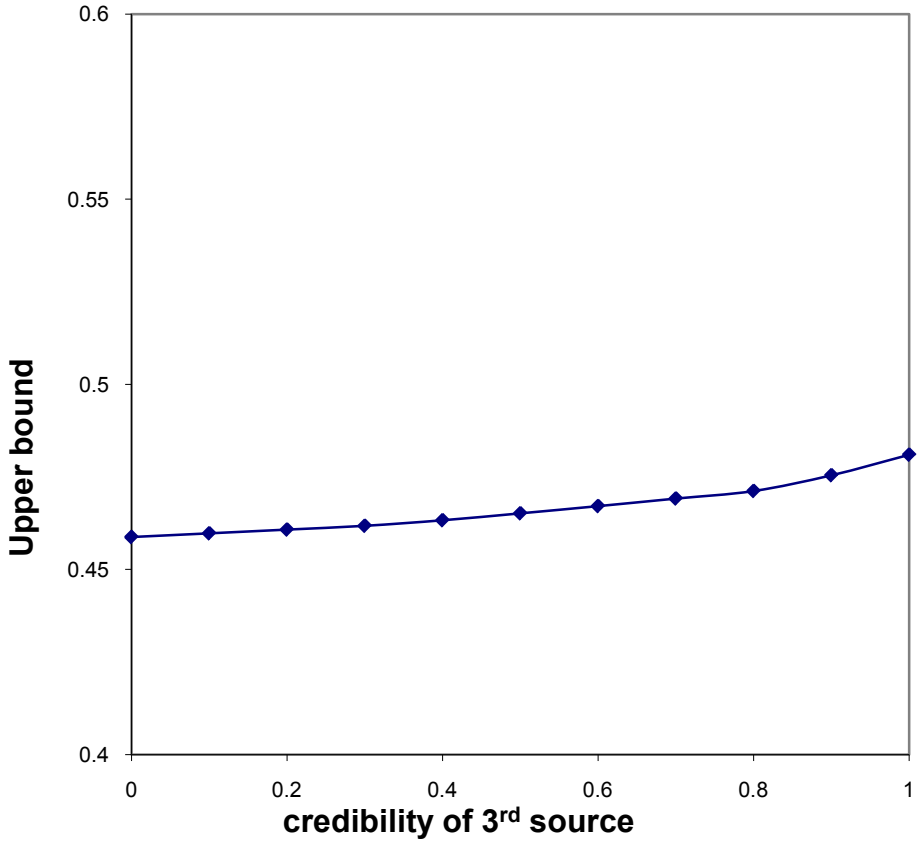

Figure 6.26 Variation of upper bound on margin of failure with the credibility of source S_3

The variation in the lower/upper bound on the margin of safety/failure as the credibility of source 3 increases depends on the evidence distribution on the interval ranges from source 3, effect of uncertain parameters on margin of safety/failure and number of uncertain parameters. The difference between lower and upper bounds for both margin of safety and margin of failure increases with increase in number of uncertain parameters used in the analysis. The validity of this statement is intuitively obvious as the uncertainty of the system increase with increase in the number of uncertain parameters used in the analysis.

6.6 SUMMARY

We found in this chapter that the sum of the lower bound on margin of safety and the upper bound on margin of failure is always equal to 1 in all cases as expected. As the number of alpha cuts used in the numerical computation of the bounds on the margins of safety and failure changed, the values of the computed bounds are found to vary. However, with increasing number of the alpha cuts, the bounds are found to converge to the values reported in this work. Irrespective of the number of sources of evidence, when the assumed fuzzy membership function of the allowable shear stress changes from the triangular to the trapezoidal shape, the lower and upper bounds tend to shrink the ranges of the margins of safety and failure. The widening or shrinking of the ranges of the margins of safety and failure is observed to depend on the available evidence and the influence of the uncertain parameters on the output or response parameter of the system. In general, the procedure proposed for considering the credibilities of the various sources of evidence (WFTI) is applicable for combining evidence to evaluate the safety/failure of any uncertain system in the presence of evidence on the uncertain parameters from different sources. The methodology presented in this chapter provides an alternative framework for combining evidence from multiple sources using fuzzy theory. In the next chapter, a general optimization model using modified PSO coupled with modified game theory is proposed to solve multi-objective optimization problems.

CHAPTER 7

DESIGN OPTIMIZATION OF ENGINEERING SYSTEMS USING PARTICLE SWARM OPTIMIZATION

7.1 OVERVIEW

This chapter proposes particle swarm optimization (PSO) based algorithms to solve engineering optimization problems involving different types of design variables (continuous, discrete and/or mixed) and single or multiple objective functions. The original PSO algorithm is modified to include dynamic maximum velocity function and bounce method, is described in section 7.2, to enhance the computational efficiency and solution accuracy. The procedure to use a closest discrete approach (CDA) in the modified PSO to solve optimization problems with discrete design variables is considered in section 7.3. Several engineering applications for single objection optimization problems are considered in section 7.4. A new modified game theory approach (MGT) is coupled with the modified PSO, is proposed in section 7.5, to solve multi-objective optimization problems. Several engineering applications like the design of 2-bar and 25-bar trusses, design of I-beam and design of gear box for multi-objective optimization is considered in section 7.6. This chapter is concluded by a summary in the last section.

7.2 MODIFIED PARTICLE SWARM OPTIMIZATION

Particle swarm optimization algorithm [76,88,102,125,144,153,160,161,164,194], described in section 3.4 of chapter 3, is considered along with modification to include

dynamic velocity function for maximum adaptable velocity for the particles, bounce method and dynamic penalty function to the optimization algorithm.

7.2.1 Dynamic velocity function

The adaptable velocity obtained from equation (3.31) is limited by the dynamic velocity function $\vec{V}_{\max} = \left[v_{1\max}, v_{2\max}, \ldots, v_{n\max}\right]^T$, as proposed in this work, to improve the convergence of the algorithm. The maximum velocity for t^{th} variable, $v_{t\max}$, is defined as

$$v_{t\max} = e^{-ai+b},\ t = 1, 2, \ldots, n \tag{7.1}$$

where a and b are constants evaluated as

$$a = \frac{\log\left(\frac{v_f}{v_i}\right)}{i_{\max}}.i \tag{7.2}$$

$$b = a + \log\left(v_f\right) \tag{7.3}$$

where v_i and v_f represent, respectively, the initial and final limits for the maximum velocity of the t^{th} variable used in the algorithm. Introduction of the exponentially decaying function $\vec{V}_{\max}$ in the algorithm will boost the particles to converge faster to the optimal solution in the first few iterations of the algorithm. All the components of $\vec{V}_{\max}$ are assumed to be same in the matlab program; thus the maximum velocity for all variables will be equal to the constant value assumed for the components of $\vec{V}_{\max}$. Introduction of the exponentially decaying function $\vec{V}_{\max}$ in the algorithm will boost the particles to converge faster to the optimal solution in the first few iterations of the algorithm. For example, if the maximum number of iterations, $i_{\max}$ = 100 and maximum velocity limits

are $v_{i\max} = 1$ and $v_{f\max} = 0.01$ then the maximum velocity of the particle in any particular iteration can be found from equation (7.1) which is shown graphically in Figure 7.1. The limits for maximum velocities (initial and final limits) depends on the range of the design variables and thus they problem dependent. As the design thumb rule, final value, $\vec{V}_{f\max}$ depends on the accuracy on the design variables values required for the optimum solutions and its effect on the function value and the initial value, $\vec{V}_{i\max}$ depends on the range of the design variables allowed in the problem.

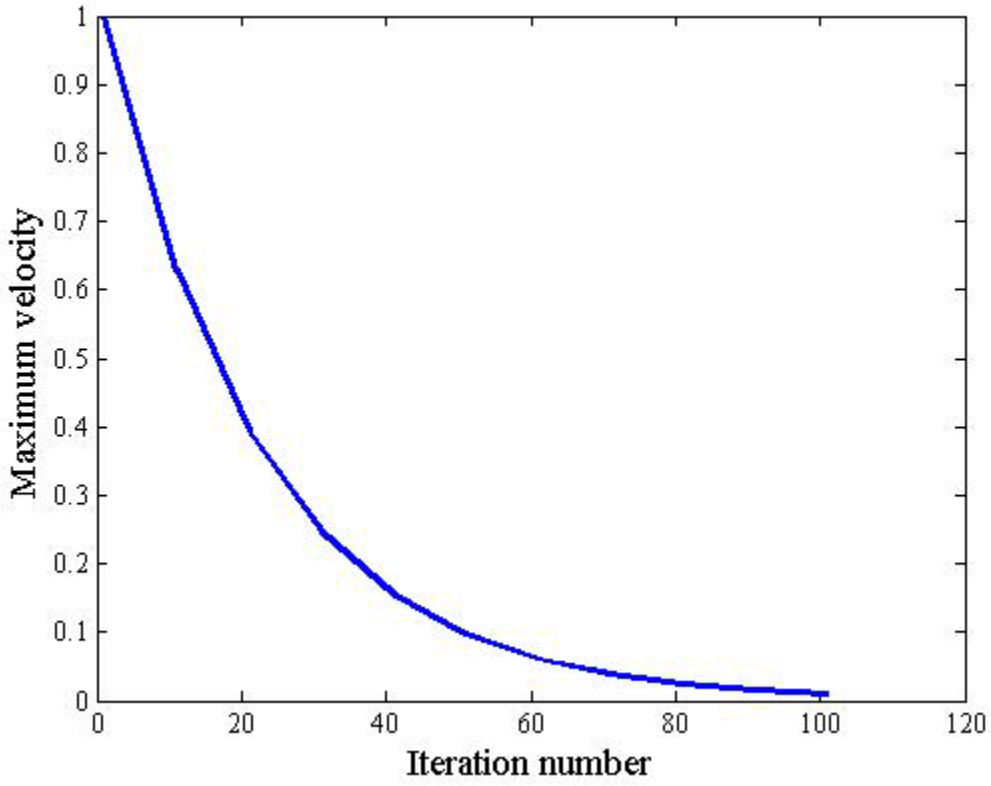

Figure 7.1 Variation of maximum velocity with iteration number

All the components of $\vec{V}_{\max}$ are assumed to be same in the Matlab program; thus the maximum velocity for all variables will be equal to the constant value assumed for the

components of $\vec{V}_{\max}$. The values for these limits of maximum velocity depend on the ranges of the design variables and they vary from one problem to other.

7.2.2 Bounce method

This method was introduced by Krink, Vestertroem, and Riget [115] to bounce away the particles that cluster around a potentially sub-optimal position. In this method, particles bounce back the boundaries with negative velocity once the new updated position, as obtained from equation (3.31), crosses the minimum/maximum position limit specified in the optimization problem. This provided a significant improvement in the performance of the algorithm for the optimization of highly multimodal objective functions by avoiding the particles to form a cluster and stagnate.

7.2.3 Dynamic penalty function

In general, any constrained optimization problem can be solved by converting it into an unconstrained one by penalizing the objective function when one or more constraints are violated using a penalty function. The basic constrained optimization problem with only inequality constraints is of the form:

Find $\vec{X}$ which minimizes $f(\vec{X})$ subjected to the constraint $g_j(X) \le 0, j = 1,2,\cdots,m$. This problem can be converted into an unconstrained minimization problem by constructing a function of the form:

$$\phi_k = \phi\left(\vec{X}, r_k\right) = f(\vec{X}) + r_k \sum_{j=1}^{m} G_j\left[g_j(\vec{X})\right] \tag{7.4}$$

where r_k is a positive constant known as the static penalty parameter. The value of this parameter is very high when the solution converges to that of the original constrained problem. In the case of exterior penalty approach, G_j is taken as:

$$G_j = \max\left[0, g_j(\vec{X})\right] \tag{7.5}$$

If r_k is not static, then the procedure is called a dynamic penalty function approach. The dynamic penalty function stated by Joines and Houck [94] is given by

$$\phi_k = f(\vec{X}) + A(i).B(\vec{X}) \tag{7.6}$$

$$A(i) = (ct * i)^{\alpha} \tag{7.7}$$

$$B(\vec{X}) = \sum_{j=1}^{m}\left[H(G_j).(G_j)^{\gamma(G_j)}\right] \tag{7.8}$$

$$H(G_j) = a.(1 - 1/(e^{G_j})) + b \tag{7.9}$$

where i denotes the iteration number, and $H(G_j)$ denotes a continuous assignment function; $\gamma(G_j)$ is the power of the maximum violated function and depends on the value of G_j as obtained from equation (7.5). If $G_j \le 1$, then the power $\gamma(G_j) = 1$; otherwise, $\gamma(G_j) = 2$. Moreover, the constants in equations (7.7) and (7.9) are selected as ct = 0.5, $\alpha = 2$, a = 150 and b = 10.

7.3 CONSTRAINED OPTIMIZATION

The general constrained optimization problem can be formulated as:

$$\text{Find } \vec{X} = \begin{Bmatrix} x_1 \\ x_2 \\ \vdots \\ x_n \end{Bmatrix} \tag{7.10}$$

which minimize $f(\vec{X})$ (7.11)

subject to

$$g_j(X) \le 0, j = 1, 2, \cdots, m \tag{7.12}$$

$$l_j(X) = 0, j = 1, 2, ..., p \tag{7.13}$$

$$x_i^{\min} \le x_i \le x_i^{\max}, i = 1, 2, ..., n \tag{7.14}$$

7.3.1 Approach for discrete design variables

7.3.1.1 General form

A mixed discrete nonlinear programming problem (MDNLP) is often stated in the following form:

$$\text{Find } \vec{X} = \begin{Bmatrix} x_1 \\ x_2 \\ \vdots \\ x_n \end{Bmatrix} \tag{7.15}$$

which minimizes $f(\vec{X})$ (7.16)

subject to

$$g_j(\vec{X}) \le 0, j = 1, 2, ..., m \tag{7.17}$$

$$x_i^{\min} \le x_i \le x_i^{\max}, i = 1, 2, ..., p \tag{7.18}$$

$$x_{p+i} \in D_i,\ D_i = \left\{ d_{i,1}, d_{i,2}, ..., d_{i,r} \right\},\ i = 1, 2, ..., q \tag{7.19}$$

where p denotes the number of continuous design variables, q denotes the number of discrete design variables with $n = p + q$, m denotes the number of non-linear behavior constraints and D_i is the set of discrete values for the i^{th} discrete design variable. In general, the number of discrete values r is different for each discrete design variable.

7.3.1.2 Closest discrete approach

This work uses an approach called the closest discrete approach [206] (CDA) to handle discrete design variables for any MDNLP (stated in equations 7.15 to 7.19). After the selection of initial random population in the modified PSO for all the design variables, including the discrete design variables, we select those discrete values from the discrete variable set which are closest to the corresponding randomly generated continuous values of discrete design variables in the population. These selected discrete values are used in place of the continuous values generated in the algorithm for discrete design variables. This process is repeated for all iterations of the modified PSO algorithm to make sure that at any point of time, the population consists of continuous values for continuous design variables and discrete values for discrete design variables. When we encounter a case where a continuous value obtained for any particular discrete design variable is equidistant from two adjacent discrete values among the permissible discrete set, then we choose one of the two discrete values using a random number. If the random number generator produces a value less than 0.5 then we choose the smaller discrete value and if it is greater than or equal to 0.5 then we choose the higher discrete value for that particular discrete design variable. This method is totally different from the existing penalty function approach for handling discrete variables in the literature.

7.4 APPLICATIONS WITH SINGLE OBJECTIVE FUNCTION

Two engineering design problems with single objective function are solved to validate the proposed approaches using modified PSO. The design of a welded beam, with continuous design variables, is considered by applying the dynamic velocity function to limit the maximum velocity of the design variables in the algorithm. The design of a pressure vessel with mixed discrete design variables is considered to illustrate the MDNLP where CDA is used to handle the discrete design variables.

7.4.1 Design of a welded beam

The design of the welded beam [169,215] described in section 4.4 of chapter 4 is considered. The beam is made of low-carbon steel of length L and cross-sectional dimensions *t* and *b* that is welded to a fixed support. The weld length is *l* on both top and bottom surfaces and the beam is required to support a load P. The weld is in the form of a triangle of depth *h*. The material cost of the welded beam is minimized subject to constraints on the shear stress in the weld, bending stress in the beam, deflection of the beam and the buckling stress of the beam. By treating *h*, *l*, *t* and *b* as the design variables x_1, x_2, x_3 and x_4, respectively, the problem can be stated as

$$\text{Find } \vec{X} = \begin{Bmatrix} x_1 \\ x_2 \\ x_3 \\ x_4 \end{Bmatrix} = \begin{Bmatrix} \text{height of the weld, } h \\ \text{length of the weld, } l \\ \text{thickness of beam, } t \\ \text{width of beam, } b \end{Bmatrix} \tag{7.20}$$

which minimizes the material cost of the welded beam

$$f(\vec{X}) = \begin{Bmatrix} \text{cost per unit} \\ \text{volume of the} \\ \text{weld metal} \end{Bmatrix} \times \begin{Bmatrix} \text{weld} \\ \text{volume} \end{Bmatrix} + \begin{Bmatrix} \text{cost per unit} \\ \text{volume of the} \\ \text{low carbon steel} \end{Bmatrix} \times \begin{Bmatrix} \text{volume of the} \\ \text{low carbon steel} \\ \text{beam} \end{Bmatrix} \quad (7..21)$$

Equation (7.21) can be rewritten with suitable cost per unit volumes as:

$$f(\vec{X}) = 1.1047 x_1^2 x_2 + 0.04811 x_3 x_4 (L + x_2) \quad (7.22)$$

subject to [169]

$$g_1(\vec{X}) = \tau(\vec{X}) - \tau_{\max} \le 0 \quad (7.23)$$

$$g_2(\vec{X}) = \sigma(\vec{X}) - \sigma_{\max} \le 0 \quad (7.24)$$

$$g_3(\vec{X}) = x_1 - x_4 \le 0 \quad (7.25)$$

$$g_4(\vec{X}) = 1.10471 x_1^2 x_2 + 0.04811 x_3 x_4 (L + x_2) - 5.0 \le 0 \quad (7.26)$$

$$g_5(\vec{X}) = 0.125 - x_1 \le 0 \quad (7.27)$$

$$g_6(\vec{X}) = \delta(\vec{X}) - \delta_{\max} \le 0 \quad (7.28)$$

$$g_7(\vec{X}) = P - P_c(\vec{X}) \le 0 \quad (7.29)$$

The geometric constraints are given by

$$0.1 \le x_i \le 2.0, i = 1,4 \quad (7.30)$$

$$0.1 \le x_i \le 10.0, i = 2,3 \quad (7.31)$$

where

$\tau = \sqrt{(\tau')^2 + 2\tau'\tau''\cos\theta + (\tau'')^2}$ = Shear stress induced in the welded beam (7.32)

$\tau' = \dfrac{P}{\sqrt{2}.x_1 x_2}$ = Primary torsional stress acting over the weld throat area (7.33)

$\tau'' = \dfrac{MR}{J}$ = Secondary torsional stress (7.34)

$$M = P\left(L + \frac{x_2}{2}\right) = \text{Moment of } P \text{ about center of gravity of the weld group} \quad (7.35)$$

$$R = \sqrt{\left[\frac{{x_2}^2}{4} + \left(\frac{x_1 + x_3}{2}\right)^2\right]} = \text{Radius of gyration} \quad (7.36)$$

$$J = 2\left(\frac{x_1 x_2}{\sqrt{2}}\left[\frac{{x_2}^2}{12} + \left(\frac{x_1 + x_3}{2}\right)^2\right]\right) = \text{Polar moment of inertia of the weld group} \quad (7.37)$$

$$\sigma(\vec{X}) = \frac{6PL}{x_4 x_3^2} = \text{Bending stress of the welded beam} \quad (7.38)$$

$$\delta(\vec{X}) = \frac{4PL^3}{Ex_3^3 x_4} = \text{Beam deflection at the end (Beam is assumed as cantilever beam)} \quad (7.39)$$

$$P_c(\vec{X}) = \frac{4.013\sqrt{EG(x_3^2 x_4^6/36)}}{L^2}\left(1 - \frac{x_3}{2l}\sqrt{\frac{E}{4G}}\right) = \text{Beam buckling load} \quad (7.40)$$

The data are: $P = 6000\,lb$, $L = 14$ in, $E = 30\times10^6$ psi, $G = 12\times10^6$ psi, $\delta_{\max} = 0.25$ in, $\tau_{\max} = 13{,}600$psi, and $\sigma_{\max} = 30{,}000$ psi. The proposed modified PSO algorithm is implemented in a Matlab code to include dynamic velocity function for the maximum velocity, bounce method for the position (or variable value) which exceeds the specified variable limits and penalty function approach for constraint violation. For the PSO parameters, namely, population size = 24, $i_{\max}$= 2200, $c_1 = c_2 = 2$, iw_{max}= 0.9, iw_{min}= 0.3, $\vec{V}_{f\max} = 0.01$ and $\vec{V}_{i\max} = 1$ for all i, stopping convergence criterion (in terms of change in the objective function value) = 10^{-8} for over 140 continuous iterations, the optimum solution given in Table 7.1 is obtained. The convergence history is shown in Fig 7.2. The number of function evaluations made to obtain this optimum solution is 24, 864 in 0.967 seconds (CPU time depends on the computer system configuration). The constraint

values at the optimum solution are found to be: $g_1(x) = -4.36 \times 10^{-11}$, $g_2(x) = -1.38 \times 10^{-7}$, $g_3(x) = -5.24 \times 10^{-15}$, $g_4(x) = -2.619$, $g_5(x) = -0.1194$, $g_6(x) = -2.34 \times 10^{-1}$ and $g_7(x) = -8.18 \times 10^{-12}$. The program is run for 20 times and is observed that optimum solution had been reached within a range of 0.01 of the optimal solution shown in Table 7.1 for 85% of the time. In the remaining 15% cases, the solutions were limited by the maximum number of iterations permitted and the difference between the terminal solution and the optimal solution reported in Table 7.1 was observed to vary between 0.01 and 0.20. This shows the robustness of the present algorithm. Deb [51] used simple genetic algorithms with binary representation and a traditional penalty function to obtain the optimum solution as shown in Table 7.1 which required 40, 080 function evaluations. Ray and Liew [175] solved this problem using a society and civilization algorithm using 33, 095 function evaluations. The present modified PSO approach can be seen to yield the solution more efficiently compared to the other two approaches.

Table 7.1 Comparison of optimum solutions for the design of welded beam

Design variables	Deb (1991) [51]	Ray and Liew (2003) [175]	Present Solution
x_1	0.2489	0.2444382760	0.2443689758
x_2	6.1730	6.2379672340	6.2177066318
x_3	8.1739	8.2885761430	8.2914713905
x_4	0.2533	0.2445661820	0.2443689758
$f(\vec{X}^*)$	2.43311600	2.3854347	2.3809871315

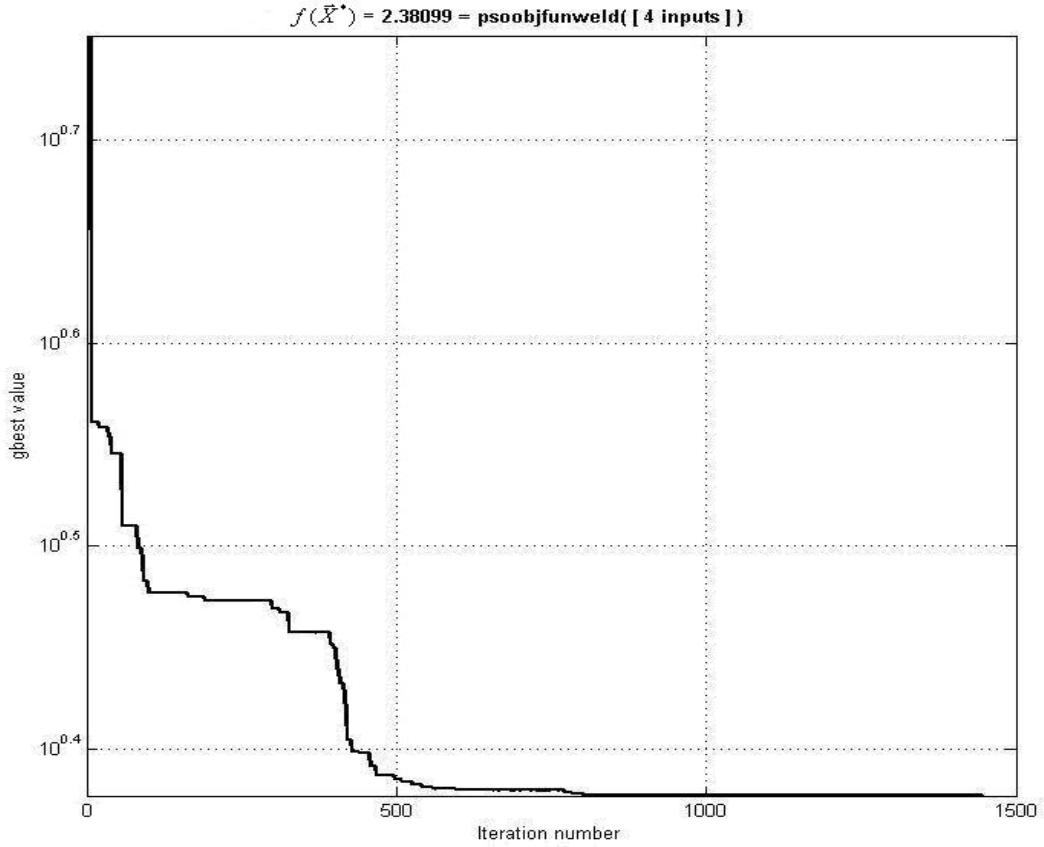

Figure 7.2 Convergence history for the design of welded beam

7.4.2 Design of a pressure vessel

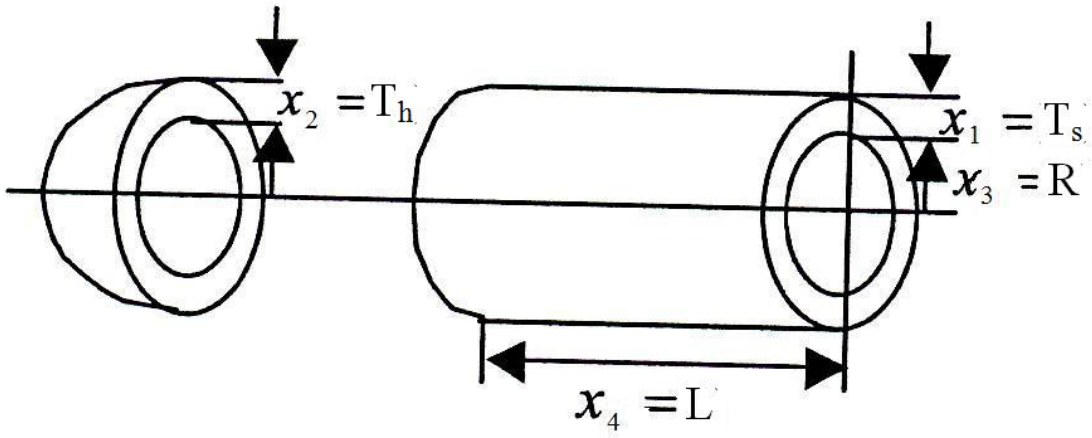

Figure 7.3 Pressure vessel

The design of the pressure vessel [79] shown in Figure 7.3 is considered with minimization of the combined cost of materials, forming and welding as the objective with constraints to satisfy the ASME code. The design variables x_1, x_2, x_3 and x_4 represent the thickness of the shell (T_s), the thickness of the spherical head (T_h), the inner radius (R), and the length of the shell (L) respectively, with x_1 and x_2 assumed to be discrete. The problem can be stated as:

Find $\vec{X}$ which minimizes the cost

$$f(\vec{X}) = 0.6224x_1x_3x_4 + 1.7781x_2x_3^2 + 3.1661x_1^2x_4 + 19.84x_1^2x_3 \tag{7.41}$$

subject to [79]

$$g_1(\vec{X}) : -x_1 + 0.0193x_3 \le 0 \tag{7.42}$$

$$g_2(\vec{X}) : -x_2 + 0.00954x_3 \le 0 \tag{7.43}$$

$$g_3(\vec{X}) : -\pi x_3^2 x_4 - 4/3(\pi x_3^3) + 1296000 \le 0 \tag{7.44}$$

$$g_4(\vec{X}) : x_4 - 240 \le 0 \tag{7.45}$$

with

$$0.0625 \le x_1, x_2 \le 6.1875 \text{ in increments of } 0.0625 \tag{7.46}$$

$$10 \le x_3, x_4 \le 200 \tag{7.47}$$

The modified PSO is applied by using a matlab code that incorporates CDA to handle discrete variables along with the dynamic velocity function for the maximum velocity, bounce method when the position (variable value) exceeds the specified variable limits and penalty function approach for constraint violation. For the PSO parameters, population size = 24, $i_{\max}$= 1000, $c_1 = c_2$ = 2, iw_{max}= 0.9, iw_{min}= 0.3, $\vec{V}_{f\max} = 0.1 \text{and} \vec{V}_{i\max} = 2$ for all i, stopping convergence criteria = 10^{-8} for over 120 continuous iterations, we obtain the optimum solution given in Table 7.2 and the convergence history is shown in Fig 7.4. The number of function evaluations made to obtain this optimum solution is 17, 448 in 6.255 seconds (CPU time depends on the computer system configuration). The program is run 20 times and the optimum solution is reached in 50% of the time as the problem has several local minima and thus the final solution is trapped in these local minimums. Coello Coello [49] used genetic algorithm with a dominance based tournament selection scheme to handle constraints to obtain the optimum solution as shown in Table 7.2 which required 80, 000 function evaluations. As the number of function evaluations required is the least among all the available solutions for both the welded beam and pressure vessel problems, the proposed modified PSO is established to be computationally efficient.

Table 7.2 Comparison of optimum solutions for the design of pressure vessel

Design variables and constraints	Deb and Gene [52]	Coello Coello [49]	Hu et al [79]	Liu and Lin [126]	Present solution
x_1	0.9375	0.8125	0.8125	0.8125	0.8125
x_2	0.5000	0.4375	0.4375	0.4375	0.4375
x_3	48.3290	40.3239	42.09845	42.098442	42.098445595
x_4	112.6790	200.0000	176.6366	176.636642	176.63659584
$g_1(\vec{X}^*)$	-0.04750	-0.034324	0.0	0.0	$-9.4\text{x}10^{-14}$
$g_2(\vec{X}^*)$	-0.038941	-0.052847	-0.03588	-0.035881	$-3.5\text{x}10^{-2}$
$g_3(\vec{X}^*)$	-3652.87683	-27.10584	$-5.820\text{x}10^{-11}$	-0.016762	$-1.1\text{x}10^{-8}$
$g_4(\vec{X}^*)$	-127.32100	-40.000	-63.3634	-63.363358	$-6.33\text{x}10^{1}$
$f(\vec{X}^*)$	6410.3811	6288.7445	6059.131296 6059.71602*	6059.71484	6059.714335

* indicates the true objective function value corresponding to the reported optimum design vector.

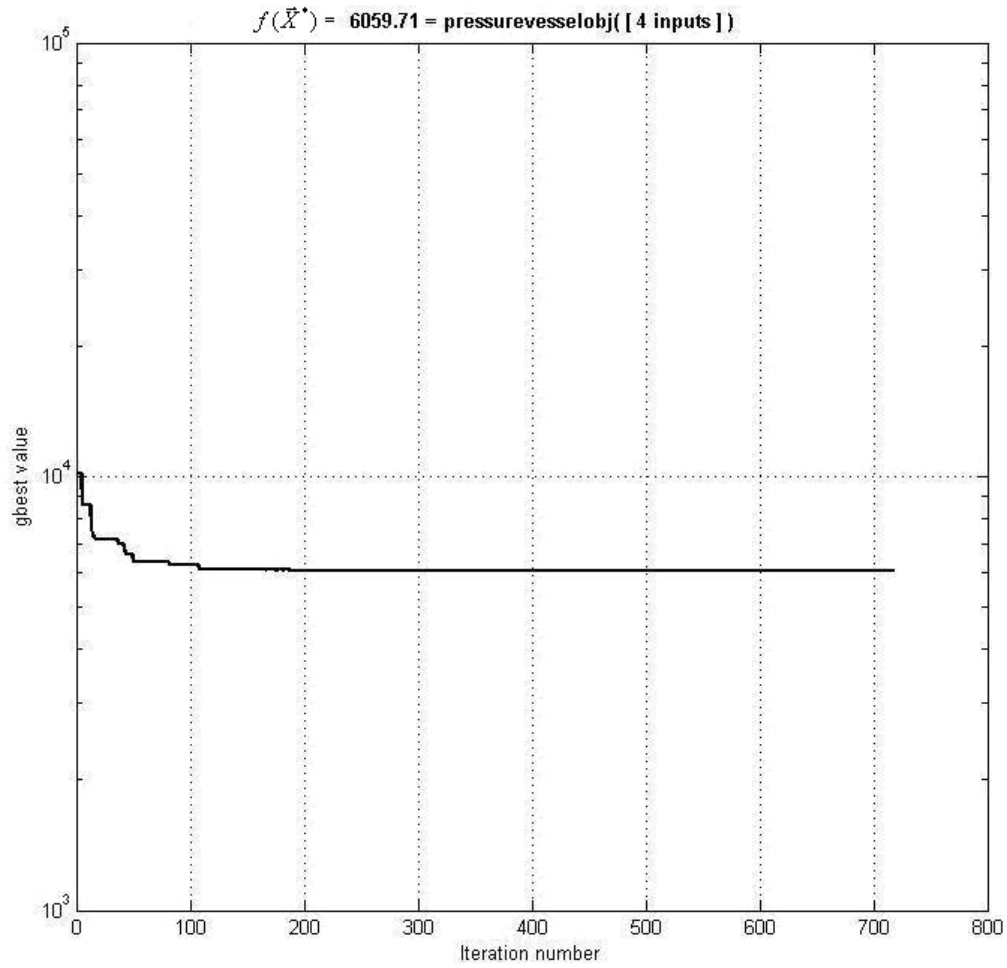

Fig 7.4 Convergence history for the design of pressure vessel

7.5 MODIFIED GAME THEORY APPROACH (MGT) FOR MULTIOBJECTIVE OPTIMIZATION

7.5.1 General problem

A multiobjective optimization problem (MOP) [77] is often stated in the following form:

$$\text{Find } \vec{X} = \begin{Bmatrix} x_1 \\ x_2 \\ \vdots \\ x_n \end{Bmatrix} \tag{7.48}$$

$$\text{which minimizes } f_i(\vec{X}),\ i = 1, 2, ...k \tag{7.49}$$

subject to

$$g_j(X) \le 0, j = 1, 2, ..., m \tag{7.50}$$

$$x_i^{\min} \le x_i \le x_i^{\max}, i = 1, 2, ..., n \tag{7.51}$$

7.5.2 Proposed MGT

A modified game theory approach was proposed by Rao and Freiheit [166] where the worst function value for any particular objective function is obtained by the maximum/minimum of its value evaluated at optimum value for each one of the objective functions except the particular objective function under consideration. This works satisfactorily as long as the objective functions are conflicting in nature i. e., if one objective function increases then other objective function decreases. In general, it cannot be assumed that all objective functions are conflicting in many engineering applications; so there is need to use an alternative procedure for the selection of worst value of each objective function in order to apply the modified game theory for the multi-objective optimization. In the proposed MGT, the selection of the worst value for each of the objective functions is made differently. The following algorithm is proposed for implementing the new MGT with modified PSO.

1. Minimize each of the k objectives stated in equation (7.49) subject to the constraints of equations (7.50) and (7.51) by using the modified PSO and find the corresponding optimal values of the objectives as $f_i(\vec{X}_i^*)$.

2. Maximize each of the k objectives stated in equation (7.49) subject to constraints of equations (7.50) and (7.51) by using the modified PSO and find the worst values of the objectives as F_{wi}.

3. Normalize each of the objectives so that no objective is favored by its magnitude and also assures that it lies between zero and one:

$$f_{ni}(\vec{X}) = \frac{f_i(\vec{X}) - f_i(\vec{X}_i^*)}{F_{wi} - f_i(\vec{X}_i^*)} \tag{7.52}$$

where F_{wi} is the worst value of the i^{th} objective function and $f_i(\vec{X}_i^*)$ is the optimum value (best) obtained in step 1 of the i^{th} objective.

4. Formulate a supercriterion $F(\vec{Y})$ as follows:

$$F(\vec{Y}) = FC - S \tag{7.53}$$

where

$$FC = C_1 f_{n1}(\vec{X}) + C_2 f_{n2}(\vec{X}) + \ldots.. + C_{k-1} f_{n(k-1)}(\vec{X}) + (1 - C_1 - C_2 - \ldots. - C_{k-1}) f_{nk}(\vec{X}) \tag{7.54}$$

$$S = \prod_{i=1}^{k} \left[1 - f_{ni}(\vec{X})\right] \tag{7.55}$$

$$\vec{Y} = \begin{Bmatrix} x_1 \\ x_2 \\ \vdots \\ x_n \\ C_1 \\ C_2 \\ \vdots \\ C_{k-1} \end{Bmatrix} \quad \text{where } 0 \le C_i \ge 1,\ i = 1,2,\ldots,k-1 \tag{7.56}$$

5. Minimize $F(\vec{Y})$ to find $\vec{Y}^*$ which yields the solution of the multiobjective optimization problem stated in equations (7.48) to (7.51).

7.5.3 Test Problem for Multi-objective optimization using modified game theory

To demonstrate the computational efficiency and the quality of results obtained using the new modified game theory, the multi-objective optimization problem presented by Deb *et al.* [53] is considered as the test problem:

Find $\vec{X}$ which minimizes

$$f_1(\vec{X}) = 1 - \exp\left(-\sum_{i=1}^{3} \left(x_i - \frac{1}{\sqrt{3}} \right)^2 \right) \tag{7.57}$$

and $f_2(\vec{X}) = 1 - \exp\left(-\sum_{i=1}^{3} \left(x_i + \frac{1}{\sqrt{3}} \right)^2 \right)$ for $-4 \le x_i \le 4$, $i = 1,2,3$. (7.58)

The Matlab code of the new MGT used the PSO parameters - population size = 50, $i_{\max}$= 2000, $c_1 = c_2 = 2$, iw_{max}= 0.9, iw_{min}= 0.3, $\vec{V}_{f\max} = 0.01$ and $\vec{V}_{i\max} = 1$ for all i, and stopping convergence criterion = 10^{-8} for over 150 continuous iterations of the algorithm - and the resulting optimal solution is given by $x_1 = x_2 = x_3 = -0.54715$ and $C_1 = 0.1$. This solution can be seen to be a particular Pareto-optimal solution. This optimum solution lies in the

optimal solution range given in the Deb's paper. Deb measures the extent of convergence to a known set of Pareto-optimal set which was explained in detail in his paper. The mean values for this convergence matrix using Non-dominated Sorting Genetic Algorithm-II (NSGA-II) for real coded and binary coded algorithms are 0.001931 and 0.002571, respectively. The present program was run 20 times and it was found that each run yielded the same optimal solution, accuracy upto 4^{th} decimal places, which makes the mean variation from the optimum solution equal to 0.000002 (almost equal to zero). This establishes the computational efficiency of the proposed modified PSO with new modified game theory algorithm.

7.6 ENGINEERING APPLICATIONS WITH MULTIPLE OBJECTIVE FUNCTIONS

Four engineering design problems with multiple objective functions are solved to validate the proposed new MGT approach. The optimum designs of a 2-bar truss and an I-beam are considered using the proposed modified PSO algorithm, coupled with the new MGT approach, with two objective functions in each case. The optimal designs of a 25-bar truss and a gear box are solved by considering three objective functions in each case using the procedure developed in this work.

7.6.1 Design of a 2-bar truss

The 2-bar truss [169] shown in Fig 7.4 is symmetric about the y-axis. The design problem corresponding to the truss is formulated as:

Find $\vec{X} = \begin{Bmatrix} x_1 \\ x_2 \end{Bmatrix} = \begin{Bmatrix} A / A_{ref} \\ x / h \end{Bmatrix}$ (7.59)

to minimizes $\left\{ f_1(\vec{X}), f_2(\vec{X}) \right\}$ (7.60)

where

$f_1(\vec{X}) = 2\rho h x_2 \sqrt{1 + x_1^2 A_{ref}}$ = Weight of the truss (7.61)

$f_2(\vec{X}) = \dfrac{Ph(1 + x_1^2)^{1.5} \sqrt{(1 + x_1^4)}}{2\sqrt{2} E x_1^2 x_2 A_{ref}}$ = Total displacement of joint 3 (7.62)

subject to the stress constraints

$\sigma_i(\vec{X}) - \sigma_0 \le 0,\ i = 1,2$ (7.63)

where

$\sigma_1(\vec{X}) = \dfrac{P(1 + x_1)\sqrt{(1 + x_1^2)}}{2\sqrt{2} x_1 x_2 A_{ref}}$ = stress induced in member 1 (7.64)

$\sigma_2(\vec{X}) = \dfrac{P(x_1 - 1)\sqrt{(1 + x_1^2)}}{2\sqrt{2} x_1 x_2 A_{ref}}$ = stress induced in member 2 (7.65)

$x_i^{\min} \le x_i \le x_i^{\max}$; i = 1,2 (7.66)

with $x_1^{\min} = 0.1,\ x_2^{\min} = 0.1,\ x_1^{\max} = 2.0$ and $x_2^{\max} = 2.5,$

$E = 30 \times 10^6\ psi,\ \rho = 0.283\, lb / in^3,\ P = 10000\, lb,\ \sigma_0 = 20000\, psi,$

$h = 100\, in.$ and $A_{ref} = 1 in^2$

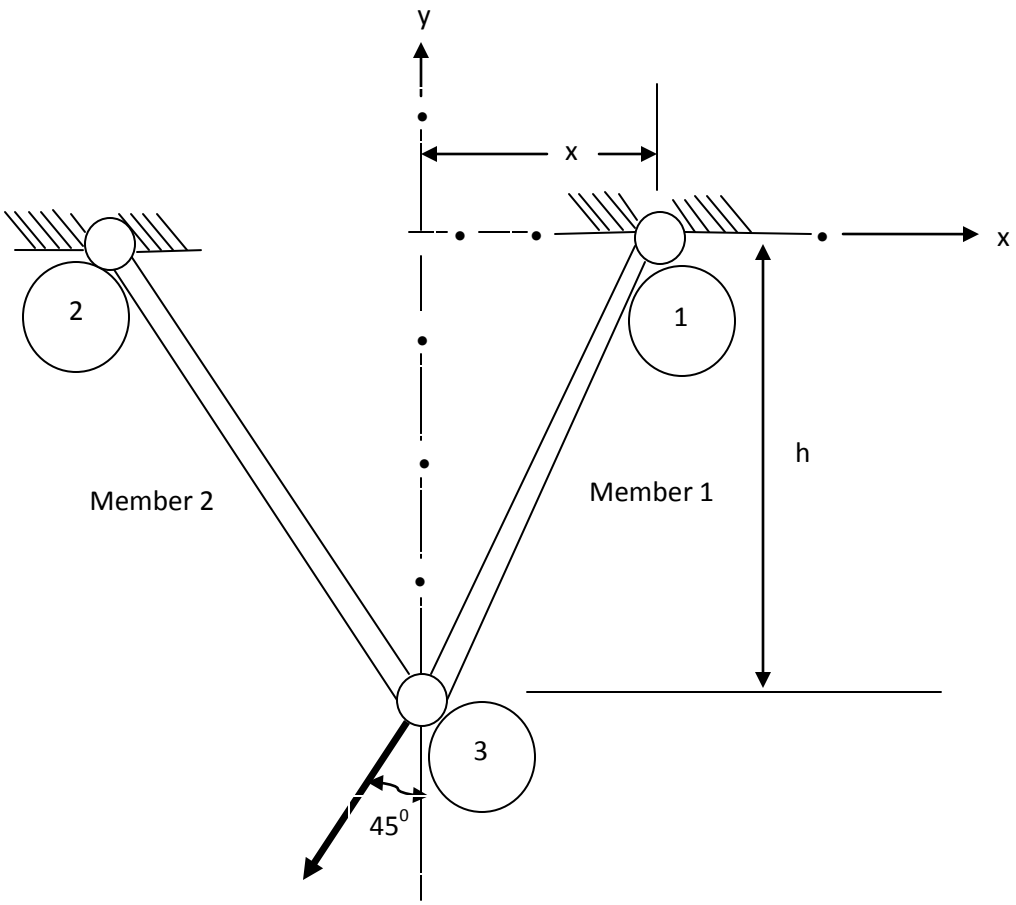

Figure 7. 5 Two-bar truss

The matlab code using the PSO parameters, population size = 50, $i_{\max}$= 1500, $c_1 = c_2 = 2$, iw_{max}= 0.9, iw_{min}= 0.4, $\vec{V}_{i\min} = 0.1 \text{and} \vec{V}_{i\max} = 2$ for all i, and stopping convergence criteria = 1e-10 for over 120 continuous iterations in the algorithm, is used to find the optimal solution and given in Table 7.3. The constraints for the optimum solution for minimization of f_1 are 0 and -2.413e4. The constraints for the optimum solution for minimization of f_2 are -1.5968e4 and -2.0293e4. The constraints for the optimum solution for multi-objective optimization of f_1 and f_2 are -0.7784e4 and -2.1603e4. The implication of C_1 = 1 implies C_2 = 0 in the optimum solution is that it emphasizes f_1 compared to f_2.

Table 7.3 Comparison of optimal solutions of 2-bar truss

Quantity	Rao [169]	Present solution
$f_1(\vec{X})$ Design variables	36.1493 [0.6743,0.5295]	36.1273 [0.6577,0.5333]
$f_2(\vec{X})$ Design variables	0.0182 [0.8612,2.5]	0.0182 [0.8645,2.5]
$\{f_1(\vec{X}), f_2(\vec{X})\}$ Design variables C_1	81.4137, 0.0408 [0.7681,1.1408]	59.9527,0.0554 [0.7680,0.8401] 1

7.6.2 Design of an I-Beam

A simply supported I-beam [78] is shown in Fig 7.5. The design variables and applied loads P and Q are also shown in Fig 7.5 and the optimization problem is formulated as follows:

$$\text{Find } \vec{X} = \begin{Bmatrix} x_1 \\ x_2 \\ x_3 \\ x_4 \end{Bmatrix} \tag{7.67}$$

which minimizes (f_1, f_2) (7.68)

where

$f_1(\vec{X}) = 2x_2x_4 + x_3(x_1 - 2x_4)$ = Area of cross section (7.69)

$$f_2(\vec{X}) = \frac{PL^3}{48EI} = \text{Deflection at the mid span} \tag{7.70}$$

$$I = \frac{x_3(x_1 - 2x_4)^3 + 2x_2x_4[4x_4^2 + 3x_1(x_1 - 2x_4)]}{12} \tag{7.71}$$

subject to stress constraint

$$\frac{M_Y}{Z_Y} + \frac{M_Z}{Z_Z} \le \sigma_b \tag{7.72}$$

where M_Y, M_Z are the maximal bending moments in the Y and Z directions, respectively and σ_b is the permissible bending stress for the material. This stress constraint can be rewritten as:

$$\frac{180000x_1}{x_3(x_1 - 2x_4)^3 + 2x_2x_4[4x_4^2 + 3x_1(x_1 - 2x_4)]} + \frac{15000x_2}{(x_1 - 2x_4)x_3^3 + 2x_4x_2^3} \le 16 \tag{7.73}$$

The geometric constraints are given by

$$10 \le x_1 \le 80, 10 \le x_2 \le 50, 0.9 \le x_3 \le 5 \text{ and } 0.9 \le x_4 \le 5 \tag{7.74}$$

The length of the I-beam is L = 200 cm, external loads are P = 600 kN and Q = 50 kN, the Young's modulus of elasticity, E = 2 x 104 kN/cm^2 and σ_b = 16 kN/cm^2. The matlab code uses the PSO parameters, namely, population size = 50, $i_{\max}$= 2000, $c_1 = c_2 = 2$, iw_{max}= 0.9, iw_{min}= 0.3, $\vec{V}_{i\min} = 0.05$ and $\vec{V}_{i\max} = 5$ for all i, and stopping convergence criteria = 1e-8 for over 150 continuous iterations in the algorithm and the resulting optimal solution is shown in Table 7.4. The stress constraint for the optimum solution for minimization of f_1 is -1.164e-10. The stress constraint for the optimum solution for minimization of f_2 is -13.9875. The stress constraint for the optimum solution for multi-objective optimization of f_1 and f_2 is -7.8443e-7.

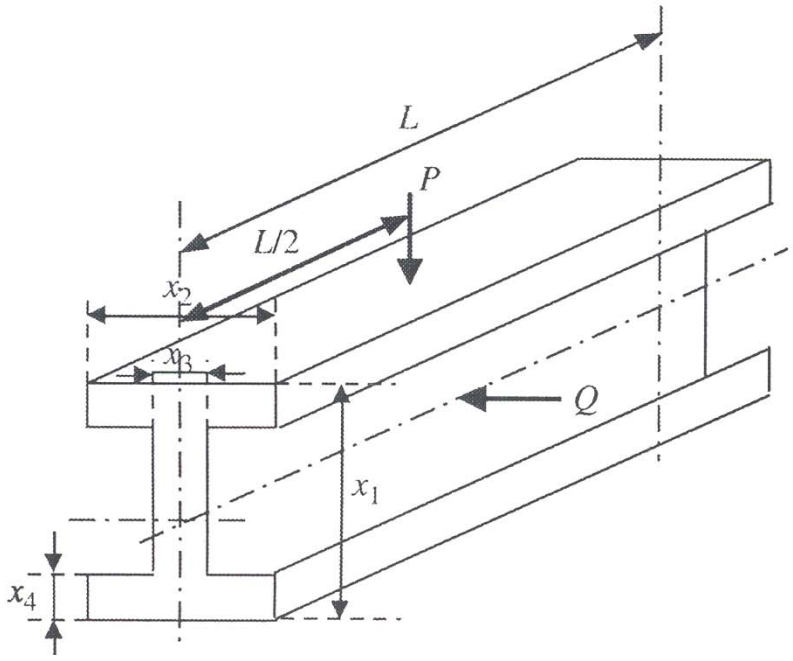

Figure 7.6 An I-beam

Table 7.4 Comparison of optimal solutions of an I-Beam

Quantity	Huang *et al* [78]	Hajela and Shih [73]	Present solution
$f_1(\vec{X})$	127.4124	-	127.4129
Design variables	[60.47,41.44,0.9,0.9]	-	[60.65,41.35,0.9,0.9]
$f_2(\vec{X})$	0.0059	-	0.0059
Design variables	[80,50,5,5]	-	[80,50,5,5]
$\begin{Bmatrix} f_1(\vec{X}) \\ f_2(\vec{X}) \end{Bmatrix}$	276.4525 0.0143	206.14 0.0205	132.5374 0.0375
Design variables	[80,50,0.9,2]	[80,39.79,0.9,1.72]	[80,34.53,0.9,0.9]
C_1			1

7.6.3 Design of a Gear box

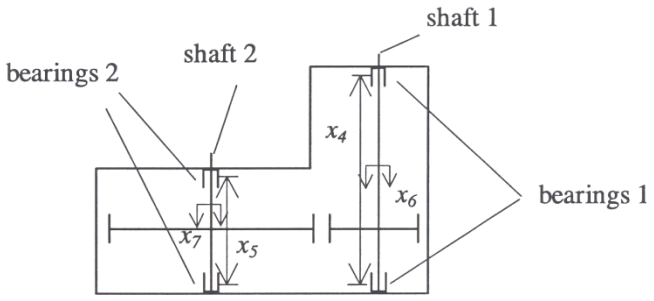

Figure 7.7 Gear box

The multiobjective optimization problem of the gear box [119], shown in Fig 7.6, can be stated as follows

$$\text{Find} \quad \vec{X} = \begin{Bmatrix} x_1 \\ x_2 \\ \vdots \\ x_7 \end{Bmatrix} = \begin{Bmatrix} \text{gear face width (cm)} \\ \text{teeth module (cm)} \\ \text{number of teeth of pinion} \\ \text{distance between bearing 1 (cm)} \\ \text{distance between bearing 2 (cm)} \\ \text{diameter of shaft 1 (cm)} \\ \text{diameter of shaft 2 (cm)} \end{Bmatrix} \tag{7.75}$$

$$\text{which minimizes} \quad F(\vec{X}) = \left\{ f_1(\vec{X}), f_2(\vec{X}), f_3(\vec{X}) \right\} \tag{7.76}$$

where

$$f_1(\vec{X}) = 0.7854 x_1 x_2^2 \left(\frac{10 x_3^2}{3} + 14.9334 x_3 - 43.0934 \right) - 1.508 x_1 (x_6^2 + x_7^2) + 7.4777 (x_6^3 + x_7^3) + 0.7854 (x_4 x_6^2 + x_5 x_7^2) = \text{Weight of the gear box} \tag{7.77}$$

$$f_2(\vec{X}) = \frac{\sqrt{\left(\frac{745 x_4}{x_2 x_3} \right)^2 + 1.69 \times 10^8}}{0.1 x_6^3} = \text{Stress developed in shaft 1} \tag{7.78}$$

$$f_3(\vec{X}) = \frac{\sqrt{\left(\frac{745x_5}{x_2x_3}\right)^2 + 1.575\times10^8}}{0.1x_7^3} = \text{Stress developed in shaft 2} \quad (7.79)$$

subject to [119]

$$g_1 = \frac{27}{x_1x_2^2x_3^3} - 1 \le 0 \text{ (bending stress of teeth constraint)} \quad (7.80)$$

$$g_2 = \frac{397.5}{x_1x_2^2x_3^2} - 1 \le 0 \text{ (contact stress of teeth constraint)} \quad (7.81)$$

$$g_3 = \frac{1.93x_4^3}{x_2x_3x_6^4} - 1 \le 0 \text{ (transverse displacement of shaft 1)} \quad (7.82)$$

$$g_4 = \frac{1.93x_5^3}{x_2x_3x_7^4} - 1 \le 0 \text{ (transverse displacement of shaft 2)} \quad (7.83)$$

g_5 to g_9 are related to torque :

$$g_5 = x_2x_3 - 40 \le 0,\ g_6 = \frac{x_1}{x_2} - 12 \le 0, g_7 = 5 - \frac{x_1}{x_2} \le 0, g_8 = 1.9 - x_4 + 1.5x_6 \le 0 \text{ and}$$

$$g_9 = 1.9 - x_5 + 1.1x_7 \le 0 \quad (7.84)$$

Stress constraints in shafts 1 and 2 are

$$g_{10} = f_2(\vec{X}) - 1300 \le 0 \text{ and } g_{11} = f_3(\vec{X}) - 1100 \le 0 \quad (7.85)$$

The geometric constraints are given by

$$2.6 \le x_1 \le 3.6, 0.7 \le x_2 \le 0.8, 17 \le x_3 \le 28, 7.3 \le x_4 \le 8.3, 7.3 \le x_5 \le 8.3, 2.9 \le x_6 \le 3.9$$

$$\text{and } 5.0 \le x_7 \le 5.5 \quad (7.86)$$

The matlab code uses the PSO parameters, namely, population size = 50, $i_{\max}$= 2000, $c_1 = c_2 =$ 2, iw_{max}= 0.9, iw_{min}= 0.3, $\vec{V}_{i\min} = 0.1 \text{and} \vec{V}_{i\max} = 0.2$ for all i, and stopping convergence criteria = 1e-8 for over 150 continuous iterations in the algorithm to find the

optimal solution given in Table 7.5. The active constraint for the optimum solution for minimization of f_1 is g_7. The nearest to zero constraints, namely g_7 and g_8 for the optimum solution for minimization of f_2 are -5.465e-9 and -1.557e-9. The nearest to zero constraint is g7 and its value for the optimum solution for minimization of f_3 is -8.333e-11. The nearest to zero constraint is g7 and its value for the optimum solution for multi-objective optimization of f_1 , f_2 and f_3 is -1.5714e-5.

Table 7.51 Comparison of optimal solutions of Gear box design

Objective function	Huang *et al* [78]	Present solution
$f_1(\vec{X})$ Design variables	-	2939.275 [3.5,0.7,17.0,7.3,7.3,3.1,5.2]
$f_2(\vec{X})$ Design variables	-	693.0318 [3.6,0.719,28.0,7.75,7.69,3.9,5.30]
$f_3(\vec{X})$ Design variables	-	754.314 [3.6,0.719,28.0,7.78,7.30,3.33,5.5]
$\{f_1(\vec{X}), f_2(\vec{X}), f_3(\vec{X})\}$ Design variables C_1 C_2	3425.0,879.8,797.6 [3.58,0.71,18,8.24,8.23,3.61,5.4] Not given Not given	3295.2857,693.0359,754.3154 [3.5,0.7,17.0,7.75,7.3,3.9,5.5] 0.3525 0.3555

7.6.4 Design of a 25-bar truss

The 25-bar truss (shown in Fig 7.7) is considered to support two load conditions given in Table 7.6 and is to be designed to minimize (i) the weight, (ii) sum of deflections

of node 1 under the two load conditions and (iii) negative of the fundamental natural frequency of the truss subject to stress and buckling constraints. The allowable maximum stress limit, $\sigma_{\max}$, for all members is assumed to be same in both tension and compression. The cross section of each member of the truss is assumed to be thin tubular with nominal diameter D and thickness t = D/100 so that the area of the member is $0.0099\pi D^2$. The diameters of these members are grouped into eight different sets D-1 to D-8 as shown in Table 7.7 and the eight diameters D-1 to D-8 are chosen to be the design variables. The minimum and maximum allowable limits for each of the variables (D-1 to D-8) are taken as 0.04 m and 0.32 m, respectively. The buckling stress in the i^{th} member is calculated as

$$\sigma_{bi} = \frac{-100.01\pi E A}{8 L_i^2},\ i = 1, 2, \cdots, 25 \tag{7.87}$$

The objectives of the multiobjective optimization problem of the 25-bar truss are stated as follows

$$f_1(\vec{X}) = 9.8125 \sum_{i=1}^{25} \rho A_i l_i \tag{7.88}$$

$$f_2(\vec{X}) = \sum_{p=1}^{2} (\delta_{xp}^2 + \delta_{yp}^2 + \delta_{zp}^2)^{1/2} \tag{7.89}$$

$$f_3(\vec{X}) = -\omega_n \tag{7.90}$$

where i is the element number, δ_{xp}, δ_{yp} and δ_{zp} are the x, y and z components of displacement of node 1 under load condition p (p = 1, 2), and ω_n is the fundamental natural frequency of vibration of the truss. The constraints are:

$$\left|\sigma_{ip}(\vec{X})\right| \le \sigma_{\max},\ i = 1, 2, \ldots, 25,\ \ p = 1, 2 \tag{7.91}$$

$$-\sigma_{ip}(\vec{X}) \le -\sigma_{bp},\ i = 1,2,...,25,\ \ p = 1,2 \tag{7.92}$$

where $\sigma_{ip}(\vec{X})$ is the stress in element i in load condition p.

The data are taken as: Young's modulus of elasticity, $E = 6.9 \times 10^{10}\ pa$, material density, $\rho = 2770\, kg/m^3$ and allowable maximum stress limit, $\sigma_{\max} = 2.76 \times 10^{8}\ pa$. The bounds for the variables c_1 and c_2 used in the supercriterion of MGT are taken as 0.1 and 0.7, respectively. These values are suggested for cooperative game theory used in the literature.

Table 7.6 Loads acting on Twenty five bar truss

	Load condition 1 (N)			
	Node-1	Node-2	Node-3	Node-4
F_x	0	0	0	0
F_y	88960	-88960	0	0
F_z	-22240	-22240	0	0
	Load condition 2 (N)			
F_x	4448	0	224	224
F_y	44480	44480	0	0
F_z	-22240	-22240	0	0

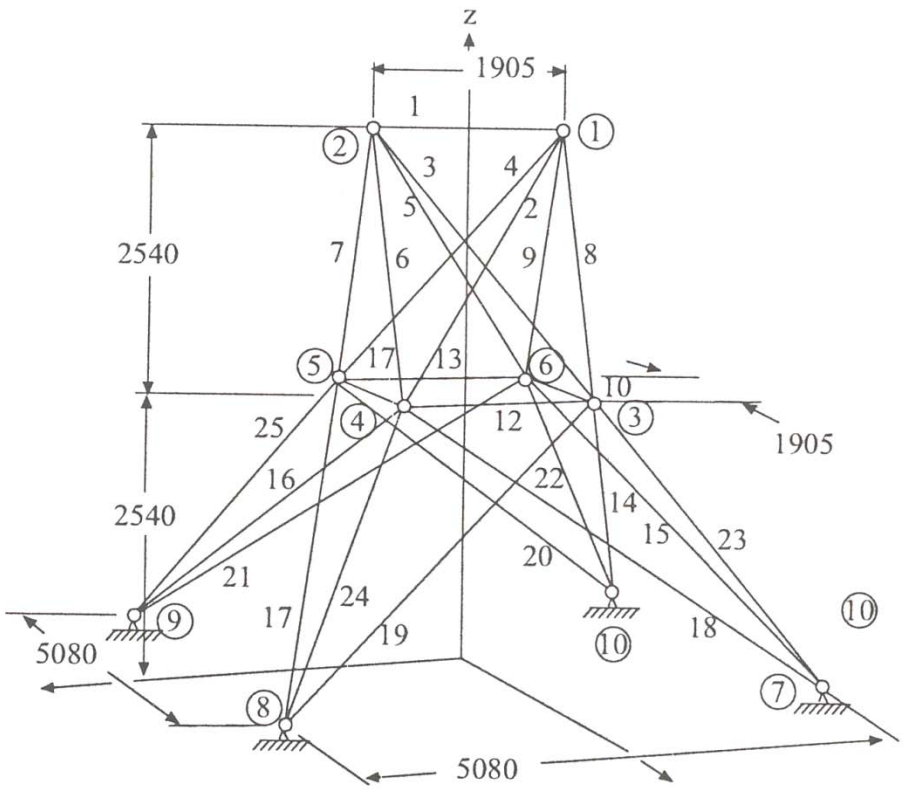

Figure 7.8 Twenty five bar truss

Table 7.7 Diameter groups for the elements of the truss

Set No.	Area groups
D-1	D_1
D-2	$D_2=D_3=D_4=D_5$
D-3	$D_6=D_7=D_8=D_9$
D-4	$D_{10}=D_{11}$
D-5	$D_{12}=D_{13}$
D-6	$D_{14}=D_{15}=D_{16}=D_{17}$
D-7	$D_{18}=D_{19}=D_{20}=D_{21}$
D-8	$D_{22}=D_{23}=D_{24}=D_{25}$

(i) Solution with continuous design variables:

The matlab code uses the PSO parameters: population size = 50, $i_{\max}$= 2000, $c_1 = c_2 =$ 2, iw_{max}= 0.9, iw_{min}= 0.4, $\vec{V}_{i\min} = 0.01$ and $\vec{V}_{i\max} = 0.3$ for all i, and stopping convergence criteria = 1e-8 for over 150 continuous iterations in the algorithm. The optimal solution is given in Table 7.8 and the results are compared with those available in the literature in Table 7.10. The constraints are not normalized in this optimization problem. The active constraints for the optimum solution for minimization of f_1 are buckling load for the element numbers 2, 5, 7, 8, 19, 20 for load condition 1 with constraint values, -3.576e-7, -3.427e-7, -3.248e-6, -3.218e-6, -8.196e-7, -7.897e-7 respectively and 13,16, 24 for load condition 2 with constraint values, -6.23e-4, -1.259e-6, -6.705e-7 respectively. The constraints which are close to being active for the optimum solution for maximization of f_2 are buckling load for the element numbers 3, 6, 8, 9 for load condition 1 with constraint values, -0.3677, -0.3677, -0.2198, -0.2198 respectively and 24 for load condition 2 with constraint value, -0.151. There are no active constraints nor close to the active constraints found for all the other optimum solutions in the Table 7.8.

Table 7.8 Optimal solution of twenty five bar truss with continuous variables

Quantity	Min. of f1	Min. of f2	Min. of f3	Max. of f1	Max. of f2	Max. of f3	Multi-objective
D-1	0.04	0.32	0.04	0.32	0.243183	0.3068	0.04
D-2	0.1286	0.32	0.1268	0.32	0.130186	0.32	0.151133
D-3	0.1243	0.32	0.1253	0.32	0.123353	0.32	0.159884
D-4	0.04	0.32	0.1546	0.32	0.309489	0.04	0.094876
D-5	0.0508	0.32	0.04	0.32	0.076901	0.32	0.04
D-6	0.1084	0.32	0.32	0.32	0.109956	0.1577	0.194687
D-7	0.1421	0.32	0.2489	0.32	0.141700	0.32	0.210814
D-8	0.1290	0.32	0.32	0.32	0.128059	0.0978	0.32
Objective function value	1031.4009	0.007925	-114.0441	7269.9078	0.049019	-26.49427	2981.4416 0.0239586 -104.3978

(ii) Solution with mixed discrete design variables:

The 25-bar truss problem is considered as a mixed discrete multiobjective optimization problem. The design variables (D-1 to D-4) are assumed to be discrete variables with lower and upper bounds as D = 40 mm and D = 320 mm, respectively, and are permitted to take values only in increments of 10 mm within the range. Thus, the permissible values of each of the four design variables are given by 40 mm, 50 mm, 60 mm, 70 mm, …, 310 mm and 320 mm. The design variables (D-5 to D-8) are assumed to be continuous variables. The lower and upper bounds for these continuous variables remains same as in the case of continuous variable problem. The modified PSO with CDA is used to solve this mixed discrete design optimization problem. The PSO parameters used are same as in the case of continuous variable problem. The results of optimization are shown in Table 7.9 and are compared with those available in the literature in Table 7.10. The constraints are not normalized in this optimization problem. The active constraints for the optimum solution for minimization of f_1 are buckling load for the element numbers 14, 15 for load condition 1 with constraint values, -6.407e-7, -5.960e-7 respectively and 13,16, 24 for load condition 2 with constraint values, -1.136e-5, -6.109e-7, -1.198e-5 respectively. The constraints which are close to being active for the optimum solution for maximization of f_2 are buckling load for the element numbers 19, 20 for load condition 1 with constraint values, -3.973e-4, -3.973e-4 respectively and 16, 24 for load condition 2 with constraint values, -0.0207, -0.0901. There are no active constraints nor close to the active constraints found for all the other optimum solutions in the Table 7.9.

Table 7.9 Optimal solution of twenty five bar truss with mixed discrete variables

Quantity	Min. of f1	Min. of f2	Min. of f3	Max. of f1	Max. of f2	Max. of f3	Multi-objective
D-1	0.04	0.32	0.04	0.32	0.23	0.32	0.04
D-2	0.13	0.32	0.13	0.32	0.13	0.32	0.15
D-3	0.13	0.32	0.13	0.32	0.13	0.32	0.16
D-4	0.04	0.32	0.15	0.32	0.16	0.04	0.09
D-5	0.04999	0.32	0.04000	0.32	0.04898	0.32000	0.04000
D-6	0.10846	0.32	0.32000	0.32	0.10976	0.10811	0.19766
D-7	0.14240	0.32	0.24580	0.32	0.14183	0.32000	0.21274
D-8	0.12885	0.32	0.32000	0.32	0.12879	0.09808	0.32000
Objective function value	1048.8444	0.007925	-113.1737	7269.9078	0.047364	-25.47221	3005.9747 0.0239842 -104.6054

Table 7.10 Comparison of optimal solutions of twenty five bar truss

Quantity	Rao[170] (FPS units used)	Sunar[197]	Present solution (continuous)	Present solution (mixed discrete)
C_1	0.1433	-	0.1	0.1
C_2	0.3628	-	0.1	0.1
$f_1(\vec{X})$	596.5181 (2600*)	3033.65	2981.4416	3005.9747
$f_2(\vec{X})$	0.9401 (0.02387*)	0.0232	0.0239586	0.0239842
$f_3(\vec{X})$	-100.2154	-103.141	-104.3978	-104.6054

* indicates the objective function value in SI units.

There are no active constraints nor close to the active constraints found for all the optimum solutions in the Table 7.10.

7.6.5 Discussion

The solution obtained for the problems solved for single optimization problems illustrate the computational efficiency of the proposed modified PSO. It was evident from the no. of function evaluations found in other evolutionary algorithms like genetic algorithm compared to our algorithm. This was extended to multi-objective optimization problems using the modified game theory and the results obtained to the design problems solved in this section are convincing with respect to other results reported in the literature.

7.7 SUMMARY

This chapter presents algorithms based on modified PSO to solve all types of engineering optimization problems involving single objective or multiple objectives with continuous, discrete and/or mixed design variables with constraints. Because of the convergence difficulties experienced with the original PSO algorithm with a constant value of the maximum velocity limit, the dynamic velocity function approach has been used to speed up the convergence. The bounce method provides significant improvement in the performance of the algorithms to overcome stagnation of the population. Results of single and multi objective optimization problems like welded beam design and pressure vessel design showed that the algorithm converges to the optimal solution faster than the original PSO algorithm. When the new MGT, combined with the modified PSO, is used to solve multiobjective optimization problems, the best compromise (optimal) solution from the Pareto-optimal front has been found efficiently. The results of the 25-bar truss multiobjective optimization problem illustrate the effectiveness and efficiency of the new approach when all the objective functions are not totally conflicting. The results obtained for the 25-bar truss with all design variables taken as continuous or as mixed discrete are found to be comparable to another. In the next chapter 7, a new method was proposed using modified PSO, modified game theory and vertex method to solve multi-objective optimization problems with uncertain parameters.

CHAPTER 8

MULTI-OBJECTIVE OPTIMIZATION OF UNCERTAIN ENGINEERING SYSTEMS USING PARTICLE SWARM OPTIMIZATION

8.1 OVERVIEW

This chapter proposes a novel method using modified particle swarm optimization (PSO) based algorithm to solve multi-objective optimization of uncertain engineering problems involving different types of design variables (continuous, discrete and/or mixed). The information for each of the uncertain parameters is assumed to be available in the form of percentage tolerance on the data, implying the existence of large epistemic uncertainty in the parameters. The vertex method, described in section 8.2, is used to reduce the widening of the function value interval due to multi-occurrences of variables when interval analysis is used in finding the response function of the system. The computational aspects of the vertex method are described in section 8.3. A modified game theory approach (MGT) is coupled with the modified PSO to solve multiobjective optimization problems as described in section 8.4. A dynamic penalty function is used to handle constraints in all constrained optimization problems. A standard weighted convex sum is coupled with the modified PSO to solve a two objective welded beam design optimization problem. This chapter is concluded by a summary in the last section.

8.2 ENGINEERING APPLICATION

8.2.1 GENERAL MULTIOBJECTIVE OPTIMIZATION PROBLEM

A multiobjective optimization problem (MOP) is solved using modified PSO with modified game theory as described in section 7.5 of chapter 7. Two engineering design problems are solved to validate the proposed approach using the modified PSO coupled with the vertex method. The vertex method is used to calculate the belief function, as one of the objectives, for the safe design of the system. The design of a welded beam, with continuous design variables, is considered by applying the dynamic velocity function to limit the maximum velocity of the design variables along with bounce method in the algorithm. The design of a 25-bar truss with continuous as well as mixed discrete design variables are considered where closest discrete approach (CDA) is used to handle the discrete design variables.

8.2.2 Design of a welded beam

The data are: $P = 6000\,\text{in}$, $L = 14\,\text{in}$, Young's modulus of the beam, $E = 30\times10^{6}\,\text{psi}$, shear modulus of the beam, $G = 12\times10^{6}\,\text{psi}$, maximum deflection allowed on the beam, $\delta_{\max} = 0.25\,\text{in}$, maximum allowable shear stress in the beam, $\tau_{\max} = 13{,}600\,\text{psi}$, and maximum allowable bending stress in the beam, $\sigma_{\max} = 30{,}000\,\text{psi}$. This design problem is solved with different number of uncertain parameters in each of the following cases. The information for each of the uncertain parameters is assumed to be available in the form of percentage tolerance on the parameters, implying the existence of large epistemic uncertainty in the parameters. We assume equal evidence for positive and negative tolerances on these parameters. Belief is

calculated for safe design (satisfying all constraints) using vertex method as described in section 8.3. A standard weighted convex sum ($f_1 + f_2$) is used for this two objective optimization as in this case the magnitudes of both f_1 and f_2 are comparable.

Case a: Four uncertain parameters

In this case, all the four design variables are considered as uncertain parameters. The uncertainty on these parameters is expressed as percentage tolerance on the nominal values of the parameters. Let ±x% tolerance is given on any uncertain parameter. This information can be translated as equal intervals defined as [(1-x/100), 1] and [1, (1+x/100)]. An equal evidence of 0.5 each for these intervals is assumed. For example, ±1% tolerance on any parameter can be translated as [0.99, 1.00] and [1.00, 1.01] times the parameter with 0.5 evidence each for the intervals.

Case b: Eleven uncertain parameters

In this case, all the parameters in equations (7.22) to (7.40) including the design parameters are considered as uncertain parameters. These uncertain parameters are x_1, x_2, x_3, x_4, *P, L, E, G,* $\delta_{\max}$, $\tau_{\max}$ and $\sigma_{\max}$. The uncertainty is assumed to be of similar form as in case a.

The proposed modified PSO algorithm is implemented in a matlab code to include dynamic velocity function for the maximum velocity, bounce method for the position (or variable value) which exceeds the specified variable limits, penalty function approach for constraint violation and vetex method to calculate belief for satisfying all constraints of the design. For the PSO parameters, namely, population size = 10, i_{max} = 800, $c_1 = c_2 = 2$,

$iw_{max} = 0.9$, $iw_{min} = 0.3$, $\vec{V}_{i\min} = 0.01$ and $\vec{V}_{i\max} = 1$ for all i, stopping convergence criterion (in terms of change in the objective function value) = $1e-8$ for over 200 continuous iterations, the optimum solutions with four uncertain parameters and eleven uncertain parameters with ±1% tolerance assumed on the design parameters as given in Table 8.1 are obtained. The variation of material cost with increase in percentage tolerance on the design variables is as shown in Figure 8.1. The default value of ±2% tolerance on all other parameters is assumed in case b. The belief for case a is found to be constant at 0.875. The belief for case b is found to be within the range 0.828 and 0.859. The active constraint values at the optimum solution for case a are found to be: $g_1(x) = -4.36 \text{x} 10^{-11}$, $g_2(x) = -1.38 \text{x} 10^{-7}$, $g_3(x) = -5.24 \text{x} 10^{-15}$, and $g_7(x) = -8.18 \text{x} 10^{-12}$. There are no active constraints are found for the other optimum solutions in Table 8.1.

Table 8.1 Comparison of optimum solutions for the design of welded beam

Design variables	Optimum Solution	Present solution case a (4 uncertain parameters)	Present solution case b (11 uncertain parameters)
x_1	0.2443689758	0.246833737	0.249724604
x_2	6.2177066318	6.217170236	5.847808155
x_3	8.2914713905	8.375730427	8.500404914
x_4	0.2443689758	0.246833892	0.249870491
$f(\vec{X}^*)$	2.3809871315	2.429322628	2.432504205

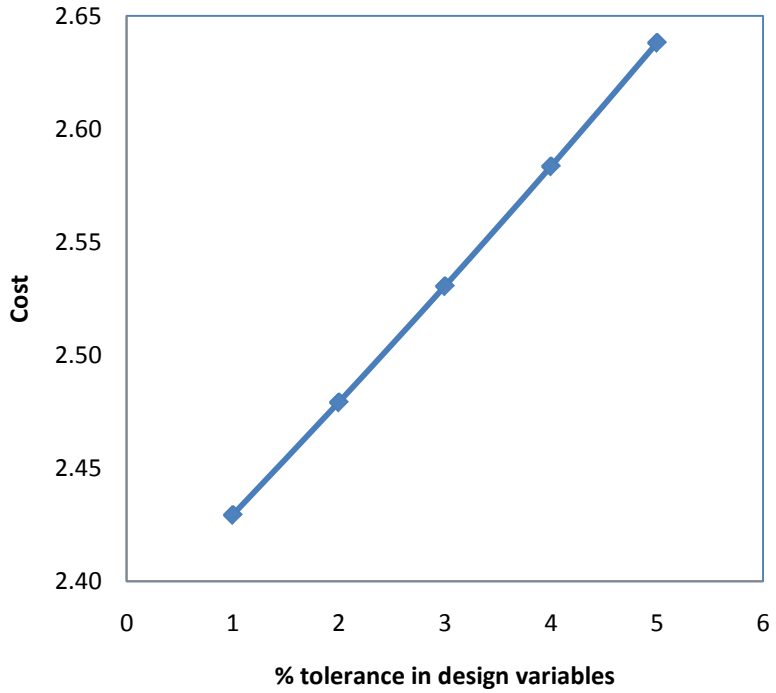

(a)

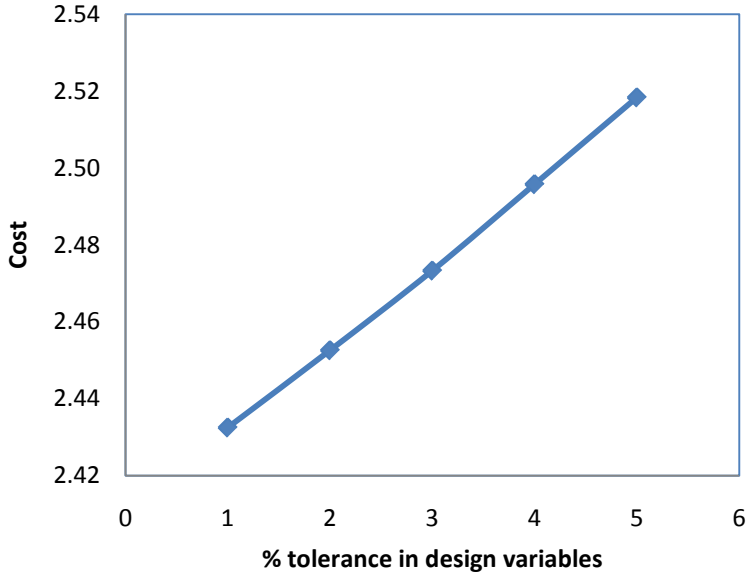

(b)

Figure 8.1 Variation of cost vs percentage tolerance on design variables for cases (a) and (b)

8.2.3 Design of a 25-bar truss

The 25-bar truss as described in section 7.6.4 of chapter 7 is considered with the exception that the maximization of belief is considered along with other three objective functions in the optimization problem. Thus, the truss is designed to minimize (i) the weight, (ii) sum of deflections of node 1 under the two load conditions, (iii) negative of the fundamental natural frequency of the truss and (iv) belief for safety design, subject to stress and buckling constraints.

The objectives of the multi-objective optimization problem of the 25-bar truss are stated as follows

$$f_1(\vec{X}) = 9.8125 \sum_{i=1}^{25} \rho A_i l_i \tag{8.1}$$

$$f_2(\vec{X}) = \sum_{p=1}^{2} (\delta_{xp}^2 + \delta_{yp}^2 + \delta_{zp}^2)^{1/2} \tag{8.2}$$

$$f_3(\vec{X}) = -\omega_n \tag{8.3}$$

$$f_4 = -Belief \ \ for \, the \, safe \, design \tag{8.4}$$

where i is the element or bar number, δ_{xp}, δ_{yp} and δ_{zp} are the x, y and z components of displacement of node 1 under load condition p (p = 1, 2), and ω_n is the fundamental natural frequency of vibration of the truss. The constraints are:

$$\left|\sigma_{ip}(\vec{X})\right| \le \sigma_{\max}, \ i = 1, 2, \ldots, 25, \ \ p = 1, 2 \tag{8.5}$$

$$-\sigma_{ip}(\vec{X}) \le -\sigma_{bp}, \ i = 1, 2, \ldots, 25, \ \ p = 1, 2 \tag{8.6}$$

where $\sigma_{ip}(\vec{X})$ is the stress in element i in load condition p.

The data are taken as: Young's modulus of elasticity, $E = 6.9 \times 10^{10}\, pa$, material density, $\rho = 2770\, kg/m^3$ and allowable maximum stress limit, $\sigma_{\max} = 2.76 \times 10^8\, Pa$. The lower and upper bounds for the variables c_1, c_2, and c_3 used in the supercriterion of MGT are taken as 0.1 and 0.7, respectively. These values have been suggested for cooperative game theory used in the literature. The information for each of the uncertain parameters is assumed to be available in the form of percentage tolerance on the parameters. We assume equal evidence for positive and negative tolerances on these parameters. Belief is calculated for safe design (satisfying all constraints) using vertex method as described in sections 5.2 and 5.3 with ±1% tolerance on the design parameters is assumed in both cases. There are no active constraints nor close to the active constraints found for all the optimum solutions of the uncertainty cases in the Tables 8.2, 8.3 and 8.4. The optimum solutions for the uncertainty cases are greater for minimization problems and smaller for maximization problems than the corresponding optimum solutions for the deterministic cases. This is the reason for no active constraints for the optimum solutions for the uncertainty cases.

8.2.3.1 Solution with continuous design variables:

The matlab code uses the PSO parameters: population size = 24, $i_{\max}$= 2000, $c_1 = c_2 =$ 2, iw_{max}= 0.9, iw_{min}= 0.4, $\vec{V}_{i\min} = 0.01 \text{and} \vec{V}_{i\max} = 0.3$ for all i, and stopping convergence criteria = 1e-8 for over 150 continuous iterations in the algorithm. The optimal solution is given in Table 8.2 and the results are compared with those available in the literature in Table 8.4.

Table 8.2 Optimal solution of twenty bar truss with continuous variables

Quantity	Min. of f1	Min. of f2	Min. of f3	Max. of f1	Max. of f2	Max. of f3	Multi-objective
D-1	0.04	0.32	0.04	0.32	0.243183	0.3068	0.04
D-2	0.13	0.32	0.1282	0.32	0.130186	0.32	0.1499
D-3	0.1256	0.32	0.1266	0.32	0.123353	0.32	0.1499
D-4	0.04	0.32	0.152	0.32	0.309489	0.04	0.12
D-5	0.0532	0.32	0.04	0.32	0.076901	0.32	0.0401
D-6	0.1096	0.32	0.32	0.32	0.109956	0.1577	0.2
D-7	0.1437	0.32	0.2463	0.32	0.141700	0.32	0.2078
D-8	0.1302	0.32	0.32	0.32	0.128059	0.0978	0.32
Objective function value	1054.123	0.007925	-113.744	7269.9078	0.049019	-26.49427	2979.8 0.0255 -105.997

8.2.3.2 Solution with mixed discrete design variables:

The 25-bar truss problem is considered as a mixed discrete uncertain multi-objective optimization problem. The design variables (D-1 to D-4) are assumed to be discrete with lower and upper bounds as D = 40 mm and D = 320 mm, respectively, and are permitted to take values only in increments of 10 mm within the range. Thus, the permissible values of each of the four design variables are given by 40 mm, 50 mm, 60 mm, 70 mm, …, 310 mm and 320 mm. The design variables (D-5 to D-8) are assumed to be continuous variables. The lower and upper bounds for these continuous variables remain same as in the case of continuous variable problem. The modified PSO with CDA is used to solve this mixed discrete design optimization problem. The matlab code uses the PSO parameters: population size = 10, i_{max} = 800, $c_1 = c_2 = 2$, iw_{max} = 0.9, iw_{min} = 0.3, $\vec{V}_{i\min} = 0.01$ and $\vec{V}_{i\max} = 0.2$ for all i, stopping convergence criterion (in terms of change in the objective function value) = $1e-8$ for over 200 continuous iterations. The results of optimization are shown in Table 8.3 and are compared with those available in the literature in Table 8.4. In all these cases, the maximum belief for the safe design is found to be 1. With increase in uncertain parameters, we observe the objective function values are increased as indicated from Tables 8.2 and 8.3. This increase for 25-bar truss is more dominant when compared to welded beam problem due to more number of constraints in case of 25-bar truss problem. The multi-objective solution for uncertain optimization using modified game theory indicated in Table 8.4 is compared with latest available results from literature. We observe that relative importance to f_1 in our optimum solution is high compared to other reported solutions.

Table 8.3 Optimal solution of twenty bar truss with mixed discrete variables

Quantity	Min. of f1	Min. of f2	Min. of f3	Max. of f1	Max. of f2	Max. of f3	Multi-objective
D-1	0.04	0.32	0.06	0.32	0.23	0.32	0.05
D-2	0.14	0.32	0.14	0.32	0.13	0.32	0.15
D-3	0.13	0.32	0.13	0.32	0.13	0.32	0.15
D-4	0.05	0.32	0.05	0.32	0.16	0.04	0.06
D-5	0.0616	0.32	0.0589	0.32	0.04898	0.32000	0.0791
D-6	0.1239	0.32	0.1468	0.32	0.10976	0.10811	0.1245
D-7	0.1440	0.32	0.1748	0.32	0.14183	0.32000	0.1971
D-8	0.1379	0.32	0.1486	0.32	0.12879	0.09808	0.1500
Objective function value	1177.5	0.007925	-77.2603	7269.9078	0.047364	-25.47221	1597.819 0.0333 -72.0487

Table 8.4 Comparison of optimal solutions of 25 bar truss

Quantity	Sunar [197]	optimal solution (continuous) Kiran and Rao [107]	optimal (mixed discrete) Kiran and Rao [107]	Present solution (continuous)	Present solution (mixed discrete)
C_1	-	0.1	0.1	0.1	0.2209
C_2	-	0.1	0.1	0.1	0.2411
C_3	-	-	-	0.1	0.3022
$f_1(\vec{X})$	3033.65	2981.4416	3005.9747	2979.8	1597.819
$f_2(\vec{X})$	0.0232	0.0239586	0.0239842	0.0255	0.0333
$f_3(\vec{X})$	-103.141	-104.3978	-104.6054	-105.997	-72.0487

8.2.4 Design of a composite simply supported beam

Design the composite laminate to minimize the weight and maximize the critical buckling load of the simply supported beam with center load, as shown in Figure 8.2. The composite is E-Glass/epoxy laminate. The laminate is symmetrical and consists of 8 layers with fiber orientations at $[90/45/-45/0]_s$.

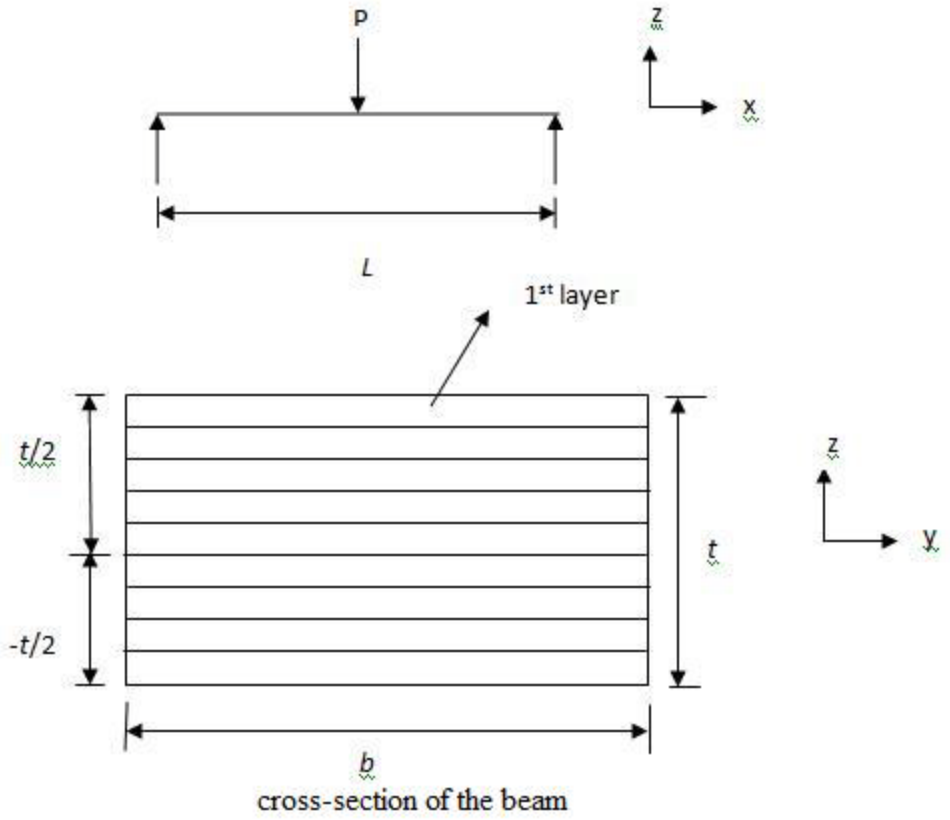

Figure 8.2 Simply supported composite beam with cross-section shown separately

The longitudinal modulus in the fiber direction can be predicted by using the rule of mixtures (ROM) as

$$E_1 = E_f V_f + E_m(1 - V_f) \tag{8.7}$$

The transverse modulus as predicted by inverse ROM formula is given by

$$\frac{1}{E_2} = \frac{V_m}{E_m} + \frac{V_f}{E_f} \tag{8.8}$$

The mechanics of materials approach leads to ROM equation for the in-plane Poisson ratio and is given by

$$v_{12} = v_f V_f + v_m V_m \tag{8.9}$$

Inplane shear modulus as given by inverse ROM equation is

$$\frac{1}{G_{12}} = \frac{V_m}{G_m} + \frac{V_f}{G_f} \tag{8.10}$$

The interlaminar shear modulus can be computed with the semiempirical stress-partitioning parameter (SPP) technique as [14]:

$$G_{23} = G_m \left[\frac{V_f + \eta_{23}(1 - V_f)}{\eta_{23}(1 - V_f) + V_f G_m / G_f} \right] \tag{8.11}$$

$$\eta_{23} = \frac{3 - 4v_m + G_m / G_f}{4(1 - v_m)} \tag{8.12}$$

$$G_{13} = G_{12} \tag{8.13}$$

We have formulated two cases for the optimization problem of the composite simply supported beam.

Case 1: Deterministic optimization problem

Find *t* (thickness of the beam) such that

$$\text{Maximize } f_1(\vec{X}) = \frac{\pi^2}{12}\left(\frac{E_{bxx} t^3}{L^2} \right) = \text{buckling load} \tag{8.14}$$

$$\text{Minimize } f_2(\vec{X}) = \rho_c \, L \, b \, t = \text{weight of the composite} \tag{8.15}$$

where ρ_c is the density of composite material and subject to

$$w_{max} - 0.005 \leq 0, \sigma_{1t} - F_{1t}/FS \leq 0, \; \sigma_{2t} - F_{2t}/FS \leq 0, \; \sigma_6 - F_6/FS \leq 0,$$
$$\sigma_{1c} - F_{1c}/FS \leq 0, \text{and } \; \sigma_{2c} - F_{2c}/FS \leq 0 \tag{8.16}$$

Normalizing the constraints given by equation (8.16) as

$$\frac{w_{max}}{0.005} - 1 \leq 0, \sigma_{1t}\frac{FS}{F_{1t}} - 1 \leq 0,\ \sigma_{2t}\frac{FS}{F_{2t}} - 1 \leq 0,\ \ \sigma_6\frac{FS}{F_6} - 1 \leq 0, \qquad \sigma_{1c}\frac{FS}{F_{1c}} - 1 \leq 0, \text{ and}$$

$$\sigma_{2c}\frac{FS}{F_{2c}} - 1 \leq 0 \tag{8.17}$$

Case 2: Uncertain optimization problem here the problem is formulated with the addition of 3rd objective given by

$$f_3 = -Belief\ for\ the\ safe\ design$$

with the same constraints as stated in the deterministic optimization problem.

The following are the material properties of the fiber and matrix for the composite material:

Young's modulus of fiber E_f = 72.3 *GPa*, Young's modulus of matrix E_m = 5.05 *GPa*, fiber volume fraction V_f = 0.6, Possion's ratio of fiber ν_f = 0.22, Possion's ratio of matrix ν_m = 0.35, and density ρ_c= 2.076 x10^3 kg/m^3.

The strength values are known per unit ply thickness (t = 0.001 m):

Longitudinal tensile strength F_{1t} = 1020 *MPa*, transverse tensile strength F_{2t} = 40 *MPa*, inplane shear strength F_6 = 60 *MPa*, longitudinal compressive strength F_{1c} = 620 *MPa*, and transverse compressive strength F_{2c} = 140 *MPa*. The factor of safety, FS, is assumed as 3.5. The weight of the composite, W_c, is given by

$W_c = \rho_c V_c$ where ρ_c = density of composite and V_c= volume of the composite.

In addition, P = 500 N, L = 1 m and all layers have equal thickness. Using laminate theory, we design the laminate so that the stresses in the layers are within the maximum strength limits divided by the factor of safety and maximum deflection of the beam is less

than 0.005 m. Assume the width to be equal to two times the thickness of the beam. We assume strength values of the lamina to vary linearly with the number of layers (the thickness of each layer). The critical buckling load for the beam is calculated using the formula given in the Table B.2. In the optimization problems, we are interested to find the dimensions of the beam to maximize the load carrying capacity without buckling in the axial direction. The maximum deflection for the beam is calculated using the formula given for the point load in the Table B.1. The stresses developed in the beam are calculated using the procedure described in Appendix-B. The calculation of $[\bar{Q}]$ for the each layer with fiber orientation angle θ is done using equation B.11. The bending stiffness matrix [D] is calculated by using equation B.25. The longitudinal, transverse and inplane shear stresses are calculated using the value of k = 8 in equations B.28, B.29 and B.30. The matlab built-in optimization function fmincon( ) is used to solve the single objective optimization problems. We have used laminate theory, described in Appendix-B, to find maximum deflection and stress induced in the composite laminate. The optimal solutions for single objective optimization for Case 1 (deterministic) are obtained as given in Table 8.5. The constraints as stated by equation 8.17 for the single optimization problem solution t = 0.012068 are -0.0002,-0.9987,-0.9861, -0.9918,-0.9978 and -0.9960. The first constraint, as stated by equation 8.17, is only the active constraint for the optimum solution t = 0.012067 in Table 8.5. There is no active constraint for all other optimum solutions in Table 8.5. Thus, we obtained the range for both buckling load and weight of the composite from single objective optimizations as given in Table 8.5. For Case 1, the optimum solution using modified game theory with modified PSO is obtained as given in Table 8.6. In Case 2, we have taken all the material properties (E_1, E_2, ν_f

and ν_m), load, P , and the thickness (t) of beam. The matlab code uses the PSO parameters: population size = 12, $i_{\max}$= 800, $c_1 = c_2$ = 2, iw_{max}= 0.9, iw_{min}= 0.4, $\vec{V}_{i\min} = 0.001$ and $\vec{V}_{i\max} = 0.05$ for all i, and stopping convergence criteria = 1e-8 for over 350 continuous iterations in the algorithm. The optimum solutions with six uncertain parameters with ±5% tolerance as given in Table 8.6 are obtained. We found that the optimum solution obtained for uncertain optimization gives lower value for weight of the composite where as deterministic optimization gives larger value of critical buckling load of the beam. The optimum solutions for the multi-objective optimization problems with seven uncertain parameters with ±3%, ±4%, and ±5%, tolerances respectively, using the modified game theory are obtained as given in Table 8.7. The modified game theory gives different solutions from the pareto-optimal solutions with difference in the importance of one objective function over other as obtained in Table 8.7.

Table 8.5 Comparison of optimal solutions of single objective composite beam

Quantity	Design Variable t	Function value	No. of function evaluations
f_1 *maximization*	0.1	11700 kN	8
f_1 *minimization*	0.0120686	20.561 kN	49
f_2 *minimization*	0.0120676	0.604647 kg	40
f_2 *maximization*	0.1	41.52 kg	8

Table 8.6 Comparison of optimal solutions of composite beam

Quantity	Present solution for case 1	Present solution for case 2
$x_1 = t$ in m	0.063894	0.019256
C_1	0.7	0.7
C_2	0.3	0.2
C_3	N/A	0.1
$f_1(\vec{X})$ in kN	3051.94	84.0462
$f_2(\vec{X})$ in kg	16.9504	1.5457
$f_3(\vec{X})$	N/A	1
$\frac{w_{max}}{0.005} - 1$	-0.9932	-0.75386
$\sigma_{1t}\frac{FS}{F_{1t}} - 1$	-0.9999	-0.99967
$\sigma_{2t}\frac{FS}{F_{2t}} - 1$	-0.9999	-0.99657
$\sigma_6\frac{FS}{F_6} - 1$	-0.9999	-0.99797
$\sigma_{1c}\frac{FS}{F_{1c}} - 1$	-0.9999	-0.99947
$\sigma_{2c}\frac{FS}{F_{2c}} - 1$	-0.9999	-0.99902

Table 8.7 Comparison of optimal solutions of uncertain composite beam

Quantity	±3% tolerance	±4% tolerance	±5% tolerance
$x_1 = t$ in m	0.048646	0.0201833	0.019256
C_1	0.56110	0.7	0.7
C_2	0.33874	0.199999	0.2
C_3	0.10016	0.09999	0.1
$f_1(\vec{X})$ in kN	1346.93	96.198	84.0462
$f_2(\vec{X})$ in kg	9.8256	1.6913	1.5457
$f_3(\vec{X})$	1	1	1
$\frac{w_{max}}{0.005} - 1$	-0.98473	-0.78625	-0.75386
$\sigma_{1t}\frac{FS}{F_{1t}} - 1$	-0.99998	-0.99972	-0.99967
$\sigma_{2t}\frac{FS}{F_{2t}} - 1$	-0.99978	-0.99703	-0.99657
$\sigma_6\frac{FS}{F_6} - 1$	0.99987	0.99824	-0.99797
$\sigma_{1c}\frac{FS}{F_{1c}} - 1$	-0.99996	-0.99954	-0.99947
$\sigma_{2c}\frac{FS}{F_{2c}} - 1$	-0.99993	-0.99915	-0.99902

This composite simply supported beam is solved again with assuming equal thickness (t_1) for the layers with the fiber orientations 0 and 90 degrees and equal thickness (t_2) for the layers with the fiber orientations -45 and 45 degrees. The same optimization problems

are again solved with two design variables t_1 and t_2 for both cases namely deterministic case and uncertainty case. The bounds on these design variables is [0.001,0.015].

The optimal solutions for single objective optimization for Case 1 (deterministic) are obtained as given in Table 8.8. The constraints as stated by equation 8.16 for the single optimization problem solution t_1 = 0.015, t_2 = 0.015 are -0.9989, -0.9999, 0.9999,-0.9999, -0.9999 and -0.9999. The constraints as stated by equation 8.16 for the single optimization problem solution t_1 = 0.002, t_2 = 0.001 are 0, -0.9984, -0.9857, -0.9923, -0.9974 and -0.9952. The constraints as stated by equation 8.16 for the single optimization problem solution t_1 = 0.001, t_2 = 0.002 are 0, -0.9986, -0.9791, -0.9914, -0.9978 and -0.9940.

Table 8.8 Comparison of optimal solutions of single objective composite beam

Quantity	Design Variables	Function value	No. of function evaluations
f_1 maximization	t_1 =0.015 t_2 =0.015	20217.80 kN	11
f_1 minimization	t_1 =0.0010 t_2 =0.00202	20.561 kN	51
f_2 minimization	t_1 =0.002007 t_2 =0.00100	0.60092 kg	41
f_2 maximization	t_1 =0.015 t_2 =0.015	59.788 kg	11

For Case 1, the optimum solution using modified game theory with modified PSO is obtained as given in Table 8.9. In Case 2, we have taken all the material properties (E_1, E_2, ν_f and ν_m), load, P , and the thickness (t_1 and t_2) of the layers. The matlab code uses the PSO parameters: population size = 12, $i_{\max}$= 800, $c_1 = c_2 = 2$, iw_{max}= 0.9, iw_{min}= 0.4, $\vec{V}_{i\min} = 0.001 \text{and} \vec{V}_{i\max} = 0.05$ for all i, and stopping convergence criteria = 1e-8 for over 350 continuous iterations in the algorithm. The optimum solutions with seven uncertain parameters with ±5% tolerance as given in Table 8.8 are obtained. We observe as the no. of objective functions increase from two to three and with uncertainty tolerance on the parameters, there is considerable shift in the constants C_1, C_2 and C_3 in the optimum solution when compared to the deterministic solution. The results obtained in Table 8.9 followed the same trend as the results obtained in the Table 8.6. In both cases, the optimum solutions obtained for uncertainty problems minimize more weight to the composite but compromise on achieving maximum buckling load on the beam. There are no active constraints nor close to the active constraints found for all the optimum solutions in the Table 8.9.

Table 8.9 Comparison of optimal solutions of composite beam

Quantity	Present solution for case 1	Present solution for case 2
$x_1 = t_1$ in m	0.01178	0.00352
$x_1 = t_2$ in m	0.015	0.00230
C_1	0.1	0.7
C_2	0.9	0.19998
C_3	N/A	0.10002
$f_1(\vec{X})$ in kN	14367	149.06
$f_2(\vec{X})$ in kg	47.64	2.2587
$f_3(\vec{X})$	N/A	1

8.3 SUMMARY

This chapter presents algorithms based on modified PSO coupled with vertex method to solve all types of uncertain engineering optimization problems involving multiple objectives with continuous, discrete and/or mixed design variables with constraints. When convergence difficulties are experienced with the original PSO algorithm by using a constant value of the maximum velocity limit, the dynamic velocity function approach is found to speed up the convergence. The bounce method provides significant improvement in the performance of the algorithms to overcome stagnation of the population. When the MGT, combined with the modified PSO and vertex method, is used to solve uncertain multi-objective optimization problems; the best compromise

(optimal) solution from the pareto-optimal front has been found efficiently. The results of the 25-bar truss multi-objective optimization problem illustrate the effectiveness and efficiency of the new approach when all the objective functions are not totally conflicting. The results obtained for the 25-bar truss with all design variables taken as continuous or as mixed discrete are found to be comparable to one another. A novel attempt is made to formulate and design a simply supported composite beam optimization problem with uncertain parameters. These results are indicative of the power to solve the uncertain engineering problems using the proposed method. In the next chapter, a comparison of various warranty policies for both repairable and non-repairable products with different failure distributions and the formulation of an automobile warranty optimization problem are considered.

CHAPTER 9

WARRANTY COST OPTIMIZATION FOR AN AUTOMOBILE USING PARTICLE SWARM OPTIMIZATION

9.1 OVERVIEW

Different non-renewing warranty policies including the free replacement warranty (FRW) policy, pro-rated warranty (PRW) policy, and combined FRW/PRW policy, are considered in the context of automobile warranty problems in section 9.2. All these warranty policies are non-renewing type. In addition a procedure is described to find the total warranty cost from manufacturer's view point for all types of policies using two types of failure distributions, namely the exponential and Weibull distributions for each warranty policy in section 9.2. A comparison of different warranty policies for both repairable and non repairable products is considered in sections 9.3. The optimization problems are solved using a modified particle swarm optimization (PSO) when both continuous and discrete design variables are involved. For the discrete optimization problem, a closest discrete approach (CDA) to handle discrete design variables, in conjunction with the modified PSO is used. The continuous and discrete optimization problems are solved for the two failures distributions-exponential and Weibull-for the failure of subsystems. A general automobile warranty problem, close to reality, is formulated and the total warranty cost is minimized with a constraint on the total failure

probability of the system in section 9.4. In section 9.5, a sensitivity analysis is conducted by varying the constraint on the total failure probability of the system followed by a discussion in section 9.6. This chapter is concluded by a summary in the last section.

9.2 WARRANTY POLICIES

For the different warranty policies discussed in chapter 3 for both 1-dimensional and 2-dimensional warranties, the procedure to find the total expected warranty cost is discussed.

9.2.1 One-dimensional warranty policies

In the one-dimensional warranty policies [16,20,46,82,91,155,157,158], two simple policies, namely Free Replacement Warranty (FRW) and Pro-Rated Warranty (PRW), a combination policy, namely FRW/PRW, and a procedure to find the expected warranty cost from the manufacturer's view point for two failure distributions (exponential and Weibull) are considered.

9.2.1.1 Policy-1: Free Replacement Warranty (FRW) Policy [25, 28]

The manufacturer agrees to repair or provide replacement for the failed items free of charge up to a time W from the time of initial purchase. This is a non-renewing and one-dimensional warranty policy applicable for both non-repairable and repairable products.

Case-1: Non- repairable products **[24, 26]**

i) If there is only one failure in the warranty period then the expected total unit cost to the manufacturer, $E[c_s(W)]$, is given by

$$E[c_s(W)\,] \cong c_s[1 + F(W)] \tag{9.1}$$

where c_s is the manufacturer's or supplier's cost and *F(W)* is the failure distribution *F(t)* when $t = W$.

ii) If there are multiple failures within the warranty period,

let *N(W)* be equal to the number of replacements in the interval [0,*W*]. The expected value of *N(W)* is given by *E[N(W)]= M(W)*, where *M(•)* is the ordinary renewal function [29, 68] associated with the distribution function *F(•)*. The expected total unit cost to the manufacturer, $E[c_s(W)]$, is given by

$$E[c_s(W)] = c_s[1 + N(W)] = c_s[1 + M(W)] \tag{9.2}$$

For exponential failure time distribution,

$$F(t) = 1 - e^{-\lambda t} \qquad (t \geq 0 \text{ and } \lambda > 0) \tag{9.3}$$

with the mean, the mean failure time, μ, given by

$$\mu = 1/\lambda \tag{9.4}$$

where λ is a constant and θ, in equation (3.38), is given by $\theta = \{\lambda\}$. The renewal function associated with the distribution function of equation (9.3) is given by [29]

$$M(t) = \lambda t \tag{9.5}$$

For Weibull distribution, the failure time distribution is given by

$$F(t) = 1 - e^{-(\lambda t)^{\beta}} \qquad (t \geq 0,\ \lambda > 0 \text{ and } \beta > 0) \tag{9.6}$$

where β is the shape parameter of the distribution and θ, in equation (3.38), is given by $\theta = \{\lambda, \beta\}$ and the mean is given by

$$\mu = \frac{1}{\lambda}\Gamma\left(1 + \frac{1}{\beta}\right) \tag{9.7}$$

where Γ is the gamma function. There is no analytical solution available for the renewal function associated with the distribution function of equation (9.6). The approximate solution for $M(t)$, for large values of t, is given by [19,29]

$$M(t) \cong \frac{t}{\mu} + \frac{\sigma^2}{2\mu^2} - \frac{1}{2} \tag{9.8}$$

where σ^2 is the variance given by

$$\sigma^2 = \frac{1}{\lambda^2}\left[\Gamma\left(1+\frac{2}{\beta}\right) - \left\{\Gamma\left(1+\frac{1}{\beta}\right)\right\}^2\right] \tag{9.9}$$

Series approximation

Leadbetter [122] has proposed a series expansion for *M(t)* in terms of t^β. We assume the scale factor of the Weibull distribution, α, to be equal to 1. If *F(t)* can be expanded into an infinite series as

$$F(t) = 1 - e^{-t^\beta} = \sum_{r=1}^{\infty} \frac{(-1)^{r-1}}{\Gamma(1+\beta r)} C_r (t^\beta)^r \tag{9.10}$$

with the coefficient C_r given by

$$C_r = \frac{\Gamma(1+\beta r)}{r!} \tag{9.11}$$

Then the renewal function, *M(t)*, associated with the distribution function represented by equation of (9.10), can be represented by the infinite series

$$M(t) = \sum_{r=1}^{\infty} \frac{(-1)^{r-1}}{\Gamma(1+\beta r)} A_r (t^\beta)^r \tag{9.12}$$

where the coefficients A_r are given by

$$A_1 = C_1 \tag{9.13}$$

$$A_j = C_j - \sum_{r=1}^{\infty} A_r C_{j-r} \text{ for } j > 1 \tag{9.14}$$

For $t < 1$, we obtain an approximation for *M(t)* as

$$M(t) \cong \sum_{r=1}^{k} \frac{(-1)^{r-1}}{\Gamma(1+\beta r)} A_r (t^\beta)^r \tag{9.15}$$

where k is some finite value and the accuracy of $M(t)$ depends on the value of k used. In order to obtain values of the renewal function for other values of the scale factor, α, we use the relationship $M(t\ ;\ \alpha) = M(t/\alpha\ ;\ 1)$. The series approximation used for the renewal function given by equations (9.12) to (9.15) is incorporated into a matlab program to compute the desired values of $M(t)$ for the automobile warranty problem considered in this work.

Case-2: Repairable products

i) When repair is as "good as new":

The cost to the manufacturer of replacing a single repairable product is given by

$$c_s(W) = c_s + c_r N_r(W) \tag{9.16}$$

where c_r is the expected cost of supplying the repaired product and $N_r(W)$ is the number of repairs required in $[0,\ W)$. The expected total unit cost to the manufacturer, $E[c_s(W)]$, is given by [28]

$$E[c_s(W)] = c_s + c_r M(W) \tag{9.17}$$

where $M(W)$ is the renewal function. The renewal function is defined as $M(W) = \sum_{r=1}^{\infty} N_r(W)$.

ii) When repair is not perfect, i.e., products are not as good as new:

Let the original product have a lifetime X_1 with distribution $F(\bullet)$ and the repaired items have lifetimes $X_2, X_3, \ldots\ldots$ identically distributed with distribution $G(\bullet)$. The delayed renewal function (see equation 9.20), $M_d(t)$, is given by [122]

$$M_d(t) = F(t) + \int_0^t M_G(t-x) f(x)\, dx \tag{9.18}$$

where $M_G(\bullet)$ is the ordinary renewal function corresponding to G. The expected total unit cost to the manufacturer is given by

$$E[c_s(W)] = c_s + c_r M_d(W) \tag{9.19}$$

For example, if the failure distribution is exponential, then the delayed renewal function is obtained as follows. Let the new and repaired items have exponentially distributed lifetimes with respective parameters λ_1 and λ_2 (with $\lambda_1 < \lambda_2$). Then

$$M_d(t) = 1 - e^{-\lambda_1 t} + \int_0^t \lambda_2(t-x)\lambda_1 e^{-\lambda_1 x}\, dx \tag{9.20}$$

$$= \lambda_2 t - \frac{(\lambda_2 - \lambda_1)}{\lambda_1}(1 - e^{-\lambda_1 t}) \tag{9.21}$$

iii) When minimal repair as "good as old":

For each item sold, failures over the warranty period occur according to a non-stationary Poisson process with an intensity function, $\lambda(t)$, given by $\lambda(t) = r(t)$ where *r(t)* is the failure rate associated with the failure distribution *F(t).* The expected number of times the product is returned for repairs over the warranty period, $E[N(W)]$, is given by

$$E[N(W)] = \int_0^W r(t)dt \tag{9.22}$$

If the average repair cost is equal to c_r, then the expected repair cost to service the warranty is given by

$$E[c_r(W)] = c_r E[N(W)] \tag{9.23}$$

Using equation (9.22), equation (9.23), can be expressed as

$$E[c_r(W)] = c_r \int_0^W r(t)dt \tag{9.24}$$

If the failure time distribution is Weibull with parameters β and λ, then the failure rate is given by

$$r(t) = \beta\lambda(\lambda t)^{\beta-1} \tag{9.25}$$

Equations (9.24) and (9.25) yield

$$E[c_r(W)] = c_r\,(\lambda W)^{\beta} \tag{9.26}$$

If the seller's cost is not constant, but is a function of time, $c_s = c_s(t)$, then the renewal function can be obtained as [27]

$$M^*(W) = \int_0^W c_s(t)\, dM(t) \tag{9.27}$$

A standard approach is to express the discounted cost as $c_s(t) = c_s e^{-\delta t}$ where δ is the discount rate. For the exponential distribution, the expected repair cost to service the warranty is given by [28]

$$E[c_r(W)] = \frac{c_r \lambda [1 - e^{-\delta W}]}{\delta} \tag{9.28}$$

The expected total unit cost to the manufacturer, $E[c_s(W)]$, is given by

$$E[c_s(W)] = c_s + E[c_r(W)] \tag{9.29}$$

where $E[c_r(W)]$ is given by equation (9.26) for the Weibull failure distribution model (and exponential failure distribution when $\beta = 1$) and for discounted cost of an exponential distribution as given by equation (9.28).

9.2.1.2 Policy 2: Pro-Rated Warranty (PRW) Policy

The manufacturer agrees to refund a fraction of the purchase price when the product fails before time *W* from the time of the initial purchase. The buyer or customer receives a cash rebate and is not constrained to buy a replacement product. The cash rebate to the customer may be of different types:

Policy 2a: When the refund is a linear function given by

$$q_1 = \begin{cases} \left(1 - \frac{t}{W}\right) c_b, & 0 \le t < W \\ 0, & \text{otherwise} \end{cases} \tag{9.30}$$

where c_b is the purchase price of the product.

Policy 2b: When the refund is a proportional linear function given by

$$q_2 = \begin{cases} \propto \left(1 - \frac{t}{W}\right) c_b, & 0 \le t < W \\ 0, & \text{otherwise} \end{cases} \tag{9.31}$$

where $0 < \propto < 1$.

Policy 2c: The refund is a quadratic function given by

$$q_3 = \begin{cases} \left(1 - \frac{t}{W}\right)^2 c_b, & 0 \le t < W \\ 0, & \text{otherwise} \end{cases} \tag{9.32}$$

Out of all the above forms, the most common type of PRW is policy 2a. The total expected warranty cost from the manufacturer's view point for this policy can be computed as follows. The cost to the manufacture of a single product sold under this policy is given by

$$c_s(W) = c_s + q(x_1) \tag{9.33}$$

where c_s is the actual manufacturing cost of the product, q is rebate function and x_1 is the lifetime of the product supplied. The rebate function is linear as given by equation (9.30). The manufacturer's expected cost of the product sold under this policy during the period [*0, W*] is given by

$$E[c_s(W)] = c_s + \int_0^W q(t)\, dF(t) \tag{9.34}$$

Substituting equation (9.30) and *F(0)* = 0 into equation (9.34) and simplifying, we obtain the manufacturer's expected warranty cost of the product as

$$E[c_s(W)] = c_s + c_b[F(W) - \frac{\mu_W}{W}] \tag{9.35}$$

where

$$\mu_W = \int_0^W t\, dF(t), \tag{9.36}$$

c_s is the manufacturer's cost and c_b is the buyer's cost. From manufacturer's view point, the average profit per unit $= c_b - E[c_s(W)]$. Using equation (9.35), we obtain

Average profit per unit $= c_b\left(1 - F(W) + \frac{\mu_W}{W}\right) - c_s$ (9.37)

where $c_b\left(1 - F(W) + \frac{\mu_W}{W}\right)$ is the expected cost to the customer/consumer and c_s is the supplier's cost.

For exponential model, the failure distribution is given by

$F(t) = 1 - e^{-\lambda t} \qquad t \geq 0$ (9.38)

Substituting equation (9.38) in equation (9.36), we obtain

$\mu_W = \frac{1}{\lambda}[1 + (1 + \lambda W)e^{-\lambda W}]$ (9.39)

The expected warranty cost of the product is obtained by substituting equation (9.39) in equation (9.35) as

$E[c_s(w)] = c_s + c_b[1 - \frac{(1-e^{-\lambda W})}{\lambda W}]$ (9.40)

For Weibull model with $\beta = 2$, the failure distribution is given by

$F(t) = 1 - e^{-(\lambda t)^2} \qquad t \geq 0$ (9.41)

Substituting equation (9.41) into equation (9.36), we obtain

$\mu_W = We^{-(\lambda W)^2} - \frac{\sqrt{\pi}}{2\lambda}\text{erf}\,(\lambda W)$ (9.42)

Using equations (9.42) and (9.35), the expected warranty cost of the product can be found as

$E[c_s(W)] = c_s + c_b[1 - 2e^{-(\lambda W)^2} + \frac{\sqrt{\pi}}{2\lambda W} erf\ (\lambda W)]$ (9.43)

where *erf* is called the error function. The error function is defined as

$erf(\lambda W) = \frac{2}{\sqrt{\pi}}\int_0^{\lambda W} e^{-u^2}\, du$

9.2.1.3 Policy-3: Combined Free Replacement Warranty/Pro-Rated Warranty (FRW/PRW) policy

Under this policy, the manufacturer agrees to provide a free replacement of the original product up to time W_1 from the time of initial purchase and any failure in the interval from W_1 *to* W $(> W_1)$ results in a pro-rate refund. The warranty does not renew. From the manufacturer's view point, the rebate function as per the policy is represented as

$$q(t) = \begin{cases} c_s, & 0 \le t < W_1 \\ c_b(W-t)/(W-W_1), & W_1 \le t < W \\ 0, & otherwise \end{cases} \tag{9.44}$$

where c_b is the purchase or buyer's price of the product. The expected rebate over the warranty period $[0,W)$ is given by

$$E[q(t)] = \int_0^W q(t)\, dF(t)$$

$$= \int_0^{W_1} q(t)\, dF(t) + \int_{W_1}^{W} q(t)\, dF(t) \tag{9.45}$$

Substituting equation (9.44) in equation (9.45), we obtain

$$E[q(x)] = \mathrm{c_s} \int_0^{W_1} f(x)dx + \mathrm{c_b} \int_{W_1}^{W} \frac{(W-x)}{(W-W_1)} f(x)dx \tag{9.46}$$

which can be simplified as

$$E[q(x)] = c_s F(W_1) + \frac{c_b}{W-W_1}\left\{W\big(F(W) - F(W_1)\big) - \mu_W + \mu_{W_1}\right\} \tag{9.47}$$

The expected warranty cost to the manufacturer/seller is given by

$$E[c_s(W_1, W)] = c_s + E[q(x)] \tag{9.48}$$

Equations (9.47) and (9.48) yield:

$$E[c_s(W_1, W)] = c_s(1 + F(W_1)) + \frac{c_b}{W-W_1}\left\{W\big(F(W) - F(W_1)\big) - \mu_W + \mu_{W_1}\right\} \tag{9.49}$$

For the failure distributions represented by equations (9.38) and (9.41), the expected warranty costs for this policy can be obtained by substituting, respectively, equations (9.39) and (9.42) in equation (9.49).

9.2.2 Two-dimensional warranty policy [One-dimensional approach]

In the two-dimensional warranty policies [48, 50, 136, 137], a simple non renewing policy, namely the Free Replacement Warranty (FRW), is considered. The procedure to find the corresponding expected warranty cost from the manufacturer's view point can be computed as indicated below.

Policy-4: Free Replacement Policy (FRP)

Under this policy the manufacturer agrees to repair or provide a replacement for the failed product free of charge up to a time W or up to a usage U, whichever occurs first, from the time of initial purchase. The warranty region is a rectangle $[0, W) \times [0, U)$ as shown in Figure 9.1. U and W are the parameters of the policy. This policy does not renew. Let $X_c(t)$ and $Y_c(t)$ represent the age and usage of the product at time t, respectively. Let $Y(t)$ represent the total usage over the interval $[0,t)$, with the first sale at $t = 0$. If no product failure has occurred in $[0, t)$, then

$$X_c(t) = t \quad \text{and} \quad Y_c(t) = Y(t) \tag{9.50}$$

This is also true if all the failed items are repaired with their repair times equal to zero. In contrast, if the product is not repairable and if there have been one or more failures in $[0, t)$ then

$$X_c(t) < t \text{ and } Y_c(t) < Y(t) \tag{9.51}$$

In the one-dimensional approach, we model $Y_c(t)$ as a function of $X_c(t)$. This function characterizes the product usage as a function of the age of the product. This relationship is assumed to be linear with a non negative coefficient *R* as:

$$Y_c(t) = R.X_c(t) \tag{9.52}$$

where *R* represents the usage per unit time or usage rate, and may vary from user to user. We can model it as a random variable with density function *g(r)* so that

$$G(r) = P(R \leq r) \tag{9.53}$$

Three different forms of *G(r)* reflecting different usage rates across the population of buyers are given below:

ii) *R* uniformly distributed over [*a, b*], with $0 \leq a \leq b$:

$$g(r) = \begin{cases} \frac{1}{[b-a]}, & for\ \ a \leq r \leq b \\ 0, & otherwise \end{cases} \tag{9.54}$$

iv) $R = a + A[b\text{-}a]$, with $0 \leq a \leq b$, and A is a random variable with a Beta density function:

$$f_A(x) = \frac{dF_A(x)}{dx} = \frac{x^{p-1}(1-x)^{q-1}}{B(p,q)}, \qquad 0 \leq x \leq 1 \tag{9.55}$$

where $B(p, q)$ is the Beta function, p and q are two parameters (positive real numbers). We assume that all the values of *R* are in the interval [*a, b*].

v) *R* distributed according to the Gamma distribution :

$$g(r) = \frac{r^{p-1}\exp(-r)}{\Gamma(p)}, \qquad 0 \leq r < b,\ p > 0 \tag{9.56}$$

$$\Gamma(z) = \int_0^\infty t^{z-1}\, e^{-t} dt$$

We assume that *R* is uniformly distributed as defined by equation (9.54) in this policy.

When the usage rate $R = r$ warranty stops at time X_r or W, if

(iii) $X_r = \frac{U}{r}$ when $r \geq \gamma_1$ (9.57)

(iv) W when $r < \gamma_1$ where $\gamma_1 = U/W$ (9.58)

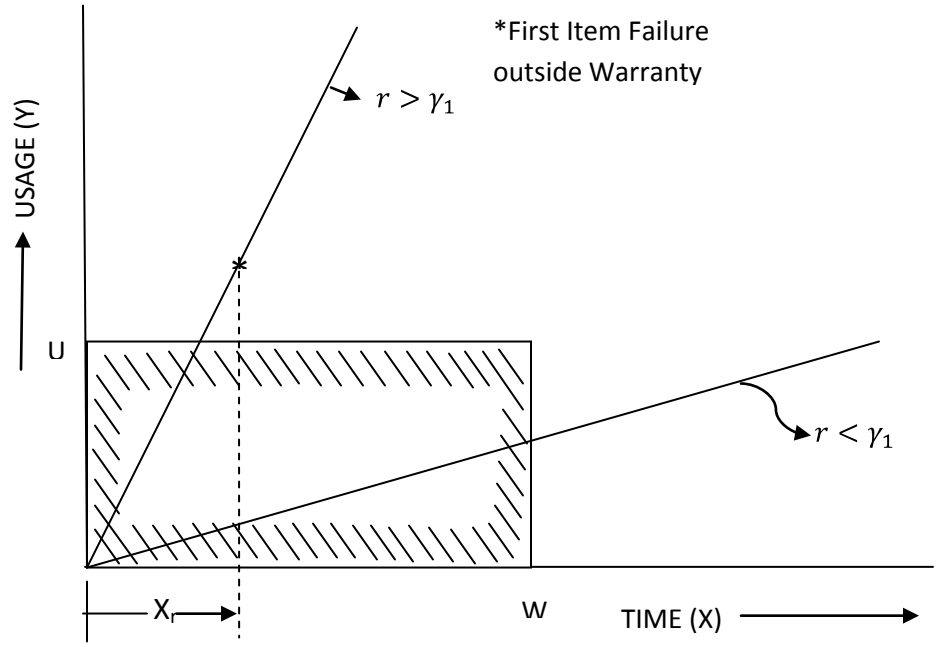

Figure 9.1 Warranty region for policy 4

Repairable products [89]

When a product fails, it is repaired using minimal repair. As a result, when $R = r$, we have

$X_c(t) = t$ and $Y_c(t) = rt$ (9.59)

For repairable products, $\overline{N}\left(\frac{t}{r}\right)$ is assumed to be a non stationary Poisson process with intensity function. We assume a simple linear model for the intensity function, $\lambda\left(\frac{t}{r}\right)$, as

$\lambda\left(\frac{t}{r}\right) = \theta_0 + \theta_1 r + (\theta_2 + \theta_3 r)t$ (9.60)

where $\theta_i \geq 0$ for $0 \leq i \leq 3$.

Let *N*(*W,U*) denote the number of failures under warranty and *N*(*W, U/r*) the number of failures under warranty when *R* = *r*. Then, [28],

$$P\{N(W,U) = n\} = \int_0^\infty P\{N(W,U) = n/r\}\ dG(r) \tag{9.61}$$

Minimal repair, i.e., no change to failure rate after item is repaired is considered. As a result, we have

$$N(W,U/r) = \begin{cases} \overline{N}\left(\frac{W}{r}\right) & if \quad r < \gamma_1 \\ \overline{N}(\left(\frac{U}{r}\right)/r) & if \quad r \geq \gamma_1 \end{cases} \tag{9.62}$$

Since $\overline{N}\left(\frac{t}{r}\right)$ is a non stationary Poisson process with intensity $\lambda\left(\frac{t}{r}\right)$ (given by equation (9.60)), the expected value of *N*(*W, U/r*) is given by

$$E[N(W,U/r)] = \begin{cases} \int_0^W \lambda\left(\frac{t}{r}\right)\ dt & if \quad r < \gamma_1 \\ \int_0^{X_r} \lambda\left(\frac{t}{r}\right)\ dt & if \quad r \geq \gamma_1 \end{cases} \tag{9.63}$$

Using the conditional expectation argument, the expected number of failures over the warranty region is given by

$$E\{N(W,U)\} = E\left\{E[N\left(W,\frac{U}{r}\right)]\right\} \tag{9.64}$$

Using equation (9.63), equation (9.64) can be simplified as

$$E\{N(W,U)\} = \int_0^{\gamma_1}\int_0^W \lambda\left(\frac{t}{r}\right)\ dt\ dG(r) + \int_{\gamma_1}^\infty \lambda\left(\frac{t}{r}\right)\ dt\ dG(r) \tag{9.65}$$

where, *dG(r) = g(r)dr*. We assume R to be uniformly distributed over [*a, b*] as given by equation (9.54) and thus changing the limits of integration in equation (9.65) to a to b and substituting $\lambda\left(\frac{t}{r}\right)$ from equation (9.60), we obtain

$$E\{N(W,U)\} = \int_a^{\gamma_1}\left\{(\theta_0 + \theta_1 r)W + \frac{(\theta_2+\theta_3 r)W^2}{2}\right\} g(r)dr$$

$$+ \int_r^b \{(\theta_0 + \theta_1 r)X_r + (\theta_2 + \theta_3 r){X_r}^2/2\}\, g(r)dr \quad (9.66)$$

Substituting $g(r) = 1/(b\text{-}a)$ and $X_r = U/r$ in equation (9.66), we obtain

$$E\{N(W,U)\} = \frac{1}{(b-a)}\left\{\left(\theta_0 W + \frac{\theta_1 W^2}{2}\right)(\gamma_1 - a) + \left(\theta_2 W + \frac{\theta_3 W^2}{2}\right)\frac{({\gamma_1}^2 - a^2)}{2} + \left(\theta_0 + \frac{\theta_3 U^2}{2}\right) log\left(\frac{b}{\gamma_1}\right) + \theta_1 U(b - \gamma_1) + 0.5\theta_2 U^2 \frac{(b-\gamma_1)}{b\gamma_1}\right\} \quad (9.67)$$

The expected total warranty cost per unit sale is given by

$$E\{C_s(W,U)\} = c_s + c_r E\{N(W,U)\} \quad (9.68)$$

where c_r is the cost of minimal repair.

The marginal density functions of W and U, denoted by $f_1(W)$ and $f_2(U)$, are exponential with means $1/\lambda_1$ and $1/\lambda_2$, respectively, and their corresponding 1-D renewal functions are M_1(W) and M_2(U), respectively and are given by

$$M_1(W) = \lambda_1 W \text{ and } M_2(U) = \lambda_2 U \quad (9.69)$$

Using Laplace transformation and scale change property of 2-D Laplace transform, Kim and Rao [106] derived the relation between M_0 and M_ρ as

$$M_0\left(\frac{W}{1-\rho}, \frac{U}{1-\rho}\right) = \frac{M_\rho(W,U)}{1-\rho} = \frac{E[N(W,U)]}{1-\rho} \quad (9.70)$$

Analogous to the univariate theory, the 2-D renewal function, $M_\rho(W,U) \equiv E[N(W,U)]$ is given by $M_\rho(W,U) = \sum_{n=1}^{\infty} F^{(n)}(W,U)$ (9.71)

where the superscript n represents n-fold convolution and the subscript ρ denotes the correlation coefficient between the random variables W and U.

When ρ =0, Downton (1970) [62] derives the relation for $F^{(n)}(W,U)$, which is given by

$$F^{(n)}(W,U) = P_n(\lambda_1 W).P_n(\lambda_2 U) \quad (9.72)$$

Using Equations (9.71) and (9.72) as derived by Kim and Rao [106], we get

$$M_0\left(\frac{W}{1-\rho},\frac{U}{1-\rho}\right) = \sum_{n=1}^{\infty} P_n\left(\frac{\lambda_1 W}{1-\rho}\right) . P_n\left(\frac{\lambda_2 U}{1-\rho}\right) \quad (9.73)$$

where $P_n(x)$ is the incomplete gamma function and is defined as follows

$$P_n(W) = \int_0^W \frac{v^{n-1}\exp(-v)}{\Gamma(n)}\, dv \quad (9.74)$$

where Γ is called gamma function and is defined as

$$\Gamma(n) = \int_0^{\infty} t^{n-1}e^{-t}\, dt \quad (9.75)$$

Thus, we obtain from the equations (9.70) and (9.73)

$$\frac{E[N(W,U)]}{1-\rho} = \sum_{n=1}^{\infty} P_n\left(\frac{\lambda_1 W}{1-\rho}\right) . P_n\left(\frac{\lambda_2 U}{1-\rho}\right) \quad (9.76)$$

For the optimization problems considered in the paper, we assume $\rho = 0.5$, $n = 15$, and $\lambda_1 = \lambda_2 = \lambda$. Thus, the only unknown will be λ in equation (9.76). Minimizing the least square error function defined as

$$\left\{\frac{E[N(W,U)]}{1-0.5} - \sum_{n=1}^{15} P_n\left(\frac{\lambda W}{1-0.5}\right) . P_n\left(\frac{\lambda U}{1-0.5}\right)\right\}^2 \quad (9.77)$$

to find λ and then substitute in joint probability density function for bivariate exponential distribution as proposed by Downton (1970) [62] and is given as

$$f(W,U) = \frac{\lambda_1\lambda_2}{1-\rho}\, exp\left\{-\frac{\lambda_1 W+\lambda_2 U}{1-\rho}\right\} I_0\left\{\frac{2(\rho\lambda_1\lambda_2 WU)^{1/2}}{1-\rho}\right\} \quad (9.78)$$

where $0 \le \rho < 1$, $I_n(\cdot)$ is the modified Bessel function of the first kind of n^{th} order.

The failure probability distribution for the bivariate exponential distribution is given by

$$F = \int_0^W \int_0^U f(W, U)\, dW\, dU \quad (9.79)$$

9.3 COMPARISON OF VARIOUS WARRANTY POLICIES

For each warranty policy, the optimization problem, with continuous design variables, is formulated to minimize the total warranty cost with a constraint on the total failure probability of the system. All the sub-systems in each optimization problem are assumed to have the same warranty policy. The warranty period is assumed to be 36 months for the one-dimensional warranty policies and the warranty period is considered to be either 36 months or a distance travelled by the automobile (mileage) is 36000 miles whichever comes first for the two-dimensional warranty policy. The cost models and the data are based on the idea that as the failure rate or design variable increases, the manufacturing cost of the sub-assembly decreases. The various costs in Tables 9.2 and 9.4 are stated in dollars.

The optimization problem is given by:

Find $\vec{X} = \{x_1\ x_2 \cdots x_5\}^T$ to minimize

$$TWC(\vec{X}) = \sum_{j=1}^{5} WC(x_j) \tag{9.80}$$

subject to

$$TFPS(\vec{X}) \le TFPS_{\max} \tag{9.81}$$

where *TWC* represents the total warranty cost of the system, *WC* the warranty cost of the sub-assembly, *TFPS* the total failure probability of the system, and $TFPS_{\max}$ the maximum permissible failure probability of the system. The automobile can be considered to be a series system and hence the total failure probability of the system can be calculated as indicated in section 3.6.1. The design data (permissible discrete design variable, c_m and c_b) is used to fit a quadratic curve for each variable for each sub-system

which in turn is used to interpolate other two values (c_m and c_b) for any particular value of the design variable. The modified PSO algorithm is implemented in a matlab program to include dynamic velocity function for the maximum velocity, bounce method for the position (or variable value) which exceeds the specified variable limits and dynamic penalty function approach for constraint violation. The PSO parameters are assumed as: population size, p = 24, maximum number of iterations, $i_{\max}$= 2000, cognitive learning rate, c_1 = 2, social learning rate, $c_2 = 2$, maximum inertia weight, iw_{max}= 0.9, minimum inertia weight, iw_{min}= 0.3, minimum velocity vector, $\vec{V}_{i\min} = 0.0001$ and maximum velocity vector, $\vec{V}_{i\max} = 0.02$ for all i (for the automobile warranty problem, i = 1 to 5), stopping convergence criterion (in terms of the change in the objective function value) = 10^{-8} for over 250 continuous iterations.

9.3.1 Non-repairable products

Three optimization problems, with five continuous design variables, to minimize the total warranty cost associated with five non-repairable sub-systems of the automobile are considered. The design variables and their ranges are indicated in Table 9.1. The warranty-related design data associated with the various sub-systems are indicated in Table 9.2 where c_m denotes the manufacturer's cost and c_b the buyer's cost. The warranty policy used in the optimization problems and the corresponding optimum solutions are obtained when $TFPS_{\max}$ = 0.4 are indicated in Table 9.5. The lowest value of the optimum solutions of the optimization problems is obtained for FRW with Weibull failure distribution, $\beta = 2$.

Table 9.1 Warranty-related design data for non-repairable sub-systems of an automobile

Design variable, λ (in month^{-1})	Sub-assembly associated	Range of the design variable, λ (in month^{-1})
x_1	Brakes (control systems)	[0.001,0.01]
x_2	Exhaust system	[0.002,0.016]
x_3	Hvac system	[0.003,0.009]
x_4	Electrical battery	[0.004,0.012]
x_5	Safety system	[0.004,0.01]

Table 9.2 Design data assumed for each design variable for non-repairable products

Sub-assembly	Variables	Different permissible discrete values			
Brakes (control systems)	x_1	0.004	0.006	0.008	0.01
	c_m	110	90	80	70
	c_b	120	100	88	75
Exhaust system	x_2	0.002	0.007	0.011	0.016
	c_m	125	95	85	65
	c_b	145	112	89	66
Hvac system	x_3	0.004	0.006	0.009	
	c_m	200	180	150	
	c_b	300	260	220	
Electrical battery	x_4	0.004	0.008	0.011	0.012
	c_m	135	110	80	75
	c_b	160	140	120	105
Safety system	x_5	0.004	0.006	0.008	0.01
	c_m	112	94	82	72
	c_b	120	100	86	75

9.3.2 Repairable products

The three optimization problems with five continuous design variables to minimize the total warranty cost associated with five repairable sub-systems of the automobile are considered in the formulation. The design variables and their ranges are indicated in Table 9.3. The warranty-related design data associated with the various sub-systems are indicated in Table 9.4 where c_m denotes the manufacturer's cost and c_r the repair cost. The warranty policy used in the optimization problems and the corresponding optimum solutions are obtained when $TFPS_{\max}$ = 0.1 are indicated in Table 9.5. The lowest value of the optimum solutions of the optimization problems is obtained for the 2-dimensional FRW (exponential distribution).

Table 9.3 Warranty-related design data for repairable sub-systems of an automobile

Design variable, λ $*$ (in month^{-1})	Sub-assembly associated	Range of the design variable, λ $*$ (in month^{-1})
x_1	Engine	[0.00001,0.004]
x_2	Transmission system	[0.00005,0.0045]
x_3	Suspension system	[0.00005,0.0046]
x_4	Chassis system	[0.00002,0.0046]
x_5	Fuel system	[0.00002,0.0048]

*It is has no units when design variable represent θ for 2-dimensional FRW

Table 9.4 Design data assumed for each design variable for repairable products

Sub-assembly	Variables	Different permissible discrete values			
Engine	x_1	0.00001	0.001	0.0025	0.004
	c_m	1150	1030	940	850
	c_r	120	105	90	80
Transmission system	x_2	0.00005	0.0015	0.003	.0045
	c_m	340	320	280	250
	c_r	50	50	45	45
Suspension system	x_3	0.00005	0.0023	0.0032	.0046
	c_m	460	420	380	345
	c_r	80	80	75	65
Chassis system	x_4	0.00002	0.0013	0.0025	0.0046
	c_m	470	430	380	330
	c_r	130	110	90	70
Fuel system	x_5	0.00002	0.0014	0.0032	0.0048
	c_m	370	325	265	235
	c_r	125	105	85	70

Table 9.5 Results of optimization problems of various warranty policies

Policy No.	Policy Description	Optimum Total Warranty Cost ($)
Non-repairable and non-renewing		
1	FRW (Weibull distribution, $\beta = 2$)	613.24
2	PRW (Weibull distribution, $\beta = 2$)	671.31
3	Combined FRW/PRW (Weibull distribution, $\beta = 2$)	717.65
Repairable and non-renewing		
1	FRW (Minimum repair, exponential distribution)	3530.08
2	2-Dimensional FRW (exponential distribution)	2820.55
3	FRW (Minimum repair, Weibull distribution, $\beta = 2$)	2824.33

Thus, we conclude that the FRW and 2-dimensional FRW are the most economical warranty policies for non-repairable and repairable items, respectively.

9.4 FORMILATION OF AN AUTOMOBILE WARRANTY OPTIMIZATION PROBLEM

An optimization problem with discrete design variables is formulated to minimize the total warranty cost with a constraint on the total failure probability of the system. A typical example of an automobile [8,116,121,131,132,147,151,196] is considered to illustrate the approach. In general, an automobile consists of more than 2500 parts in the various sub-assemblies of the system. In order to make the system realistic, versatile and reasonably complex, the warranty cost associated with 12 important sub-systems of the automobile is considered in the formulation. The warranty-related design variables associated with the various sub-systems are indicated in Table 9.6. The warranty period is assumed to be 36 months for the one-dimensional warranty policies and the warranty period is considered to be either 36 months or the distance travelled by the automobile (mileage) to be 36000 miles whichever comes first for the two-dimensional warranty policy.

Table 9.6 Warranty-related design variables of an automobile

Design variable	Sub-assembly associated	Variable notation*	No. of discrete values considered within the range	Range of the design variable
x_1	Brake	λ	16	[0.001,0.01]
x_2	Engine	θ_2	7	[0.0002,0.003]
x_3	Transmission	θ_2	9	[0.00015,0.0038]
x_4	Exhaust	λ	9	[0.002,0.016]
x_5	Suspension	λ	9	[0.0012,0.0026]
x_6	HVAC system	λ	9	[0.002,0.009]
x_7	CAB system	λ	6	[0.0015,0.011]
x_8	Chassis system	θ_2	9	[0.0002,0.003]
x_9	Electric Battery	λ	12	[0.002,0.012]
x_{10}	Fuel system	λ	7	[0.003,0.012]
x_{11}	Safety stem	λ	12	[0.002,0.01]
x_{12}	Other components	λ	16	[0.0011,0.0045]

*Unit for λ is month^{-1}and θ_2 is a dimensionless quantity

Different vendors or suppliers are assumed for each of the sub-assemblies (or its components) as shown in Table 9.7. In Table 9.7, c_m denotes the manufacturer's cost, c_b the buyer's cost, c_r the repair cost, θ_2 the coefficient used in equation (9.60) and λ the failure time distribution parameter. The units of the costs (c_m, c_b and c_r) are stated in dollars. The cost models and the data are based on the idea that as the failure rate or design variable increases, the manufacturing cost of the sub-assembly decreases for each vendor. Without loss of generality, the vendors are denoted as first, second, third and so on. The use of multiple vendors for any sub-assembly or component corresponds to a real

world scenario in the context of an automobile manufacturer. Warranty period, W, is stated in terms of months and the usage, U, is stated in terms of thousands of miles. The various warranty policies discussed in section 3.6.2 are considered for each of the sub-assemblies and the corresponding model parameters are given in Table 9.8.

Table 9.7 Design data assumed for each design variable

Sub-assembly	Vendor	Variables	Different permissible discrete values			
brakes (control systems)	First	$\lambda(x_1)$	0.004	0.006	0.008	0.01
		c_m	110	90	80	75
	Second	$\lambda(x_1)$	0.003	0.005	0.007	0.009
		c_m	110	100	90	80
	Third	$\lambda(x_1)$	0.002	0.0035	0.0065	0.0085
		c_m	105	100	95	85
	Fourth	$\lambda(x_1)$	0.001	0.0045	0.0075	0.0095
		c_m	115	105	90	80
engine (engine components)	First	$\theta_2(x_2)$	0.001	0.0025	0.003	
		c_m	1000	950	900	
		c_r	100	95	90	
	Second	$\theta_2(x_2)$	0.0002	0.0011	0.002	0.0028
		c_m	1100	1000	970	940
		c_r	100	95	90	90
transmission	First	$\theta_2(x_3)$	0.001	0.0025	0.0036	
		c_m	300	280	250	
		c_r	50	45	45	
	Second	$\theta_2(x_3)$	0.00015	0.002	0.0034	
		c_m	310	290	270	
		c_r	50	45	45	
	Third	$\theta_2(x_3)$	0.0005	0.0026	0.0038	
		c_m	305	280	250	
		c_r	50	45	45	
exhaust system	First	$\lambda(x_4)$	0.002	0.0085	0.016	
		c_m	100	80	70	
		c_b	110	85	80	
	Second	$\lambda(x_4)$	0.004	0.008	0.012	
		c_m	100	90	80	
		c_b	110	95	85	
	Third	$\lambda(x_4)$	0.006	0.01	0.015	
		c_m	105	95	85	
		c_b	115	100	95	

Table 9.7 Design data assumed for each design variable (continued)

Sub-assembly	Vendor	Variables	Different permissible discrete values		
suspension	First	$\lambda(x_5)$	0.0013	0.002	0.0026
		c_m	400	380	350
		c_r	80	80	75
	Second	$\lambda(x_5)$	0.0012	0.0017	0.0022
		c_m	410	390	370
		c_r	80	80	75
	Third	$\lambda(x_5)$	0.0014	0.0018	0.0025
		c_m	405	380	350
		c_r	80	80	75
hvac system	First	$\lambda(x_6)$	0.0035	0.006	0.008
		c_m	200	180	170
		c_b	300	280	270
	Second	$\lambda(x_6)$	0.002	0.007	0.009
		c_m	210	190	160
		c_b	300	280	260
	Third	$\lambda(x_6)$	0.004	0.0065	0.0085
		c_m	195	180	160
		c_b	300	280	260
CAB system	First	$\lambda(x_7)$	0.004	0.008	0.01
		c_m	600	550	530
		c_b	640	600	590
	Second	$\lambda(x_7)$	0.0015	0.007	0.011
		c_m	610	560	530
		c_b	640	600	580
chassis system	First	$\theta_2(x_8)$	0.001	0.002	0.003
		c_m	400	380	350
		c_r	100	100	90
	Second	$\theta_2(x_8)$	0.0002	0.0018	0.0025
		c_m	410	390	370
		c_r	100	100	90
	Third	$\theta_2(x_8)$	0.0006	0.0022	0.0029
		c_m	405	380	350
		c_r	100	100	90

Table 9.7 Design data assumed for each design variable

Sub-assembly	Vendor	Variables	Different permissible discrete values			
electrical battery	First	$\lambda(x_9)$	0.003	0.007	0.011	0.012
		c_m	110	90	80	75
		c_b	150	140	130	125
	Second	$\lambda(x_9)$	0.002	0.006	0.009	0.0115
		c_m	110	100	90	80
		c_b	150	140	130	125
	Third	$\lambda(x_9)$	0.005	0.0092	0.01	0.0105
		c_m	105	100	95	85
		c_b	150	140	130	125
fuel system	First	$\lambda_1(x_{10})$	0.004	0.008	0.01	
		c_m	300	275	260	
		c_r	100	95	90	
		λ_2	0.007	0.01	0.012	
	Second	$\lambda_1(x_{10})$	0.003	0.006	0.009	0.012
		c_m	320	290	270	260
		c_r	100	95	90	90
		λ_2	0.006	0.009	0.012	0.015
safety system	First	$\lambda(x_{11})$	0.002	0.0065	0.008	0.01
		c_m	110	90	80	75
	Second	$\lambda(x_{11})$	0.003	0.005	0.007	0.009
		c_m	110	100	90	80
	Third	$\lambda(x_{11})$	0.0035	0.004	0.006	0.0085
		c_m	105	100	95	85
other components	First	$\lambda(x_{12})$	0.0014	0.0016	0.002	0.0023
		c_m	110	90	85	80
	Second	$\lambda(x_{12})$	0.0013	0.0024	0.0037	0.0045
		c_m	110	100	90	80
	Third	$\lambda(x_{12})$	0.0012	0.0025	0.003	0.0035
		c_m	105	100	95	85
	Fourth	$\lambda(x_{12})$	0.0011	0.0015	0.0034	0.0042
		c_m	115	105	90	80

Table 9.8 Warranty policies assumed for the design variables

Sub-assembly	Design variable	Type of Sub-assembly and warranty	Model description and the parameters assumed
Brake Safety	x_1 x_{11}	Non-renewing, 1-D, Non repairable FRW	Weibull model W = 36 months for brakes β = 2 for safety β = 1.75
Engine Transmission Chassis	x_2 x_3 x_8	Non-renewing, repairable, 2-D	Weibull model , U = 36000 miles, W = 36 months G(r) is uniformly distributed over [0,3] using 1-D approach, $\lambda\left(\frac{t}{x}\right)$ is assumed to be linear, $\theta_1 = \theta_3 = \theta_0$ for engine θ_0= 0.0001 , for transmission θ_0=0.0002, for chassis θ_0= 0.00015.
Exhaust CAB	x_4 x_7	Non-renewing , 1-D, Non repairable PRW	Weibull model β = 2 , W = 36 months
Suspension	x_5	Non-renewing, 1-D, repairable FRW minimal repair	Weibull model β = 1.5 , W = 36 months
HVAC Electrical battery	x_6 x_9	Non-renewing, 1-D combined FRW/PRW	Weibull model β = 2, for HVAC W_1=24 months, W_2= 36 months for electrical battery W_1=12 months, W_2=36 months
Fuel system	x_{10}	Non-renewing, 1-D, repairable FRW repair is not perfect	Exponential distribution, λ_1- before, λ_2- after, W = 36 months
Other systems	x_{12}	Non-renewing, 1 D, Non repairable FRW	Gamma distribution, β = 2 , W = 36 months

9.4.1 Problem statement for automobile warranty problem

The automobile warranty problem can be stated in mathematical form as follows:

$$\text{Find } \vec{X} = \begin{Bmatrix} x_1 \\ x_2 \\ \vdots \\ x_{12} \end{Bmatrix} \tag{9.82}$$

to minimize

$$TWC(\vec{X}) = 2WC(x_1) + \sum_{j=2, j\neq 5}^{12} WC(x_j) + 2WC(x_5) \tag{9.83}$$

subject to

$$TFPS(\vec{X}) \leq TFPS_{\max} \tag{9.84}$$

where TWC represents the total warranty cost of the system, WC the warranty cost of the sub-assembly, $TFPS$ the total failure probability of the system, and $TFPS_{\max}$ the maximum permissible failure probability of the system. The automobile can be considered to be a series system and hence the total failure probability of the system can be calculated as indicated in section 3.6.1. The warranty cost of the brakes and suspension are multiplied by a factor 2 to account for both the left and right side sub-assemblies of the automobile. The total failure probability of the serious system, using equation (3.45), can be expressed as

$$TFPS(\vec{X}) = 1 - \prod_{j=1}^{12} (1 - FP(x_j)) \tag{9.85}$$

where $FP(x_j)$ represents the failure probability of j^{th} sub-assembly.

Several automobile warranty optimization problems with varying $TFPS_{\max}$ are solved for two cases. In each case, we assume two types of design variables for the optimization

problems namely- continuous design variables and discrete design variables. The two cases are designated as:

Case a: By assuming the failure distribution models of all the sub-assemblies to be exponential.

Case b: By assuming the failure distribution models of all the sub-assemblies as indicated in Table 8 (Weibull distributions).

9.4.2 Numerical results and discussion

The continuous and discrete warranty optimization problems are solved using a modified particle swarm optimization (PSO) technique. The modified PSO algorithm is implemented in a matlab program to include dynamic velocity function for the maximum velocity, bounce method for the position (or variable value) which exceeds the specified variable limits and dynamic penalty function approach for constraint violation. The design data for each sub-system, shown in Table 9.7, is used to fit a quadratic curve which in turn is used to interpolate for any particular value of design variable in the case of continuous design variable optimization problem (in similar way as done in section 9.3). The discrete optimization problem is solved using a modified particle swarm optimization [61] using Closest Discrete Approach (CDA) to handle the discrete design variables. The PSO parameters are assumed as: population size, p = 50, maximum number of iterations, $i_{\max}$= 2000, cognitive learning rate, c_1= 2, social learning rate, $c_2 = 2$, maximum inertia weight, iw_{max}= 0.9, minimum inertia weight, iw_{min}= 0.3, minimum velocity vector, $\vec{V}_{i\min} = 0.0001$ and maximum velocity vector, $\vec{V}_{i\max} = 0.02$ for all i (for the automobile warranty problem, i = 1 to 12), stopping convergence criterion (in

terms of the change in the objective function value) = 1e-8 for over 400 continuous iterations. The optimum solutions are obtained through several matlab program runs with varying values of the maximum permissible failure probability of the system for case (a) for both continuous and discrete design variables and the results obtained are shown in Figure 9.2.

Table 9.9 Comparison of optimal solutions of warranty problems for case a

Quantity	Continuous solution for case a	Discrete solution for case a
x_1	0.00103	0.008
x_2	0.000708	0.0002
x_3	0.00015	0.00015
x_4	0.00216	0.002
x_5	0.0026	0.0025
x_6	0.002	0.002
x_7	0.001502	0.0015
x_8	0.0002	0.0002
x_9	0.00203	0.002
x_{10}	0.00927	0.009
x_{11}	0.00677	0.008
x_{12}	0.00335	0.0023
TWC	4376.391	4378.640
TFPS	0.79945	0.797179

Table 9.10 Comparison of optimal solutions of warranty problems for case b

Quantity	Continuous solution for case b	Discrete solution for case b
x_1	0.003097	0.002
x_2	0.0002066	0.0002
x_3	0.0001504	0.00015
x_4	0.002935	0.002
x_5	0.002599	0.0025
x_6	0.00200	0.004
x_7	0.004114	0.007
x_8	0.000202	0.0002
x_9	0.002055	0.002
x_{10}	0.003562	0.003
x_{11}	0.003740	0.002
x_{12}	0.004322	0.0023
TWC	4307.2151	4338.763
TFPS	0.39973	0.39388

The optimum solutions for both continuous and discrete automobile warranty optimization problems with the failure distributions assumed as per case a for various sub-assemblies are tabulated in Table 9.9 and those with failure distributions assumed as per case b for various sub-assemblies are tabulated in Table 9.10.

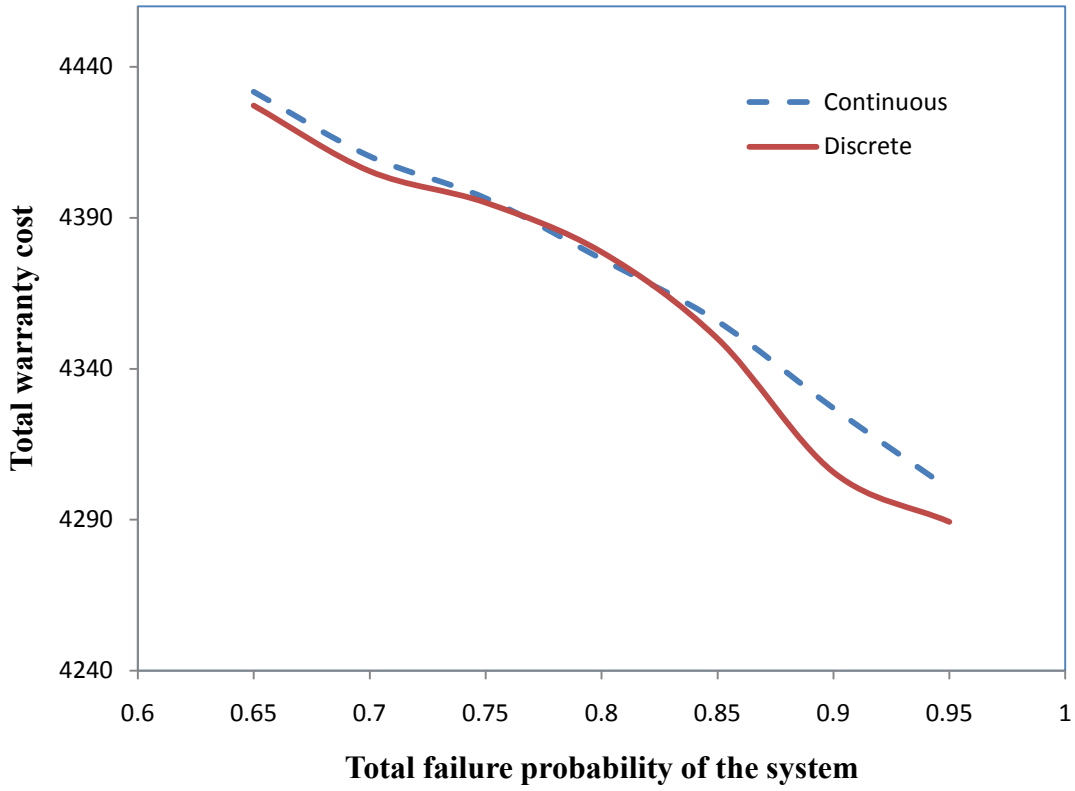

Figure 9.2 Minimum total warranty cost vs $TFPS_{max}$ with continuous and discrete design variables (Exponential failure distribution)

The optimum solutions are obtained through several matlab program runs with varying values of maximum permissible failure probability of the system for case (b) for both continuous and discrete design variables and the results obtained are shown in Figure 9.3.

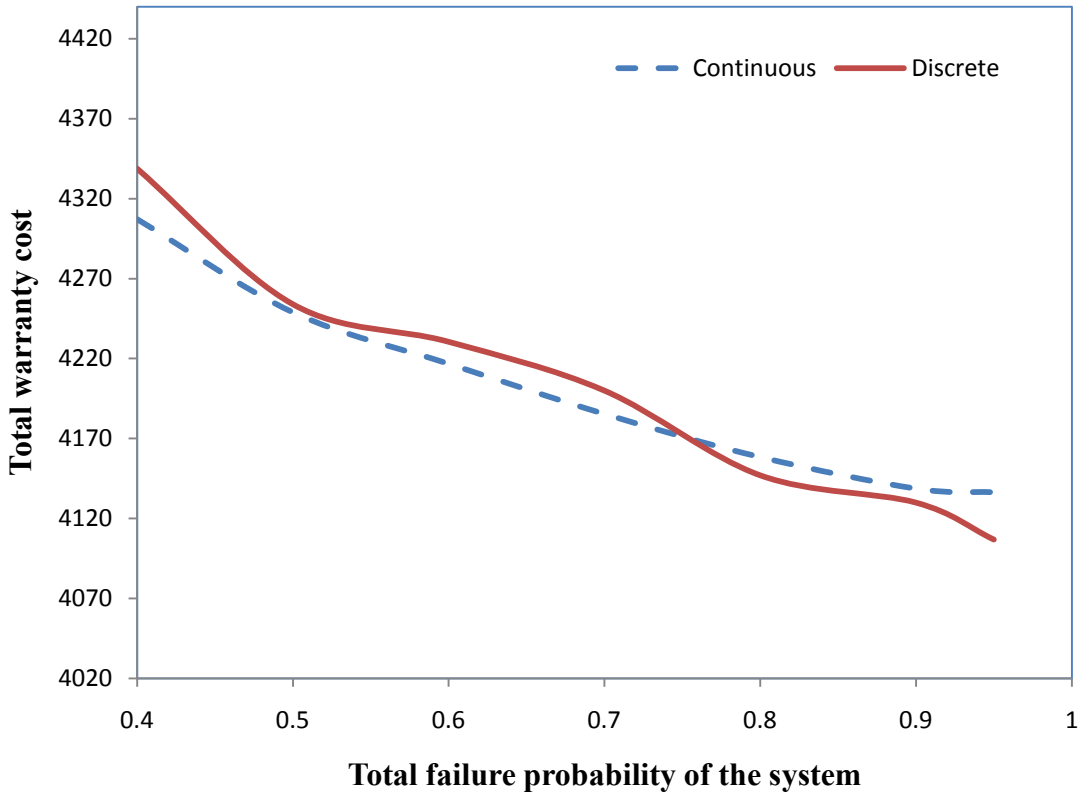

Figure 9.3 Total warranty cost vs $TFPS_{max}$ with continuous and discrete design variables (Weibull failure distribution)

As the total failure probability of the system decreases, the total warranty cost increases as expected. In case of discrete design variables for both cases (a) and (b), we observe that the curve is not smooth and has some bumps. It is due to the fact that different vendors have their own pricing criteria to determine the costs with respect to the failure probability of the product, profit margin. In figures 9.4a to 9.4*l*, first one plot is drawn between the failure probability calculated at the end of the warranty period vs design variable and the second plot is drawn between failure probability with different values of the warranty period (in case of 2-D warranty policies, we assume $W=U$) at mean value of the design variable for each of the sub-assemblies in the discrete optimization problem.

The dash line curves represent the exponential failure distribution model as represented by case (a) and the solid line curves represent the Weibull failure distribution model as represented by case (b) in Figures 9.4a to 9.4*l*. All the plots of Figures 9.4a to 9.4*l* show an increasing trend with respect to the x-axis. In the case of 2-D warranty policies (as in the case of engine, transmission and chassis), the exponential failure distribution is assumed for both cases (a) and (b). For the fuel system sub-assembly, the curves coincide because both the cases assume the same exponential failure time distribution. These plots (Figures 9.4a to 9.4*l*) are obtained using a separate matlab programs by using all the information given in Tables 9.6 to 9.8 to compare both the failure distribution models (in both cases a and b) for the failure probability for each of the design variables and in order to have comparable spread for the total failure probability of the system for both cases. Thus, it can be seen that design or formulation of the data for the automobile problem taken care of the total failure probability of the system spread in the design space for both cases.

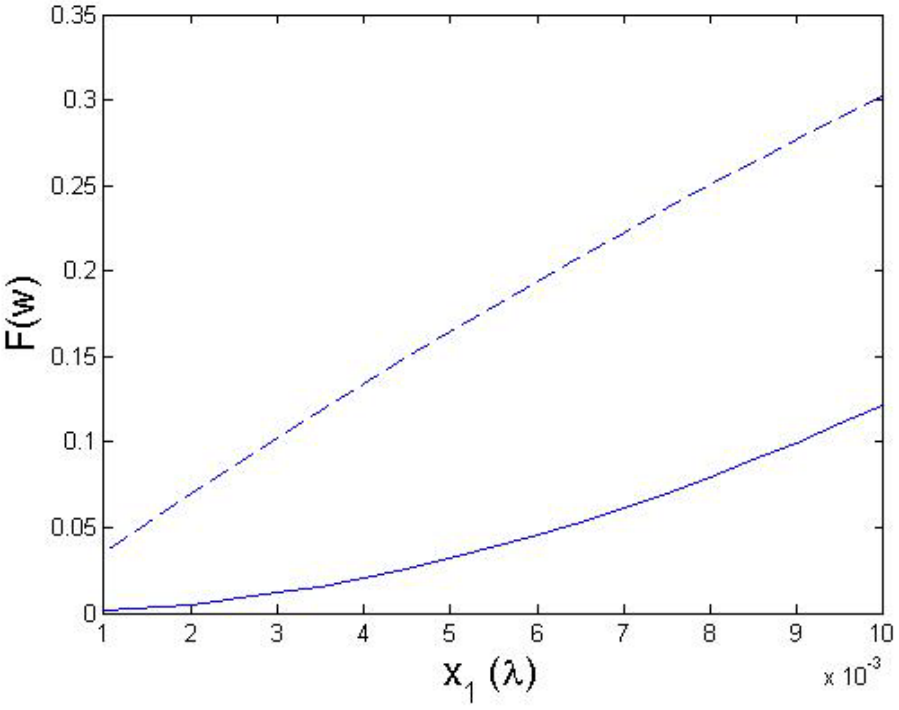

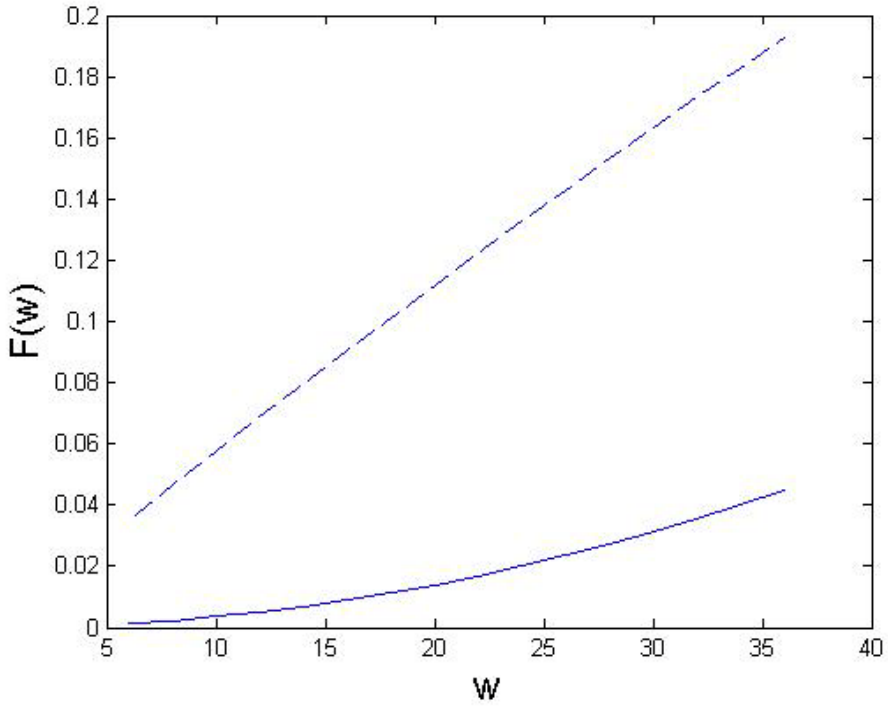

Figure 9.4a $F(W)$ vs x_1 and $F(W)$ vs W at the mean value of x_1

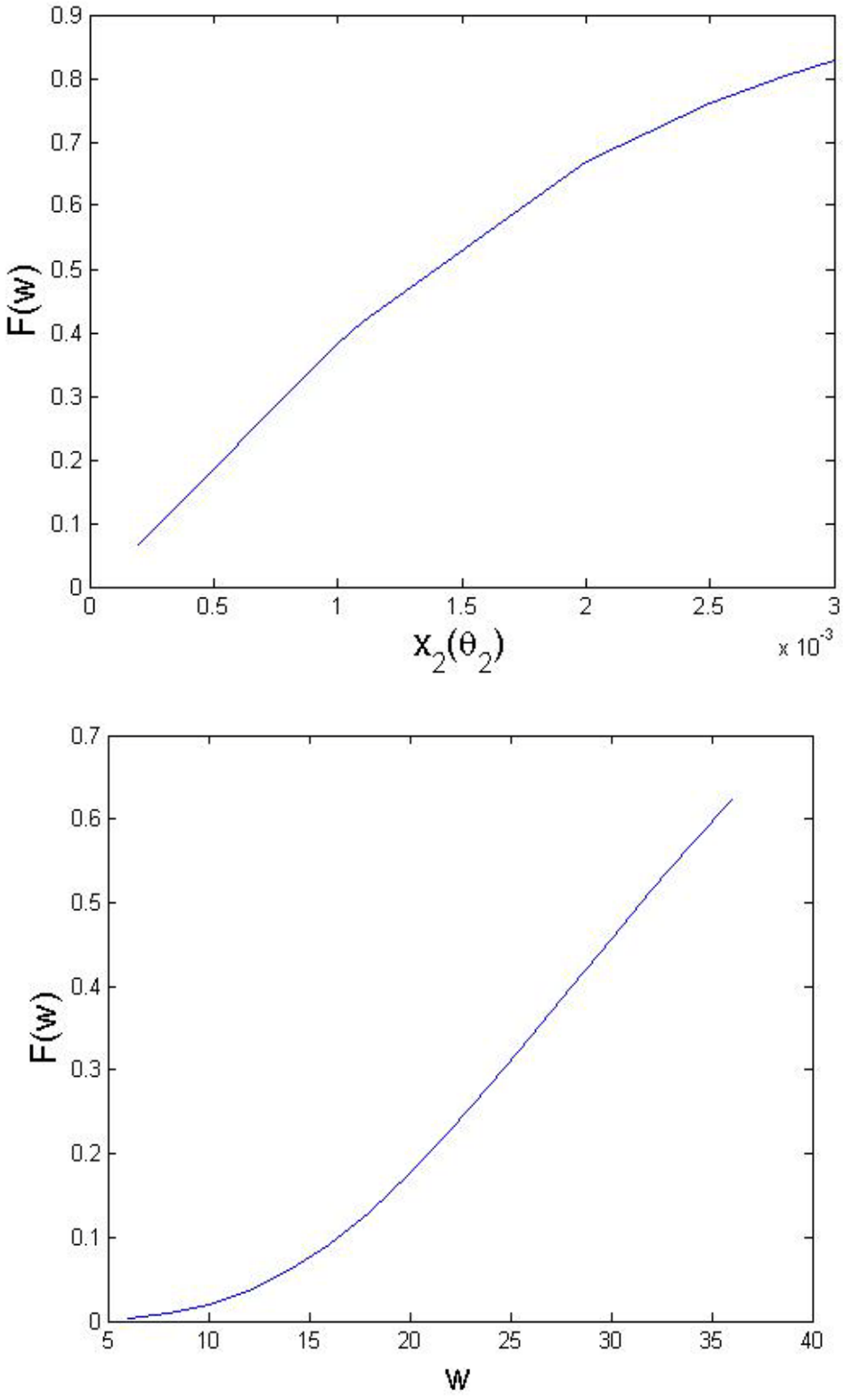

Figure 9.4b $F(W)$ vs x_2 and $F(W)$ vs W at the mean value of x_2

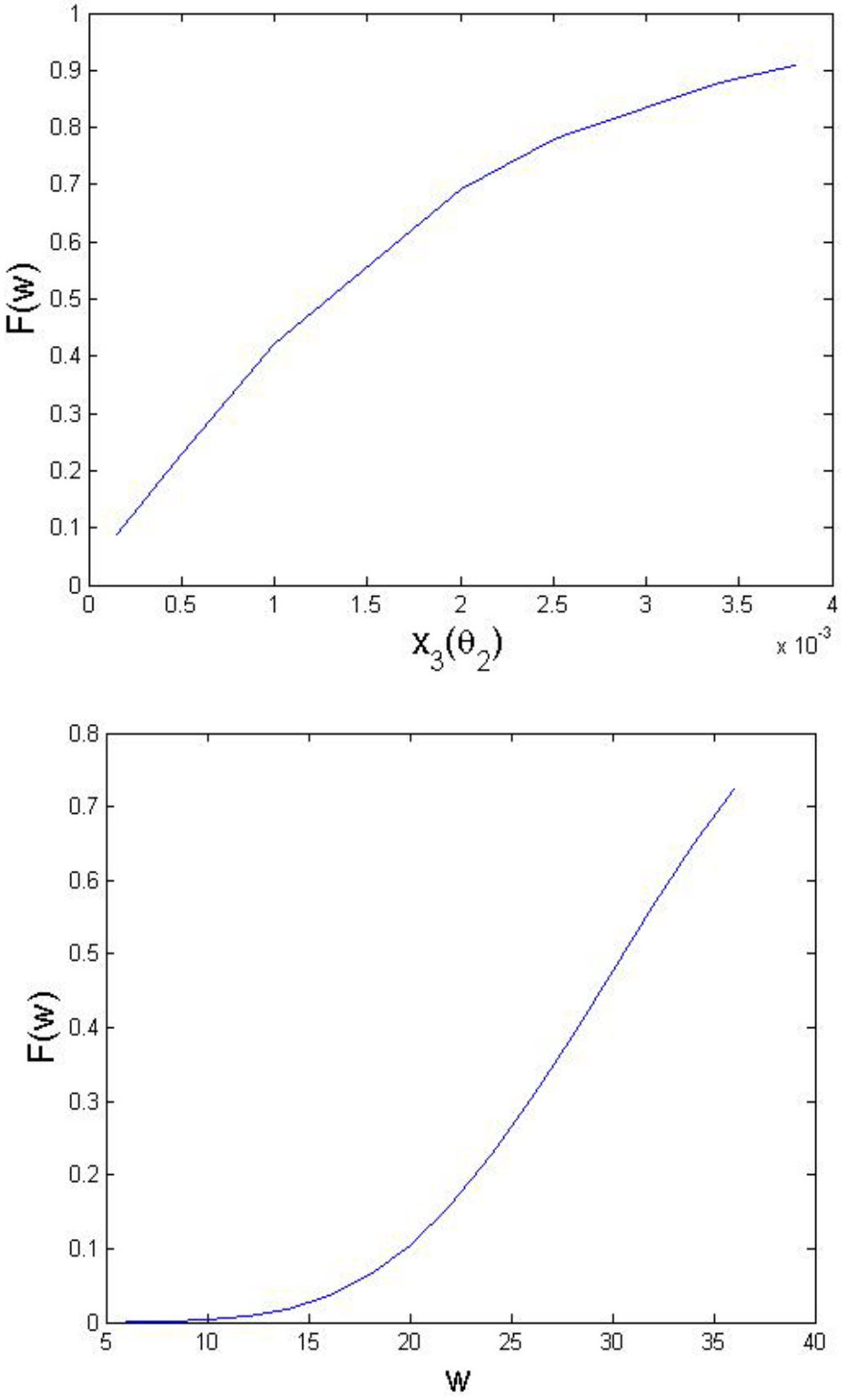

Figure 9.4c $F(W)$ vs x_3 and $F(W)$ vs W at the mean value of x_3

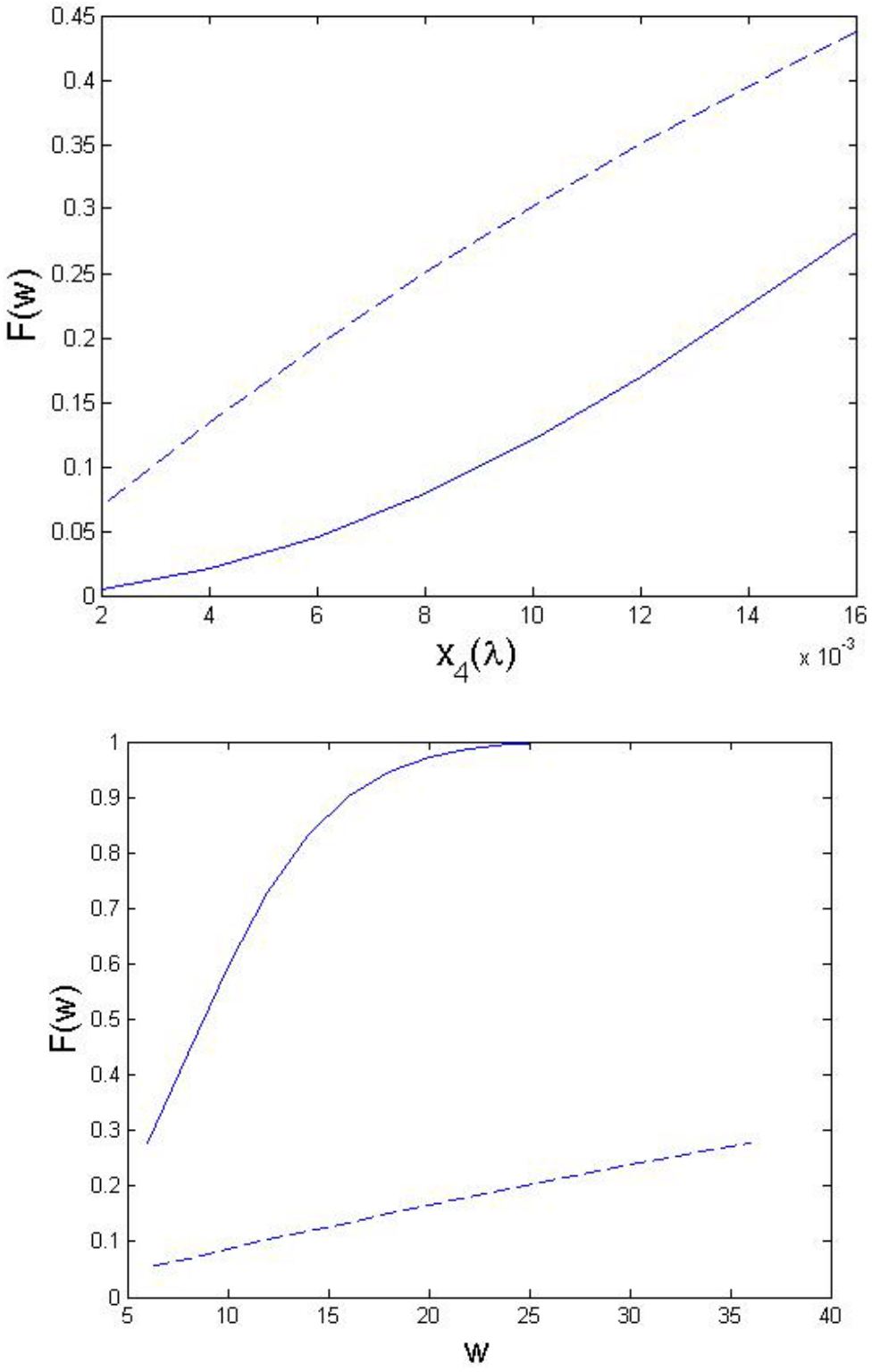

Figure 9.4d $F(W)$ vs x_4 and $F(W)$ vs W at the mean value of x_4

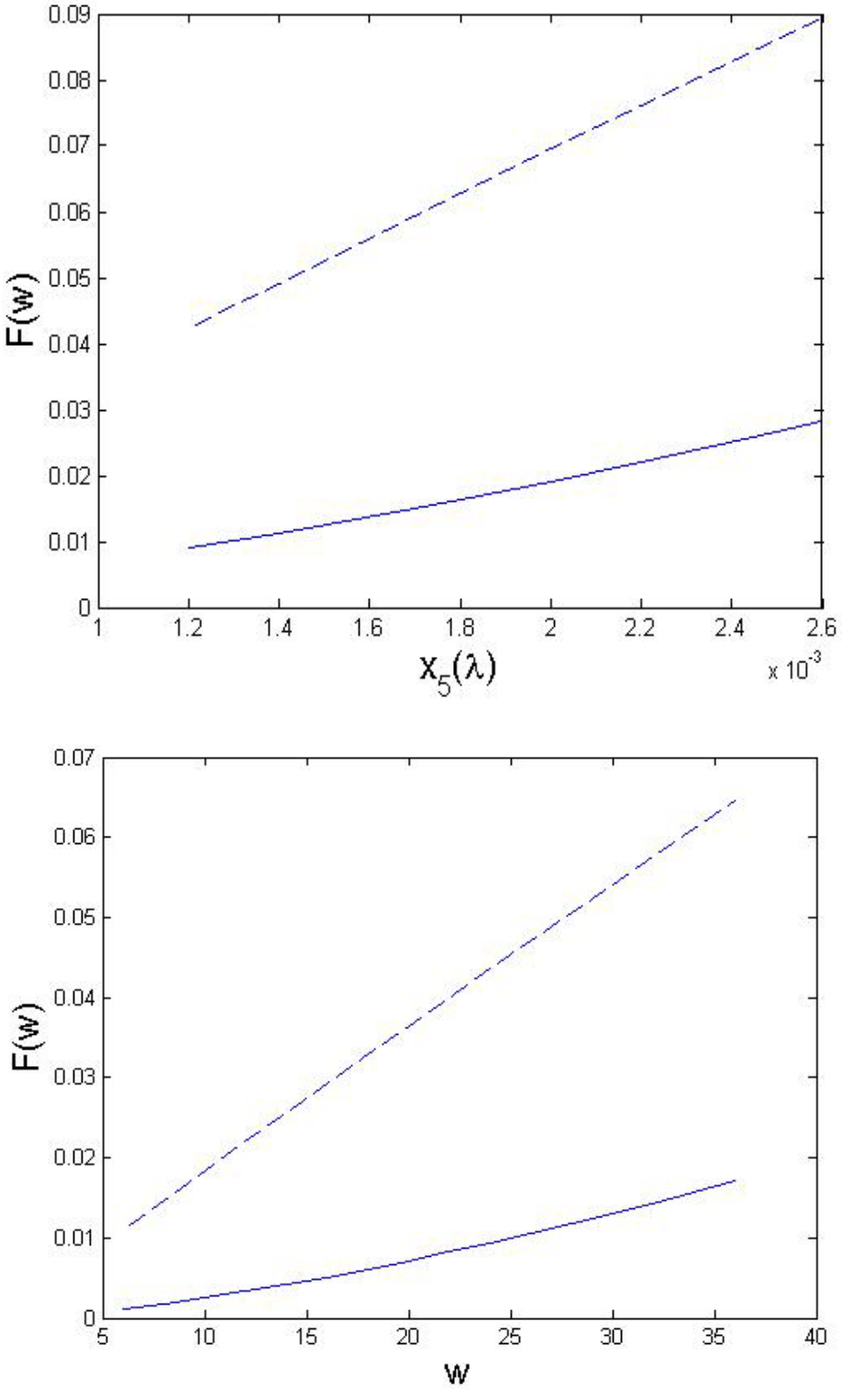

Figure 9.4e $F(W)$ vs x_5 and $F(W)$ vs W at the mean value of x_5

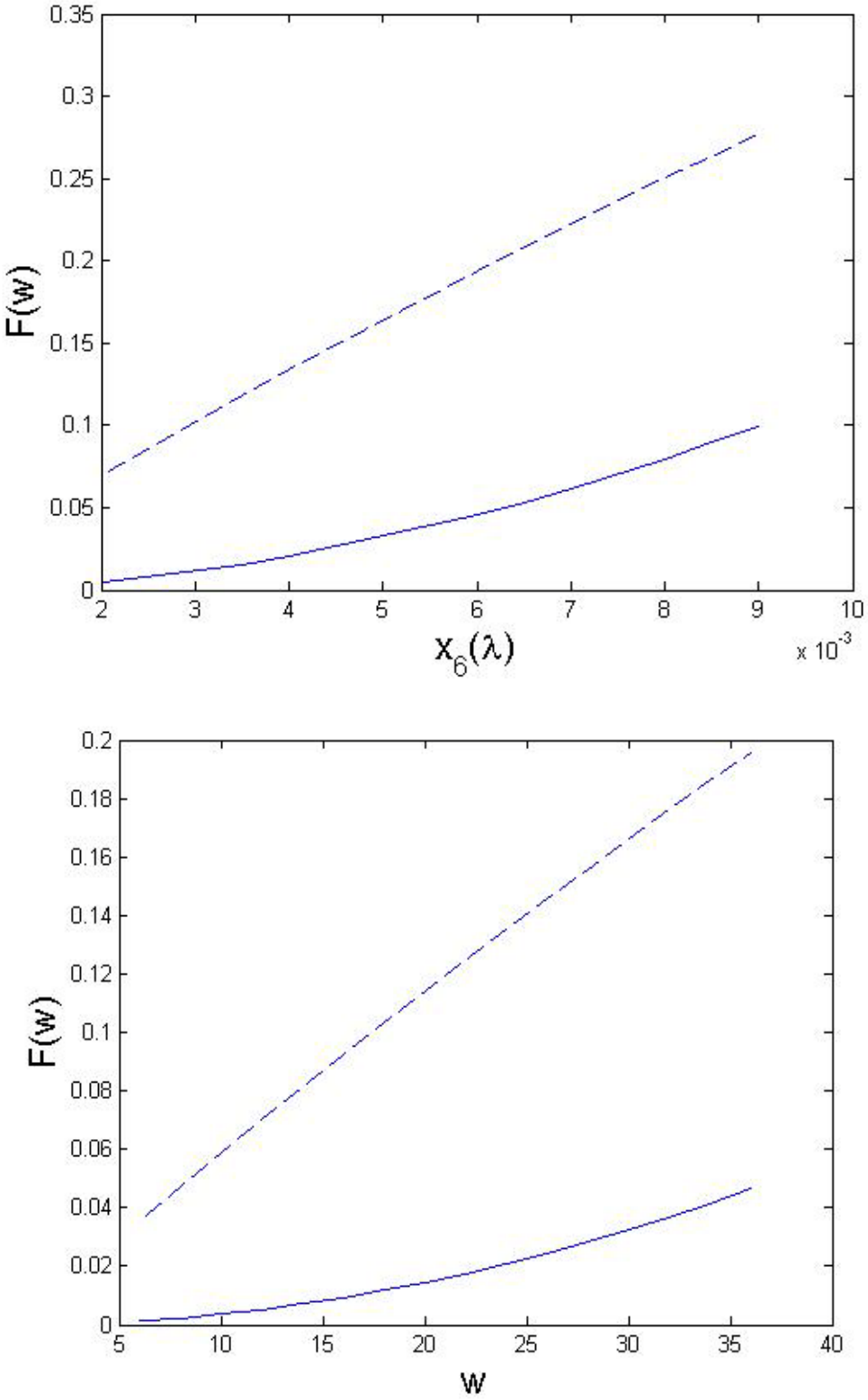

Figure 9.4f $F(W)$ vs x_6 and $F(W)$ vs W at the mean value of x_6

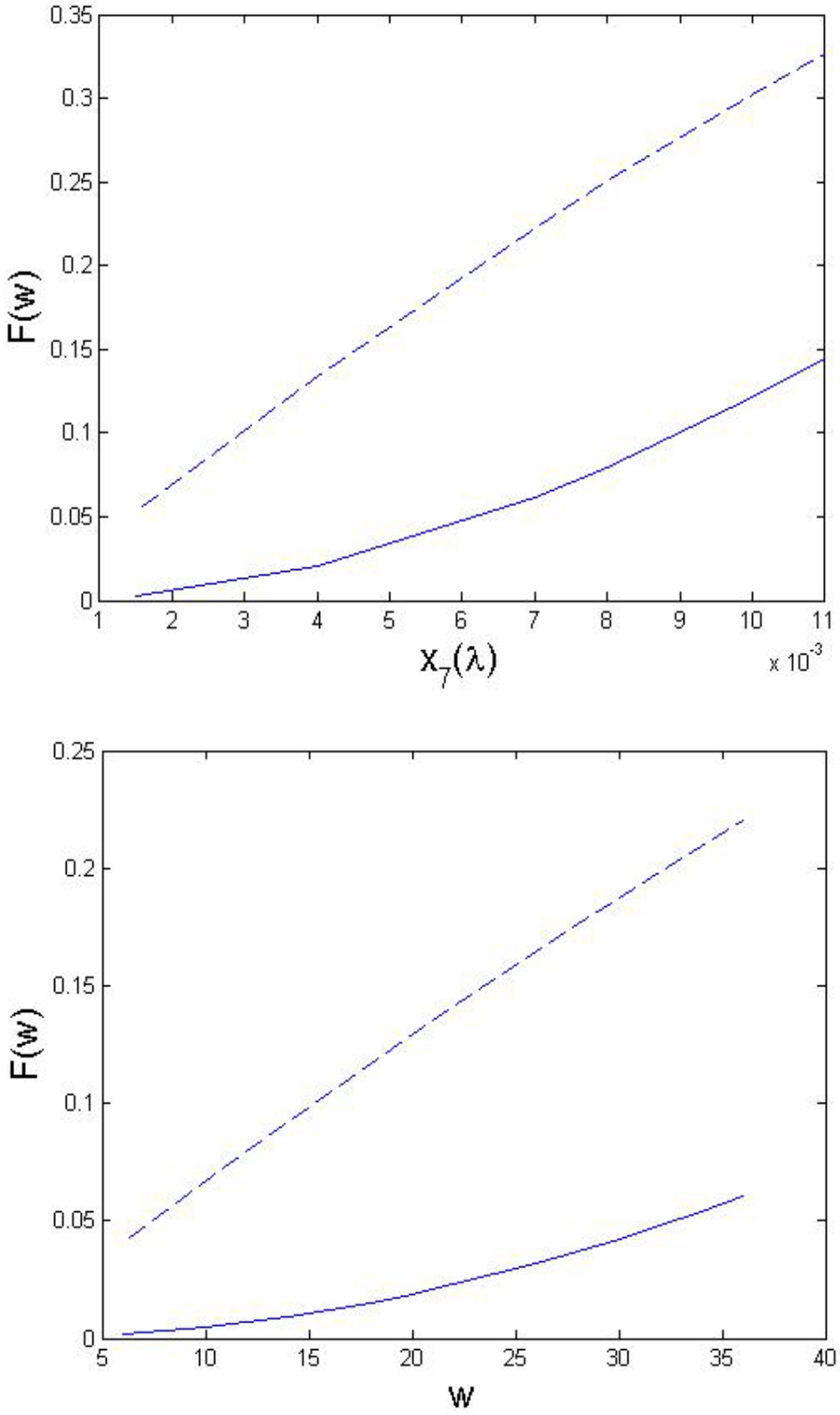

Figure 9.4g $F(W)$ vs x_7 and $F(W)$ vs W at the mean value of x_7

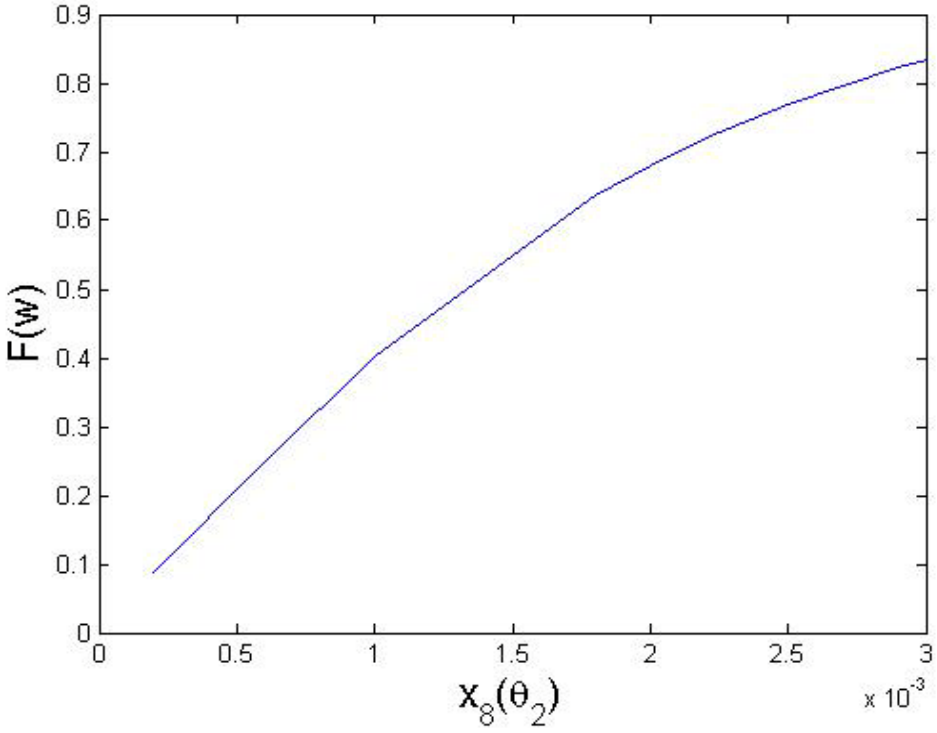

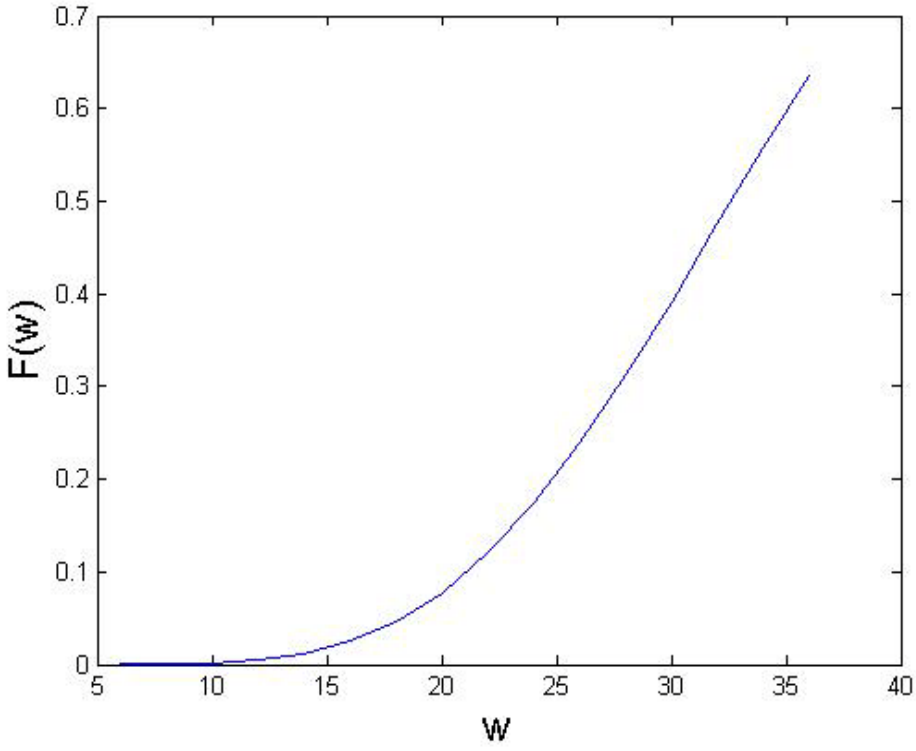

Figure 9.4h $F(W)$ vs x_8 and $F(W)$ vs W at the mean value of x_8

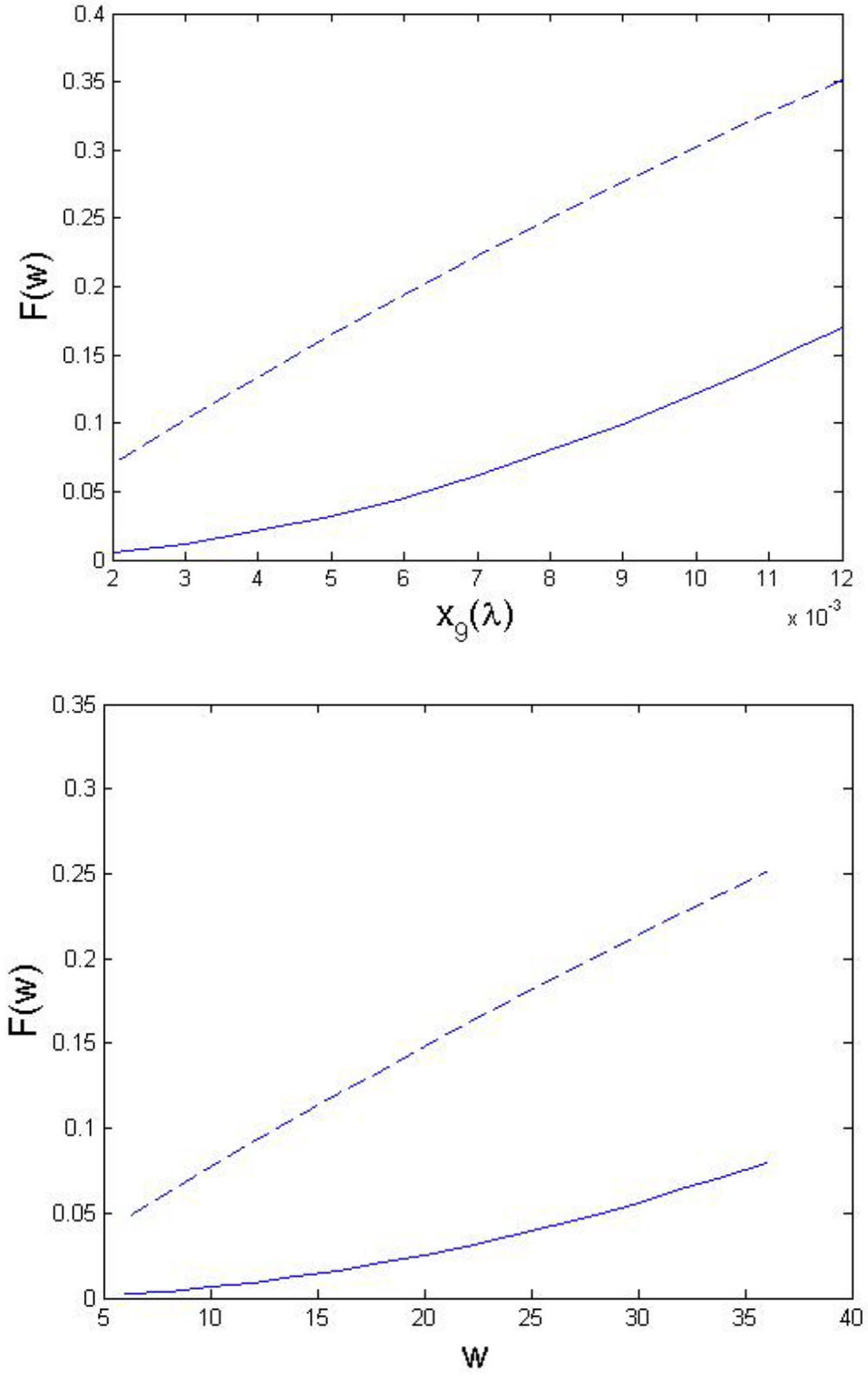

Figure 9.4i $F(W)$ vs x_9 and $F(W)$ vs W at the mean value of x_9

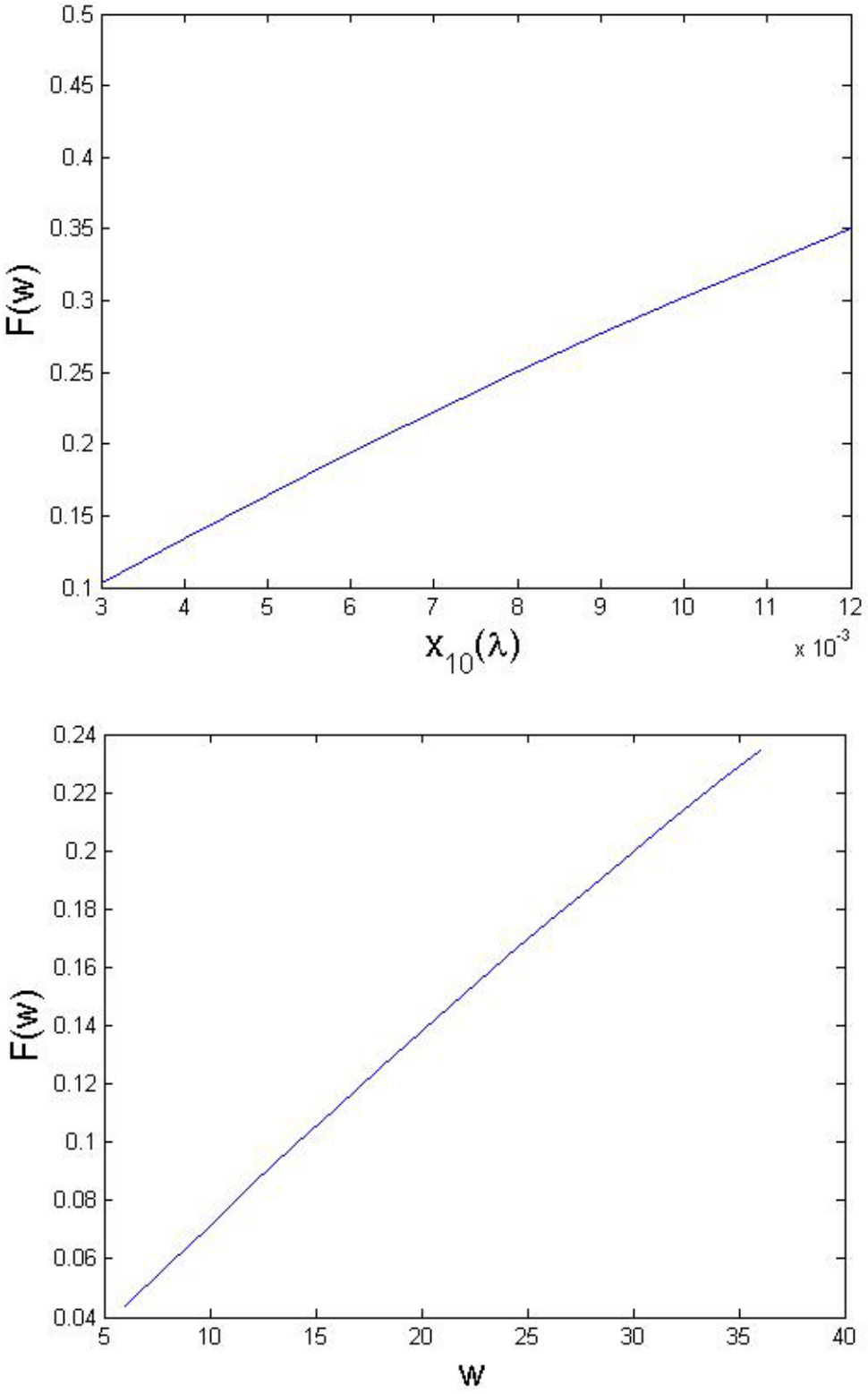

Figure 9.4j $F(W)$ vs x_{10} and $F(W)$ vs W at the mean value of x_{10}

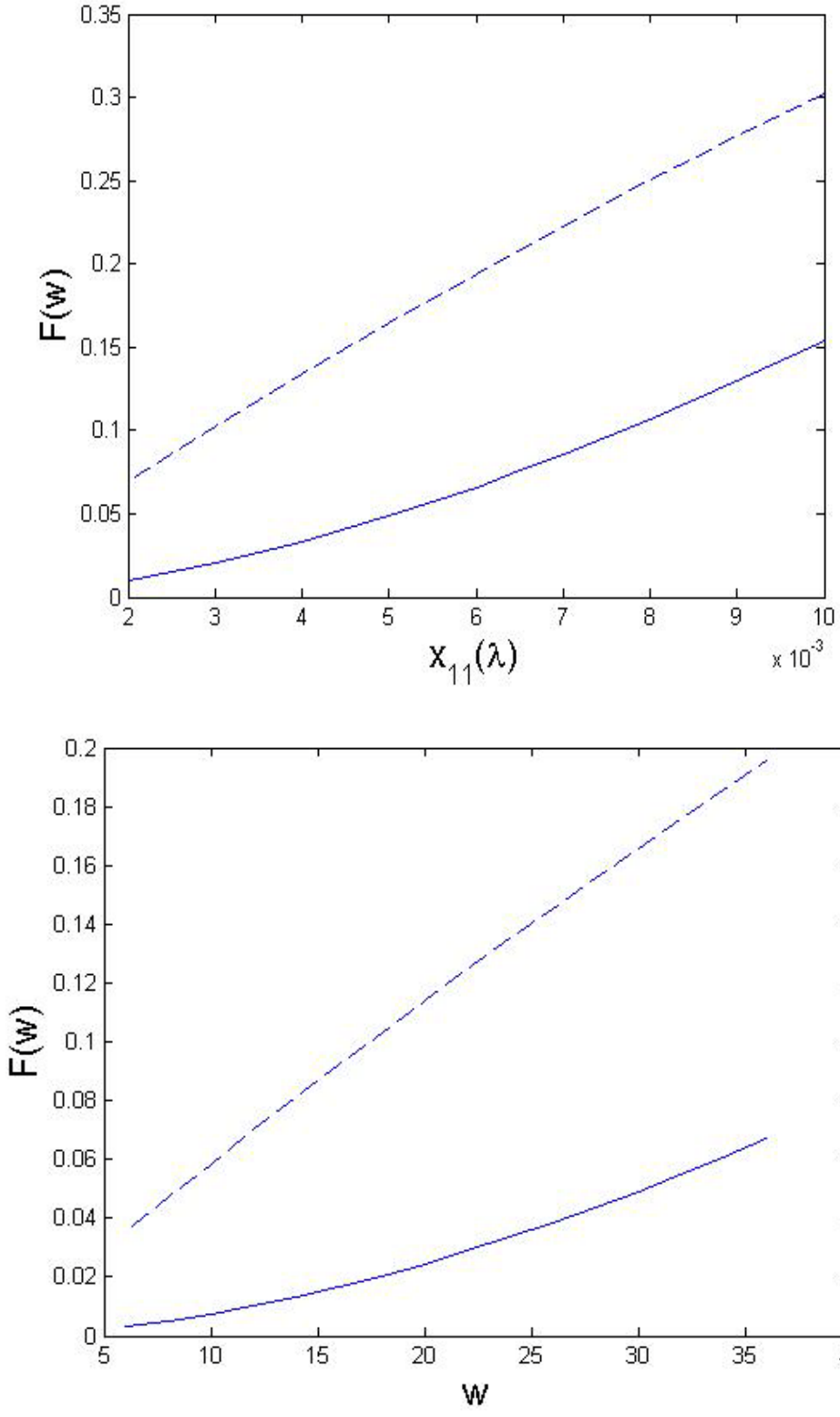

Figure 9.4k $F(W)$ vs x_{11} and $F(W)$ vs W at the mean value of x_{11}

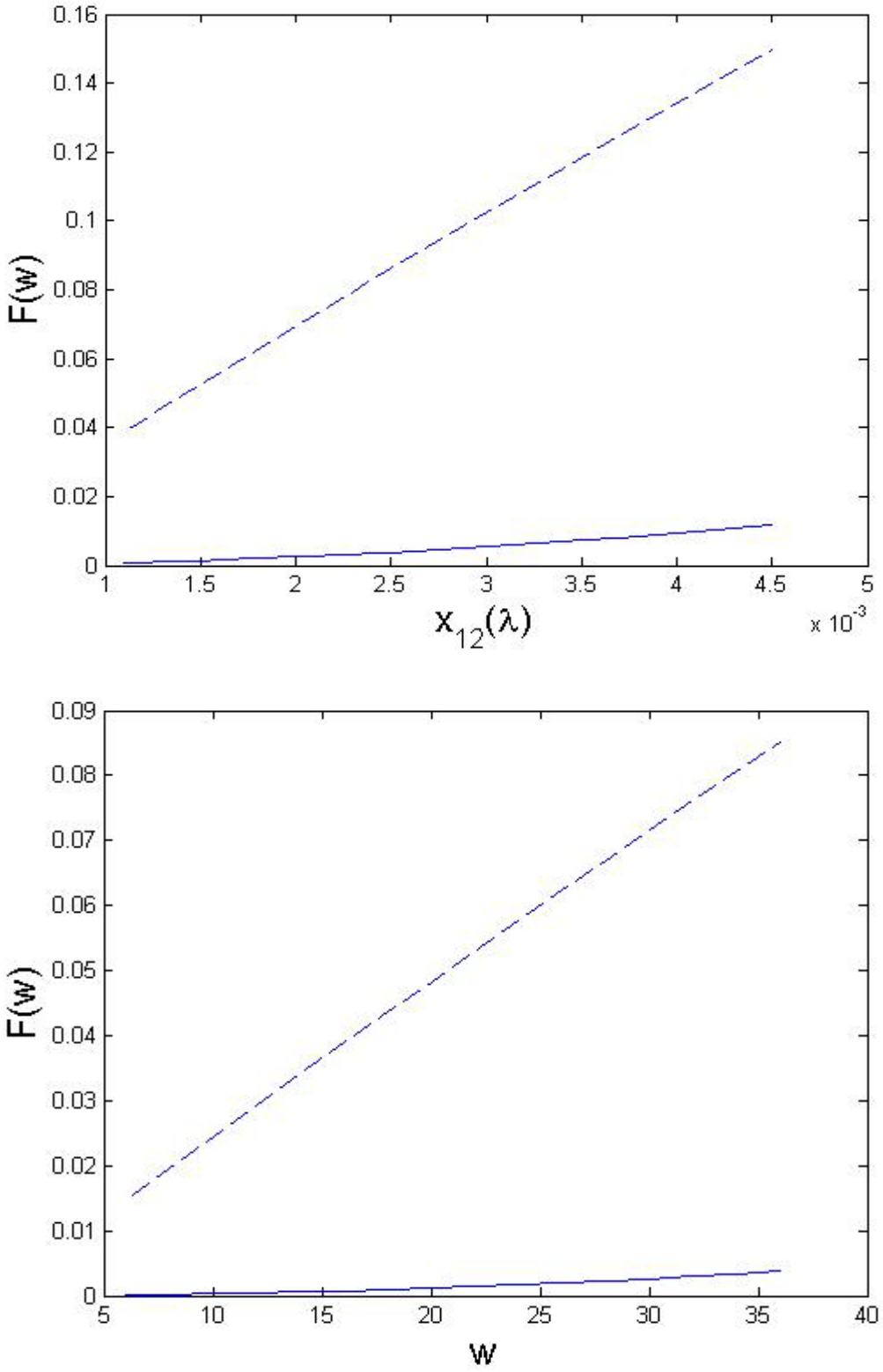

Figure 9.4*l* $F(W)$ ***vs*** x_{12} **and** $F(W)$ ***vs*** W **at the mean value of** x_{12}

9.5 SENSITIVITY ANALYSIS

Sensitivity analysis of the total failure probability of the system *TFPS* (constraint) and the warranty cost *TWC* (objective function) has been conducted with respect to the design variables and the results are shown in Figures 9.5(a)-9.5(c) and 9.6(a)-9.6(c), respectively. Figures 9.5(a) -9.5(c) and 9.6(a) -9.6(c) indicate the variations of *TFPS* and *TWC* when the optimum values of the discrete design variables are changed over the range ±20% (approximately). Depending on the location of the optimum discrete design variable with its permissible range, up to 2 values smaller and up to 2 values larger than the optimum value are considered for the sensitivity study. This sensitivity analysis has been carried with reference to the discrete optimum solution of case b when $TFPS_{\max}$ = 0.4. For the design variables associated with the sub-assemblies of the engine, transmission, hvac and chassis systems, the results of the sensitivity analysis are shown in Figures 9.5(a) and 9.6(a). For the design variables associated with the sub-assemblies of exhaust system, cab system, electrical battery and safety system, the results of the sensitivity analysis are shown in Figures 9.5(b) and 9.6(b). For the rest of the design variables, namely brakes, suspension, fuel systems and other components, the sensitivity analysis results are shown in Figures 9.5(c) and9.6(c). The constraint, $TFPS_{\max}$ = 0.4, is shown as dotted line in Figures 9.5(a) to 9.5(c) and the optimum warranty cost, *TWC* = $4338.8, is shown as dotted line in Figures 9.6(a) to 9.6(c). The sensitivity analysis with respected *TFPS* indicates that as the discrete design variable increases, *TFPS* increases as expected.

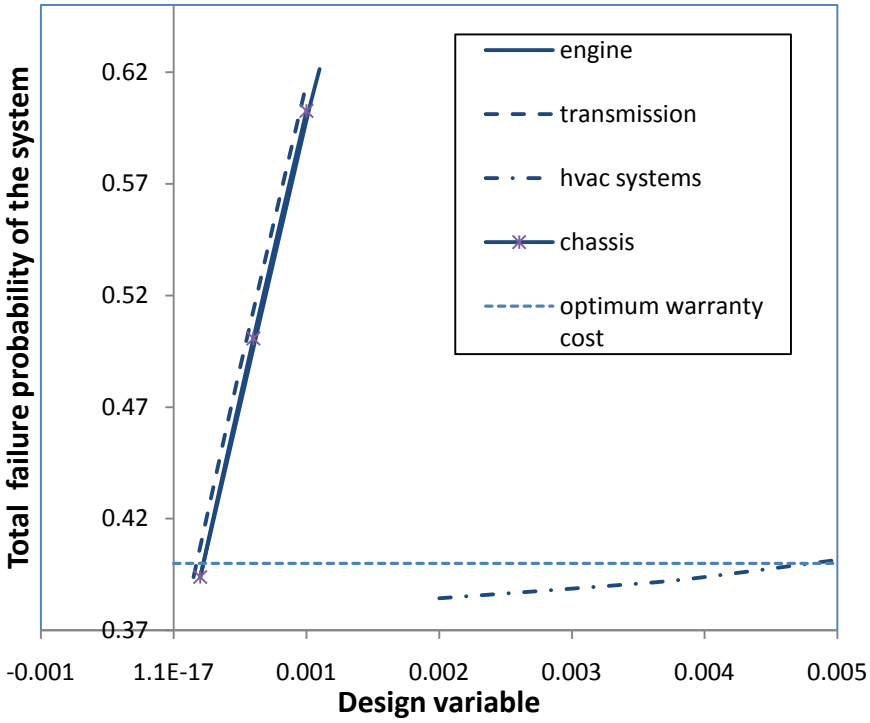

Figure 9.5a *TFPS vs* Design variables $(x_{2,}, x_3, x_6, x_8)$

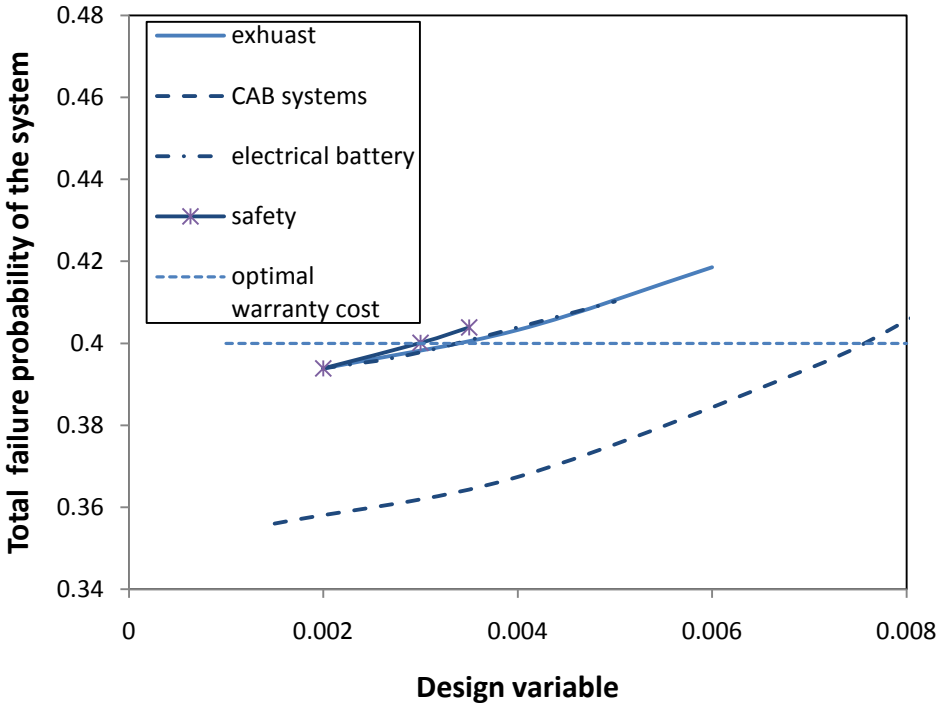

Figure 9.5b TFPS vs Design variables $(\mathrm{x}_{4,}, \mathrm{x}_7, \mathrm{x}_9, \mathrm{x}_{11})$

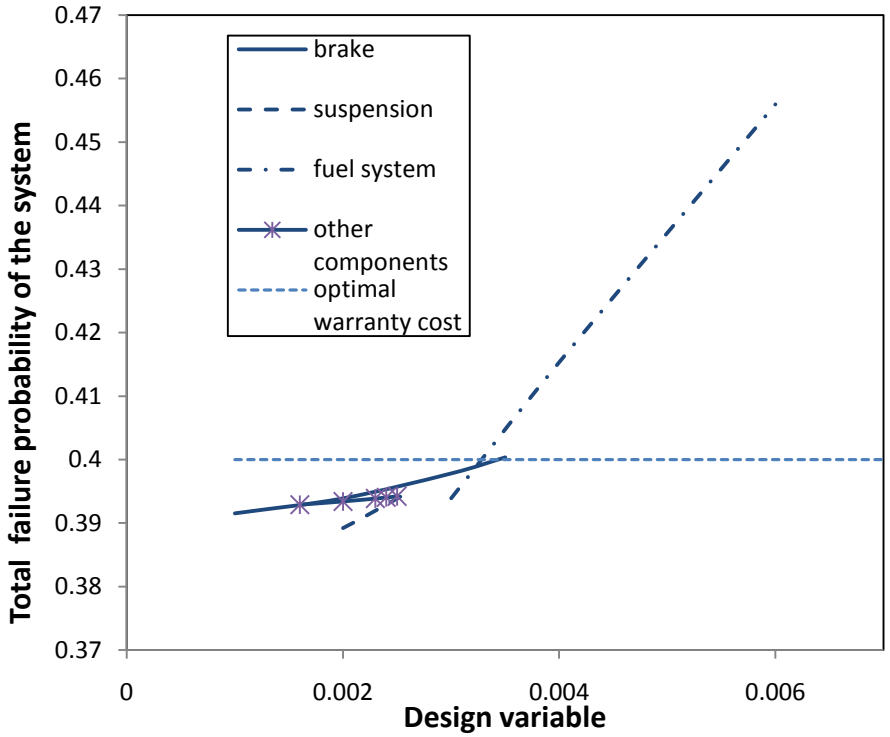

Figure 9.5c *TFPS vs* Design variables $(x_{1,}, x_5, x_{10}, x_{12})$

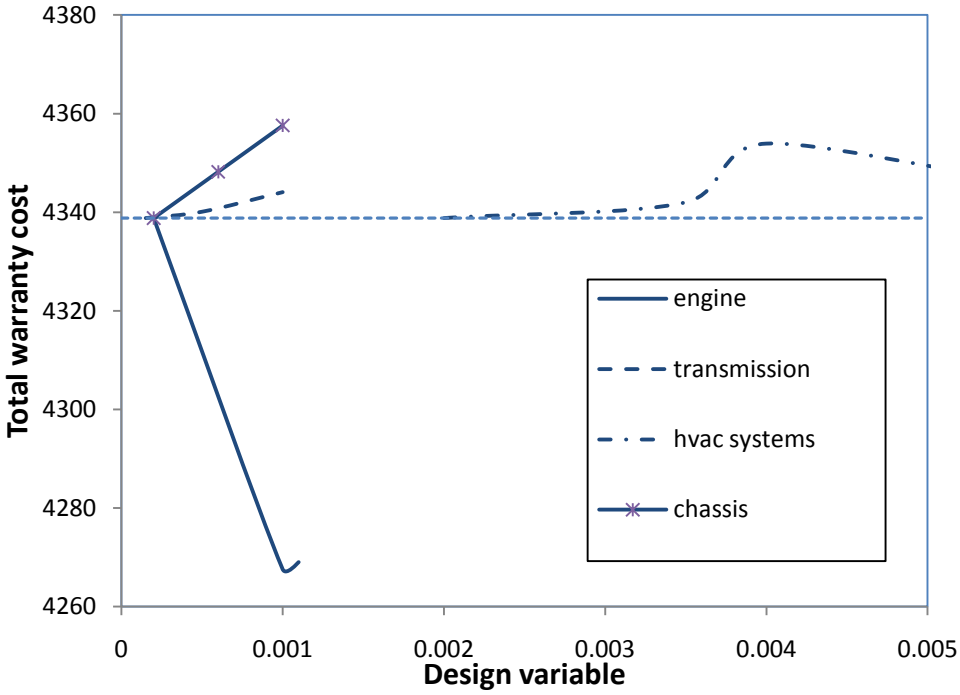

Figure 9.6a *TWC vs* Design variables $(x_{2,}, x_3, x_6, x_8)$

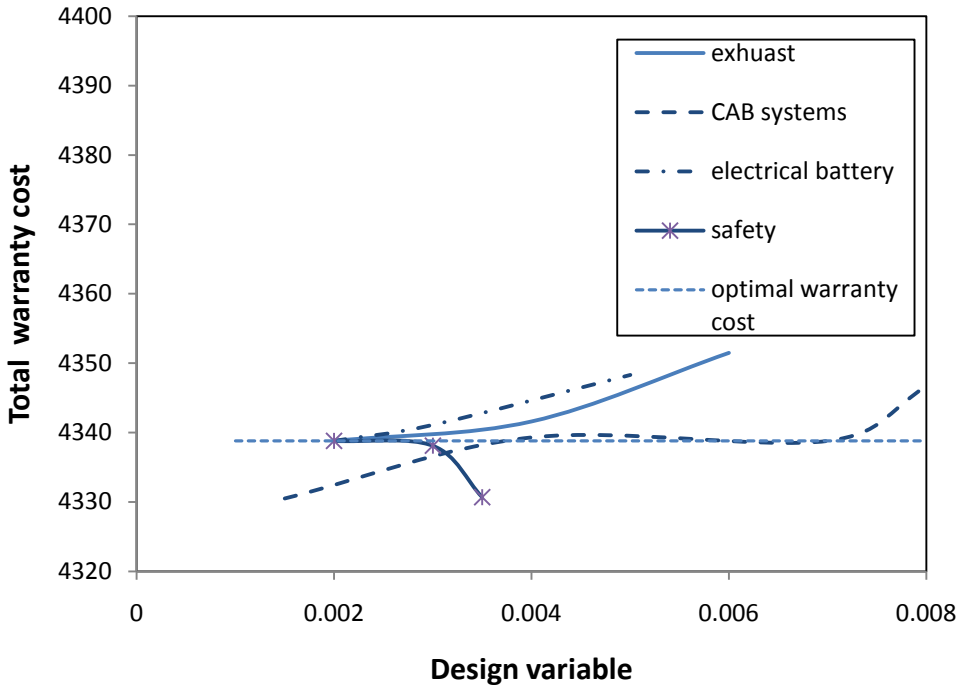

Figure 9.6b *TWC vs* Design variables $(x_{4,}, x_7, x_9, x_{11})$

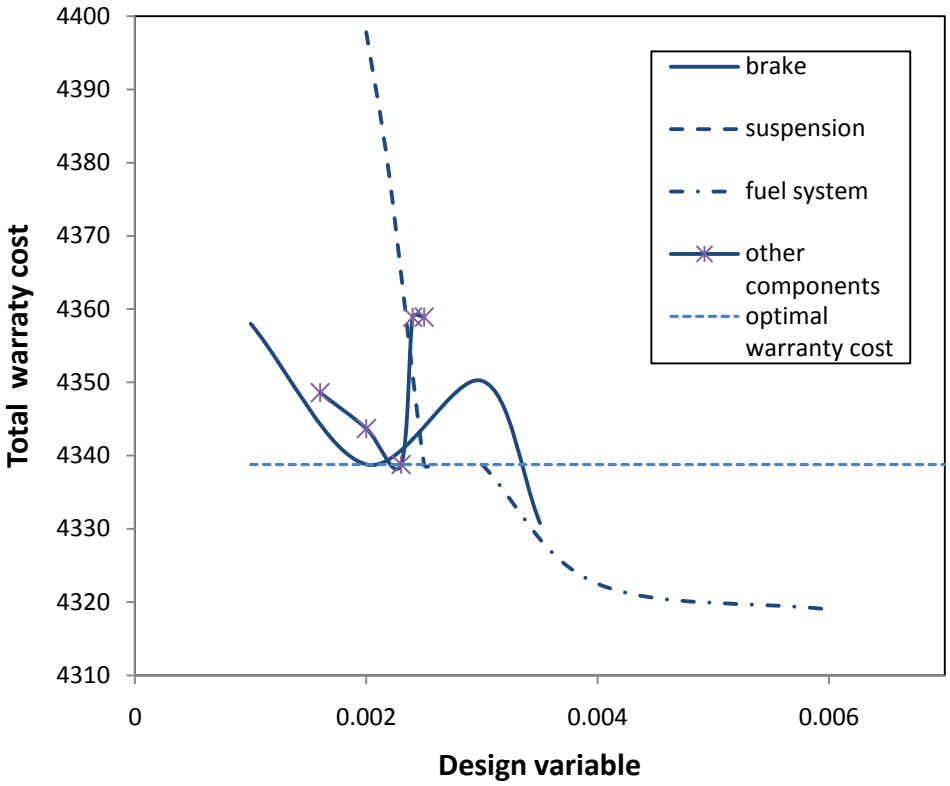

Figure 9.6c *TWC vs* Design variables $(x_{1,}, x_5, x_{10}, x_{12})$

9.6 DISCUSSION

We have studied three warranty policies for both repairable and non-repairable products for an automobile example to illustrate us the best warranty policy among them which yield minimum total warranty cost. Thus, we concluded that the FRW and 2-dimensional FRW are the most economical warranty policies for non-repairable and repairable items, respectively. In this study, an automobile warranty problem has been formulated by making it as close to reality as possible. The problem formulated results in both discrete and continuous design spaces, with the number of potential design points on the order of 10^{11} in the discrete design space. The discrete optimization problem is closer than the continuous optimization problem to the reality. The modified PSO algorithm is used to find the optimum solutions for different values of the maximum permissible total failure probability of the system for both the exponential and Weibull failure distribution models (cases a and b) with results shown in Figures 9.3 and 9.4. Both continuous and discrete design variable optimization problems as the total failure probability of the system decreases, the total warranty cost also decreases for both cases a and b. When you fit a quadratic curves for the discrete design variable and its corresponding sub-assembly costs from different vendors for each assembly, and with fact that vendors have their own pricing criteria, we can see some points above and below the quadratic curve and thus make some discrete design variables take less warranty cost than their corresponding continuous design variables obtained from quadratic curve. This is the reason for the crossing of the curves in figures 9.3 and 9.4.

The sensitivity analysis results show that the engine, transmission and chassis system sub-assemblies are more sensitive to the *TFPS*. Engine and suspension sub-

assemblies are more sensitive to the *TWC* of the system. Sensitivity curve with respect to *TWC* for hvac sub-assembly increases and then decreases as the design variable increases; this is due to the fact that vendor have their own pricing criteria. The sensitivity analysis with respected *TWC* indicates that as the discrete design variable increases, TWC increases except for engine, brake and other system sub-assemblies for the automobile. This exception is due to the fact that vendors pricing criteria don't match among different vendors.

9.7 SUMMARY

In this chapter a comprehensive study of the various non-renewing one-dimensional and two dimensional warranty policies has been made from an automobile manufacturer's view point. The total warranty costs as well as the probability of failure of the system corresponding to different parameters assumed for the failure time distributions of the sub-assemblies are calculated. Two types of failure time distributions-the exponential and Weibull types-are used for the sub-assembly lives. The automobile warranty optimization problem has been formulated with both discrete and continuous design variables based on the various warranty policies discussed. The results obtained (using the modified PSO) will give the manufacturer an insight on the probable warranty cost based on the reliability desired for the automobile.

CHAPTER 10
CONCLUSIONS

This work studies various combination rules to combine evidences from multiple sources to understand the procedure of combining evidences in depth and how the conflict among the evidences can be treated. The solutions of different optimization problems, which are framed and solved for combining two sources of evidences, indicate the similarities and distinctions among various combination rules as discussed in section 4.2. The proposed selection procedure described in section 4.3 guides the user or analyst to select the most suitable combination rule for combining various evidences obtained from multiple sources based on the nature of evidence sets. At the same time, the user or analyst is free to use other rules for combining the evidences. Evidence sets given in Table 4.7 are constructed in such a way that the applied combination rule gives more satisfactory/logical results compared to other combination rules in each of the five cases described in section 4.4. For each of the cases described in section 4.4, if any combination rule other than the one suggested is used for combining the evidences we may get misleading results which may not convergence to actual reality when more and more evidence/information becomes available. We also considered an example, in which data is available in various forms of evidence namely deterministic, probabilistic, fuzzy and Dempster's bpa to combine evidence.

When evidences on several uncertain parameters are available from a number of sources (experts) in an engineering problem, and if the response of the system involves mathematical expressions, DST or Zhang's combination rule can be used. In the case of

the safety analysis of the welded beam problem, evidences of two and four uncertain parameters are combined in sections 5.4.1 and 5.4.2, to find the maximum shear stress induced in the weld. A modified DST method is presented in section 5.5 to combine evidences from multiple sources, when the sources of evidence have different credibilities. The variations in the belief and plausibility have been observed to depend on the number of interval ranges for the interval-valued data for combining the evidences. An essential feature of knowledge representation in engineering applications is the ability to represent and manage imprecise concepts and the example presented in chapter 5 represents an initial step in this direction.

The sum of the lower bound on margin of safety and the upper bound on margin of failure is always equal to 1 in all cases as, indicated in section 6.4. As the number of alpha cuts used in the numerical computation of the bounds on the margins of safety and failure changed, the values of the computed bounds are found to vary. However, with increasing number of the alpha cuts, the bounds are found to converge to the values reported in this work. Irrespective of the number of sources of evidence, when the assumed fuzzy membership function of the allowable shear stress changes from the triangular to the trapezoidal shape, the lower and upper bounds tend to shrink the ranges of the margins of safety and failure. The widening or shrinking of the ranges of the margins of safety and failure is observed to depend on the available evidence and the influence of the uncertain parameters on the output or response parameter of the system. In general, the procedure proposed for considering the credibilities of the various sources of evidence (WFTI) is applicable for combining evidences to evaluate the safety/failure of any uncertain system in the presence of evidences on the uncertain parameters from

different sources. The methodology presented in chapter 6 provides an alternative framework for combining evidence from multiple sources using fuzzy theory.

The chapter 7 presents algorithms based on modified PSO to solve all types of engineering optimization problems involving single objective or multiple objectives with continuous, discrete and/or mixed design variables in the presence of constraints. Because of the convergence difficulties experienced with the original PSO algorithm with a constant value of the maximum velocity limit, the dynamic velocity function approach has been used to speed up the convergence. The bounce method provides a significant improvement in the performance of the algorithm to overcome stagnation of the population. Results of single objective optimization problems like welded beam design and pressure vessel design showed that the algorithm converges to the optimal solution faster than the original PSO algorithm. When the new MGT, combined with the modified PSO, is used to solve multi-objective optimization problems, the best compromise (optimal) solution from the Pareto-optimal front has been found efficiently. The results of the 25-bar truss multi-objective optimization problem illustrate the effectiveness and efficiency of the new approach when all the objective functions are not totally conflicting. The results obtained for the 25-bar truss with all design variables taken as continuous or as mixed discrete are found to be comparable to another. A novel attempt is made to formulate and design a composite simply supported beam optimization problem with uncertain parameters.

The chapter 8 presents algorithms based on modified PSO coupled with vertex method to solve uncertain engineering optimization problems involving multiple objectives with continuous, discrete and/or mixed design variables with constraints. When convergence

difficulties are experienced with the original PSO algorithm by using a constant value of the maximum velocity limit, the dynamic velocity function approach is found to speed up the convergence. The bounce method provides a significant improvement in the performance of the algorithms to overcome stagnation of the population. When the MGT, combined with the modified PSO and vertex method, is used to solve uncertain multi-objective optimization problems, the best compromise (optimal) solution from the Pareto-optimal front has been found efficiently. The results of the 25-bar truss multi-objective optimization problem illustrate the effectiveness and efficiency of the new approach when all the objective functions are not totally conflicting. The results obtained for the 25-bar truss with all design variables taken as continuous or as mixed discrete are found to be comparable to another. These results are indicative of the power to solve the uncertain engineering problems using the proposed method.

The present research focuses on minimization of warranty cost for servicing warranties in 1-dimension and 2-dimensions both for repairable and non-repairable products. A comprehensive study of the various non-renewing one-dimensional and two dimensional warranty policies has been conducted from an automobile manufacturer's view point in chapter 9. The total warranty cost and the probability of failure of the system corresponding to different parameters assumed for the failure time distributions of the sub-assemblies are calculated. Two types of failure time distributions-the exponential and Weibull types-are used for the sub-assembly lives. The automobile warranty optimization problem has been formulated for both discrete and continuous optimization problems based on the various warranty policies discussed. The results obtained using the modified

PSO will give manufacturer an insight on the probable total warranty cost based on the reliability desired for the automobile.

We have summarized the present research work in this chapter and the future scope of the research is described in the next chapter.

CHAPTER 11
FUTURE SCOPE OF WORK

Using a procedure similar to the one described in chapter 4, other rules of combining evidences can be explored and suitable selection procedures can be developed to apply these rules. A Weighted Dempster Shafer Theory for Interval-valued data (WDSTI) and Weighted Fuzzy Theory for Interval-valued Data (WFTI) are proposed to combine evidences from multiple sources, to evaluate the safety/failure of any uncertain system in the presence of evidence on the uncertain parameters, when the multiple sources of evidence have different credibilities. These approached can be explored for other engineering applications. The scope of the automobile example considered in chapter 9 can be expanded to include more sub-assemblies (or design variables) of the automobile to obtain more realistic optimum total warranty costs. This work can be extended to include the actual data available to the real world auto manufacturers instead of the data assumed in Tables 9.6 to 9.8. The proposed method using modified particle swarm optimization (PSO) based algorithm to solve multi-objective optimization of uncertain engineering problems involving different types of design variables (continuous, discrete and/or mixed). We can apply this algorithm to solve many optimization problems in the area of composite structures, aerospace structures and civil engineering. We can also explore design of composite structures by expanding the problem solved in chapter-8 for multi-objective optimization using uncertain parameters. We can also solve real world automobile optimization examples with inherent uncertainty present in the formulation of the problem. We can expand the example problem in chapter 4 to combine various forms

of evidences available from different sources with different credibilities for complex engineering applications.

REFERENCES

1. Agarwal, H, Renaud, J. E, Preston, E. L., and Padmanabhan, D., "Uncertainty quantification using evidence theory in multidisciplinary design optimization", Reliability Engineering and System Safety, Vol. 85, 281-294, 2004.

2. Ai-ling, C., Gen-ke, Y. and Zhi-ming, W.U., "Hybrid discrete particle swarm optimization algorithm for capacitated vehicle routing problem", Chen et al./ J Zhejiang Univ Science A, Vol. 7(4), 607-614, 2006.

3. Alim, S., "Application of Dempster-Shafer theory for interpretation of seismic parameters", Journal of Structural Engineering, Vol. 114(9), 2070-2084, 1988.

4. Anderson. E., "Product price and warranty terms: an optimization model", Naval Reserach Logistics, Vol. 28, 739-741, 1977.

5. Arora, J.S., Huang, M.W. and Hsieh, C.C., "Method for optimization of nonlinear problems with discrete variables: a review", Structural Optimization, Vol. 8, 69-85, 1994.

6. Arrow, Kenneth J., "Social choice and individual values", 2nd Edition, John Wiley & Sons, New York 1951.

7. Atiqullah, M.M. and Rao, S.S., "Simulated annealing and parallel processing: An implementation for constrained global design optimization", Eng. Opt, Vol. 32, 659-685, 2000.

8. Attardi, L., Guida, M., and Pulcini, G., "A mixed weibull regression model for the wnalysis of wutomotive warranty data", Reliability Engineering and System Safety, Vol. 87, 265-273, 2005.

9. Bae, H.R., "Uncertainty quantification and optimization of structural response using evidence theory", PhD Dissertation, Wright State University, 2004.

10. Baik, J., Murthy, D.N.P., and Jack, N., "Two-dimensional failure modeling with minimal repair", Novel Research Logistics, Vol. 51, 345-362, 2004.

11. Balachandran, K.R., Maschmeyer, R. A. and Livingstone, J. L., "Product warranty period: A Markovian approach to estimation and analysis of repair and replacement costs", The Accounting Review LVI, Vol. 1, 115-123, 1981.

12. Balcer, Y, and Sahin, I., "Replacement costs under warranty: Cost moments and time variability", Operations Research, Vol. 34(4), 554-559, 1986.

13. Banks, A., Vincent, J. and Anyakoha, C., "A review of particle swarm optimization. Part I: background and development", Nat compu, Vol. 6, 467-484, 2007.

14. Barbero, E.J., "Introduction to composite materials design", Taylor & Francis, 1999.

15. Bastiere, A., "Methods for multisensory classification of airborne targets integrating evidence theory", Aerospace Science and Technology, Vol. 2(6), 401-411, 1998.

16. Barlow, R.E., and Proschan, F.," Mathematical theory of reliability", Wiley, New York, 1965.

17. Beer, M., "Uncertain structural design based on nonlinear fuzzy analysis", ZAMM.Z.Angew. Math. Mech, Vol. 84(10-11), 740-753, 2004.

18. Ben-Haim, Y., and Elishakoff, I., "Convex models of uncertainty in applied mechanics", Elsevier Science, Amsterdam, 1990.

19. Beynon, M, Curry, B, and Morgan, P, "The Dempster-Shafer theory of evidence: an alternative approach to multicriteria decision modeling", Omega, Vol. 28, 37-50, 2000.

20. Bhattacharya, P., "On the Dempster-Shafer evidence theory and non-hierarchical aggregation of belief structures", IEEE Transactions on Systems, Man, and Cybernetics-Part A: Systems and Humans, Vol. 30, 526-536, 2000.

21. Biondini, F., Bontempi, F., and Malerba, P.G., "Fuzzy reliability rnalysis of concrete structures", Computers and Structures, Vol. 82, 1033-1052, 2004.

22. Bi, Y. Wu, S., Huang, X. and Guo, G., "Combining multiple sets of rules for improving classification via measuring their closeness", Q.Yang and G.Webb (Eds.): PRICAI, 1068-1072, 2006.

23. Blaquiere, Austin, Francoise Gerard, and George Leitmann, "Quantitative and qualitative games", Academic Press, New York, 1969.

24. Blischke, W.R., "Mathematical models for analysis of warranty policies", Mathl Compt. Modelling, Vol. 13(7), 1-16, 1990.

25. Blischke, W.R., and Murthy, D.N.P., "Product warranty handbook", Marcel Dekker, New York, 1996.

26. Blischke, W.R., and Murthy, D.N.P., "Product warranty management- I: A taxonomy for warranty policies", European Journal of Operation Research, Vol. 62, 127-148, 1992.

27. Blischke, W.R., and Murthy, D.N.P., "Reliability: modeling, prediction, and optimization", John Wiley and Sons, New York, 2000.

28. Blischke, W.R., and Murthy, D.N.P., "Warranty cost analysis", Marcel Dekker, New York, 1994.

29. Blischke, W.R., and Schaeuer, E.M.,"Applications of renewal theory on analysis of the free-replacement warranty", Novel Research Logistics, Vol. 28, 193-205, 1981.

30. Blischke,W.R. and Scheuer, E.M., "Calculation of the cost of warranty policies as a function of estimated life distribution", Naval Research Logistics, Vol. 22(4), 681-696, 1975.

31. Bloch, I., "Some aspects of Dempster-Shafer evidence theory for classification of multi-modality medical images taking partial volume effect into account", Pattern Recognition Letters Vol. 17(8), 905-919, 1996.

32. Bonarini, A., Bontempi. G., "A Qualitative simulation approach for fuzzy dynamical models", ACM TOMACS 4, 1994.

33. Boston, J. R., "A signal detection system based on Dempster-Shafer theory and comparison to fuzzy detection", IEEE Transactions on Systems Man and Cybernetics Part CApplications and Reviews Vol. 30(1), 45-51, 2000.

34. Boston, J.R., Baloa, L., Liu, D., Simaan, M.A., Choi, S., and Antaki, J., " Combination of data approaches to heuristic control and fault detection", In Proceeding of IEEE Conference on Control Applications, Vol. 1, 98-103, 2000.

35. Borotschnig, H., Paletta, L., Prantl, M. and Pinz, A., "A Comparison of probabilistic, possibilistic and evidence theoretic fusion scheme for active object recognition", Computing, Vol. 62, 293-319, 1999.

36. Butler, A.C, Sadeghi, F, Rao, S. S and LeClair, S. R., "Computer-aided design/engineering of bearing systems using Dempster-Shafer theory", Artificial Intelligence for Engineering Design, Analysis and Manufacturing, Vol. 9, 1-11, 1995.

37. Cao, K. and Zhu, Q., "Belief combination for uncertainty reduction in microarray gene expression pattern analysis", Y.Shi et al. (Eds.): ICCS, 844-851, 2007.

38. Cai, Y.P., Huang, G.H., Lu, H.W., Yang, Z.F. and Tan, Q., "An interval valued fuzzy robust programming approach for municipal waste management planning under uncertainty", Engineering Optimization, Vol. 41, 399-418, 2009.

39. Campos, F. and Souza, F.M.C., "Extending Dempster-Shafer theory to overcome counter intuitive results", Proceeding of NLP-KE, 729-734, 2005.

40. Cao, Y.J. and Wu, Q.H., "Mechanical design optimization by mixed variable evolutionary programming", Electrical Engineering and Electronics, 443-446, 1997.

41. Chandramohan, A., Rao, M.V. and Arumugam, M.S., "Two new and useful defuzzyfication methods based on root mean square value", Soft Comput, Vol. 10, 1047-1059, 2006.

42. Chang, Y.C., Wright, J.R., and Engel, B.A., "Evidential reasoning for assessing environmental impact", Civil Engineering Systems, Vol. 14(1), 55-77, 1996.

43. Chen, L. and Rao, S.S., "A modified Dempster-Shafer theory for multicriteria optimization", Engineering Optimization, Vol. 30(3-4), 177-201, 1998.

44. Chen, S.Q., "Comparing probabilistic and fuzzy set approach for design in the presence of uncertainty", PhD Dissertation, Virginia Polytechnic Institute and State University, 2000.

45. Chukova S., and Hayakawa Y., "Warranty cost analysis: non-renewing warranty with repair time", Applied Stochastic Models in Business and Industry, Vol. 20, 59-71, 2004.

46. Chukova, S.S., Dimitrov, B.N., and Rykov, V.V., "Warranty Analysis", Plenum Publishing Corporation, Vol. 2, 3486-3508, 1993.

47. Chun Y.H. and Kwei T., "Cost analysis of two-attribute warranty policies on the product usage rate", IEEE Transactions on Engineering Management, Vol. 46(2), 201-209, 1999.

48. Coello coello, C.A., "A proposal for multiobjective particle swarm optimization", In Congress on Evolutionary Computation, Piscataway, Newjersery, USA, IEEE Service Center, Vol. 2, 1051-1056, 2002.

49. Coello Coello, C.A., "Use of a self-adaptive penalty approach for engineering optimization problems", Computers Industry, Vol. 41, 113-127, 2000.

50. Curley, S.P., "The application of dempster shafer theory demonstrated with justification provided by legal evidence", Judgment and Decision Making, Vol. 2, 257-276, 2007.

51. Deb, K., “Optimal design of a welded beam via genetic algorithms”, AIAA Journal, Vol. 29, 2013-2015, 1991.

52. Deb, K., Gene, A.S., “A robust optimal design techniques for mechanical component design”, In Evolutionary Algorithms in Engineering Applications, Edited by D. Dasgupta and Z. Michalewicz, 497-514, 1997(Springer-Verlag: Berlin).

53. Deb, K., Pratap, T., Agarwal, S., and Meyarivan, T., “A fast and elitist multi-objective genetic algorithm: NSGA-II”, IEEE Trans. on Evolutionary Computation, Vol. 6(2), 182-197, 2002.

54. Dempster, A. P., “Upper and lower probabilities induced by a multivalued mapping”, The Annals of Statistics, Vol. 28, 325-339, 1967.

55. Dempster, A.P., “The dempster shafer calculus for statisticians”, Harvard University, 2007.

56. Deng, H. and Yeh, C.H., “Simulation based evaluation of defuzzification based approaches to fuzzy multiattribute decision making”, IEEE Transaction on Systems, Man and Cybernetics-Part A: Systems and Humans, Vol. 36(5), 2006.

57. Deutsch-McLeish, M, “A Study of probabilities and belief functions under conflicting evidence: comparisons and new methods”, University of Guelph, Vol. 521, 41-49, 1991.

58. Dhingra, A.K. and Rao, S.S., “A cooperative fuzzy game theoretic approach to multiple objective design optimization”, European Journal of Research, Vol. 83, 547-567, 1995.

59. Dhingra, A.K. and Rao, S.S., “An Integrated kinematic-kineto static approach to optimal design of planar mechanisms using fuzzy theories”, ASME Journal of Mechanical Design, Vol. 113(3), 306-311, 1991.

60. Dhingra, A.K., Rao S.S., and Miura, H., “Multiobjective decision making in a fuzzy environment with applications to helicopter design”, AIAA Journal, Vol. 28, 703-710, 1990.

61. Dong, W. M., and Shah, H. C., “Vertex method for computing functions of fuzzy variables”, Fuzzy Sets and Systems, Vol. 24, 65-78, 1987.

62. Downton, F., “Bivariate exponential distributions in reliability theory”, Journal of Royal Statistical Society B, Vol. 32,408-417, 1970.

63. Eberhart, R.C. and Shi, Y., "Comparing inertia weights and constriction factors in particle swarm optimization", In Proc. of the 2000 Congress on Evolut Comput., Vol. 1, 84-88, 2000.

64. Elbeltagi, E., Hegazy, T. and Grierson, D., "Comparison among five evolutionary based optimization algorithms", Advanced Engineering Informatics, Vol. 19, 43-53, 2005.

65. Eliashberg, J., Singpurwalla, N.D., and Wilson, S.P., "Calculating the reserve for a time and usage indexed warranty", Management Science, Vol. 43(7), 966-975, 1997.

66. Ferson, S., Kreinovich, V Ginzburg, L., Myers, D. S. and Sentz, K., "Constructing probability boxes and Dempster-Shafer structures", SAND Report, 2003.

67. Foo, J.L., Kalivarapu, V.K. and Winer, E., "Implementation of digital pheromones for use in particle swarm optimization", AIAA, 2006.

68. Frees, E.W., "Warranty analysis and renewal function estimation", Naval Research Logistics Quarterly, Vol. 33, 361-372, 1986.

69. Frees, E.W., and Nam, S.H., "Approximating expected warranty costs", Management Science, Vol. 34, 1441-1449, 1988.

70. Fu, J.F., Fenton, R.G. and Cleghorn, W.L., "A mixed integer-discrete-continuous programming method and its application to engineering design optimization", Engineering Optimization, Vol. 17, 263-280, 1991.

71. George, T. and Pal, N.R., "Quantification of conflict in dempster shafer framework: a new approach", International Journal of General Systems, Vol. 24(4), 407-423, 1996.

72. Glickman, T.S. and Berger, P.D., "Optimal price and protection period decisions for a product under warranty", Management Science, Vol. 22, 1381-1389, 1976.

73. Hajela, P. and Shih, C.J., "Multiobjective optimum design in mixed integer and discrete design variable problems", AIAAA Journal, Vol. 28 (4), 670-675, 1990.

74. Ha-Rok, B., "Uncertainty quantification and optimization of structural response using evidence theory", PhD Dissertation, Wright State University, 2004.

75. Halpern, J.Y. and Fagin, R., "Two views of belief: belief as generalized probability and belief as evidence", Artificial Intelligence, Vol. 54, 275-317, 1992.

76. He, S., Prepain, E. and Wu, H., "An improved particle swarm optimizer for mechanical design optimization problems", Engineering Optimization, Vol. 3, 585-605, 2004.

77. Hori, S., Tanaka, K. and Wang, H.O., "Multiobjective structure design for mechanical systems", IEEE, 116-121, 2002.

78. Huang, H.Z., Gu, Y.K. and Du, X., "An interactive fuzzy multiobjective optimization method for engineering design", Engineering Application of Artificial Intelligence, Vol.19, 451-460, 2006.

79. Hu, X., Eberhart, R.C. and Shi, Y., "Engineering optimization with particle swarm", In IEEE Swarm Intelligence Symposium, Indianapolis, IN, 2003.

80. Hu, X. and Eberhart, R.C., "Solving constrained nonlinear optimization problems with particle swarm optimization", in Proc. of the 6th World Multiconference on Systemics, Cybernetics and Informatics, Orlando, 2002.

81. Hu, Y., Gao, J., Hu, L. M. and Dong, H.M., "A New method of determining the basic belief assignment in D-S Evidence theory", Proceeding of the Second International Conference on Machine learning and cybernetics, Xi'an, IEEE, 3208-3211, 2003.

82. Hu, X.J., Lawless, J.F., and Suzuki, K., " Nonparametric estimation of a lifetime distribution when censoring times are missing", Technometrics, Vol. 40, 3-13, 1998.

83. Inagaki, T., "Interdependence between safety-control policy and multiple-sensor Schemes via Dempster-Shafer theory", IEEE Transactions on Reliability, Vol. 40(2), 182-188, 1991.

84. Isaacs, Rufus, "Differential games", John Wiley and Sons, Inc., New York, 1965.

85. Iskandar, B.P. and Murthy, D.N.P., "Repair-replace stratergies for two-dimensional warranty policies", Mathematical and Computer Modelling, Vol. 38, 1233-1241, 2003.

86. Iskandar, B.P., Murthy, D.N.P., and Jack N., "A new repair-replace stratergy for items sold with a two-dimensional warranty", Computers and Operations Research, Vol. 32, 669-682, 2005.

87. Iskandar, B.P., Wilson, R.J., and Murthy, D.N.P., "Two-dimensional combination warranty policies", RAIRO=Operations Research, Vol. 28(1), 57-75, 1994.

88. Izui, K., Nishiwaki, S. and Yoshimura, M., "Swarm algorithm for single- and multi-objective optimization problems incorporating sensitivity analysis", Engineering Optimization, Vol. 39, 981-998, 2007.

89. Jack, N., and Schouten, F.V.D., "Optimal repair-replace strategies for a warranted product", Int. J. production Economics, Vol. 67, 95-100, 2000.

90. Jack, N., and Murthy, D.N.P., "A Servicing stratergy for items sold under warranty", Journal of Operational Research Society, Vol. 52, 1284-1288, 2001.

91. James, R.B., "Warranties planning, analysis and implementation", McGraw-Hill, Inc., New York, 1994.

92. Jayaraman, R., "On minimizing expected warranty costs in 1-dimension and 2-dimensions with different repair options", PhD Dissertation, University of Texas tech, 2008.

93. Jiang, J., Guo, J., Luo. P.F., Sheng, Lie, F.S., and Sun, Z.K., "Multisensor multipleattribute data association", In Proceedings., CIE International Conference of Radar 393 – 396, 1996.

94. Joines, J.A. and Houck, C.R., "On the use of non stationary penalty functions to solve nonlinear constrained optimization problems with genetic algorithms", In Proc. Of the First IEEE Conf. on Evolut. Compu., 579-584, 1994.

95. Jones, R.M., "Mechanics of composite materials", Hemisphere Publishing Corporation, 1975.

96. Joshi, A, V., Sahasrabudhe, S.C. and Shankar, K., "Sensitivity of combination schemes under conflicting conditions and a new method", Indian Institute of Technology, Vol. 991, 1995.

97. Jousselme, A.L., Grenier, D. and Bosse, E., "Anew distance between two bodies of evidence", Information Fusion, Vol. 2, 91-101, 2001.

98. Jousselme, A.L., Liu, C., Grenier, D. and Bosse, E., "Measuring ambiguity in the evidence theory", IEEE Transactions on systems, Man, and Cybernetics Part A: Sustems and Humans, 2005.

99. Kangas, A.S. and kangas, J., "probability, possibility and evidence: approach to consider risk and uncertainty in forestry decision analysis", Forest Policy and Economics, Vol. 6, 169-188, 2004.

100. Kaufmann, A. and Gupta, M.M., "Introduction to fuzzy arithmetic", Van Nostrand Reinhold Company Inc., 1985.

101. Kendall, D. G., "Foundations of a theory of random sets in:harding", E., and D. Kendall (eds.), Stochastic Geometry, New York, 322-376, 1974.

102. Kennedy, J. and Eberhart, R.C., "A discrete binary version of the particle swarm algorithm", IEEE, 4104-4108, 1997.

103. Kennedy, J. and Eberhart, R.C., "Particle swarm optimization", in Pros. of IEEE International Conference on Neural Networks, 1942-1948, 1995 (IEEE Press: Piscataway, NJ).

104. Kenney, R.L., and Raiffa, H., "Decisions with multiple objectives: preferences and value tradeoffs", John Wiley, New York, 1976.

105. Kickert, Walter, J. M., "Fuzzy theories on decision-making", Martinus Nijhoff Social Sciences Division, Leiden, 1978.

106. Kim, H. G. and Rao, B. M., "Expected warranty cost of two-attribute free-replacement warranties based on a bivariate exponential distribution", Computers & Industrial Engineering, Vol. 38, 425-434, 2000.

107. Kiran, K. A. and Rao, S. S., "Multi-objective optimization of engineering systems using game theory and particle swarm optimization", Engineering Optimization, 2009 (Accepted)

108. Kitayama, S., Arakawa, M. and Yamazaki, K., "Penalty function approach for the mixed discrete nonlinear problems by particle swarm optimization", Struct Multidisc Optim, Vol. 32, 191-202, 2006.

109. Kitayama, S. and Yasuda, K., "A method for mixed integer programming problems by particle swarm optimuzation", Electrical Engineering, Vol. 157, 40-49, 2006.

110. Klir, G.J. and Wierman, M. J., "Uncertainty-based information: elements of generalized information theory", Physica-Verlag, Heidelberg, 1998.

111. Kohlas, J. and Monney, P.A., "Theory of evidence—a survey of its mathematical foundations, applications and computational aspects", Mathematical Methods of Operations Research Vol. 39, 35-68, 1994.

112. Kolakowski, Z., "On some aspects of the modified Tsai-wu criterion in thin walled composite structures", Thin-Walled Structures, Vol. 41, 357-574, 2003.

113. Köyluoglu, U., Cakmak, A.S., and Nielsen, S. R. K., "Interval algebra to deal with pattern loading and structural uncertainties", Journal of Engineering Mechanics, Vol. 121, 1149-1157, 1995.

114. Kozine, I. O. and Utkin, L. V., “An approach to combining unreliable pieces of evidence and their propagation in a system response analysis”, Reliability Engineering and System Safety, Vol. 85, No. 1-3, 103-112, 2004.

115. Krinck, T., Vestertroem, J.S. and Riget, J., “Particle swarm optimization with spatial particle extension”, Proceedings of the IEEE Congress on Evolutionary Computation (CEC 2002), Hawaii, 2002.

116. Krivtsov, V., and Frabkstein, M., ” Automotive component reliability: should it be measured in time or mileage?”, IEEE, 601-603, 2006.

117. Kuhn, H.W., and Tucker, A.W., “Nonlinear programming”, In Proceedings of Second Berkeley Symposium, Math. Stat. Prob., 481-492, 1951.

118. Kurupati, A. and Azaram, S., “Immune network simulation with multiobjective genetic for multidisciplinary design optimization”, Eng. Opt., Vol. 33, 245-260, 2000.

119. Kurpati, A., Azarm, S. and Wu, J., “Constraint handling improvements for multiobjective genetic algorithms”, Struct Multidisc Optim, Vol. 23, 204-213, 2002.

120. Laskey, K. B. and Cohen, M. S., “Applications of the Dempster-Shafer theory of evidence for simulation”, Proceedings of the 18th Conference on Winter Simulation, 440-444, 1986.

121. Lawless, J., Hu, J., and Cao, J., “Methods for the estimation of failure distributions and rates from automotive warranty data”, Lifetime Data Analysis, Vol. 1, 227-240, 1995.

122. Leadbetter, M.R.,” On Series expansion for the renewal moments”, Biometrika, Vol. 50, 75-80, 1963.

123. Lefevre, E., Colot, O. and vannooreberghe, P., “Belief function combination and conflict management”, Information Fusion, Vol. 3, 149-162, 2002.

124. Levi, F., Gobbi, M. and Mastinu, G., “An application of multi objective stochastic optimization to structural design”, Struct Multidisc Optim, Vol. 29, 272-284, 2005.

125. Liu, J., Fan, X. and Qu, Z., “An improved particle swarm optimization with mutation based on similarity”, Third International Conference on Natural Computation, IEEE, 2007.

126. Liu, J.L. and Lin, J.H., "Evolutionary computation of unconstrained and constrained problems using a novel momentum-type particle swarm optimization", Engineering Optimization, Vol. 39, 287-305, 2007.

127. Liu, X.W., "Parameterized defuzzification with maximum entropy weighting function another view of the weighting function expectation method", Mathematical and Computer Modelling, Vol. 45, 177-188, 2007.

128. Liu, W., "Analyzing the degree of conflict among belief functions", Artificial Intelligence, Vol. 170, 909-924, 2006.

129. Luna, M., "Interval analysis-based multi-objective optimization of wing structures", PhD Dissertation, University of Miami, 2007.

130. Luo, Z. and Li, D., "Multi-source information integration in intelligent systems using the plausibility measure", IEEE International Conference on Multisensor Fusion and Integration for Intelligent Systems: 403- 409, 1994.

131. Majesle, K.D., "A mixture model for automotive warranty data", Reliability Engineering and System Safety, Vol. 81, 71-77, 2003.

132. Majeske, K.D., and Herrin, G.D., "Determining warranty benefits for automobile design changes", Proceeding Annual Reliability and Maintainability Symposium, 94-99, 1998.

133. Mamer, J.W., "Cost analysis of pro-rata and free replacement warranties", Naval Research Logistics Quarterly, Vol. 29(2), 345-356, 1982.

134. Mamer, J.W., "Discounted and per unit costs of product warranty", Management Science, Vol. 33(7), 916-930, 1987.

135. Manna, D.K., Pal, S., and Sinha, S., "A Use-rate failure model for two-dimensional warranty", Computers and Industrial Engineering, Vol. 52, 229-240, 2007.

136. Manna, D.K., Pal, S., and Sinha, S., "Optimal determination of warranty region for 2D policy: A customer perspective", Computers and Industrial Engineering, Vol. 50, 161-174, 2006.

137. Manna, D.K., Pal, S., and Sinha, S., "A note on calculating cost of two-dimensional warranty policy", Computers and Industrial Engineering, Vol. 54, 1071-1077, 2006.

138. Marschak, Jacob, and Roy Radner, "Economic theory of teams", Yale University Press, New Haven, 1972.

139. Menezes, M.A.J., and Currim, I.S., "An approach for determination of warranty length", International Journal of Research in Marketing, Vol. 9, 177-195, 1992.

140. Moller, B., Graf, W., and Bee, M., "Fuzzy structural analysis using α – level optimization", Computational Mechanics, Vol. 26, 547-565, 2000.

141. Moskowitz, H. and Chun, Y.H., "A Bayseian approach to the two-attribute warranty policy", Krannert Graduate School of Management, Purdue University, West Lafayette, Indiana, 950, 1988.

142. Moskowitz, H., and Chun, Y.H., "A Poisson regression model for two-attribute warranty policies", Novel Research Logistics, Vol. 41, 355-376, 1994.

143. Muhanna, R. L. and Mullen, R. L., "Uncertainty in mechanics problems - interval-based approach", Journal of Engineering Mechanics, ASCE, Vol. 127, No. 6, 557-566, 2001.

144. Mullen, R. L., and Muhanna, R. L., "Bounds of structural response for all possible loadings", Journal of Structural Engineering, ASCE, Vol. 125(1), 98-106, 1999.

145. Murphy, C.K., "Combining belief functions when evidence conflicts", Decision Support systems, Vol. 29, 1-9, 2000.

146. Murthy, D.N.P., and Blischke, W.R., "Product warranty management –II: An integrated framework for study", European Journal of Operations Research, Vol. 62, 261- 281, 1992.

147. Murthy, D.N.P., and Blischke, W.R., "Product warranty management –III: A review of mathematical models", European Journal of Operations Research, Vol. 62, 1-34, 1992.

148. Murthy, D.N.P., "A usage dependent model for warranty costing", European Journal of Operations Research, Vol. 57, 1, 89-99, 1992.

149. Murphy, R. R., "Dempster-Shafer theory for sensor fusion in autonomous mobile robots", IEEE Transactions on Robotics and Automation Vol. 14(2), 197-206, 1998.

150. Murthy, D.N.P., Iskandar, B.P., and Wilson, R.J., "Two-dimensional failure-free warranty policies: two-dimensional point process models", Operations Research, Vol. 43, 356-366, 1995.

151. Murthy, D.N.P., Xie, M, and Jiang, R., "Weibull model", John Wiely and Sons, New York, 2003.

152. Myrick, A., "Analysis of warranty cost based on reliability", Proceeding Annual Reliability and Maintainability Symposium, 228-232, 1990.

153. Naka, S., Genji, T. and Yura, T. and Fukuyama, Y., "Particle distribution state estimation using hybrid particle swarm optimization", in Proc. of IEEE Power Engineering Society Winter Meeting, Columbus, Ohio, 2001.

154. Nash, J., "The bargaining problem", Econimetrica, Vol. 18, 155-162, 1950.

155. Nguyen, D.G., and Murthy D.N.P., "A general model for estimating warranty costs for repairable products", IIE Transactions, Vol.16, 379-386, 1984b.

156. Nguyen, D.G., and Murthy, D.N.P., "An optimal policy for serving warranty", Operational Research Society, Vol. 37(11), 1081-1088, 1986a.

157. Nguyen, D.G., and Murthy, D.N.P., "Cost analysis of warranty policies", Naval Research Logistics, Vol. 31, 525-541, 1984b.

158. Nguyen, D.G., and Murthy, D.N.P., "Optimal replace-repair strategy for servicing products sold with warranty", European Journal of Operational Research, Vol. 39, 206-212, 1989.

159. Oberkampf, W. L., and Helton J. C., "Investigation of evidence theory for engineering applications," Non-Deterministic Approaches Forum, Paper No. AIAA-2002-1569, 2002.

160. Pang, W. Wang, K.P., Zhou, C.G. and Dong, L.J., Modified "Fuzzy discrete particle swarm optimization for solving travelling salesman problem", Proceeding of the Fourth International Conference on Computer and Information Technology, IEEE, 2004.

161. Pant, M., Radha, T. and Singh, V. P., "A new technique for efficient initialization applied to particle swarm optimization", International Conference on Computer Aided Engineering, 760-767, 2007.

162. Parikh, C. R., Pont, M. J and Jones, N. B, "Application of Dempster- Shafer Theory in condition monitoring systems: A case study", Pattern Recognition Letters, Vol. 22(6-7), 777-785, 2001.

163. Patankar, J.G., and Mitra, A., "A Multi objective model for warranty cost estimation using multiple products", Computer Operations Research, Vol. 16(4), 341-351, 1989.

164. Peer, E., Vanden Bergh, F., and Engelbrecht, A., "Using neighborhoods with the generated convergence PSO", In swarm Intelligence Symposition, Piscataway, Newjersey, USA, IEEE Service Center, 235-242, 2003.

165. Perez, R.E. and Behdinan, K., "Particle swarm approach for structural design optimization", Computers and Structures, Vol. 85, 1579-1588, 2007.

166. Rao, S.S. and Freiheit, T.I., "A modified game theory approach to multi-objective optimization", Journal of Mechanical Design (ASME), Vol. 113, 286-291, 1991.

167. Rao, S.S. and Sawyer, P., "Fuzzy finite element approach for the analysis of imprecisely defined systems", AIAA Journal, Vol. 33(12), 2364-2370, 1995.

168. Rao, S.S., "Description and optimum design of fuzzy mechanical systems", Transaction of the ASME, Vol. 109, 391-408, 1998.

169. Rao, S. S., "Engineering optimization theory and practice", 3rd Edition, John Wiley, New York, 1996.

170. Rao, S.S., "Game theory approach for multi-objective structural optimization", Computer & Structures, 25, 119-127, 1987.

171. Rao, S.S., "Multiobjective optimization of fuzzy structural system", International Journal for Numerical Methods in Engineering, Vol. 24, 1157-1171, 1987.

172. Rao, S.S., "Optimum design of structures in a fuzzy environment", AIAA Journal, Vol. 25, 1633-1636, 1987.

173. Rao, S.S., "Reliability-based design", McGraw- Hill, New York, 1992.

174. Rao, S.S., Venkayya, V.B., and Khot, N.S., "Game theory approach for the integrated design of structures and controls", AIAA Journal, Vol. 26(4), 463-469, 1988.

175. Ray, T. and Liew, K.M., "Society and civilization: An optimization algorithm based on the simulation of social behavior", IEEE Trans. on Evolut. Comput., Vol. 7, 386-396, 2003.

176. Reddy, J.N., "Mechanics of composite materials: selected works of Nicholas J. Pagano", Kluwer Academix Publishers, 1994.

177. Reddy, J.N., "Mechanics of laminated composite plates and shells, Theory and Analysis", CRC Press, Boca Raton, 2004.

178. Reddy, M.J. and Kumar, D.N., "An efficient multi-objective optimization algorithm based on swarm intelligence for engineering design", Engineering Optimization, Vol. 39, 49-68, 2007.

179. Ritchken, P.H., and Tapiero, C.S., "Warranty design under buyer and seller risk aversion", Naval Research Quarterly, Vol. 33, 657-671, 1986.

180. Ross, T. J., "Fuzzy logic with engineering applications", McGraw-Hill, Inc., 1995.

181. Ruthven, I. and Lalmas, M., "Using Dempster Shafer's theory of evidence to combine aspects of information use", Journal of Intelligent Information System, Vol. 19(3), 267-301, 2002.

182. Sahin, I. and Polatoglu, H., "Maintenance strategies following the expiration of warranty", IEEE Transactions on reliability. Vol. 45(2), 220-228, 1996.

183. Sahin, I., "Conformance quality and replacement costs under warranty", Production and Operations Management. Vol. 2(4), 242-261, 1993.

184. Salukvadze, M. E., "Vector-valued optimization problems in control theory", Academic Press, New York, 1979.

185. Sentz, K., "Combination of evidence in Dempster-Shafer theory", PhD Dissertation, Binghamton University, 2002.

186. Shafer, G., "A Mathematical theory of evidence", Princeton University Press, Princeton, NJ, 1976.

187. Shenoy, P. P., "Using Dempster-Shafer's belief-function theory in expert systems", In Proceedings of SPIE The International Society for Optical Engineering, Vol. 2(14), 1992.

188. Shukla, S.K., "Teaching game theory for computer engineering", Proceeding of the IEEE International Conference on Microelectronic Systems Education, 2005.

189. Sim, K.B. and Kim, J.Y., "Solution of multiobjective optimization problems: coevolutionary algorithm based on evolutionary game theory", Artif Life Robotics, Vol. 8, 174-185, 2004.

190. Smarandache, F., "An in-depth look at information fusion rules and the unification of fusion theories", University of New Mexico, 2004.

191. Smets, P., "Analyzing the combination of conflicting belief functions", Information Fusion Vol. 8, 387-412, 2007.

192. Smets, P., "The transferable belief model for expert judgements", Analysis and Management of Uncertainty: Theory and Applications. B. M. Ayyub, M. M. Gupta and L. N. Kanal. New York, North-Holland. Vol. 13, 165-170, 1992.

193. Smith, R.M. and Klir, G.J., "On measuring uncertainty in evidence theory", IEEE, 317-321, 1999.

194. Song, M.P. and Gu, G.C., "Research on particle swarm optimization: A review", Proceeding of the Third International Conference on Machine Learning and Cybernetics, Shanghai, IEEE, 26-29, 2004.

195. Straffin, Philip D., "Game theory and strategy", The Mathematical Association of America, 1993.

196. Summit, R., and Cerone, P., "Costing a new car warranty", Asia-Pacific Journal of Operation Research, 20, 89-101, 2003.

197. Sunar, M. and Kahraman, R., "A comparative study of multi-objective optimization methods in structural design", Turk J Engin Environ Sci, Vol. 25, 69-78, 2001.

198. Suresh, S., Sujit, P.B. and Rao, A.K., "Particle swarm optimization approach for multiobjective composite box beam design", Composite Structures, Vol. 81, 598-605, 2007.

199. Syan, Y.R., Lee, E.S. and Jia, L., "Convexity and upper semi continuity of fuzzy sets", Computers and Mathematical with application, Vol. 48, 117-129, 2004.

200. Tchamova, A., "Evidence reasoning theory with application to the identity estimation and data association systems", Mathematics and Computers in Simulation Vol. 43, 139-142, 1997.

201. Thomas, M.U., "Optimal warranty policies for non-repairable products", IEEE Transactions on Reliability, Vol. 32(3), 282-288, 1983.

202. Tianlu, C. and Peiwen, Q., "Target recognition based on modified combination rule", Journal of Systems Engineering and Electronics, Vol. 17, 279-283, 2006.

203. Tonon, F. and Bernardini, A., "A random set approach to the optimization of uncertain structures", Computers and Structures, Vol. 68, 583-600, 1998.

204. Van den bergh, F., "An analysis of particle swarm optimizers", PhD Dissertation, Department of Computer Science, University of Pretoria, Pretoria, South Africa, 2002.

205. Vasseur, P., Pegard, C., Mouaddib, E.M., and Delahoche, L., "Perceptual organization approach based on Dempster-Shafer theory", Pattern Recognition Vol. 32(8), 1449-1462, 1999.

206. Venter, G. and Sobieszczanski-Sobieski, J., "Particle swarm optimization", AIAA J, Vol. 41(7), 1583-1589, 2003.

207. Vincent, T.L., and Grantham, W.J., "Optimality in parametric systems", John Wiley and Sons, New York, 1981.

208. Vincent, T.L., "Game theory as a design tool", ASME Journal of Mechanisms, Transmissions, and Automated Design, Vol. 105, 1983.

209. Von Neumann, J., and Morgenstern, O., "Theory of games and economic behavior", Princeton University Press, Princeton, 1944.

210. Voorbraak, F, "On the justification of Dempster's rule of combination", Artificial Intelligence, Vol. 48, 171-197, 1991.

211. Walley, P., "Statistical reasoning with imprecise probabilities", Chapman and Hall, London, 1991.

212. Wang, Y, Qiao, Y, and Pei, Z, "Combining evidence and its application in synthesis decision", Proceeding of the Second International Conference on Machine Learning and Cybernetics, Xi'an, IEEE, 1796-1801, 2003.

213. Wood, K.L, Otto, K.N., and Antonsson, E.K., "Engineering design calculations with fuzzy parameters, Fuzzy Sets and Systems", Vol. 52, 1-20, 1992.

214. Yager, R., "On the Dempster-Shafer framework and new combination rules", Information Sciences, Vol. 41, 93-137, 1987.

215. Yokota, T., Taguchi, T. and Gen, M., "A solution method for optimal cost problem of welded beam by using genetic algorithms", Computer and Industrial Engineering, Vol. 37, 379-382, 1997.

216. Yong, D., WenKang, S., ZhenFu, Z. and Qi, L., "Combining belief functions based on distance of evidence", Decision Support Systems, Vol. 38 489-493, 2004.

217. Yu, M., and Xu, C., "Multi-objective fuzzy optimization of structures based on generalized fuzzy decision-making", Vol. 53(2), 411-417, 1994.

218. Zadeh, L.A., "A Simple view of the dempster shafer theory of evidence and its implication for the rule of combination", The Ai Magazine Summer, 85-90, 1986.

219. Zadeh, L. A., "Fuzzy sets as a basis for a theory of possibility", Fuzzy Sets and Systems, Vol. 1, 3-28, 1978.

220. Zadeh, L., “Fuzzy sets”, IEEE Information Control, Vol. IC-8, 338–353, 1965.

221. Zhang, L., ” Representation, independence, and combination of evidence in the Dempster-Shafer theory”, Advances in the Dempster-Shafer Theory of Evidence, R. R. Yager, J. Kacprzyk and M. Fedrizzi. New York, John Wiley & Sons, Inc.: 51-69, 1994.

222. Zhou, C.L., Kang, S.W., Yong, D. and Fu, Z.Z., “A new fusion approach based on distance of evidences”, Journal of Zhejiang University Science, 476-482, 2005.

Appendix-A

A description of the steps involved in the application of the various combination rules considered in this study is given below for two examples: The robbery example, with evidences as indicated in Table 4.2, and the automobile example, with evidences as shown in Table 4.4.

Robbery Example:

(i) Dempster's rule

Step 1: Using Dempster's rule, calculate the combined bpa values as shown in Table A.1.

Table A.1 Combination of bpa values for sources E_1 and E_2

E_1 / E_2	$m\{A\} = 0.5$	$m\{B\} = 0.1$	$m\{C\} = 0.1$	$m\{\Theta\} = 0.3$
$m\{A\} = 0.6$	0.30	0.06	0.06	0.18
$m\{B\} = 0.1$	0.05	0.01	0.01	0.03
$m\{C\} = 0.1$	0.05	0.01	0.01	0.03
$m\{\Theta\} = 0.2$	0.10	0.02	0.02	0.06

Step 2: Determine the value of k, using equation (4.3), as

$$k = 0.06 + 0.06 + 0.05 + 0.01 + 0.05 + 0.01 = 0.24$$

Step 3: Using DST combination rule (equation (4.1)), find the values of bpa as:

$$m\{A\} = \frac{0.30 + 0.18 + 0.1}{1 - 0.24} = 0.7631$$

$$m\{B\} = \frac{0.01 + 0.03 + 0.02}{1 - 0.24} = 0.0789$$

$$m\{C\} = \frac{0.01 + 0.03 + 0.02}{1 - 0.24} = 0.0789$$

$$m\{\Theta\} = \frac{0.06}{1 - 0.24} = 0.0789$$

Step 4: Compute the belief values as $Bel\{A\} = m\{A\} = 0.7631$, $Bel\{B\} = m\{B\} = 0.0789$ and $Bel\{C\} = m\{C\} = 0.0789$.

Step 5: Find the plausibility values, using equation (3.10), as $Pl\{\text{A}\} = 1 - Bel\{B\} - Bel\{C\} = 0.8421$, $Pl\{B\} = 0.1578$ and $Pl\{C\} = 0.1578$.

(ii) Yager's rule

Step 1: compute the combined ground probability mass assignments, using equation (4.7) to obtain $q\{A\} = 0.58, q\{B\} = 0.06$ and $q\{C\} = 0.06$.

Step 2: Determine the ground probability mass assignments to the null set and the universal set using exactly the same procedure as in the case of Dempster's rule except for the normalization to obtain $q\{\phi\} = 0.24$ and $q\{\Theta\} = 0.06$.

Step 3: Find the basic probability assignment of the universal set, using equation (4.9), as $m^{Y}\{\Theta\} = 0.30$.

Step 4: Calculate the belief values *Bel{A}* = *q{A}* = 0.58, *Bel{B}* = *q{B}* = 0.06 and *Bel{C}* = *q{C}* = 0.06.

Step 5: Determine the plausibility values, using equation (3.10), as *Pl{A}* = 1 - *Bel{B}* - *Bel{C}* = 0.88, *Pl{B}* = 0.36 and *Pl{C}* = 0.36.

(iii) Inagaki's extreme rule

Step 1: Calculate the ground probability mass assignment to the null set, $q\{\phi\}$, and the universal set, $q\{\Theta\}$, using exactly the same procedure as in the case of Yager's rule: $q\{\phi\} = 0.24$ and $q\{\Theta\} = 0.06$.

Step 2: With the value of $p = \dfrac{1 - q(\Theta)}{1 - q(\phi) - q(\Theta)} = 1.3428$, equation (4.23) is used to obtain

$m^U\{A\} = 0.58 * p = 0.7788, \quad m^U\{B\} = 0.06 * p = 0.0805$ and $m^U\{C\} = 0.06 * p = 0.0805.$

Step 3: Determine the belief values as *Bel{A}* = $m^U\{A\}$ = 0.7788, *Bel{B}* = 0.0805 and *Bel{C}* = 0.0805.

Step 4: Find the plausibility values, using equation (3.10), as *Pl{A}* = 0.8388, *Pl{B}* = 0.1405 and *Pl{C}* = 0.1405.

(iv) Zhang's rule

Step 1: Compute the combined bpa values as in the case of Dempster's rule (Table A.1).

Step 2: Indicate the intersection measures (r) for the combined bpa values from sources E_1 and E_2 as shown in Table A.2 (values are assumed to be known from the data of the problem).

Step 3: Determine the combined bpa values from sources E_1 and E_2 using Zhang's rule (Eq. (4.31) without multiplying with the re-normalization constant $\widetilde{k}$) as shown in Table A.3.

Table A.2 Values of intersection measure (*r*) for combined bpa values from sources E_1 and E_2

E_1 / E_2	$m\{A\} = 0.5$	$m\{B\} = 0.1$	$m\{C\} = 0.1$	$m\{\Theta\} = 0.3$
$m\{A\} = 0.6$	1	0	0	1/3
$m\{B\} = 0.1$	0	1	0	1/3
$m\{C\} = 0.1$	0	0	1	1/3
$m\{\Theta\} = 0.2$	1/3	1/3	1/3	1/3

Table A.3 Combined bpa values from sources E_1 and E_2 using Zhang's rule before re-normalization

E_2 \ E_1	$m\{A\}=0.5$	$m\{B\}=0.1$	$m\{C\}=0.1$	$m\{\Theta\}=0.3$
$m\{A\}=0.6$	0.3	0	0	0.06
$m\{B\}=0.1$	0	0.01	0	0.01
$m\{C\}=0.1$	0	0	0.01	0.01
$m\{\Theta\}=0.2$	0.03333	0.006666	0.006666	0.02

Step 4: Re-normalizing the combined bpa values given in Table A.3 as indicated in Table A.4

Table A.4 Combined bpa values from sources E_1 and E_2 using Zhang's rule after re-normalization

E_1 / E_2	$m\{A\} = 0.5$	$m\{B\} = 0.1$	$m\{C\} = 0.1$	$m\{\Theta\} = 0.3$
$m\{A\} = 0.6$	0.642857	0	0	0.128571
$m\{B\} = 0.1$	0	0.021428	0	0.021428
$m\{C\} = 0.1$	0	0	0.021428	0.021428
$m\{\Theta\} = 0.2$	0.071429	0.014285	0.014285	0.042857

Step 5: Find the value of bpa values using Zhang's rule (equation (4.27) to obtain $m\{A\} = 0.842857, m\{B\} = 0.057143,\ \ m\{C\} = 0.057143,$ and $m\{\Theta\} = 0.042857.$

Step 6: Calculate the belief values as *Bel{A}* = $m\{A\}$ = 0.842857, *Bel{B}* = $m\{B\}$ = 0.057143 and *Bel*$\{C\}$ = $m\{C\}$=0.057143.

Step 7: Determine the plausibility values from equation (3.10) as *Pl*$\{$A$\}$ = 1 - *Bel{B}* - *Bel{C}* = 0.885714, *Pl{B}* = 0.1 and *Pl{C}* = 0.1.

(v) Murphy's rule

Step 1: Calculate the mean bpa set E_m from E_1 and E_2, and the combined bpa values are calculated as in the case of Dempster's rule.

Step 2: Find the belief values as $Bel\{A\} = m\{A\} = 0.7598$, $Bel\{B\} = m\{B\} = 0.0789$ and $Bel\{C\} = m\{C\} = 0.0789$.

Step 3: Determine the plausibility values using equation (4.2) as $Pl\{A\} = 1 - Bel\{B\} - Bel\{C\} = 0.8421$, $Pl\{B\} = 0.1611$ and $Pl\{C\} = 0.1511$.

Table A.5 Combination of bpa values for sources E_1 and E_2 using Murphy's rule

E_m / E_m	$m\{A\} = 0.55$	$m\{B\} = 0.1$	$m\{C\} = 0.1$	$m\{\Theta\} = 0.25$
$m\{A\} = 0.55$	0.3025	0.055	0.055	0.1375
$m\{B\} = 0.1$	0.055	0.01	0.01	0.025
$m\{C\} = 0.1$	0.055	0.01	0.01	0.025
$m\{\Theta\} = 0.25$	0.1375	0.025	0.025	0.0625

Automobile Example:

(i) Dempster's rule

Step 1: Using Dempster's rule, calculate the combined bpa values as shown in Table A.4.

Table A.6 Combination of bpa values for sources E_1 and E_2

E_1 / E_2	$m\{I\} = 0.5$	$m\{II\} = 0.3$	$m\{\Theta\} = 0.2$
$m\{I\} = 0.6$	0.30	0.18	0.12
$m\{II\} = 0.1$	0.05	0.03	0.02
$m\{\Theta\} = 0.3$	0.15	0.09	0.06

Step 2: Determine the value of *k*, using equation (4.3), as

$$k = 0.18 + 0.05 = 0.23$$

Step 3: Using DST combination rule (equation (4.1)), find the values of bpa as:

$$m\{I\} = \frac{0.30 + 0.12 + 0.15}{1 - 0.23} = 0.74026$$

$$m\{II\} = \frac{0.03 + 0.02 + 0.09}{1 - 0.23} = 0.1818$$

$$m\{\Theta\} = \frac{0.06}{1 - 0.23} = 0.07792$$

Step 4: Compute the belief values as *Bel{I}* = *m*{I} = 0.74026,and *Bel{II}* = *m*{II} = 0.1818.

Step 5: Find the plausibility values, using equation (3.10), as $Pl\{\mathrm{I}\} = 1 - Bel\{II\} = 0.81818$, and $Pl\{II\} = 0.25974$.

(ii) Yager's rule

Step 1: compute the combined ground probability mass assignments, using equation (4.7) to obtain $q\{I\} = 0.57, \text{and } q\{II\} = 0.14$.

Step 2: Determine the ground probability mass assignments to the null set and the universal set using exactly the same procedure as in the case of Dempster's rule except for the normalization to obtain $q\{\phi\} = 0.23$, $q\{\Theta\} = 0.06$.

Step 3: Find the basic probability assignment of the universal set, using equation (4.9), we obtain $m^{Y}\{\Theta\} = 0.29$.

Step 4: Calculate the belief values $Bel\{I\} = q\{I\} = 0.57$ and $Bel\{II\} = q\{II\} = 0.14$.

Step 5: Determine the plausibility values, using equation (3.10), as $Pl\{I\} = 1 - Bel\{II\} = 0.86$ and $Pl\{II\} = 0.43$.

(iii) Inagaki's extreme rule

Step 1: Calculate the ground probability mass assignment to the null set, $q\{\phi\}$, and the universal set, $q\{\Theta\}$, using exactly the same procedure as in the case of Yager's rule: $q\{\phi\} = 0.23 \text{ and } q\{\Theta\} = 0.06$.

Step 2: With the value of $p = \dfrac{1 - q(\Theta)}{1 - q(\phi) - q(\Theta)} = 1.3239$, equation (4.23) is used to obtain $m^{U}\{I\} = 0.57 * p = 0.7546$ and $m^{U}\{II\} = 0.06 * p = 0.0805$.

Step 3: Determine the belief values as $Bel\{I\} = m^U\{I\} = 0.7546$ and $Bel\{II\} = 0.0805$.

Step 4: Find the plausibility values, using equation (3.10), as $Pl\{I\} = 0.81465$ and $Pl\{II\} = 0.24535$.

(iv) Zhang's rule

Step 1: Compute the combined bpa values as in the case of Dempster's rule (Table A.6).

Step 2: Indicate the intersection measures (r) for the combined bpa values from sources E_1 and E_2 as shown in Table A.7 (values are assumed to be known from the data of the problem).

Step 3: Determine the combined bpa values from sources E_1 and E_2 using Zhang's rule (Eq. (4.31) without multiplying with re-normalization constant $\tilde{k}$) as shown in Table A.8.

Table A.7 Values of intersection measure (*r*) for combined bpa values from sources E_1 and E_2

E_2 \ E_1	$m\{I\} = 0.5$	$m\{II\} = 0.3$	$m\{\Theta\} = 0.2$
$m\{I\} = 0.6$	1	0	0.5
$m\{II\} = 0.1$	0	1	0.5
$m\{\Theta\} = 0.3$	0.5	0.5	0.5

Table A.8 Combined bpa values from sources E_1 and E_2 using Zhang's rule before re-normalization

E_1 / E_2	$m\{I\} = 0.5$	$m\{II\} = 0.3$	$m\{\Theta\} = 0.2$
$m\{I\} = 0.6$	0.3	0	0.06
$m\{II\} = 0.1$	0	0.03	0.01
$m\{\Theta\} = 0.3$	0.075	0.045	0.03

Step 4: Re-normalizing the combined bpa values given in Table A.8 as indicated in Table A.9

Table A.9 Combined bpa values from sources E_1 and E_2 using Zhang's rule after re-normalization

E_1 / E_2	$m\{I\} = 0.5$	$m\{II\} = 0.3$	$m\{\Theta\} = 0.2$
$m\{I\} = 0.6$	0.5454	0	0.10909
$m\{II\} = 0.1$	0	0.05454	0.01818
$m\{\Theta\} = 0.3$	0.1363	0.08181	0.05454

Step 5: Find the value of bpa values using Zhang's rule (equation (4.23) to obtain $m\{I\} = 0.7909$ and $m\{II\} = 0.1545,$ and $m\{\Theta\} = 0.0545.$

Step 6: Calculate the belief values as *Bel{I}* = *m*{I} = 0.79091 and *Bel{II}* = *m*{*II*} = 0.15455.

Step 7: Determine the plausibility values from equation (3.10) as *Pl*{I} = 1 - *Bel{II}* = 0.84545, and *Pl{II}* = 0.20909.

(v) Murphy's rule

Step 1: Calculate the mean bpa set E_m from E_1 and E_2, and the combined bpa values are calculated as in the case of Dempster's rule (Table A.10).

Step 2: Find the belief values as *Bel{I}* = *m*{*I*} = 0.740385 and *Bel{II}* = *m*{*II*} = 0.179487.

Step 3: Determine the plausibility values using equation (4.2) as *Pl*{I} = 1 - *Bel{II}* = 0.820513 and *Pl{II}* = 0.259615.

Table A.10 Combination of bpa values for sources E_1 and E_2 using Murphy's rule

E_1 / E_2	$m\{I\} = 0.55$	$m\{II\} = 0.2$	$m\{\Theta\} = 0.25$
$m\{I\} = 0.55$	0.3025	0.11	0.1375
$m\{II\} = 0.2$	0.11	0.04	0.05
$m\{\Theta\} = 0.25$	0.1375	0.05	0.0625

Appendix-B

B.1 INTRODUCTION

Composite materials are formed by the combination of two or more materials to form a single structure with an identifiable interface. The properties of that new structure are dependent upon the properties of the constituent materials as well as the properties of the interface. The main constituents of composite materials, or composites, are fibers and matrix. In the more familiar world of metals, the mixing of different materials typically forms bonds at the atomic level (alloys), composites typically form molecular bonds in which the original materials retain their identity and mechanical properties. Additionally, where metal alloys (steel, brass, etc.) have isotropic characteristics (the same in all directions), composites can have very selective directional properties to meet specific application needs. The fibers provide most of the strength Thus, composites are typically highly engineered materials targeted at specific applications. The many advantages of composites may be summarized as:

1. Stronger and stiffer than metals on a density basis
    - For the same strength, lighter than steel by 80% and aluminum by 60%
    - Superior stiffness-to-weight ratios
2. Capable of high continuous operating temperatures
    - Up to 250°F in many composites
3. Highly corrosion resistant
    - Essentially inert in the most corrosive environments

4. Electrically insulating properties are inherent in most composites (depending on reinforcement selected).

B.2 MECHANICS OF COMPOSITE MATERIALS

The study of strength of composite materials is a complicated task, to meet several requirements, it must be easy to use but moreover it has to be effective and must fit to any case; which is a challenge considering the numerous fibers and matrices present in the aeronautical industry. They all have distinctive behaviors and properties which confer on them specific applications.

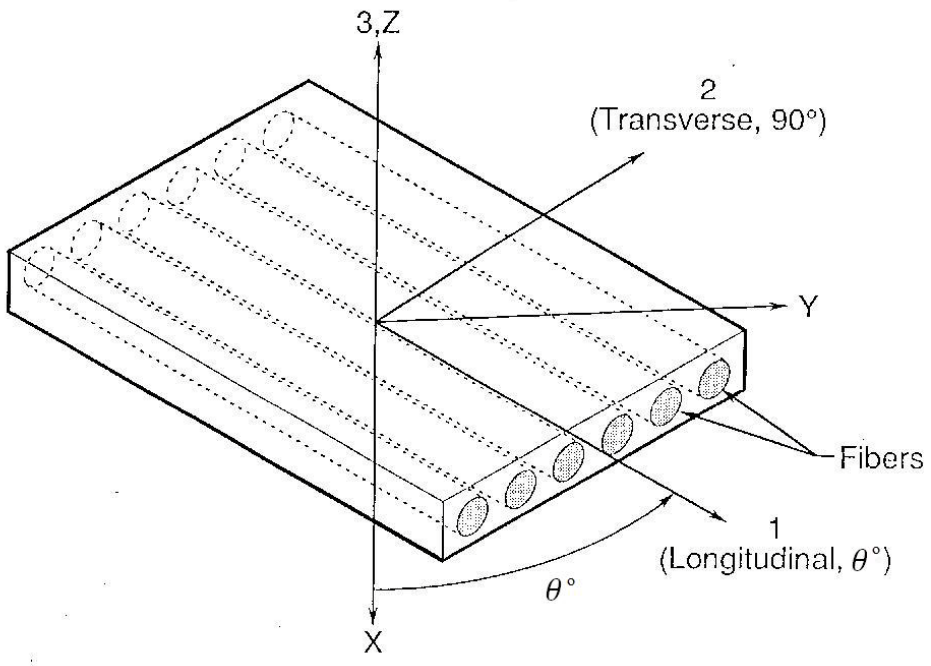

Figure B.1 composite laminate in local and global coordinate system

The mechanics of composite materials deals mainly with the analysis of stresses and strains in the laminate [112,177]. This is usually performed by analyzing the stresses and strains in each lamina first. The results for all the laminas are then integrated over the length of the laminate to obtain the overall quantities.

Consider a laminate shown in figure B.1. The 1-direction is called the fiber direction, while the 2- and 3-directions are called the matrix directions or the transverse directions. This 1-2-3 coordinate system is called the principal material coordinate system. The stresses and strains in the layer (also called a lamina) will be referred to the principal material coordinate system. The *x*-*y*-*z* coordinate system is called transformed or laminate or local coordinate system. The angle θ is measured counterclockwise from *x*-axis to the 1-axis.

In the analysis of fiber-reinforced composite materials, the assumption of plane stress is usually used for each layer. This is mainly because fiber reinforced materials are utilized in beams, plates, cylinders, and other structural shapes which have at least one characteristic geometric dimension in an order of magnitude less than the other two dimensions.

The stresses σ on an element are related to the strains ε by the following relations:

$$\begin{Bmatrix} \varepsilon_1 \\ \varepsilon_2 \\ \varepsilon_3 \\ \gamma_{23} \\ \gamma_{13} \\ \gamma_{12} \end{Bmatrix} = \begin{bmatrix} 1/E_1 & -\upsilon_{21}/E_2 & -\upsilon_{31}/E_3 & 0 & 0 & 0 \\ -\upsilon_{12}/E_1 & 1/E_2 & -\upsilon_{32}/E_3 & 0 & 0 & 0 \\ -\upsilon_{13}/E_1 & -\upsilon_{23}/E_2 & 1/E_3 & 0 & 0 & 0 \\ 0 & 0 & 0 & 1/G_{23} & 0 & 0 \\ 0 & 0 & 0 & 0 & 1/G_{23} & 0 \\ 0 & 0 & 0 & 0 & 0 & 1/G_{23} \end{bmatrix} \begin{Bmatrix} \sigma_1 \\ \sigma_2 \\ \sigma_3 \\ \tau_{23} \\ \tau_{13} \\ \tau_{12} \end{Bmatrix} \quad \text{(B.1)}$$

where $[\sigma] = [\sigma_1\ \sigma_2\ \sigma_3\ \tau_{23}\ \tau_{13}\ \tau_{12}]^T$, $[\varepsilon] = [\varepsilon_1\ \varepsilon_2\ \varepsilon_3\ \gamma_{23}\ \gamma_{13}\gamma_{12}]^T$ and E_1, E_2, and E_3 are the extensional moduli of elasticity along the 1, 2, and 3 directions, respectively. Also, υ_{ij} (i, j = 1, 2, 3) are the different Poisson's ratios, while G_{12}, G_{23}, and G_{13} are the three shear moduli.

$$\begin{Bmatrix} \varepsilon_1 \\ \varepsilon_2 \\ \varepsilon_3 \\ \gamma_{23} \\ \gamma_{13} \\ \gamma_{12} \end{Bmatrix} = \begin{bmatrix} S_{11} & S_{12} & S_{13} & 0 & 0 & 0 \\ S_{21} & S_{22} & S_{23} & 0 & 0 & 0 \\ S_{31} & S_{32} & S_{33} & 0 & 0 & 0 \\ 0 & 0 & 0 & S_{44} & 0 & 0 \\ 0 & 0 & 0 & 0 & S_{55} & 0 \\ 0 & 0 & 0 & 0 & 0 & S_{66} \end{bmatrix} \begin{Bmatrix} \sigma_1 \\ \sigma_2 \\ 0 \\ 0 \\ 0 \\ \tau_{12} \end{Bmatrix} \quad \text{(B.2)}$$

The compact form of the equation (B.2) is

$$\varepsilon = [S]\{\sigma\}$$

where $\{\varepsilon\}$ and $\{\sigma\}$ represent the 6 × 1 strain and stress vectors, respectively, and [S] is called the compliance matrix.

The inverse of the compliance matrix [S] is called the stiffness matrix [Q] given, in general, as follows:

$$\begin{Bmatrix}\sigma_1\\ \sigma_2\\ \sigma_3\\ \tau_{23}\\ \tau_{13}\\ \tau_{12}\end{Bmatrix} = \begin{bmatrix} Q_{11} & Q_{12} & Q_{13} & 0 & 0 & 0\\ Q_{21} & Q_{22} & Q_{23} & 0 & 0 & 0\\ Q_{31} & Q_{32} & Q_{33} & 0 & 0 & 0\\ 0 & 0 & 0 & Q_{44} & 0 & 0\\ 0 & 0 & 0 & 0 & Q_{55} & 0\\ 0 & 0 & 0 & 0 & 0 & Q_{66}\end{bmatrix} \begin{Bmatrix}\varepsilon_1\\ \varepsilon_2\\ \varepsilon_3\\ \gamma_{23}\\ \gamma_{13}\\ \gamma_{12}\end{Bmatrix} \tag{B.3}$$

The material constants appearing in the compliance matrix are not all independent. A material is called transversely isotropic if its behavior in the 2-direction is identical to its behavior in the 3-direction. For this case, $E_2 = E_3$, $\upsilon_{12} = \upsilon_{13}$, and $G_{12} = G_{13}$. In addition, we have the following relation:

$$G_{23} = \frac{E_2}{2(1+\upsilon_{23})} \tag{B.4}$$

A material is called isotropic if its behavior is the same in all three 1-2-3 directions. In this case, $E_1 = E_2 = E_3 = E$, $\upsilon_{12} = \upsilon_{23} = \upsilon_{13} = \upsilon$, and $G_{12} = G_{23} = G_{13} = \mathrm{G}$. In addition, we have the following relation:

$$G = \frac{E}{2(1+\upsilon)} \tag{B.5}$$

Reduced compliance matrix:

$$\begin{Bmatrix}\varepsilon_1\\ \varepsilon_2\\ \gamma_{12}\end{Bmatrix} = \begin{bmatrix} S_{11} & S_{12} & 0\\ S_{12} & S_{22} & 0\\ 0 & 0 & S_{33}\end{bmatrix} \begin{Bmatrix}\sigma_1\\ \sigma_2\\ \tau_{12}\end{Bmatrix} \tag{B.6}$$

Reduced stiffness matrix:

$$\begin{Bmatrix}\sigma_1\\ \sigma_2\\ \tau_{12}\end{Bmatrix} = \begin{bmatrix} Q_{11} & Q_{12} & 0\\ Q_{12} & Q_{22} & 0\\ 0 & 0 & Q_{33}\end{bmatrix} \begin{Bmatrix}\varepsilon_1\\ \varepsilon_2\\ \gamma_{12}\end{Bmatrix} \tag{B.7}$$

$$[Q] = \begin{bmatrix} Q_{11} & Q_{12} & Q_{13} \\ Q_{12} & Q_{22} & Q_{23} \\ Q_{13} & Q_{23} & Q_{33} \end{bmatrix} \tag{B.8}$$

If the material is homogenous and orthotropic:

$$[Q] = \begin{bmatrix} Q_{11} & Q_{12} & 0 \\ Q_{12} & Q_{22} & 0 \\ 0 & 0 & Q_{33} \end{bmatrix} \tag{B.9}$$

Transformed reduced stiffness matrix:

$$[\bar{Q}] = \begin{bmatrix} \bar{Q}_{11} & \bar{Q}_{12} & 0 \\ \bar{Q}_{12} & \bar{Q}_{22} & 0 \\ 0 & 0 & \bar{Q}_{33} \end{bmatrix} \tag{B.10}$$

There is two ways to calculate the $\bar{Q}_{ij}$ terms: The first way is given by

$$[\bar{Q}] = [T]^{-1}[Q][T]^{-T} \tag{B.11}$$

where $[T]$ is the transformation matrix given as follows:

$$[T] = \begin{bmatrix} m^2 & n^2 & 2mn \\ n^2 & m^2 & -2mn \\ -mn & mn & m^2 - n^2 \end{bmatrix} \tag{B.12}$$

The inverse of the matrix $[T]$ is $[T]^{-1}$ given as follows:

$$[T]^{-1} = \begin{bmatrix} m^2 & n^2 & -2mn \\ n^2 & m^2 & 2mn \\ mn & -mn & m^2 - n^2 \end{bmatrix} \tag{B.13}$$

where $m = cos\theta$ and $n = sin\theta$

The second way is to calculate each term of $[\bar{Q}]$ as follows [95]

$$\bar{Q}_{11} = Q_{11}cos\theta^4 + 2(Q_{12} + 2Q_{33})sin\theta^2cos\theta^2 + Q_{22}sin\theta^4 \quad \text{(B.14)}$$

$$\bar{Q}_{12} = Q_{11} + Q_{22} - 4Q_{33}sin\theta^2cos\theta^2 + Q_{12}(cos\theta^4 + sin\theta^4) \quad \text{(B.15)}$$

$$\bar{Q}_{21} = \bar{Q}_{12} \quad \text{(B.16)}$$

$$\bar{Q}_{11} = Q_{11}sin\theta^4 + 2(Q_{12} + 2Q_{33})sin\theta^2cos\theta^2 + Q_{22}cos\theta^4 \quad \text{(B.17)}$$

$$\bar{Q}_{13} = (Q_{11} - Q_{12} - 2Q_{33})sin\theta cos\theta^3 + (Q_{12} - Q_{22} + 2Q_{33})sin\theta^3cos\theta \quad \text{(B.18)}$$

$$\bar{Q}_{31} = \bar{Q}_{13} \quad \text{(B.19)}$$

$$\bar{Q}_{23} = (Q_{11} - Q_{12} - 2Q_{33})sin\theta^3cos\theta + (Q_{12} - Q_{22} + 2Q_{33})sin\theta cos\theta^3 \quad \text{(B.20)}$$

$$\bar{Q}_{32} = \bar{Q}_{23} \quad \text{(B.21)}$$

$$\bar{Q}_{33} = (Q_{11} + Q_{22} - 2Q_{12} - 2Q_{33})sin\theta^2cos\theta^2 + Q_{33}(cos\theta^4 + sin\theta^4) \quad \text{(B.22)}$$

The stiffness matrices of a laminate are defined as:

Extensional stiffness

$$A_{ij} = \sum_{k=1}^{N}\left(\bar{Q}_{ij}\right)_k (z_k - z_{k-1}) \quad \text{(B.23)}$$

Coupling stiffness

$$B_{ij} = \frac{1}{2}\sum_{k=1}^{N}\left(\bar{Q}_{ij}\right)_k (z_k^2 - z_{k-1}^2) \quad \text{(B.24)}$$

Bending stiffness

$$D_{ij} = \frac{1}{3}\sum_{k=1}^{N}\left(\bar{Q}_{ij}\right)_k (z_k^3 - z_{k-1}^3) \quad \text{(B.25)}$$

Where k is the total number of plies in the laminate, z_k and z_{k-1} are the distances from the reference plane to the two surfaces of the k^{th} ply; and $\left(\bar{Q}_{ij}\right)_k$ are the elements of the stiffness matrix of the k^{th} ply. With the following definitions of the stiffness matrices, the expressions for the in-plane forces and moments become [2]

$$\begin{Bmatrix} N_x \\ N_y \\ N_z \end{Bmatrix} = \begin{bmatrix} A_{11} & A_{12} & A_{16} \\ A_{12} & A_{22} & A_{26} \\ A_{16} & A_{26} & A_{66} \end{bmatrix} \begin{Bmatrix} \varepsilon_x^0 \\ \varepsilon_y^0 \\ \gamma_{xy}^0 \end{Bmatrix} + \begin{bmatrix} B_{11} & B_{12} & B_{16} \\ B_{12} & B_{22} & B_{26} \\ B_{16} & B_{26} & B_{66} \end{bmatrix} \begin{Bmatrix} k_x^0 \\ k_y^0 \\ k_z^0 \end{Bmatrix} \tag{B.26}$$

Bending moments:

$$\begin{Bmatrix} M_x \\ M_y \\ M_z \end{Bmatrix} = \begin{bmatrix} B_{11} & B_{12} & B_{16} \\ B_{12} & B_{22} & B_{26} \\ B_{16} & B_{26} & B_{66} \end{bmatrix} \begin{Bmatrix} \varepsilon_x^0 \\ \varepsilon_y^0 \\ \gamma_{xy}^0 \end{Bmatrix} + \begin{bmatrix} D_{11} & D_{12} & D_{16} \\ D_{12} & D_{22} & D_{26} \\ D_{16} & D_{26} & D_{66} \end{bmatrix} \begin{Bmatrix} k_x^0 \\ k_y^0 \\ k_z^0 \end{Bmatrix} \tag{B.27}$$

where $\varepsilon_x^0, \varepsilon_y^0, \gamma_{xy}^0$ are the in-plane deformations and k_x^0, k_y^0, k_z^0 are the curvatures. When the laminate is symmetrical, $[B] = 0$. The in-plane stresses in the k^{th} layer are calculated as

$$\sigma_{xx}^{(k)}(x,z) = \frac{M(x)z}{b}\left(\bar{Q}_{11}^{(k)} D_{11}^* + \bar{Q}_{22}^{(k)} D_{12}^* + \bar{Q}_{16}^{(k)} D_{16}^*\right) \tag{B.28}$$

$$\sigma_{yy}^{(k)}(x,z) = \frac{M(x)z}{b}\left(\bar{Q}_{12}^{(k)} D_{11}^* + \bar{Q}_{22}^{(k)} D_{12}^* + \bar{Q}_{26}^{(k)} D_{26}^*\right) \tag{B.29}$$

$$\sigma_{xy}^{(k)}(x,z) = \frac{M(x)z}{b}\left(\bar{Q}_{16}^{(k)} D_{11}^* + \bar{Q}_{26}^{(k)} D_{12}^* + \bar{Q}_{66}^{(k)} D_{16}^*\right) \tag{B.30}$$

where D_{ij}^* are terms from the inverse of the D matrix.

In general, the maximum stress does not occur at the top or bottom of a laminated beam. The maximum stress location through the beam thickness depends on the lamination scheme. The 0° layers take the most axial stress.

Also of importance is the response of the composite to a load applied transverse to the fibre direction. The stiffness and strength of the composite are expected to be much lower in this case, since the matrix is not shielded from carrying stress to the same degree as for axial loading. Prediction of the transverse stiffness of a composite from the elastic properties of the constituents is far more difficult than the axial value.

$$\sigma_{xy}^{(k)}(x,z) = -Q_x(x)\left(\bar{Q}_{11}^{(k)}D_{11}^{*} + \bar{Q}_{12}^{(k)}D_{12}^{*} + \bar{Q}_{66}^{(k)}D_{16}^{*}\right)\left(\frac{z^2-z_k^2}{2}\right) + G^{(k)} \quad \text{(B.31)}$$

If the laminate bottom is stress free, we have $G^{(1)}=0$

$$G^{(k+1)} = -Q_x(x)\left(\bar{Q}_{11}^{(k)}D_{11}^{*} + \bar{Q}_{12}^{(k)}D_{12}^{*} + \bar{Q}_{66}^{(k)}D_{16}^{*}\right)\left(\frac{z_{k+1}^2 - z_k^2}{2}\right) + G^{(k)}$$

$$= \sigma_{xz}^{(k)}(x, z_{k+1}) \quad \text{(B.32)}$$

where $Q_x(x) = \frac{\partial M(x)}{\partial x}$ (B.33)

The maximum deflection (W_{max}) for various boundary conditions and different loads for the composite laminate beam with dimensions length (a), width (b) and height (h) are given in the Table B.1. We assume F_0 and $Q_0$to be center load and uniformly distributed load (UDL) for the simply supported beam, F_1 and Q_1 to be center load and UDL for the fully clamped beam, F_2 and $Q_2$to be end load and UDL for the cantilever beam [176]

Table B.1 Maximum deflections for various beams for each load case

W_{max}	Point load	Uniformly distributed load
Simply supported	$\frac{F_0.b.a^3}{48.E_{xx}^b.l_{yy}}$	$\frac{5Q_0.b.a^4}{384.E_{xx}^b.l_{yy}}$ at $x=\frac{a}{2}$
Fully clamped	$\frac{F_1.b.a^3}{192.E_{xx}^b.l_{yy}}$	$\frac{Q_1.b.a^4}{384.E_{xx}^b.l_{yy}}$ at $x=\frac{a}{2}$
Cantilever	$\frac{F_2.b.a^3}{3.E_{xx}^b.l_{yy}}$	$\frac{Q_1.b.a^4}{8.E_{xx}^b.l_{yy}}$ at $x=a$

where $E_{xx}^b=\frac{b}{l_{yy}D_{11}^*}$ and $l_{yy}=\frac{b.h^3}{12}$ (B.34)

These equations are identical in form to those of Euler-Bernoulli; the solutions for deflections of isotropic beams can be readily used for laminated beams by replacing the modulus *E* with E_{xx}^b and multiplying loads and mass inertias with b (width).

Similarly, we can calculate critical buckling load, N_{cr}, for different cases as tabulated in Table B.2

Table B.2 Critical buckling load for various beams

	N_{cr}
Simply supported	$\left(\frac{\pi^2}{12}\right)\frac{E_{xx}^{b}.h^3}{a^2}$
Fully clamped	$\left(\frac{\pi^2}{3}\right)\frac{E_{xx}^{b}.h^3}{a^2}$
Cantilever	$\left(\frac{\pi^2}{48}\right)\frac{E_{xx}^{b}.h^3}{a^2}$

To conclude the analysis of composite materials, there is one essential feature, the weight of a part made of composite materials. It can be calculated as [14]

Weight = $\rho_c \times V_c$

where ρ_c= Density of composite material and V_c is volume of the composite.

Appendix-C Computer Programs

C.1 MATLAB PROGRAMS FOR COMPOSITE SIMPLY SUPPORTED BEAM

The following is the matlab program required for constraint function for the two variable case for the composite problem described in page 253 and is needed to obtain optimum solutions tabulated in Table 8.8. It doesn't require any input parameters. It should be used along with matlab program

Constraint function

```
function [c,ceq]= constraintcomposite(x)
% global f3;
format long
P=500;
L=1;
t1=x(1);
t2=x(2);
t=4*(t1+t2);
b=2*t;
Ef=72.3e9;
Em=5.05e9;
Vf=0.6;
muf=.22;
mum=.35;
%For isotropic materials
Gm=Em/(2*(1+mum));
Gf=Ef/(2*(1+muf));
%Rule of mixtures
```

```
E1=Ef*Vf+Em*(1-Vf);
%Inverse rule of mixtures
E2=Em*Ef/(Ef*(1-Vf)+Em*Vf);
%Inverse rule of mixtures
G12=Gm/(1-Vf+Vf*(Gm/Gf));
%Rule of mixtures
mu12=muf*Vf+mum*(1-Vf);
G13=G12;
%With Semiempirical stress-partitioning parameter (SPP) technique
n23=(3-4*mum+Gm/Gf)/(4*(1-mum));
G23=Gm*(Vf+n23*(1-Vf))/(n23*(1-Vf)+Vf*Gm/Gf);
F1t=floor((4*t1+4*t2)/0.001)*1020e6;
F2t=floor((4*t1+4*t2)/0.001)*40e6;
F6=floor((4*t1+4*t2)/0.001)*60e6;
F1c=floor((4*t1+4*t2)/0.001)*620e6;
F2c=floor((4*t1+4*t2)/0.001)*140e6;
rho=2.076e3; %Density of composite in kg/m3
FS=3.5; %Factor of safety

%we have delta=1-mu12*mu21=1-((mu12)^2)*(E2/E1);
%calculation of Q plane stress reduced stiffness
delta=1-((mu12)^2)*(E2/E1);
Q11=E1/delta;
Q12=mu12*E2/delta;
Q21=Q12;
Q22=E2/delta;
Q66=G12;
```

```
Q26=0;
Q62=Q26;
Q16=Q26;
Q61=Q16;

Q=[Q11 Q12 Q16
   Q21 Q22 Q26
   Q61 Q62 Q66];
%theta orientations of layers
theta=[90 45 -45 0 0 -45 45 90];

for i3=1:8
T=zeros(3);
m=cosd(theta(i3));
n=sind(theta(i3));
T=[m^2 n^2 2*m*n
  n^2 m^2 -2*m*n
  -m*n m*n m^2-n^2];
Qbar(:,:,i3)=inv(T)*Q*(inv(T))';
end

%calculating h1, h2,....from thickness
h(1)=-2*(t1+t2);
h(2)=h(1)+t1;
h(3)=h(2)+t2;
h(4)=h(3)+t2;
h(5)=h(4)+t1;
```

```
h(6)=h(5)+t1;
h(7)=h(6)+t2;
h(8)=h(7)+t2;
h(9)=2*(t1+t2);
D=zeros(3);
for k=1:8
   D=D+((h(k+1)^3-h(k)^3)/3)*Qbar(:,:,k);
end

Dstar=inv(D);
Iyy=(b*t^3)/12;
D11star=Dstar(1,1);
Ebxx=12/(t^3*D11star);
%calculating maximum deflection
wmax=abs((P*b*(L^3))/(48*Ebxx*Iyy));
C3=-P*b*L;
%calculating bending moment
bmmax=-0.25*C3;
j=1;
M=[bmmax;0;0];
%finding stresses
for i3=1:8
sigmastress1(:,:,i3)=(1/b)*h(i3)*Qbar(:,:,i3)*Dstar;
ss1(:,1,i3)=sigmastress1(:,:,i3)*M;
sigmastress2(:,:,i3)=(1/b)*h(i3+1)*Qbar(:,:,i3)*Dstar;
ss2(:,1,i3)=sigmastress2(:,:,i3)*M;
sigmastress3(:,:,i3)=(1/b)*h(i3)*Qbar(:,:,i3)*Dstar;
```

```
ss3(:,1,i3)=sigmastress3(:,:,i3)*M;
sigmastress4(:,:,i3)=(1/b)*h(i3+1)*Qbar(:,:,i3)*Dstar;
ss4(:,1,i3)=sigmastress4(:,:,i3)*M;
sigmastress5(:,:,i3)=(1/b)*h(i3)*Qbar(:,:,i3)*Dstar;
ss5(:,1,i3)=sigmastress5(:,:,i3)*M;
sigmastress6(:,:,i3)=(1/b)*h(i3+1)*Qbar(:,:,i3)*Dstar;
ss6(:,1,i3)=sigmastress6(:,:,i3)*M;
sslt(j)=ss1(1,:,i3);
sstt(j)=ss3(2,:,i3);
ssis(j)=ss5(3,:,i3);
j=j+1;
sslt(j)=ss2(1,:,i3);
sstt(j)=ss4(2,:,i3);
ssis(j)=ss6(3,:,i3);
j=j+1;
end

%finding maximum and minimum stresses
cF1t=max(sslt);
cF2t=max(sstt);
cF6=max(ssis);
cF1c=-min(sslt);
cF2tc=-min(sstt);

% c = [wmax/.005-1;-0.9+x(3)+x(4);FS*cF1t/F1t-1;cF2t*FS/F2t-1;cF6*FS/F6-
1;cF1c*FS/F1c-1;cF2tc*FS/F2c-1];

% Nonlinear inequality constraints
```

```
c = [wmax/.005-1;FS*cF1t/F1t-1;cF2t*FS/F2t-1;cF6*FS/F6-1;cF1c*FS/F1c-
1;cF2tc*FS/F2c-1];

% Nonlinear equality constraints

ceq = [];
```

The following matlab program is used to calculate the objective function to find maximum buckling load for the two variable composite beam optimization problem described in page 253 and is needed to obtain optimum solution tabulated in Table 8.8. It doesn't require any input parameters. It should be used along with matlab program in the section C.3

C.2 OBJECTIVE FUNCTION FOR f_1

```
function f= objcompositef1(x)

P=500;

L=1;

t1=x(1);

t2=x(2);

t=4*(t1+t2);

b=2*t;

Ef=72.3e9;

Em=5.05e9;

Vf=0.6;

muf=.22;

mum=.35;

Gm=Em/(2*(1+mum));

Gf=Ef/(2*(1+muf));

E1=Ef*Vf+Em*(1-Vf);

E2=Em*Ef/(Ef*(1-Vf)+Em*Vf);

%PMM

% S3=0.49247-0.47603*Vf-.02748*Vf^2;
```

```
% G12=Gm*(1+(Vf*(1-Gm/Gf))/(Gm/Gf+S3*(1-Gm/Gf)))
G12=Gm/(1-Vf+Vf*(Gm/Gf));
mu12=muf*Vf+mum*(1-Vf);
G13=G12;
n23=(3-4*mum+Gm/Gf)/(4*(1-mum));
G23=Gm*(Vf+n23*(1-Vf))/(n23*(1-Vf)+Vf*Gm/Gf);
F1t=floor((4*t1+4*t2)/0.001)*1020e6;
F2t=floor((4*t1+4*t2)/0.001)*40e6;
F6=floor((4*t1+4*t2)/0.001)*60e6;
F1c=floor((4*t1+4*t2)/0.001)*620e6;
F2c=floor((4*t1+4*t2)/0.001)*140e6;
rho=2.076e3; %kg/m3
FS=3.5;
%we have delta=1-mu12*mu21=1-((mu12)^2)*(E2/E1);
%calculation of Q plane stress reduced stiffness
delta=1-((mu12)^2)*(E2/E1);
Q11=E1/delta;
Q12=mu12*E2/delta;
Q21=Q12;
Q22=E2/delta;
Q66=G12;
Q26=0;
Q62=Q26;
Q16=Q26;
Q61=Q16;

Q=[Q11 Q12 Q16
```

```
   Q21 Q22 Q26
   Q61 Q62 Q66];
theta=[90 45 -45 0 0 -45 45 90];
for i3=1:8
T=zeros(3);
m=cosd(theta(i3));
n=sind(theta(i3));
T=[m^2 n^2 2*m*n
  n^2 m^2 -2*m*n
  -m*n m*n m^2-n^2];
Qbar(:,:,i3)=inv(T)*Q*(inv(T))';
end

h(1)=-2*(t1+t2);
h(2)=h(1)+t1;
h(3)=h(2)+t2;
h(4)=h(3)+t2;
h(5)=h(4)+t1;
h(6)=h(5)+t1;
h(7)=h(6)+t2;
h(8)=h(7)+t2;
h(9)=2*(t1+t2);
% f2=rho*x(1)*b*L;
D=zeros(3);
for k=1:8
   D=D+((h(k+1)^3-h(k)^3)/3)*Qbar(:,:,k);
end
```

```
Dstar=inv(D);

Iyy=(b*t^3)/12;

D11star=Dstar(1,1);

Ebxx=12/(t^3*D11star);

wmax=abs((P*b*(L^3))/(48*Ebxx*Iyy));

C3=-P*b*L;

bmmax=-0.25*C3;

%critical buckling load

Ncr=(pi*pi/12)*(Ebxx*t^3)/L^2;

% To get buckling load in kN, we divide by 1000

f1=Ncr/1000;
```

The following matlab program is main program used to get minimization of buckling load (f_1) for the two variable composite beam optimization problem described in the page 253 and is needed to obtain optimum solutions tabulated in Table 8.8. It doesn't require any input parameters. It should be placed in the same directory as that of matlab programs in sections C.1 and C.2

C.3 MAIN MATLAB PROOGRAM FOR MINIMIZATION OF f_1

```
clc

clear all

x0 = [.004,0.004]; % Starting guess

% [c,ceq] = constraintcomposite(x0)

format long

lb=[.001;0.001];

ub=[.015;0.015];

options = optimset('LargeScale','off');
```

```
[x,fval,exitflag,output]=fmincon(@objcompositef1,x0,[],[],[],[],lb,ub,@constraintcomposite,options)

[c,ceq] = constraintcomposite(x)
```

C.4 OUTPUT OF THE MATLAB PROGRAM C.3

The following is the output of the matlab program in section C.3 to obtain optimum solution tabulated in Table 8.8. Note that all the program in the sections C.1, C.2 and C.3 should be present in the same directory.

```
Optimization terminated: Search direction less than 2*options.TolX

 and maximum constraint violation is less than options.TolCon.

Active inequalities (to within options.TolCon = 1e-006):

  lower      upper     ineqlin   ineqnonlin

    1                          1


x =    0.00100000000000   0.00202077781045

fval =   20.56167244497333

exitflag =      4

output =

       iterations: 10

        funcCount: 51

         stepsize: 1

        algorithm: 'medium-scale: SQP, Quasi-Newton, line-search'

    firstorderopt: 3.390678876522489e-006

     cgiterations: []

          message: [1x129 char]

c =

   0.00000016490047

  -0.99866403756274
```

-0.97915768799494

-0.99147974182226

-0.99780212631289

-0.99404505371284

ceq = []

f1 = 20.56167244497333

The following matlab program is in general the modified PSO algorithm described in the chapter 7 and used for the continuous optimization problems considered in the same chapter. The PSO parameters are used in this program are specifically used for the two variable composite beam optimization problem described in the page 253 and is needed to obtain optimum solutions tabulated in Table 8.9. It doesn't require any input parameters.

C.5 PSO MATLAB PROGRAM IN GENERAL

```
% a generic particle swarm optimizer
%dynamic maximum velocity is a exponential decreasing function (natural)
% Usage:
%  [optOUT]=PSO(functname,D)
% or:
%  [optOUT]=PSO(functname,D,mv,VarRange,minmax,PSOparams)
%
% Inputs:
%    functname - string of matlab function to optimize
%    D - # of inputs to the function (dimension of problem)
%
% Optional Inputs:
%    mv - max particle velocity, either a scalar or a vector of length D
%         (this allows each component to have it's own max velocity),
%         default = 4
```

```
%   VarRange - matrix of ranges for each input variable,
%     default -100 to 100, of form:
%      [ min1 max1
%        min2 max2
%          ...
%        minD maxD ]
%
%   minmax = 0, funct minimized (default)
%          = 1, funct maximized


%
%   PSOparams - PSO parameters
%     P(1) - Epochs between updating display, default = 100. if 0,
%            no display
%     P(2) - Maximum number of iterations (epochs) to train, default = 2000.
%     P(3) - population size, default = 24
%
%     P(4) - acceleration const 1 (local best influence), default = 2
%     P(5) - acceleration const 2 (global best influence), default = 2
%     P(6) - Initial inertia weight, default = 0.9
%     P(7) - Final inertia weight, default = 0.4
%     P(8) - Epoch when inertial weight at final value, default = 1500
%     P(9)- minimum global error gradient,
%               if abs(Gbest(i+1)-Gbest(i)) < gradient over
%               certain length of epochs, terminate run, default = 1e-25
%     P(10)- epochs before error gradient criterion terminates run,
%               default = 150, if the SSE does not change over 250 epochs
```

```
%                       then exit
%     P(11)- error goal, if NaN then unconstrained min or max, default=NaN
%     P(12)- type flag (which kind of PSO to use)
%              0 = Common PSO w/intertia (default)
%     P(13)- PSOseed, default=0
%            = 0 for initial positions all random

function [OUT,varargout]=compositebeampso(functname,D,varargin)
timestart=cputime;
disp(['PSO start time at ',datestr(now,13)]);
global CNT i;
CNT=0;
rand('state',sum(100*clock));
if nargin < 2
  error('Minimum number of arguments is 2');
end

if nargin == 4  % specified functname, D, mv, Varrange
  mv=varargin{1};
  if isnan(mv)
     mv=4;
  end
  VR=varargin{2}; %VarRange - matrix of ranges for each input variable
  minmax = 0;
  P = [];
  plotfcn='goplotpso';
else
```

```
  error('Wrong # of input arguments.');
end

% sets up default pso paramaters
Pdef = [20 800 10 2 2 0.9 0.4 790 1e-8 350 NaN 0 0];
Plen = length(P);
P    = [P,Pdef(Plen+1:end)]; %store default pso parameters into P

df     = P(1);
me     = P(2);
ps     = P(3);
ac1    = P(4);
ac2    = P(5);
iw1    = P(6);
iw2    = P(7);
iwe    = P(8);
ergrd  = P(9);
ergrdep = P(10);
errgoal = P(11);
trelea  = P(12);
PSOseed = P(13);

mvmax=mv;
mvmin=0.001; % minimum limit for maximum velocity
% set plotting flag
if df~=0
  plotflg=1;
```

```
else
  plotflg=0;
end
% preallocate variables for speed up
 tr = ones(1,me)*NaN;
% take care of setting max velocity and position params here
if length(mv)==1
 velmaskmin = -mv*ones(ps,D);     % min vel, psXD matrix
 velmaskmax = mv*ones(ps,D);      % max vel
else
 error('Max vel must be either a scalar or same length as prob dimension D');
end
posmaskmin  = repmat(VR(1:D,1)',ps,1);  % min pos, psXD matrix
posmaskmax  = repmat(VR(1:D,2)',ps,1);  % max pos

% 3=bounce method (see comments below inside epoch loop)
posmaskmeth = 3;
% PLOTTING
 message = sprintf('PSO: %%g/%g iterations, GBest = %%20.20g.\n',me);

% initialize population of particles and their velocities at time zero,
% construct random population positions bounded by VR

  pos(1:ps,1:D) = normmat(rand([ps,D]),VR',1);

% construct initial random velocities between -mv,mv
  vel(1:ps,1:D) = normmat(rand([ps,D]),[forcecol(-mv),forcecol(mv)]',1);
```

```
% initial pbest positions vals
 pbest = pos;

 i=1; %initializing iteration number

 out = feval(functname,pos);  % returns column of cost values (1 for each particle)

 pbestval=out;   % initially, pbest is same as pos

% assign initial gbest here also (gbest and gbestval)
if minmax == 0
        [gbestval,idx1] = min(pbestval);
end
 % preallocate a variable to keep track of gbest for all iters
 bestpos       = zeros(me,D+1)*NaN;
 gbest         = pbest(idx1,:);  % this is gbest position

 bestpos(1,1:D) = gbest;
 sentryval = gbestval;
 sentry    = gbest;
% INITIALIZE END

rstflg = 0; % for dynamic environment checking
% start PSO iterative procedures
 cnt    = 0; % counter used for updating display according to df in the options
 cnt2   = 0; % counter used for the stopping subroutine based on error convergence
```

```
 iwt(1) = iw1;
 gbestprev=gbest;
while i<me  % start epoch loop (iterations)
if i==1
   outbestval=gbestval;
end

if i>1
    out      = feval(functname,[pos;gbest]);
    outbestval = out(end,:);
    out       = out(1:end-1,:);
end

    tr(i+1)         = gbestval; % keep track of global best val
    te              = i; % returns epoch number to calling program when done
    bestpos(i,1:D+1) = [gbest,gbestval];

  % this section does the plots during iterations
   if plotflg==1
      if (rem(i,df) == 0 ) | (i==me) | (i==1)
       fprintf(message,i,gbestval);
       cnt = cnt+1; % count how many times we display (useful for movies)

       eval(plotfcn); % defined at top of script

     end  % end update display every df if statement
   end % end plotflg if statement
```

```
% check for an error space that changes wrt time/iter
% threshold value that determines dynamic environment
% sees if the value of gbest changes more than some threshold value
% for the same location
chkdyn = 1;
rstflg = 0; % for dynamic environment checking

if chkdyn==1
 threshld = 0.05;  % percent current best is allowed to change, .05 = 5% etc
 letiter  = 5; % # of iterations before checking environment, leave at least 3 so PSO has time to converge
 outorng  = abs( 1- (outbestval/gbestval) ) >= threshld;
 samepos  = (max( sentry == gbest ));

 if (outorng & samepos) & rem(i,letiter)==0
    rstflg=1;

   pbest     = pos; % reset personal bests to current positions
   pbestval  = out;
   vel       = vel; % agitate particles a little (or a lot)

  % recalculate best vals
   if minmax == 0
     [gbestval,idx1] = min(pbestval);
   end
   gbest  = pbest(idx1,:);
 end  % end if outorng
```

```
 sentryval = gbestval;
 sentry    = gbest;

end % end if chkdyn

% find particles where we have new pbest, depending on minmax choice
% then find gbest and gbestval
if rstflg == 0
 if minmax == 0
   [tempi]           = find(pbestval>=out); % new min pbestvals
   pbestval(tempi,1)  = out(tempi);   % update pbestvals
   pbest(tempi,:)     = pos(tempi,:); % update pbest positions

   [iterbestval,idx1] = min(pbestval);

   if gbestval >= iterbestval
      gbestval = iterbestval;
      gbest    = pbest(idx1,:);
   end
 end
end
  % get new velocities, positions (this is the heart of the PSO algorithm)
  % each epoch get new set of random numbers
   rannum1 = rand([ps,D]); % for Trelea and Clerc types
   rannum2 = rand([ps,D]);
```

```
% modified PSO algo with inertia wt
% get inertia weight, just a linear funct w.r.t. epoch parameter iwe
 if i<=iwe
   iwt(i) = ((iw2-iw1)/(iwe-1))*(i-1)+iw1;
 else
   iwt(i) = iw2;
 end

 a=(log(mvmax/mvmin))/(iwe-1);
 b=a+log(mvmax);
 if i<=iwe
   maxv(i) = exp(-a*i+b);
 else
   maxv(i) = mvmin;
 end
 velmaskmin = -maxv(i)*ones(ps,D);     % min vel, psXD matrix
velmaskmax = maxv(i)*ones(ps,D);      % max vel

% random number including acceleration constants
 ac11 = rannum1.*ac1;    % for common PSO w/inertia
 ac22 = rannum2.*ac2;

 vel = iwt(i).*vel...                        % prev vel
      +ac11.*(pbest-pos)...                  % independent
      +ac22.*(repmat(gbest,ps,1)-pos);          % social
```

```
% limit velocities here using masking
 vel = ( (vel <= velmaskmin).*velmaskmin ) + ( (vel > velmaskmin).*vel );
 vel = ( (vel >= velmaskmax).*velmaskmax ) + ( (vel < velmaskmax).*vel );

% update new position (PSO algo)
 pos = pos + vel;

% position masking, limits positions to desired search space
 minposmask_throwaway = pos <= posmaskmin;  % these are psXD matrices
 minposmask_keep      = pos >  posmaskmin;
 maxposmask_throwaway = pos >= posmaskmax;
 maxposmask_keep      = pos <  posmaskmax;

 if posmaskmeth == 3
  % this is the bounce method, particles bounce off the boundaries with -vel
   pos = ( minposmask_throwaway.*posmaskmin ) + ( minposmask_keep.*pos );
   pos = ( maxposmask_throwaway.*posmaskmax ) + ( maxposmask_keep.*pos );

   vel = (vel.*minposmask_keep) + (-vel.*minposmask_throwaway);
   vel = (vel.*maxposmask_keep) + (-vel.*maxposmask_throwaway);
 else
  % no change, this is the original Eberhart, Kennedy method,
  % it lets the particles grow beyond bounds if psoparams (P)
  % especially Vmax, aren't set correctly, see the literature
 end

% check for stopping criterion based on speed of convergence to desired error
```

```
    tmp1 = abs(tr(i) - gbestval);
    if tmp1 > ergrd
      cnt2 = 0;
    elseif tmp1 <= ergrd
      cnt2 = cnt2+1;
      if cnt2 >= ergrdep
       if plotflg == 1
        fprintf(message,i,gbestval);
        disp(' ');
        disp(['--> Solution likely, GBest hasn''t changed by at least ',...
           num2str(ergrd),' for ',...
              num2str(cnt2),' epochs.']);
        eval(plotfcn);
       end
       break
      end
    end
    i=i+1;
%     if i==700
%        i=799
%     end

end  % end epoch loop

 OUT=[gbest';gbestval];
 varargout{1}=[1:te];
 varargout{2}=[tr(find(~isnan(tr)))];
```

```
 disp(['PSO end time at ',datestr(now,13)]);

 fprintf('No. of function evaluations = %d\n',CNT*ps);

fprintf('Total CPU time %f sec',cputime-timestart);

return
```

The following matlab program is used to calculate the objective function to find the optimum solution using modified game theory for the two variable composite beam optimization problem described in page 253 and is needed to obtain optimum solution tabulated in Table 8.9. It doesn't require any input parameters. It should be used along with matlab programs in the sections C.5 and C.7

C.6 OBJECTIVE FUNCTION REQUIRED FOR COMPOSITE BEAM PROBLEM ALONG WITH C.5

```
function [out]= objcompgamemod(in)

warning off

global CNT i;

% i=1;

CNT=CNT+1;

const=0.5;

alpha=2;

ck=(const*i)^alpha;

consta=150;

constb=10;

% global f3;

for i2=1:size(in,1)

x1=in(i2,1);

x2=in(i2,2);

x3=in(i2,3);

P=500;
```

```
L=1;
t1=x1;
t2=x2;
t=4*(t1+t2);
b=2*t;
Ef=72.3e9;
Em=5.05e9;
Vf=0.6;
muf=.22;
mum=.35;
%For isotropic materials
Gm=Em/(2*(1+mum));
Gf=Ef/(2*(1+muf));
%Rule of mixtures
E1=Ef*Vf+Em*(1-Vf);
%Inverse rule of mixtures
E2=Em*Ef/(Ef*(1-Vf)+Em*Vf);
%Inverse rule of mixtures
G12=Gm/(1-Vf+Vf*(Gm/Gf));
%Rule of mixtures
mu12=muf*Vf+mum*(1-Vf);
G13=G12;
%With Semiempirical stress-partitioning parameter (SPP) technique
n23=(3-4*mum+Gm/Gf)/(4*(1-mum));
G23=Gm*(Vf+n23*(1-Vf))/(n23*(1-Vf)+Vf*Gm/Gf);
F1t=floor((4*t1+4*t2)/0.001)*1020e6;
F2t=floor((4*t1+4*t2)/0.001)*40e6;
```

```
F6=floor((4*t1+4*t2)/0.001)*60e6;
F1c=floor((4*t1+4*t2)/0.001)*620e6;
F2c=floor((4*t1+4*t2)/0.001)*140e6;
rho=2.076e3; %Density of composite in kg/m3
FS=3.5; %Factor of safety

%we have delta=1-mu12*mu21=1-((mu12)^2)*(E2/E1);
%calculation of Q plane stress reduced stiffness
delta=1-((mu12)^2)*(E2/E1);
Q11=E1/delta;
Q12=mu12*E2/delta;
Q21=Q12;
Q22=E2/delta;
Q66=G12;
Q26=0;
Q62=Q26;
Q16=Q26;
Q61=Q16;

Q=[Q11 Q12 Q16
   Q21 Q22 Q26
   Q61 Q62 Q66];
theta=[90 45 -45 0 0 -45 45 90];
for i3=1:8
T=zeros(3);
m=cosd(theta(i3));
n=sind(theta(i3));
```

```
T=[m^2 n^2 2*m*n
  n^2 m^2 -2*m*n
  -m*n m*n m^2-n^2];
Qbar(:,:,i3)=inv(T)*Q*(inv(T))';
end

h(1)=-2*(t1+t2);
h(2)=h(1)+t1;
h(3)=h(2)+t2;
h(4)=h(3)+t2;
h(5)=h(4)+t1;
h(6)=h(5)+t1;
h(7)=h(6)+t2;
h(8)=h(7)+t2;
h(9)=2*(t1+t2);
f2=rho*4*(t1+t2)*b*L/100;
D=zeros(3);
for k=1:8
   D=D+((h(k+1)^3-h(k)^3)/3)*Qbar(:,:,k);
end

Dstar=inv(D);
Iyy=(b*t^3)/12;
D11star=Dstar(1,1);
Ebxx=12/(t^3*D11star);
wmax=abs((P*b*(L^3))/(48*Ebxx*Iyy));
C3=-P*b*L;
```

```
bmmax=-0.25*C3;
Ncr=(pi*pi/12)*(Ebxx*t^3)/L^2;
f1=-Ncr/100000000;
j=1;
M=[bmmax;0;0];
for i3=1:8
sigmastress1(:,:,i3)=(1/b)*h(i3)*Qbar(:,:,i3)*Dstar;
ss1(:,1,i3)=sigmastress1(:,:,i3)*M;
sigmastress2(:,:,i3)=(1/b)*h(i3+1)*Qbar(:,:,i3)*Dstar;
ss2(:,1,i3)=sigmastress2(:,:,i3)*M;
sigmastress3(:,:,i3)=(1/b)*h(i3)*Qbar(:,:,i3)*Dstar;
ss3(:,1,i3)=sigmastress3(:,:,i3)*M;
sigmastress4(:,:,i3)=(1/b)*h(i3+1)*Qbar(:,:,i3)*Dstar;
ss4(:,1,i3)=sigmastress4(:,:,i3)*M;
sigmastress5(:,:,i3)=(1/b)*h(i3)*Qbar(:,:,i3)*Dstar;
ss5(:,1,i3)=sigmastress5(:,:,i3)*M;
sigmastress6(:,:,i3)=(1/b)*h(i3+1)*Qbar(:,:,i3)*Dstar;
ss6(:,1,i3)=sigmastress6(:,:,i3)*M;
sslt(j)=ss1(1,:,i3);
sstt(j)=ss3(2,:,i3);
ssis(j)=ss5(3,:,i3);
j=j+1;
sslt(j)=ss2(1,:,i3);
sstt(j)=ss4(2,:,i3);
ssis(j)=ss6(3,:,i3);
j=j+1;
end
```

```
cF1t=max(sslt);
cF2t=max(sstt);
cF6=max(ssis);
cF1c=-min(sslt);
cF2tc=-min(sstt);

cc=zeros(6,1);
g=0.0;
c = [wmax/.005-1;FS*cF1t/F1t-1;cF2t*FS/F2t-1;cF6*FS/F6-1;cF1c*FS/F1c-
1;cF2tc*FS/F2c-1];

for i1=1:6
    if cc(i1,1)>0
        if cc(i1,1)<=1
            gammaqx=1;
        else
            gammaqx=2;
        end
        thetaqx=consta*(1-1/exp(cc(i1,1)))+constb;
        hx=thetaqx*(cc(i1,1))^gammaqx;
        g=g+ck*hx;
    end
end
f1w=-20.56610040952907/100000;
f2w=59.788/100;
f1star=-20217.8581711447/100000;
f2star=0.600922712638432/100;
```

```
f1n=(f1w-f1)/(f1w-f1star);

f2n=(f2w-f2)/(f2w-f2star);

fc=x3*f1n+f2n*(1-x3);

ff=fc-(1-f1n)*(1-f2n);

out(i2,1)=ff+ck*g;

end
```

The following matlab program is main program used to get the optimum solution using modified game theory for the two variable composite beam optimization problem described in the page 253. It doesn't require any input parameters. It should be placed in the same directory as that of matlab programs in sections C.5 and C.6

C.7 MAIN OPTIMIZATION PROGRAM (DETERMINISTIC)

```
clc

clear all

format long

out=compositebeampso('objcompgamemod',3,0.05,[0.001 0.015; 0.001 0.015;0.1 0.7])
```

C.8 OUTPUT OF THE MATLAB PROGRAM IN THE SECTION C.7

The following is the output of the matlab program in the section C.7 to obtain optimum solution tabulated in Table 8.9. Note that all the program in the sections C.5,C.6 and C.7 should be present in the same directory.

```
PSO start time at 08:05:49

PSO: 1/800 iterations, GBest =  0.13553899823459714.

PSO: 20/800 iterations, GBest = 0.082996840248725612.

PSO: 40/800 iterations, GBest = 0.079821180437261385.

PSO: 60/800 iterations, GBest = 0.079821180437261385.

PSO: 80/800 iterations, GBest = 0.079821180437261385.

PSO: 100/800 iterations, GBest = 0.079821180437261385.
```

PSO: 120/800 iterations, GBest = 0.079821180437261385.

PSO: 140/800 iterations, GBest = 0.079821180437261385.

PSO: 160/800 iterations, GBest = 0.079821180437261385.

PSO: 180/800 iterations, GBest = 0.079821180437261385.

PSO: 200/800 iterations, GBest = 0.079821180437261385.

PSO: 220/800 iterations, GBest = 0.059947899703387264.

PSO: 240/800 iterations, GBest = 0.058502905280338746.

PSO: 260/800 iterations, GBest = 0.058419282352298207.

PSO: 280/800 iterations, GBest = 0.051481484515911224.

PSO: 300/800 iterations, GBest = 0.03740741548166876.

PSO: 320/800 iterations, GBest = 0.025436018410963379.

PSO: 340/800 iterations, GBest = 0.025421814124444692.

PSO: 360/800 iterations, GBest = 0.025421708813983285.

PSO: 380/800 iterations, GBest = 0.02542170805166355.

PSO: 400/800 iterations, GBest = 0.025421708044712332.

PSO: 420/800 iterations, GBest = 0.025421708030273299.

PSO: 440/800 iterations, GBest = 0.025421708029904955.

PSO: 460/800 iterations, GBest = 0.025421708029904344.

PSO: 480/800 iterations, GBest = 0.025421708029904261.

PSO: 500/800 iterations, GBest = 0.025421708029904261.

PSO: 520/800 iterations, GBest = 0.025421708029904233.

PSO: 540/800 iterations, GBest = 0.02542170802990415.

PSO: 560/800 iterations, GBest = 0.025421708029903956.

PSO: 580/800 iterations, GBest = 0.025421708029903956.

PSO: 600/800 iterations, GBest = 0.025421708029903956.

PSO: 620/800 iterations, GBest = 0.025421708029903956.

PSO: 640/800 iterations, GBest = 0.025421708029903956.

PSO: 660/800 iterations, GBest = 0.025421708029903956.

PSO: 680/800 iterations, GBest = 0.025421708029903956.

PSO: 700/800 iterations, GBest = 0.025421708029903956.

PSO: 703/800 iterations, GBest = 0.025421708029903956.

--> Solution likely, GBest hasn't changed by at least 1e-008 for 350 epochs.

PSO end time at 08:06:21

No. of function evaluations = 7030

Total CPU time 30.997399 sec

out =

0.01178069750772

0.01500000000000

0.10000000000000

0.02542170802990

The following matlab program is used to calculate the objective function for design of welded beam problem in section 7.4.1 on page 206 and is needed to obtain optimum solution tabulated in Table 7.1. It doesn't require any input parameters. It should be used along with matlab program in the sections C.5 with change the function name to "weldbeampso".

C.9 OBJECTIVE FUNCTION FOR THE DESIGN OF WELDED BEAM PROBLEM

```
function [out]= spoobjfunweld(in)

global CNT i;

CNT=CNT+1;

const=0.5;

alpha=2;

ck=(const*i)^alpha;
```

```
consta=150;
constb=10;

x1=in(:,1);
x2=in(:,2);
x3=in(:,3);
x4=in(:,4);
f=1.10471*x1.*x1.*x2+0.04811*x3.*x4.*(14.0+x2);
P=6000;
E=30e6;
G=12e6;
smax=30000;
deltamax=0.25;
shearmax=13600;
L=14;
j1=(2/2^0.5)*x1.*x2;
j2=((x2.^2)/12+((x1+x3)./2).^2);
J=j1.*j2;
S=6*P*L./(x4.*x3.*x3);
K=(4*P*L^3)./(E*(x3.^3).*x4);
pc1=1-(x3./(2.*L))*(E./(4.*G))^(1/2);
pc2=4.013.*((E.*G.*(x3.^2 ).*(x4.^6)./36)).^(1/2);
Pc=pc1.*pc2./(L*L);
M=P*(L+x2./2);
R=((x2.^2)/4+((x1+x3)./2).^2).^0.5;
A=P./(x1.*x2.*1.414);
B=M.*R./J;
```

```
T = (A.^2+2.*A.*B.*(x2./(2.*R))+B.^2).^0.5;

g1=1.10471*x1.*x1+0.04811*x3.*x4.*(14.0+x2)-5.0;


for i2=1:size(in,1)

c=zeros(7,1);

g=0.0;

c = [T(i2,1)-shearmax;S(i2,1)-smax;x1(i2,1)-x4(i2,1);0.125-x1(i2,1);g1(i2,1);K(i2,1)-
deltamax;P-Pc(i2,1)];

for i1=1:7

    if c(i1,1)>0

        if c(i1,1)<=1

            gammaqx=1;

        else

            gammaqx=2;

        end

        thetaqx=consta*(1-1/exp(c(i1,1)))+constb;

        hx=thetaqx*(c(i1,1))^gammaqx;

        g=g+ck*hx;

    end

end

out(i2,1)=f(i2,1)+ck*g;

end

out;
```

The matlab program in the sections C.5 with change the function name to "weldbeampso" and matlab program in the section C.9 should be placed in the same directory. The optimum solution obtained for design of welded beam problem in section 7.4.1 on page 206 is as shown section C.10 and is tabulated in Table 7.1 We get the following output, as described in the section C.10, when use the following code at the matlab prompt.

>> out = weldbeampso('spoobjfunweld',4,2,[0.1 2.0;0.1 10;0.1 10;0.1 2.0])

C.10 OUTPUT/ OPTIMUM SOLUTION FOR THE DESIGN OF WELDED BEAM PROBLEM

PSO start time at 16:54:58

PSO: 1/2000 iterations, GBest = 11.600078268703111.

PSO: 50/2000 iterations, GBest = 4.7268530105574857.

PSO: 100/2000 iterations, GBest = 3.6929675084922176.

PSO: 150/2000 iterations, GBest = 3.6929675084922176.

PSO: 200/2000 iterations, GBest = 3.0896019039198981.

PSO: 250/2000 iterations, GBest = 3.0896019039198981.

PSO: 300/2000 iterations, GBest = 3.0896019039198981.

PSO: 350/2000 iterations, GBest = 2.7443504894923256.

PSO: 400/2000 iterations, GBest = 2.7443504894923256.

PSO: 450/2000 iterations, GBest = 2.5690241167803718.

PSO: 500/2000 iterations, GBest = 2.4644430980423846.

PSO: 550/2000 iterations, GBest = 2.4142986651480607.

PSO: 600/2000 iterations, GBest = 2.4130985072240807.

PSO: 650/2000 iterations, GBest = 2.3871643157891791.

PSO: 700/2000 iterations, GBest = 2.3827797928594032.

PSO: 750/2000 iterations, GBest = 2.382767943345498.

PSO: 800/2000 iterations, GBest = 2.3823256886358504.

PSO: 850/2000 iterations, GBest = 2.3818374278046397.

PSO: 900/2000 iterations, GBest = 2.3816125867753861.

PSO: 950/2000 iterations, GBest = 2.3813514495268513.

PSO: 1000/2000 iterations, GBest = 2.3812658028586959.

PSO: 1050/2000 iterations, GBest = 2.3812243960409996.

PSO: 1100/2000 iterations, GBest = 2.3812010944293842.

PSO: 1150/2000 iterations, GBest = 2.3812003169795446.

PSO: 1200/2000 iterations, GBest = 2.3811865786946704.

PSO: 1250/2000 iterations, GBest = 2.3811807081169056.

PSO: 1300/2000 iterations, GBest = 2.3811796868955026.

PSO: 1350/2000 iterations, GBest = 2.3811793822946741.

PSO: 1400/2000 iterations, GBest = 2.3811790013166698.

PSO: 1450/2000 iterations, GBest = 2.3811777126040239.

PSO: 1500/2000 iterations, GBest = 2.3811455203452581.

PSO: 1550/2000 iterations, GBest = 2.3811455067987972.

PSO: 1600/2000 iterations, GBest = 2.3811442702488388.

PSO: 1650/2000 iterations, GBest = 2.3811442693440239.

PSO: 1700/2000 iterations, GBest = 2.3811442693440212.

PSO: 1750/2000 iterations, GBest = 2.3811400963891862.

PSO: 1800/2000 iterations, GBest = 2.381139995411139.

PSO: 1850/2000 iterations, GBest = 2.3811399862981615.

PSO: 1900/2000 iterations, GBest = 2.3811399849397135.

PSO: 1950/2000 iterations, GBest = 2.381139984927044.

PSO: 2000/2000 iterations, GBest = 2.3811399849269828.

PSO end time at 16:55:10

No. of function evaluations = 24000

Total CPU time 12.355279 sec

out =

0.2443

6.2159

8.2944

0.2443

2.3811

The following matlab program is used to combine evidence from two sources using Dempster's rule for the problem described in section 4.2.1 on page 76 and is needed to obtain optimum solution tabulated in Table 4.3.

C.11 DEMPSTER-SHAFER COMBINATION RULE FOR COMBINING TWO EVIDENCES E_1 AND E_2

```
function [bela belb belc pla plb plc normk]=dempster2(m1,m2)

% m1=[.1 .1 .1 .1 .1 .1 .4]; %Evidence E1

% m2=[.2 .3 .1 0 .1 .1 .2];%Evidence E2

sum=0;

a=0;

b=a;

c=a;

d=a;

e=a;

f=a;

pi=a;

for i=1:7

   for j=1:7

            sum=sum+m1(i)*m2(j);

            if i==7 && j==7

               theta=m1(i)*m2(j);

            elseif (i==1 || i==7) && (j==1 || j==7)

               a=a+m1(i)*m2(j);

            elseif (i==2 || i==7) && (j==2 || j==7)

               b=b+m1(i)*m2(j);

            elseif (i==3 || i==7) && (j==3 || j==7)

               c=c+m1(i)*m2(j);

            elseif (i==1 || i==4 || i==6) && (j==1 || j==4 || j==6) && i~=j
```

```
            a=a+m1(i)*m2(j);
        elseif (i==2 || i==4 || i==5) && (j==2 || j==4 || j==5) && i~=j
            b=b+m1(i)*m2(j);
        elseif (i==3 || i==5 || i==6) && (j==3 || j==5 || j==6) && i~=j
            c=c+m1(i)*m2(j);
        elseif (i==4 || i==7) && (j==4 || j==7)
            d=d+m1(i)*m2(j);
        elseif (i==5 || i==7) && (j==5 || j==7)
            e=e+m1(i)*m2(j);
        elseif (i==6 || i==7) && (j==6 || j==7)
            f=f+m1(i)*m2(j);
        else
            [i j];
            pi=pi+m1(i)*m2(j);
        end

    end
end

normk=1-pi;
bela=a/normk;
belb=b/normk;
belc=c/normk;
beld=d/normk;
bele=e/normk;
belf=f/normk;
pla=1-belb-belc-bele;
```

```
plb=1-bela-belc-belf;

plc=1-bela-belb-beld;

BIA=[bela pla]

BIB=[belb plb]

BIC=[belc plc]

qtheta=pi+theta;


If  m1 = [.5 .1 .1 0 0 0 .3]; %Evidence E1

 and m2 = [.6 .1 .1 0 0 0 .2];%Evidence E2
```

are given then dempster2(m1,m2) at the command prompt gives the following result.

The BIA, BIB, and BIC gives the belief intervals for A,B and C respectively.

```
>> dempster2(m1,m2);

BIA =     0.0009    0.2096

BIB =     0.0016    0.2103

BIC =    0.7888    0.9976

ans =   8.7562e-004
```

The following matlab program is used to combine evidence from four sources using Yager's rule for the problem described in section 4.4 on page 96 and is needed to obtain optimum solution tabulated in Table 4.11.

C.12 YAGER'S COMBINATION RULE FOR COMBINING FOUR EVIDENCES E_1, E_2, E_3 and E_4

```
function [bela belb belc pla plb plc]=yagers4(m1,m2,m3,m4)

%clc

% m1=[.1 .1 .1 .1 .1 .1 .4];

% m2=m1;

% m3=m1;

% m4=m1;
```

```
sum=0;
a=0;
b=a;
c=a;
d=a;
e=a;
f=a;
pi=a;

for i=1:7
   for j=1:7
      for k=1:7
         for l=1:7
            sum=sum+m1(i)*m2(j)*m3(k)*m4(l);
            if i==7 && j==7 && k==7 && l==7
               theta=m1(i)*m2(j)*m3(k)*m4(l);
            elseif (i==1 || i==7) && (j==1 || j==7) && (k==1 || k==7) && (l==1 || l==7)
               a=a+m1(i)*m2(j)*m3(k)*m4(l);
            elseif (i==2 || i==7) && (j==2 || j==7) && (k==2 || k==7) && (l==2 || l==7)
               b=b+m1(i)*m2(j)*m3(k)*m4(l);
            elseif (i==3 || i==7) && (j==3 || j==7) && (k==3 || k==7) && (l==3 || l==7)
               c=c+m1(i)*m2(j)*m3(k)*m4(l);
            elseif (i==4 || i==7) && (j==4 || j==7) && (k==4 || k==7) && (l==4 || l==7)
               d=d+m1(i)*m2(j)*m3(k)*m4(l);
            elseif (i==5 || i==7) && (j==5 || j==7) && (k==5 || k==7) && (l==5 || l==7)
               e=e+m1(i)*m2(j)*m3(k)*m4(l);
            elseif (i==6 || i==7) && (j==6 || j==7) && (k==6 || k==7) && (l==6 || l==7)
```

```
            f=f+m1(i)*m2(j)*m3(k)*m4(l);

        elseif (i==1 || i==4 || i==6 || i==7) && (j==1 || j==4 || j==6 || j==7) && (k==1 ||
k==4 || k==6 || k==7) && (l==1 || l==4 || l==6 || l==7)

            if (i==1 && j==1 && k==1 && l==1)|| (i==4 && j==4 && k==4 &&
l==4)||(i==6 && j==6 && k==6 && l==6)

                ;

            else

            a=a+m1(i)*m2(j)*m3(k)*m4(l);

            end

        elseif (i==2 || i==4 || i==5 || i==7) && (j==2 || j==4 || j==5|| j==7) && (k==2 ||
k==4 || k==5|| k==7) && (l==2 || l==4 || l==5|| l==7)

            if (i==2 && j==2 && k==2 && l==2)|| (i==4 && j==4 && k==4 &&
l==4)||(i==5 && j==5 && k==5 && l==5)

                ;

            else

            b=b+m1(i)*m2(j)*m3(k)*m4(l);

            end

        elseif (i==3 || i==5 || i==6|| i==7) && (j==3 || j==5 || j==6|| j==7) && (k==3 ||
k==5 || k==6|| k==7) && (l==3 || l==5 || l==6|| l==7)

            if (i==3 && j==3 && k==3 && l==3)|| (i==5 && j==5 && k==5 &&
l==5)||(i==6 && j==6 && k==6 && l==6)

                ;

            else

            c=c+m1(i)*m2(j)*m3(k)*m4(l);

            end

        elseif (i==4 || i==7) && (j==4 || j==7) && (k==4 || k==7) && (l==4 || l==7)

            d=d+m1(i)*m2(j)*m3(k)*m4(l);

        elseif (i==5 || i==7) && (j==5 || j==7) && (k==5 || k==7) && (l==5 || l==7)

            e=e+m1(i)*m2(j)*m3(k)*m4(l);

        elseif (i==6 || i==7) && (j==6 || j==7) && (k==6 || k==7) && (l==6 || l==7)
```

```
                f=f+m1(i)*m2(j)*m3(k)*m4(l);
            else
                pi=pi+m1(i)*m2(j)*m3(k)*m4(l);
            end
        end
    end
end

bela=a;
belb=b;
belc=c;
beld=d;
bele=e;
belf=f;
pla=1-belb-belc-bele;
plb=1-bela-belc-belf;
plc=1-bela-belb-beld;
% qtheta=pi+theta;
BIA=[bela pla]
BIB=[belb plb]
BIC=[belc plc]
```

Evidence set-2 in Table 4.8 is considered to run the program

If m1=[0.4 0.4 0 0 0 0 0.2]; %Evidence S_1

m2=[0.5 0 0.3 0 0 0 0.2]; %Evidence S_2

m3=[0.6 0.25 0 0 0 0 0.15]; %Evidence S_3

and m4=[0.7 0.2 0 0 0 0 0.1]; %Evidence S_4

are given then yagers4(m1,m2,m3,m4) at the command prompt gives the following result. The BIA, BIB, and BIC gives the belief intervals for I, II and III respectively.

```
>> yagers4(m1,m2,m3,m4)

BIA =     0.2514    0.9853

BIB =      0.0138    0.7477

BIC =      0.0009    0.7348

ans =     0.2514
```

The following matlab program is used to combine evidence from four sources using Zhang's rule for the problem described in section 4.4 on page 96 and is needed to obtain optimum solution tabulated in Table 4.11.

C.13 ZHANG'S COMBINATION RULE FOR COMBINING FOUR E_1, E_2, E_3 and E_4

```
function [bela belb belc pla plb plc]=zhangs4(m1,m2,m3,m4)

% clc

% m1=[.1 .1 .1 .1 .1 .1 .4];

% m2=m1;

% m3=m1;

% m4=m1;

sum=0;

a=0;

b=a;

c=a;

d=a;

e=a;

f=a;

pi=a;

R=zeros(7,7,7,7);

rsum=0;

for i=1:7
```

```
        if i==1
           x1=[1];
        end
        if i==2
           x1=[2];
        end
        if i==3
           x1=[3];
        end
        if i==4
           x1=[1 2];
        end
         if i==5
           x1=[2 3];
         end
         if i==6
           x1=[1 3];
         end
         if i==7
           x1=[1 2 3];
         end
for j=1:7
        if j==1
           x2=[1];
        end
        if j==2
           x2=[2];
```

```
        end
        if j==3
           x2=[3];
        end
        if j==4
           x2=[1 2];
        end
         if j==5
           x2=[2 3];
         end
         if j==6
           x2=[1 3];
         end
         if j==7
           x2=[1 2 3];
         end
    for k=1:7
        if k==1
           x3=[1];
        end
        if k==2
           x3=[2];
        end
        if k==3
           x3=[3];
        end
        if k==4
```

```
        x3=[1 2];
    end
     if k==5
        x3=[2 3];
     end
     if k==6
        x3=[1 3];
     end
     if k==7
        x3=[1 2 3];
     end
for l=1:7
    if l==1
        x4=[1];
    end
    if l==2
        x4=[2];
    end
    if l==3
        x4=[3];
    end
    if l==4
        x4=[1 2];
    end
     if l==5
        x4=[2 3];
     end
```

```
            if l==6
               x4=[1 3];
            end
            if l==7
               x4=[1 2 3];
            end

R(i,j,k,l)=length(intersect(intersect(intersect(x1,x2),x3),x4))/(length(x1)*length(x2)*lengt
h(x3)*length(x4));
            rsum=rsum+R(i,j,k,l);
            clear x4
         end
         clear x3
      end
      clear x2
   end
   clear x1
end
rsum
for i=1:7
   for j=1:7
      for k=1:7
         for l=1:7
            sum=sum+m1(i)*m2(j)*m3(k)*m4(l)*R(i,j,k,l);
            if i==7 && j==7 && k==7 && l==7
               theta=m1(i)*m2(j)*m3(k)*m4(l)*R(i,j,k,l);
            elseif (i==1 || i==7) && (j==1 || j==7) && (k==1 || k==7) && (l==1 || l==7)
               a=a+m1(i)*m2(j)*m3(k)*m4(l)*R(i,j,k,l);
```

```
elseif (i==2 || i==7) && (j==2 || j==7) && (k==2 || k==7) && (l==2 || l==7)
   b=b+m1(i)*m2(j)*m3(k)*m4(l)*R(i,j,k,l);
elseif (i==3 || i==7) && (j==3 || j==7) && (k==3 || k==7) && (l==3 || l==7)
   c=c+m1(i)*m2(j)*m3(k)*m4(l)*R(i,j,k,l);
elseif (i==4 || i==7) && (j==4 || j==7) && (k==4 || k==7) && (l==4 || l==7)
   d=d+m1(i)*m2(j)*m3(k)*m4(l)*R(i,j,k,l);
elseif (i==5 || i==7) && (j==5 || j==7) && (k==5 || k==7) && (l==5 || l==7)
   e=e+m1(i)*m2(j)*m3(k)*m4(l)*R(i,j,k,l);
elseif (i==6 || i==7) && (j==6 || j==7) && (k==6 || k==7) && (l==6 || l==7)
   f=f+m1(i)*m2(j)*m3(k)*m4(l)*R(i,j,k,l);
elseif (i==1 || i==4 || i==6 || i==7) && (j==1 || j==4 || j==6 || j==7) && (k==1 ||
k==4 || k==6 || k==7) && (l==1 || l==4 || l==6 || l==7)
   if (i==1 && j==1 && k==1 && l==1)|| (i==4 && j==4 && k==4 &&
l==4)||(i==6 && j==6 && k==6 && l==6)
      ;
   else
   a=a+m1(i)*m2(j)*m3(k)*m4(l)*R(i,j,k,l);
   end
elseif (i==2 || i==4 || i==5 || i==7) && (j==2 || j==4 || j==5|| j==7) && (k==2 ||
k==4 || k==5|| k==7) && (l==2 || l==4 || l==5|| l==7)
   if (i==2 && j==2 && k==2 && l==2)|| (i==4 && j==4 && k==4 &&
l==4)||(i==5 && j==5 && k==5 && l==5)
      ;
   else
   b=b+m1(i)*m2(j)*m3(k)*m4(l)*R(i,j,k,l);
   end
elseif (i==3 || i==5 || i==6|| i==7) && (j==3 || j==5 || j==6|| j==7) && (k==3 ||
k==5 || k==6|| k==7) && (l==3 || l==5 || l==6|| l==7)
   if (i==3 && j==3 && k==3 && l==3)|| (i==5 && j==5 && k==5 &&
l==5)||(i==6 && j==6 && k==6 && l==6)
```

```
                ;
            else
            c=c+m1(i)*m2(j)*m3(k)*m4(l)*R(i,j,k,l);
            end
        elseif (i==4 || i==7) && (j==4 || j==7) && (k==4 || k==7) && (l==4 || l==7)
            d=d+m1(i)*m2(j)*m3(k)*m4(l)*R(i,j,k,l);
        elseif (i==5 || i==7) && (j==5 || j==7) && (k==5 || k==7) && (l==5 || l==7)
            e=e+m1(i)*m2(j)*m3(k)*m4(l)*R(i,j,k,l);
        elseif (i==6 || i==7) && (j==6 || j==7) && (k==6 || k==7) && (l==6 || l==7)
            f=f+m1(i)*m2(j)*m3(k)*m4(l)*R(i,j,k,l);
        else
            pi=pi+m1(i)*m2(j)*m3(k)*m4(l)*R(i,j,k,l);
            if R(i,j,k,l)~=0
                [i j k l]
            end
        end
      end
    end
  end
end

bela=a/sum;
belb=b/sum;
belc=c/sum;
beld=d/sum;
bele=e/sum;
belf=f/sum;
```

```
pla=1-belb-belc-bele;

plb=1-bela-belc-belf;

plc=1-bela-belb-beld;

BIA=[bela pla]

BIB=[belb plb]

BIC=[belc plc]
```

Evidence set-4 in Table 4.8 is considered to run the program

If m1=[0 0 0 0.8 0.1 0 0.1]; %Evidence S_1

m2=[0 0.5 0.1 0 0 0.2 0.2]; %Evidence S_2

m3=[0.6 0 0 0 0.2 0 0.2]; %Evidence S_3

and m4=[0.6 0.1 0 0 0.2 0 0.1]; %Evidence S_4

are given then zhangs4(m1,m2,m3,m4) at the command prompt gives the following result. The BIA, BIB, and BIC gives the belief intervals for I, II and III respectively.

```
>>zhangs4(m1,m2,m3,m4);

BIA =    0.7306    0.7342

BIB =    0.2514    0.2603

BIC =     0.0087    0.0151
```

The following matlab program is used to calculate the objective function for non-repairable FRW policy optimization problem in section 9.3.1 on page 275 and is needed to obtain optimum solution tabulated in Table 7.1. It doesn't require any input parameters. It should be used along with matlab program in the sections C.5 with change the function name to "multiobjcontautomobile".

C.14 OBJECTIVE FUNCTION FOR NON-REPAIRABLE FRW POLICY OPTIMIZATION PROBLEM

```
function [out]=awcexppolicy1(in)

format long g

global CNT i;

psize=size(in);

CNT=CNT+1;

const=0.5;
```

```
alpha=2;
ck=(const*i)^alpha;
consta=150;
constb=10;
fpslimit=0.4;
%weibull distribution model is assumed for failure distribution
%Non renewing and non repairable FRW

    %brakes
    bc1=[110 90 80 70];
    b1=[.004 .006 .008 .01];
    pb=polyfit(b1,bc1,2);
    wb=36;
    wba=12;

    %exhausts
    uc1=[125 95 85 65];
    u1=[.002 .007 .011 .016];
    pu1=polyfit(u1,uc1,2);
    wu=36;
    wua=12;

    %hvac
    hc1=[200 180 150];
    h1=[.004 .006 .009];
    ph1=polyfit(h1,hc1,2);
    wh=36;
```

```
        wha=12;

        %electrical battery
        ebc1=[135 110 80 75];
        eb1=[.004 .008 .011 .012];
        peb1=polyfit(eb1,ebc1,2);
        weba=12;
        web=36;

        %safety systems
        stc1=[112 94 82 72];
        st1=[.004 .006 .008 .01];
        ps=polyfit(st1,stc1,2);
        wst=36;
        wsta=12;

for k1=1:psize(1,1)
   clear x1 x2 x3 x4 x5
        x1=in(k1,1);
        x2=in(k1,2);
        x3=in(k1,3);
        x4=in(k1,4);
        x5=in(k1,5);

        twc=0;
        fb = polyval(pb,x1);
        wb1=fb*(1+mtforweibull((x1*wb),2));
```

```
    twc=twc+2*wb1;
    fpb=1-exp(-(x1*wb)^2);

    fu1 = polyval(pu1,x2);
    wu1=fu1*(1+mtforweibull((x2*wu),2));
    twc=twc+wu1;
    fpu=1-exp(-(x2*wu)^2);

    fh1 = polyval(ph1,x3);
    wh1=fh1*(1+mtforweibull((x3*wh),2));
    twc=twc+wh1;
    fph=1-exp(-(x3*wh)^2);

    feb1 = polyval(peb1,x4);
    web1=feb1*(1+mtforweibull((x4*web),2));
    twc=twc+web1;
    fpeb=1-exp(-(x4*web)^2);

    fs = polyval(ps,x5);
    wst1=fs*(1+mtforweibull((x5*wst),2));
    twc=twc+wst1;
    fpst=1-exp(-(x5*wst)^2);

%failure of the automobile in series
tfps=1-(1-fpb)*(1-fpu)*(1-fph)*(1-fpeb)*(1-fpst);
gconst1=tfps-fpslimit;
if gconst1>0
```

```
    if gconst1<=1
        gammaqx=1;
    else
        gconst1=gconst1+1;
        gammaqx=2;
    end
    thetaqx=consta*(1-1/exp(gconst1))+constb;
    hx=thetaqx*(gconst1)^gammaqx;
    gconst1=gconst1+ck*hx;
  else
     gconst1=0;
  end
  gconst1
  out(k1,1)=twc+gconst1;
end
```

The following output is obtained for the non-repairable FRW policy optimization problem when the following command is used at command prompt of the matlab

```
 out1 = multiobjcontautomobile('awcexppolicy1',5,0.02,z)
```

```
PSO start time at 21:51:00
PSO: 1/800 iterations, GBest =   678.16842020125171.
PSO: 50/800 iterations, GBest =   641.89019107138938.
PSO: 100/800 iterations, GBest =   630.56665392052753.
PSO: 150/800 iterations, GBest =   620.63148661739399.
PSO: 200/800 iterations, GBest =   616.38943082507035.
PSO: 250/800 iterations, GBest =   615.30922288733768.
PSO: 300/800 iterations, GBest =   613.35234399898945.
PSO: 350/800 iterations, GBest =   613.30526648825139.
PSO: 400/800 iterations, GBest =   613.30525902532747.
```

PSO: 450/800 iterations, GBest = 613.30525902459135.

PSO: 500/800 iterations, GBest = 613.22880792880028.

PSO: 550/800 iterations, GBest = 613.22378263387179.

PSO: 600/800 iterations, GBest = 613.215853376822.

PSO: 650/800 iterations, GBest = 613.21292985033176.

PSO: 700/800 iterations, GBest = 613.21280476885397.

PSO: 750/800 iterations, GBest = 613.21280447210063.

PSO: 800/800 iterations, GBest = 613.21267001185515.

PSO end time at 21:59:46

No. of function evaluations = 9600

Total CPU time 284.951427 sec

out1 = 1.0e+002 *

0.00008971382571

0.00005607028943

0.00008999999998

0.00012000000000

0.00007565099235

6.13212670011855